ol. 124 No. 1, February 1, 1981 ISSN 0003-2670

ANALYTICA CHIMICA ACTA

International journal devoted to all branches of analytical chemistry

ELSEVIER SCIENTIFIC PUBLISHING COMPANY

ANALYTICA CHIMICA ACTA

International journal devoted to all branches of analytical chemistry
Revue internationale consacrée à tous les domaines de la chimie analytique
Internationale Zeitschrift für alle Gebiete der analytischen Chemie

PUBLICATION SCHEDULE FOR 1981 (incorporating the section on Computer Techniques and Optimization).

	J	F	M	A	M	J	J	A	S	O	N	D
Analytica Chimica Acta	123	124/1	124/2	125	126	127	128	129	130/1	130/2	131	132
Section on Computer Techniques and Optimization		133/1			133/2			133/3			133/4	

Scope. *Analytica Chimica Acta* publishes original papers, short communications, and reviews dealing with every aspect of modern chemical analysis, both fundamental and applied. The section on *Computer Techniques and Optimization* is devoted to new developments in chemical analysis by the application of computer techniques and by interdisciplinary approaches, including statistics, systems theory and operation research. The section deals with the following topics: Computerized acquisition, processing and evaluation of data. Computerized methods for the interpretation of analytical data including chemometrics, cluster analysis, and pattern recognition. Storage and retrieval systems. Optimization procedures and their application. Automated analysis for industrial processes and quality control. Organizational problems.

Submission of Papers. Manuscripts (three copies) should be submitted as designated below for rapid and efficient handling:

Papers from the Americas to: Professor Harry L. Pardue, Department of Chemistry, Purdue University, West Lafayette, IN 47907, U.S.A.

Papers from all other countries to: Dr. A. M. G. Macdonald, Department of Chemistry, The University, P.O. Box 363, Birmingham B15 2TT, England.

For the section on *Computer Techniques and Optimization:* Dr. J. T. Clerc, Universität Bern, Pharmazeutisches Institut, Sahlistrasse 10, CH-3012 Bern, Switzerland.

American authors are recommended to send manuscripts and proofs by INTERNATIONAL AIRMAIL.

Information for Authors. Papers in English, French and German are published. There are no page charges. Manuscripts should conform in layout and style to the papers published in this Volume. Authors should consult Vol. 121, p. 353 for detailed information. Reprints of this information are available from the Editors or from: Elsevier Editorial Services Ltd., Mayfield House, 256 Banbury Road, Oxford OX2 7DE (Great Britain).

Reprints. Fifty reprints will be supplied free of charge. Additional reprints (minimum 100) can be ordered. An order form containing price quotations will be sent to the authors together with the proofs of their article.

Advertisements. Advertisement rates are available from the publisher.

Subscriptions. Subscriptions should be sent to: Elsevier Scientific Publishing Company, P.O. Box 211, 1000 AE Amsterdam, The Netherlands. The section on *Computer Techniques and Optimization* can be subscribed to separately.

Publication. *Analytica Chimica Acta* (including the section on *Computer Techniques and Optimization*) appears in 11 volumes in 1981. The subscription for 1981 (Vols. 123–133) is Dfl. 1639.00 plus Dfl. 198.00 (postage) (total approx. U.S. $942.00). The subscription for the *Computer Techniques and Optimization* section only (Vol. 133) is Dfl. 149.00 plus Dfl. 18.00 (postage) (total approx. U.S. $86.00). Journals are sent automatically by airmail to the U.S.A. and Canada at no extra cost and to Japan, Australia and New Zealand for a small additional postal charge. All earlier volumes (Vols. 1–121) except Vols. 23 and 28 are available at Dfl. 164.00 (U.S. $84.00), plus Dfl. 13.00 (U.S. $6.50) postage and handling, per volume.

Claims for issues not received should be made within three months of publication of the issue, otherwise they cannot be honoured free of charge.

Customers in the U.S.A. and Canada who wish to obtain additional bibliographic information on this and other Elsevier journals should contact Elsevier/North Holland Inc., Journal Information Center, 52 Vanderbilt Avenue, New York, NY 10017. Tel: (212) 867-9040.

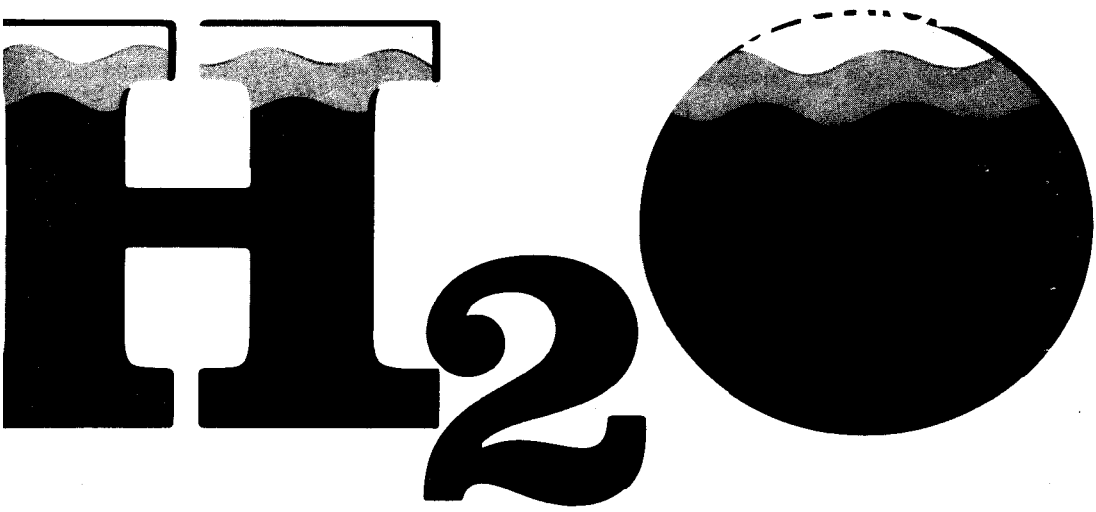

Aquamerck®

Reagent kits for the analysis of industrial, boiler feed and swimming pool water. Chemical analyses can be carried out quickly and reliably without additional equipment and with few operations.

Aquaquant®

Complete ready-to-use reagent kits with integrated 10-step color comparator. An analysis system, which offers both the qualified laboratory and the user without previous analytical experience, decisive advantages.

Merckoquant®

Test strips for use in orientating search or pre-tests for the semi-quantitative determination of ions or compounds in field and laboratory analysis.

Spectroquant®

Reagent kits for the photometric rapid analysis of important substances in water.

Please ask for our special literature.

E. Merck, Darmstadt,
Federal Republic of Germany

Electrodes of Conductive Metal Oxides: Part A

edited by SERGIO TRASATTI, *Laboratory of Electrochemistry, University of Milan, Italy*

STUDIES IN PHYSICAL AND THEORETICAL CHEMISTRY 11

The discovery by Beer in the second half of the sixties that the performances of anodes made of thermally prepared noble metal oxides were better than those of noble metals provoked something of a technological revolution in the large electrolytic industry. Since then an ever increasing number of fundamental studies have been published but the large amount of data has, until now, not been adequately assimilated.

This two-part work provides a general unifying introduction plus a state-of-the-art review of the physicochemical properties and electrochemical behaviour of conductive oxide electrodes (DSA). The text has been divided into two volumes – Part A dealing mainly with structural and thermodynamic properties and Part B, to be published in due course, dealing with kinetic and electrocatalytic aspects. This division came about due to the large amount of material to be treated and also because, in a rapidly developing field, difficulties arise in collecting all relevant material at one given moment.

The editor approaches the subject from a multidisciplinary angle, for example, the electrochemical behaviour of oxide electrodes is presented and discussed in the context of a variety of physicochemical properties – electronic structure, nonstoichiometry, crystal structure, surface structure, morphology and adsorption properties. For the first time the different groups of oxides are treated together in order to place emphasis on their similarities and differences.

This major reference work is mainly directed to electrochemists and those working on catalysis. It will also be useful to those in the fields of materials science, physical chemistry, surface and colloid chemistry and in areas where oxide surfaces may play a major role as in chromatography and photochemistry.

CONTENTS: Chapters. 1. Electronic Band Structure of Oxides with Metallic or Semiconducting Characteristics *(J. M. Honig)*. 2. Chemisorption and Catalysis on Metal Oxides *(A. Cimino and S. Carrà)*.. 3. Oxide Growth and Oxygen Evolution on Noble Metals *(L. D. Burke)*. 4. Electrochemistry of Lead Dioxide *(J. P. Pohl and H. Rickert)*. 5. Properties of Spinel-Type Oxide Electrodes *(M. R. Tarasevich and B. N. Efremov)*. 6. Physicochemical and Electrochemical Properties of Perovskite Oxides *(H. Tamura, Y. Yoneyama and Y. Matsumoto)*. 7. Properties of Conductive Transition Metal Oxides with Rutile-Type Structure *(S. Trasatti and G. Lodi)*.

1980 xvi + 366 pages
US $ 83.00 / Dfl. 170.00
ISBN 0-444-41912-8

ELSEVIER

P.O. Box 211, 1000 AE
Amsterdam, The Netherlands.

52 Vanderbilt Ave,
New York, NY 10017.

The Dutch guilder price is definitive. US $ price is subject to exchange rate fluctuations

STATISTICAL TREATMENT OF EXPERIMENTAL DATA

By J.R. GREEN, *Lecturer in Computational and Statistical Science, University of Liverpool, U.K. and* D. MARGERISON, *Senior Lecturer in Inorganic, Physical and Industrial Chemistry, University of Liverpool, U.K.*

PHYSICAL SCIENCES DATA 2

This book first appeared in 1977. In 1978 a revised reprint was published and in response to demand, further reprints appeared in 1979 and 1980. Intended for researchers wishing to analyse experimental data, this work will also be useful to students of statistics. Statistical methods and concepts are explained and the ideas and reasoning behind statistical methodology clarified. Noteworthy features of the text are numerical worked examples to illustrate formal results, and the treatment of many practical topics which are often omitted from standard texts, for example testing for outliers, stabilization of variances and polynomial regression.

What the reviewers had to say:

"The index is detailed; the format is good; the presentation is clear; and no mathematics beyond calculus is assumed".
–CHOICE

"A lot of thought has gone into this book and I like it very much. It deserves a place on every laboratory bookshelf".
–CHEMISTRY IN BRITAIN

1977. Reprinted 1978, 1979, 1980.
xiv + 382 pages
US $39.25/Dfl.90.00
ISBN: 0-444-41725-7

ELSEVIER
P.O. Box 211, 1000 AE Amsterdam, The Netherlands.
52 Vanderbilt Ave., New York, NY 10017.

The Dutch guilder price is definitive. US$ prices are subject to exchange rate fluctuations.

7/84

ANALYTICA CHIMICA ACTA
VOL. 124 (1981)

ANALYTICA CHIMICA ACTA

International journal devoted to all branches of analytical chemistry

ELSEVIER SCIENTIFIC PUBLISHING COMPANY

Anal. Chim. Acta, Vol. 124 (1981)

Printed in The Netherlands.

Analytica Chimica Acta, 124 (1981) 1—13

DETERMINATION OF TETRAMETHYLLEAD AND TETRAETHYLLEAD IN THE ATMOSPHERE BY A TWO-STEP ENRICHMENT METHOD AND GAS CHROMATOGRAPHIC—MASS SPECTROMETRIC ISOTOPE DILUTION ANALYSIS

TORBEN NIELSEN*, HELGE EGSGAARD and ELFINN LARSEN

Chemistry Department, Risø National Laboratory, DK-4000 Roskilde (Denmark)

GUSTAV SCHROLL

Department of General and Organic Chemistry, University of Copenhagen, Universitetsparken 5, DK-2100 Copenhagen Ø (Denmark)

(Received 1st September 1980)

SUMMARY

The development of a specific and sensitive technique for determining tetramethyllead (TML) in air is described. The method has been tested in different areas under differing meteorological conditions to determine the atmospheric content of TML and tetraethyllead (TEL). The advantages and limitations of the method are critically discussed. The tetraalkyllead compounds are collected on Porapak QS or N at ambient temperature, desorbed, re-collected at −80°C on a small column containing 4% Apiezon M on Chromosorb PAW-DCMS, and analysed by gas chromatography—mass spectrometry with single ion monitoring. The isotope dilution technique is used by adding known amounts of d_{12}-TML and d_{20}-TEL to the sampling columns in advance. This makes it possible to correct for decomposition during the sampling and/or during the analytical procedure. The detection limit for TML is 20 pg m^{-3}.

Inorganic lead seems to be present in all kinds of environmental samples. A large part of the amount in the biosphere probably comes from the human uses of lead [1]. It is known that inorganic mercury compounds may be converted to methylmercury compounds under natural environmental conditions [2, 3]. Laboratory studies have shown that micro-organisms in the aquatic environment can methylate inorganic lead compounds to tetramethyllead (TML) [4, 5]. Trimethyllead compounds and TML are more toxic than inorganic lead compounds [6]. It is of importance, therefore, to explore the possible biomethylation of lead and the distribution of organolead compounds from man-made sources in the environment. Recently, Chau et al. [7] demonstrated that fish caught in remote areas may contain detectable amounts of tetraalkyllead. Furthermore, Harrison and Laxen [8] observed abnormally high ratios of organolead vapour to total lead in atmospheric samples from a rural area when the air masses had passed over open sea and coastal regions adjacent to the sampling sites.

*Present address: Swedish Water and Air Pollution Research Institute, Box 5207, S-402 24 Göteborg, Sweden.

Several methods have been developed for the determination of organolead compounds in the urban atmosphere [6, 9—14]. Only a few of these are selective for TML and at the same time are sufficiently sensitive to apply to rural areas [11, 14]. However, they are inconvenient for long-term sampling in the field requiring extensive cooling during collection.

Laveskog [15] collected TML and tetraethyllead (TEL) from urban air in a small gas chromatographic column at −80°C, desorbed them by heating and determined them by gas chromatographic—mass spectrometric (g.c.—m.s.) fragmentography in his pioneering work in Stockholm in 1969. The limitations of this method are that the formation of ice-plugs in the sampling tube restricts the sampling volume to 1 l of air, and the detection limits for TML and TEL are about 10 ng m^{-3}.

This paper describes a two-step enrichment method based upon the isotope dilution technique. The sampling is performed at ambient temperatures, and the sampling volume can be increased to more than 100 l. By this method it is possible to detect 20 pg TML m^{-3}.

An important advantage of this method compared to other g.c. methods utilizing either atomic absorption spectrometric detection [11, 13] or microwave plasma detection [14], is that the use of isotope dilution m.s. makes it possible to correct for decomposition of TML during the collection and/or the subsequent analytical procedure. The method has been tested in different modifications for the determination of atmospheric TML and TEL in urban and suburban areas under varying meteorological conditions and for the determination of TML in a rural area.

EXPERIMENTAL

Apparatus and reagents

The g.c.—m.s. measurements were performed on a Perkin-Elmer F 11 gas chromatograph interfaced by a two-stage all-glass jet separator to a Varian MAT mass spectrometer, model CH 5D. The m.s. fragmentographic signal was amplified and recorded on a two-channel recorder.

TML, TEL, d_{12}-TML and d_{20}-TEL were synthesized from the respective Grignard reagents (alkylmagnesium iodides) and lead nitrate [16, 17]. The mass spectra of the tetraalkyllead compounds are shown in Fig. 1. The standards used were freshly prepared solutions in analytical grade n-pentane. The carrier gas for the desorption of tetraalkyllead from the sampling columns and for the g.c.—m.s. analysis was dried and purified helium.

Sampling procedure and concentration of tetraalkyllead in small columns

The adsorption tubes for air samples were stainless steel tubes (50 cm × 1/4 in.) packed with Porapak N or QS (ca. 3.2 g). The columns were conditioned for 4—8 h at 190°C with purified nitrogen. Known amounts of d_{12}-TML and d_{20}-TEL (ca. 3 ng of each) were added to the columns kept at room temperature with the injection port at 90°C. The columns were then kept at −20°C

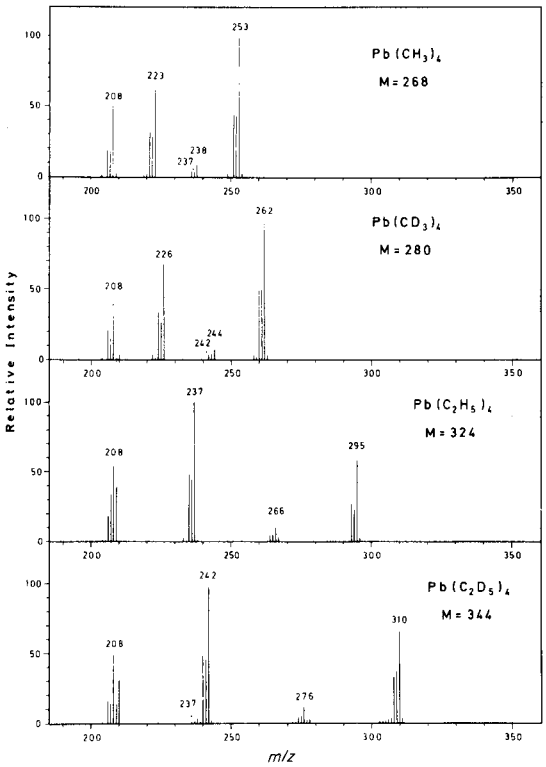

Fig. 1. The 70-eV mass spectra of tetramethyllead, d_{12}-tetramethyllead, tetraethyllead, and d_{20}-tetraethyllead.

until sampling. This was performed at about 5°C above the ambient temperature (−15 to + 25°C). The temperature increase was caused by the membrane pump (Thomas Ind. Inc., Model 107CD18 3) used for the sampling. On the inlet side the column was connected to a stainless steel tube doubled over to prevent snow or rain from entering the sampling tube. The sampling time varied in the different investigations from 2 to 26 h and the sampling volume from 13 to 190 l. In most cases a 24-h sampling time and 80—90-l sampling volumes were used. The collected samples were kept at −20°C.

Re-collection of tetraalkyllead in a small column. The g.c.—m.s. analysis of TML and TEL demands that the sample be concentrated in a small volume. Tetraalkyllead was desorbed from the sampling tube at 90°C with dried and purified helium at 50 ml min^{-1} (Fig. 2). The flow direction was opposite to that of the sampling. The re-collection of tetraalkyllead was done at −80°C in a glass U-tube (40 cm × 6 mm o.d.) filled with Chromosorb P-AW-DCMS (60—80 mesh) with 4% Apiezon M, and furnished with two teflon valves. They were closed at the end of this step and the Apiezon M column was heated to about 90°C to vapourize TML and TEL.

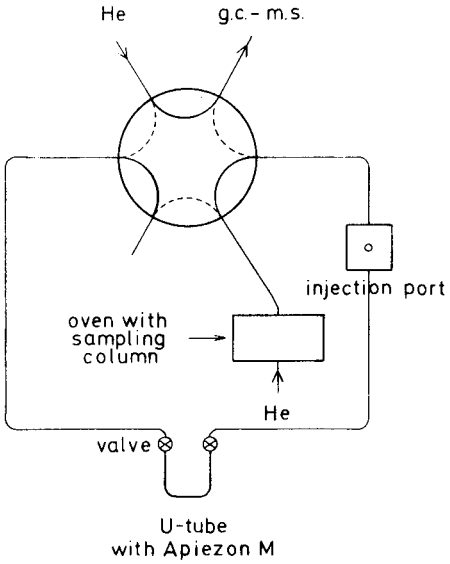

Fig. 2. Regulation of the flow-switching pattern with a six-port rotary valve. (——) Recollection of tetraalkyllead; (---) g.c.—m.s. of R_4Pb.

G.c.—m.s. procedure

The connections between the sampling tube, the U-tube with Apiezon M, and the gas chromatograph, as well as the flow direction in the U-tube are regulated with a six-port rotary valve as shown in Fig. 2. The parameters for the g.c.—m.s. are given in Table 1.

After heating the sample in the U-tube to about 90°C, the six-port rotary valve is turned, and the two teflon valves on the U-tube are opened. In this way the sample is introduced into the semi-polar g.c. column. The different methylethyllead compounds, $Me_nEt_{4-n}Pb$ (n = 0—4), are separated (Fig. 3) and detected by single ion monitoring. It was possible to monitor at only two masses with the instrument used. Therefore, to detect TML, TEL and the two deuterated standards m/z = 237 [$(CH_3)_2{}^{207}Pb^{+\cdot}$, $C_2H_5{}^{208}Pb^+$] and

TABLE 1

Parameters for the g.c.—m.s. system

G.c. column	10% EGSS-X on 80—100 mesh Chromosorb P-AW (2 m × 0.4 cm i.d., glass column)
Column temperature	100°C
Carrier gas	Helium
Flow rate	50 ml min^{-1}
Separator	100°C
Ionizing energy	70 eV (100 μA)
Ion source temperature	200°C
Detector, electron multiplier	Optimum conditions

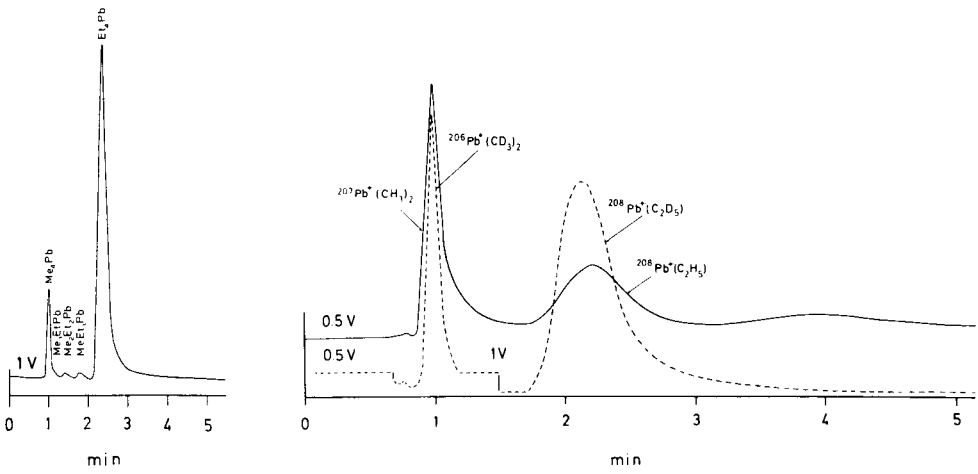

Fig. 3. Gas chromatogram of 0.1 μl of sample of leaded petrol (97 octane) detected at m/z = 237.

Fig. 4. Gas chromatogram of an air sample collected in a suburban area. TML and TEL are detected at m/z = 237 (——) and the internal standards, d_{12}-TML and d_{20}-TEL, at m/z = 242 (---).

m/z = 242 [$(CD_3)_2{}^{206}Pb^{+\cdot}$, $C_2D_5{}^{208}Pb^+$] were used (see Figs. 1 and 4). In those cases where only TML was investigated m/z = 253 [$(CH_3)_3{}^{208}Pb^+$] and m/z = 262 [$(CD_3)_3{}^{208}Pb^+$] were used, leading to enhanced sensitivity.

RESULTS AND DISCUSSION

Sampling adsorbent

The adsorbent was selected in order to comply with the following requirements: a low breakthrough volume of water vapour at ambient temperatures; high adsorption energies for TML and TEL, i.e., high breakthrough volumes at ambient temperatures and low ones at 90°C; no induced decomposition of the adsorbed TML and TEL.

The dependence of the retention volume of TML on the temperature was determined for the following six materials: Tenax GC (60—80 mesh). Porapak QS (80—100 mesh), Porapak N (80—100 mesh), and 30% Apiezon M, 20% OV-11 or 20% OV-101 on Chromosorb P-AW-DCMS (60—80 mesh). The tested materials have a low breakthrough volume for water vapour. The breakthrough volume of TML at ambient temperature was obtained by extrapolation of the linear graph of ln(retention volume) vs. 1/T, reducing the possible candidates to Porapak QS and N (Fig. 5). The breakthrough volumes for TML at 30°C were 170 l and 64 l per g of adsorbent. The adsorption energies calculated from the slopes of the linear plots were 14.6 and 14.4 kcal mol^{-1}, respectively.

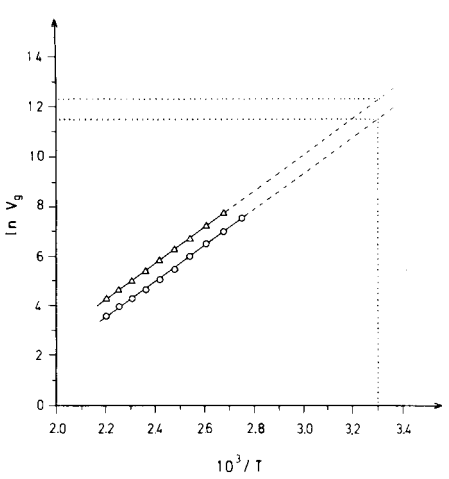

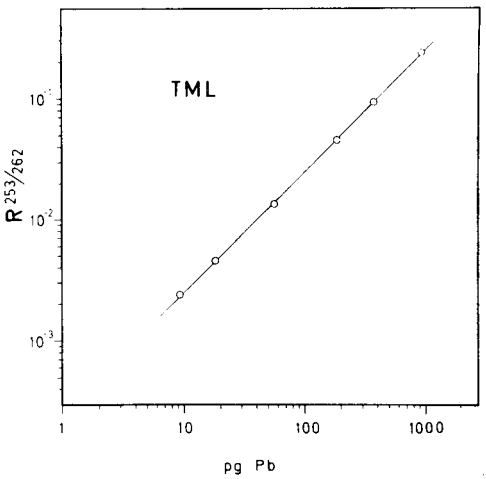

Fig. 5. The temperature dependence (K) of the retention volume V_g (ml) of TML on a Porapak QS (△) and a Porapak N (○) column (both, 100 cm × 0.29 cm o.d., 1.4 g of adsorbent).

Fig. 6. A calibration graph for TML. The ordinate shows the ratio between the peak heights of TML and d_{12}-TML at, respectively, *m/z* 253 $[(CH_3)_3{}^{208}Pb^+]$ and *m/z* 262 $[(CD_3)_3{}^{208}Pb^+]$. The abscissa shows the injected amount of TML (as Pb). In all cases the injected amount of d_{12}-TML was 3800 pg Pb.

The sample recovery was evaluated by injecting standards of TML and TEL into the Porapak QS and N columns and sampling 4—60 l of purified air. During the desorption and re-collection step, standards of d_{12}-TML and d_{20}-TEL were injected (see Fig. 2) and the recoveries of TML and TEL were determined by single ion monitoring at *m/z* = 237 and 242. The recoveries (mean ± standard deviation for 5 measurements) were 102 ± 4% for TML and 52 ± 11% for TEL for Porapak QS, and 92 ± 3% for TML and 73 ± 5% for TEL for Porapak N. The recoveries were independent of the volume of purified air, excluding the possibility that adsorbents catalyzed oxidation of TML and TEL by oxygen, as does activated carbon [6]. High recoveries for the collection of TML and TEL in Apiezon M U-tube at —80°C had been found earlier [15].

Tests of the sampling method with purified air did not indicate whether the oxidants in the atmosphere (e.g., ozone, HO˙ or $O(^3P)$) decompose the collected TML and TEL during sampling. The Porapak materials are copolymers of ethylvinyl- and divinyl-benzene. The relative reactivities of TML:TEL:*m*-xylene in the vapour phase at room temperature towards ozone are 60:20000:1; towards $O(^3P)$ they are 3:5:1, and towards HO˙, 0.4:3:1 [18]. The low selectivities of HO˙ and $O(^3P)$ indicate little possibility of causing decomposition of the collected TML and TEL during the sampling. The high selectivity of ozone and the high rate constants for the reaction between ozone and either TML or TEL indicate that during

sampling the presence of a large ozone concentration in the air may cause a considerable loss, particularly of TEL.

In other methods where sampling is done at temperatures of −80°C or lower [11, 13—15, 19], the possibility of decomposition during sampling is low. But reactive photochemical oxidants (e.g., ozone and peroxyacetyl nitrate) may also be collected, and may give rise to decomposition of TML and TEL during the subsequent analytical procedure. These aspects appear to have been disregarded except in one investigation [19].

G.c.—m.s. analysis

Discrepancies in the results for the contents of TML and TEL in urban atmospheres in different investigations have caused some discussion [6, 9, 11] about whether the method of Laveskog [15] is selective for TML and TEL or not. In the case in which a semi-polar column is used at 100°C, the retention times of TML and TEL are short compared with those of hydrocarbons with similar molecular weights. The difference between the retention time of TML and that of n-pentane is less than 30 s. The chromatogram of a sample of petrol detected at m/z = 237 (Fig. 3) contained five peaks with the same retention times as those peaks observable at m/z = 237 in a mixture of TML, TEL, Me_3PbCl and Et_3PbCl. The two latter catalyze alkyl exchange reactions of tetraalkyllead compounds [20]; therefore, it is concluded that the five peaks in Fig. 3 belong to $Me_nEt_{4-n}Pb$ (n = 0—4). The amount of TML and TEL in the petrol was about 0.4 g Pb l^{-1}, in accordance with the maximum permissible content of lead in petrol in Denmark. Thus, it appears that no compounds in the petrol interfere with the determination of TML and TEL. Furthermore, two experiments with car exhaust samples were performed. The ratio between the mass spectrometric peaks of TML measured at m/z = 253 and 237 was identical with that of a TML standard.

Apparently, the only possible compounds that may interfere with the TML and TEL determinations are certain organometallic compounds and freons. However, none of the organometallic compounds which might interfere are suspected of being present in environmental samples. Freons present in detectable amounts in the atmosphere have all molecular weights lower than 200 [21]. This also implies that the method of Laveskog [15] is selective for TML and TEL.

The detection limits for TML and TEL defined as a signal equal to twice the average noise, are 60 and 10 pg of lead respectively, measured at m/z = 237. Concerning TML separately, a mass spectrometric detection limit of about 3 pg can be obtained by measuring TML at m/z = 253 (cf. Figs. 1 and 6). Blank values for TML measured at m/z = 253 on four conditioned sampling columns did not exceed the detection limit. For a 150-l sample, 20 pg TML m^{-3} can be detected; this is 25 times lower than was attainable with previous methods [11, 14].

The ratio between the peak height of TML measured at m/z = 253 and that of d_{12}-TML measured at m/z = 262 was linearly dependent on the

injected amount of TML, keeping that of d_{12}-TML constant. The same dependence was observed when TML was measured at m/z = 237 and d_{12}-TML at m/z = 242, or TEL at m/z = 237 and d_{20}-TEL at m/z = 242.

The relative standard deviation for the preparation of standard solutions and the determination of the calibration graph was 2%; for the injection of a known amount of internal standards into the sampling columns it was 6%; and for the determination of the sampling volumes, it was 8%. Thus, if no decomposition occurs during the sampling, the coefficient of variation for atmospheric analyses would be about 10%.

Determination of TML and TEL in the atmosphere

A survey of the results is shown in Table 2. Different modifications of the sampling method were used in these investigations. In January/February 1979 the sampling was performed using internal standards (d_{12}-TML and d_{20}-TEL). Known amounts of these were added to the samples in the U-tube with Apiezon M during the re-collection step. The results of TEL were multiplied by 2 in accordance with the laboratory recovery test.

During the summer, high levels of photochemical oxidants are common, especially in suburban and rural areas [22—24]. The tests of the method in January/February, and May/June 1979 were done in connection with an investigation by the Danish Air Pollution Laboratory of the atmospheric pollution of lead in an industrialized suburban area [25]. This implied that the columns were installed in the sampling boxes on the locations 12 h before the sampling started and were removed 12 h after the sampling stopped. It was considered, therefore, that the test in May/June 1979 represents the "worst case circumstances" for field measurements in Denmark. To correct for possible degradation of the TML and TEL collected, known amounts of d_{12}-TML and d_{20}-TEL were added to the sampling columns in advance. Furthermore, two samples were collected in each case on Porapak QS and Porapak N, respectively. The sampling volumes also differed; they were 80—90 l and about 20 l, respectively. In the samples for Sept. 1979, and

TABLE 2

Atmospheric content of TML and TEL at different locations

Location	No. of samples	Date	Sampling time (h)	Adsorbent[a]	TML (ng Pb m^{-3})		TEL (ng Pb m	
					Mean	Range	Mean	Rang
Suburban, 9 sites	26	Jan./Feb. 1979	24	QS	19	2—54	7	<1—36
Petrol station	1	Feb. 1979	10	QS	1100		60	
Suburban, 9 sites	15	May/June 1979	24	QS, N	20	0.9—58	8	<1—36
Copenhagen, busy streets[b]	2	Sept. 1979	2	QS	150	140—150	45	
Stockholm, busy street	6	March 1980	10	QS, N	61	47—77		
Stockholm, quiet street	6	March 1980	10	QS, N	16	11—22		
Rural area	4	April 1980	16—26	N	1.5	0.5—2.5		

[a]QS = Porapak QS; N = Porapak, N. [b]Collected inside a bus (diesel oil).

March and April 1980 (Table 2) internal standards were added to the sampling columns in advance.

Some general conclusions may be drawn from these investigations. There does not seem to be any observable difference between the use of Porapak QS or Porapak N as adsorbent, even though the laboratory recovery experiments may indicate a minor difference. The d_{20}-TEL added to the column may decompose totally during sampling in summer as in winter, while there was no observable decomposition of d_{12}-TML in winter samples. In the test in May/June 1979 the recovery of d_{12}-TML varied considerably. Only in those cases where the recovery of d_{12}-TML was high were the measurements considered to be reliable. Thus, in the test in May/June 1979 in 30% of the 27 samples with Porapak QS as adsorbent and in 37% of the Porapak N samples, were the measurements considered satisfactory. The relative standard deviations between those results obtained with the two adsorbents were on the order of 40%. The meteorological conditions on the sampling sites indicate that episodes with photochemical oxidants were possible. But, unfortunately, no measurements of ozone or other photochemical oxidants were performed in connection with the test in May/June 1979. In Rörvik at Göteborg, Sweden, 200 km north of the investigated area, the 24-h mean values of ozone were between 62 and 106 ppb, and the maximum mean values for 1 h were between 80 and 155 ppb in this period [26].

When the results of the atmospheric content of organolead compounds are compared with those obtained in other investigations in Europe, it should be remembered that in some of these the atmospheric content of TML and TEL was determined [15, 27], in some the total content of tetraalkyllead compounds [13, 19], and in others the total content of organolead compounds passing a filter [8, 10, 12]. Furthermore, there are great variations in the relative compositions of tetraalkyllead compounds in petrol samples from different manufacturers [28]. In Denmark the average ratio of TML to TEL in petrol is 1.9 [29].

The order of the observed levels of TML (Table 2: petrol station > busy streets in urban area > quiet street in urban area ≈ suburban area > rural area) is in accordance with the observations of others. Furthermore, the levels of TML and TEL are at the same magnitude as those reported by others [6, 8–10, 12, 13, 15, 19, 27].

The mean ratio of TML to TEL in the samples January/February 1979 was 2.7 (Table 2). This implies that losses of TEL during sampling had not been of general importance in these measurements, as the ratio would be expected to be slightly higher than 1.9 [6]. Although none of the determinations of TEL in May/June 1979 is considered to be very accurate, as the recovery of d_{20}-TEL in all cases appeared to be low, the observed mean ratio of 2.5 of TML to TEL is reasonable.

In Stockholm the ratio of 3.8 between TML in a busy street and in a street without traffic (Table 2) agrees with the 4–5 times lower levels of particulate lead found at locations remote from streets in Copenhagen com-

pared with that found in busy streets, as the dominant part of the particulate lead comes from car exhausts [30].

There are differing opinions as to whether the relative content of tetraalkyllead compounds to the total content of lead is lower or higher than 5% in urban air [6, 9, 31]. In some cases in the industrialized suburban area (Table 3) the relative content of TML and TEL was lower than 4%. However, in those cases the relative levels of particulate antimony and tin were higher than normal. The locations of the sampling sites and a lead smelter in relation to the wind direction confirmed that some of the particulate lead came from the lead smelter [25]. In those cases where the contribution from this point source was small or negligible, the mean relative content of TML and TEL in the winter samples was 6.6 ± 0.5% (n = 18) and in the summer samples 7 ± 1% (n = 8). In agreement with those values, Laveskog [15] found a relative content of TML and TEL of 6—10% in most of his measurements, and Rohbock et al. [13] reported that 4—10% of the total lead in city air consists of tetraalkyllead compounds. In contrast, the measurements of the relative content of tetraalkyllead of Harrison et al. [19] ranged from 0.9 to 3.3%. It should be added that TML and TEL seem to constitute the main part of the content of tetraalkyllead compounds in petrol [28]. It is, therefore, reasonable to assume that tetraalkyllead compounds make up 5—10% of the total lead content in the air of European cities. As discussed pre-

TABLE 3

Relative atmospheric content of TML and TEL on different sites in a suburban area in winter and summer

TML (ng Pb m^{-3})	TEL (ng Pb m^{-3})	Particulate Pb[a] (ng Pb m^{-3})	% Sb rel. to particulate Pb[a]	% Sn rel. to particulate Pb[a]	% (TML + TEL) of total Pb
Winter					
30	11	420	0.6	1.2	9
15	6	290	<0.4	1.0	7
4.3	1	78	<1.3	1.8	6
54	11	1900[b]	7.9	3.0	3
14	2	1300[b]	17	8.3	1
14	<1	3100[b]	41	24	0.4
Summer					
58	—	480	1.3	3.5	11
40	20	720	1.1	1.3	8
14	5	320	<0.3	2.3	6
10	<4	480[b]	6.5	10	<3
24	<3	1400[b]	4.6	13	2

[a]From [25], airborne particulate matter was collected on Nucleopore (N 1200) and cellulose acetate (Selectron ST 69) filters in series, and analyzed by proton-induced X-ray emission [32]. [b]Contribution from a lead smelter [25].

viously [6] the proportion of tetraalkyllead in urban air in the U.S.A. and Canada is probably lower, on the order of 2—5% [11, 14].

Recent investigations have shown that the dominant amount of several organic compounds with boiling points up to 400°C, e.g. anthracene and fluoranthene, are in the vapour phase in cooled diluted exhaust gases and in urban atmospheres [33—35]. As trimethyllead chloride sublimes at 190°C [36], it cannot be excluded that if trialkyllead compounds are present in the atmosphere, the dominant proportion will be in the vapour phase. This assumption is supported by the presence of most methylmercury compounds in the gas phase in the atmosphere [37, 38]. As trialkyllead compounds are probably more chemically stable than tetraalkyllead compounds [6], their existence in the atmosphere is plausible.

As this problem is unsolved, it is difficult to assess results obtained with techniques measuring organolead compounds in relation to those obtained with those measuring tetraalkyllead compounds. Using similar methods, one group found a relative content of vapour-phase organolead compounds in urban air of 11—21% [10] and another 3—13% [12].

It was not possible in this investigation to make measurements of TML in areas where levels of the order of 0.02—0.2 ng Pb m^{-3} could be expected. Four measurements (Table 2) were made of atmospheric TML in a rural area under circumstances where the pollution with TML from the use of leaded petrol was as low as possible. Two of those samples had to be collected under strong gale conditions; the sampling site was situated more than 10 km downwind from the nearest road, and more than 25 km from the nearest town (about 20000 inhabitants), and more than 100 km from larger cities (>100,000 inhabitants). The levels of TML were 0.5 and 0.7 ng Pb m^{-3}. It seems reasonable to assume that levels of TML below these values are very uncommon on Zealand. During part of the sampling time the air masses in the two other samples had passed over areas with a higher population density as well as a road with moderate traffic situated 0.5 km from the sampling site. Thus the levels of TML were higher, 2.2 and 2.5 ng Pb m^{-3}, respectively. In all four samples the recoveries of d_{12}-TML were high. A few measurements of ozone indicated that the levels of ozone had not exceeded 50 ppb during the sampling periods [39]. Therefore, the method is considered to be very well suited to investigations of atmospheric TML in rural and remote areas under circumstances in which the levels of photochemical oxidants are low.

Conclusions

The method presented is useful for the determination of TML in air in areas with concentrations down to 20 pg m^{-3}. The method is the only one available for determining TML in air in remote areas in order to explore the possible biological formation of TML and its distribution from man-made sources in the environment. It is suitable for field measurements as TML is collected at ambient temperatures, and also because it is possible to correct for any decomposition of TML taking place during sampling, and the collected samples can easily be transported over long distances.

It would be desirable to diminish the decomposition problems, especially of TEL, during sampling in the summer. As a sensitive method for determining TML and TEL in water samples is needed [7, 40], this will be tested in the near future, if a simple modification of the present method is capable of solving this problem.

The two-step enrichment method described here may be useful for investigating other volatile organometallic compounds, e.g. tetramethyltin [41], in the atmosphere.

This work was supported by the National Agency of Environmental Protection, Denmark. Finn Palmgren Jensen and Knud Hansen of the Danish Air Pollution Laboratory are acknowledged for making the sampling boxes, assisting with the collection of samples, and for stimulating discussions. We also thank Anders Jonsson and Sven Berg, Stockholm University, for collecting the samples in Stockholm, and Bente Christensen, Tomas Fernquist, Jytte Funch, Ole Jørgensen and Tove Thomsen for skilful technical assistance.

REFERENCES

1 D. M. Settle and C. C. Patterson, Science, 207 (1980) 1167.
2 S. Jensen and A. Jernelöv, Nature, 223 (1969) 753.
3 A. Johnels, G. Tyler and T. Westermark, Ambio, 8 (1979) 160.
4 P. T. S. Wong, Y. K. Chau and P. L. Luxon, Nature, 253 (1975) 263.
5 U. Schmidt and F. Huber, Nature, 259 (1976) 159.
6 P. Grandjean and T. Nielsen, Residue Rev., 72 (1979) 97.
7 Y. K. Chau, P. T. S. Wong, O. Kramar, G. A. Bengert, R. B. Cruz, J. O. Kinrade, J. Lye and J. C. van Loon, Bull. Environ. Contam. Toxicol., 24 (1980) 265.
8 R. M. Harrison and D. P. H. Laxen, Nature, 275 (1978) 738.
9 R. M. Harrison and R. Perry, Atmos. Environ., 11 (1977) 847.
10 W. de Jonghe and F. Adams, Anal. Chim. Acta, 108 (1979) 21.
11 B. Radziuk, Y. Thomassen, L. R. P. Butler, J. C. van Loon and Y. K. Chau, Anal. Chim. Acta, 105 (1979) 255.
12 J. Birch, R. M. Harrison and D. P. H. Laxen, Sci. Total Environ., 14 (1980) 31.
13 E. Rohbock, H.-W. Georgii and J. Müller, Atmos. Environ., 14 (1980) 89.
14 D. C. Reamer, W. H. Zohler and T. C. O'Haver, Anal. Chem., 50 (1978) 1449.
15 A. Laveskog, Organolead Compounds in Auto Exhaust and Street Air, Alkyllead Compounds, Tetramethyllead and Tetraethyllead, TPM-BIL-64 (1971), revised May 1972.
16 Houben-Weyl, Methoden der Organischen Chemie, Vol. 13/2a, G. Thieme, Stuttgart, 1973, p. 54.
17 Houben-Weyl, Methoden der Organischen Chemie, Vol. 13/7, G. Thieme, Stuttgart, 1975, p. 20.
18 R. M. Harrison and D. P. H. Laxen, Environ. Sci. Technol., 12 (1978) 1384.
19 R. M. Harrison, R. Perry and D. P. H. Slater, Atmos. Environ., 8 (1974) 1187.
20 G. Calingaert, H. A. Beatty and L. Hess, J. Am. Chem. Soc., 61 (1939) 3300.
21 Stratospheric Ozone Depletion by Halocarbons: Chemistry and Transport, N.A.S.–N.C.R. Publ., 1979.
22 P. Grennfelt, Ozone Episodes on the Swedish West Coast, IVL B 337, 1976.
23 H. Ro-Poulsen, B. Andersen, L. Mortensen and L. Moseholm, Oikos, in press.
24 T. Nielsen, O. J. Nielsen, E. L. Thomsen, A. M. Hansen and B. Zachau, in preparation.
25 F. Palmgren Jensen, MST LUFT A 22 (1979), Danish Air Pollution Laboratory (in Danish).

26 P. Grennfelt, private communication, 1980.
27 B. Allvin and S. Berg, SNV PM 907, Swedish Environmental Protection Agency, Stockholm, 1977 (in Swedish).
28 W. de Jonghe, D. Chakraborti and F. Adams, Anal. Chim. Acta, 115 (1980) 89.
29 P. Grandjean and T. Nielsen, SNV PM 879 (1977), Swedish Environmental Protection Agency, Stockholm (in Danish).
30 H. Flyger, F. Palmgren Jensen and K. Kemp, Risø Report No. 338, 1976.
31 R. M. Harrison and D. P. H. Laxen, Chem. Brit., 16 (1980) 316.
32 F. Palmgren Jensen and K. Kemp, MST LUFT A 14, Danish Air Pollution Laboratory, 1979 (in Danish).
33 W. Cautreels and K. van Cauwenberghe, Atmos. Environ., 12 (1978) 1133.
34 T. Alsberg and U. Stenberg, Chemosphere, 7 (1979) 487.
35 P. S. Pedersen, J. Ingwersen, T. Nielsen and E. Larsen, Environ. Sci. Technol, 14 (1980) 71.
36 Houben-Weyl, Methoden der Organischen Chemie, Vol. 13/7, G. Thieme, Stuttgart, 1975, p. 87.
37 D. L. Johnson and R. S. Braman, Environ. Sci. Technol., 12 (1974) 1003.
38 B. A. Soldano, P. Bien and P. Kwan, Atmos. Environ., 9 (1975) 941.
39 E. Lund Thomsen, private communication, 1980.
40 H. Potter, A. W. P. Jarvie and R. N. Markall, Water Pollut. Control, (1977) 123.
41 R. S. Braman and M. A. Tomkins, Anal. Chem., 51 (1979) 12.

Analytica Chimica Acta, 124 (1981) 15—22

MONITOR FOR MEASURING THE TOTAL CONCENTRATION OF REACTIVE HYDROCARBONS IN AMBIENT AIR BASED ON THEIR CHEMILUMINESCENCE REACTION WITH OXYGEN ATOMS

P. M. HOUPT* and F. LANGEWEG

Division of Technology for Society TNO, P.O. Box 217, 2600 AE Delft (The Netherlands)

(Received 23rd September 1980)

SUMMARY

The monitor functions by measuring the intensity of the chemiluminescence radiation at 309 nm which is emitted during the reaction of hydrocarbons with $O(^3p)$ atoms. The system comprises a specially-developed stable source of atomic oxygen, a detection unit for measuring the intensity of the chemiluminescence radiation and a device for pre-concentration of the hydrocarbons to be determined. The sensitivity of the monitor depends on the concentration and reactivity of the hydrocarbons, and is greatest for unsaturated compounds. For butadiene, the detection limit is 3 ppb, and response is linear over the range 0—2500 ppb. The monitor can also serve as a detector for unsaturated hydrocarbons in gas chromatography.

The potential of the atmosphere to form smog is determined by the concentration and reactivity of the hydrocarbons present. In the atmosphere the hydrocarbons are subject to conversion to other compounds, particularly by reaction with OH radicals, which are formed as the result of photo-dissociation and in other radical reactions of impurities present in the atmosphere [1—3]. The proper analytical method to determine the smog-forming potential is therefore to measure the rate at which the concentration of OH radicals decreases as a result of their reaction with hydrocarbons. The laser magnetic resonance method described by Howard [4] is sufficiently sensitive for measuring the concentration of OH radicals. However, this principle cannot readily be embodied in an analytical instrument for practical reasons.

As Fig. 1 shows, there is an almost linear relationship between the rate constants given in the literature for the reactions of different hydrocarbons with OH radicals and with atomic oxygen in the ground state (^3p) [5, 6]. In the reaction with $O(^3p)$ atoms, hydroxyl radicals in an electronically excited state ($OH^2\Sigma$) are formed [7, 8], and measurable radiation is emitted on relaxation to the ground state. This chemiluminescence reaction makes it possible to construct a measuring instrument for determining the smog-forming potential of hydrocarbons. In 1975, Fontijn and Ellison [8] described a Reactive Hydrocarbon Analyzer based on this chemiluminescence reaction. It was developed for measuring hydrocarbons in car exhaust gases, but was

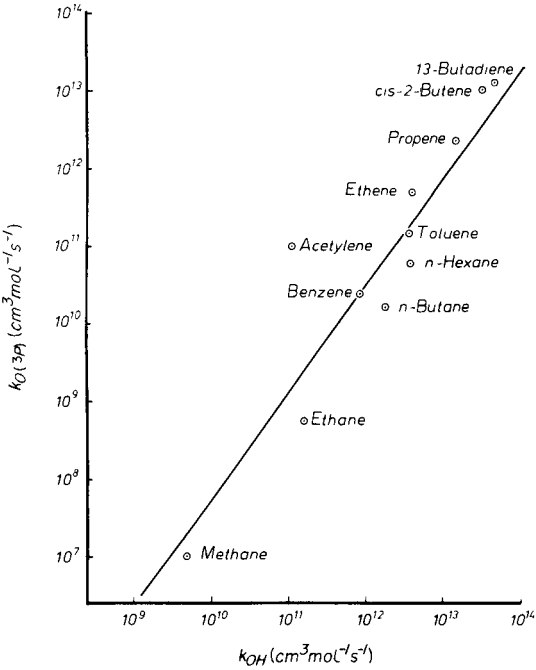

Fig. 1. Relationship between the constants of reactions of hydrocarbons with hydroxyl radicals (k_{OH}) and oxygen atoms in the ground-state ($k_{O(^3P)}$).

found to be unsuitable for measuring the relatively low concentrations of hydrocarbons in the atmosphere. The monitor described here is also based on the chemiluminescence reaction between reactive hydrocarbons and O(^{3}p) atoms, but with the proposed instrument the reactivity and concentration of hydrocarbons can be measured at the lower levels occurring in contaminated air.

DESCRIPTION OF THE MONITOR

Atomic oxygen source

An important factor for the proper functioning of the monitor is the long-term stability of the oxygen atom source. Recombination effects taking place at the glass walls [9] give a loss of oxygen atoms [10], and much research has been done to obviate this. A film of phosphoric acid on the reactor wall reduces this process considerably [11]. However, in the long term, the structure and composition of the coating change to such an extent that this results in an appreciable reduction in the yield of atomic oxygen. The source used by Fontijn and Ellison therefore is not sufficiently stable and the O(^{3}p) yield is low. The addition of 0.05—0.1% of hydrogen to the discharge gas considerably improves the stability [12]. This makes a phosphoric acid coating superfluous and provides an oxygen atom source that is stable for several months.

Detection unit

The most important part of the monitor is shown in Fig. 2A. In the tube (1), to which the discharge gas (89.9% Ar—10% O_2—0.1% H_2) is admitted by way of a pressure-drop capillary, a gas discharge is generated at low pressure by a 2450-MHz microwave cavity (2), (type EMS 214L [13]). The oxygen atoms formed in this tube are transported, at 1.5 Torr (0.2 kPa) and a velocity of 10 m s^{-1}, to the reaction chamber (8), where they react with the hydrocarbons that are supplied through another tube (9). The chemiluminescence radiation emitted passes through a quartz window (4), a diaphragm (5) and a narrow-range interference filter (6), which has maximum transmission at 309.2 nm. Finally the radiation is detected with a Hamamatsu R 106 photomultiplier (7). To reduce the amount of radiation originating from the gas discharge leaking away to the reaction space, light traps (3, Woodshorns) are incorporated in the system. The whole system, except for the discharge tube, is placed in a light-tight casing (10).

Preconcentration unit

Because the low hydrocarbon concentrations in the ambient air cannot be measured directly with the detector, a preconcentration system based on the adsorption-desorption principle is used (Fig. 2B). It consists of a stainless-steel U-tube filled with Ambersorb XE 347 (Rohm and Haas Co., Antwerp; not yet commercially available) and with Tenax [14, 15]. Ambersorb combines with the lower hydrocarbons, the higher hydrocarbons being absorbed by Tenax. To prevent bleeding, the Ambersorb is purified by Soxhlet extraction with methanol.

The fully programmed adsorption/desorption cycle proceeds as follows. Adsorption takes place for 12 min, after which time the electrically operated micro-volume valve (Carle 2013) turns and the gas current through the system is reversed. An electric current (5V, 50 A) is passed for 3 s through the wall of the U-tube. This causes the temperature in the tube to rise to 187°C, as a result of which the hydrocarbons desorb and are drawn in by the detector. The tube is then air-cooled by forced circulation for 7 min. The whole cycle takes 20 min, and thus information is supplied on the reactive hydrocarbon concentration three times in each hour.

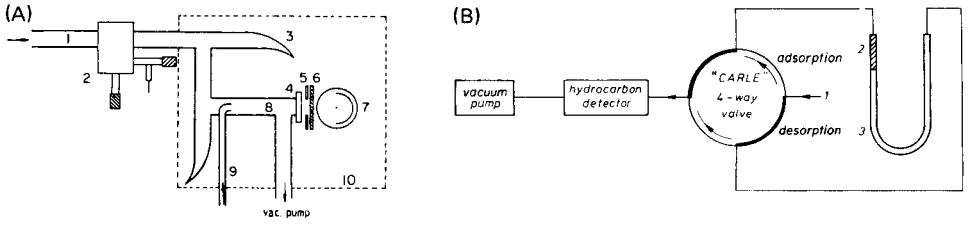

Fig. 2. Schematic diagrams of the instrument. (A) Detection unit in the reactive hydrocarbons monitor; (B) adsorption/desorption preconcentration system coupled to the detector. For details, see text. In (B), drawn in the desorption phase (the valve already turned), the U-tube is filled with Ambersorb (3) and Tenax (2), and sample is fed in by tube (1). In the adsorption phase, the hydrocarbon mixture passes first the Tenax (2) and then the Ambersorb (3).

RESULTS AND DISCUSSION

The chemiluminescence reaction

The smog-forming potential of hydrocarbons depends not only on their concentration but also on their reactivity. This means that at a given concentration of different hydrocarbons the intensity of the emitted radiation (measured at 309.2 nm) is a function of the reactivity for $O(^3p)$ atoms. The results, which are illustrated in Fig. 3, show that there is a relationship between these two quantities. Not all the points are on the dotted line, however, which is largely to be attributed to differences in reaction mechanisms (particularly reaction 1) of saturated, unsaturated and aromatic hydrocarbons with $O(^3p)$ atoms.

For saturated hydrocarbons, OH radicals are formed in the primary reaction (reaction 1) [16, 17]

$$C_nH_{2n+2} + O(^3p) \rightarrow \cdot[C_nH_{2n+1}] + OH \qquad (1)$$

This reaction is exothermic, but the remaining energy is not sufficient to supply the 4.4 eV which is required for excitation to the $^2\Sigma$-state. Besides OH radicals, other products are formed, depending on the nature of the reacting hydrocarbon [18].

Aromatics hardly form OH radicals as primary reaction products [19]. A possible explanation for the emission of hydrocarbons, including aromatics, is the occurrence of rapid follow-up reactions which do produce a vibrationally excited OH radical, e.g.,

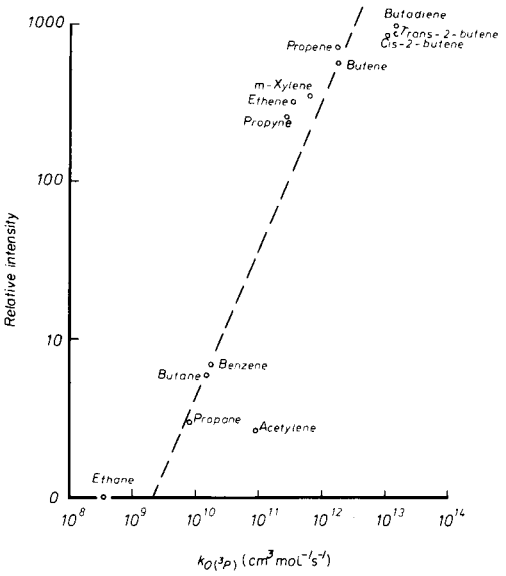

Fig. 3. Relationship between reaction rate and measured relative intensity of the emitted OH spectrum for reactions of equal concentrations of hydrocarbon with $O(^3p)$.

$$\cdot[C_nH_{2n+1}] + O_2 \rightarrow \cdot[C_nH_{2n}O] + OH^*(^2\Sigma) \quad (2)$$

This reaction is exothermic, supplying ±6 eV (579 kJ mol^{-1}), which generates sufficient energy for the electronic excitation of the OH radical to the $^2\Sigma$-state [20]. In this reaction a strong C—O bond is formed and a weak C—H bond is disrupted, so that the hydrogen atom receives an excess of energy, which again is reflected in a rapid rotation of the hydrogen atom around the oxygen atom. A rotation temperature of 960 K was measured here for the reaction of butadiene with $O(^3p)$; the same reaction with ethene supplied a temperature of about 800 K.

A strong indication that the mechanism of reaction (1) in particular can depend on the type of hydrocarbon is obtained when the ionization potentials of the hydrocarbons are plotted against the logarithms of the rate constants (Fig. 4). If it is assumed that $k = A \exp(-E/RT)$, then a linear relationship exists between E and $\log k$. This means, when reference is made

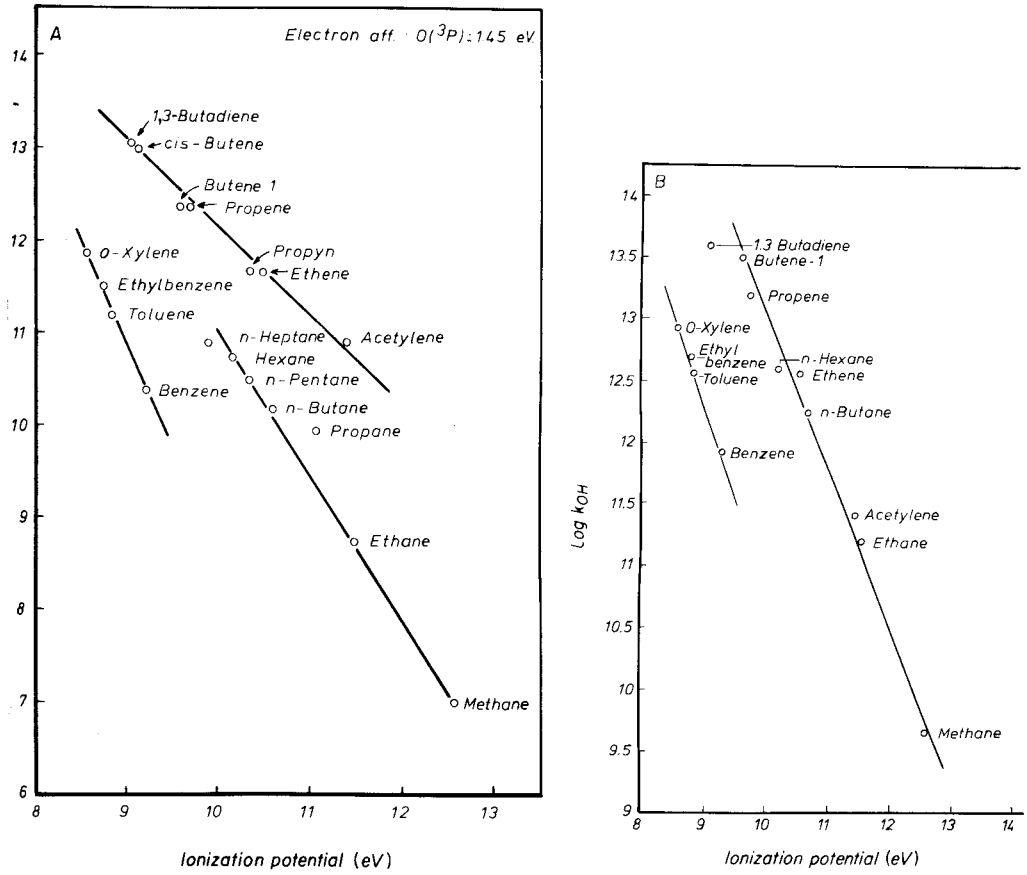

Fig. 4. Relationships between the ionization potentials of hydrocarbons and (A) log $k_{O(^3p)}$ (electron affinity for $O(^3p)$, 1.45 eV); (B) log k_{OH} (electron affinity for OH, 1.83 eV), both at 298 K.

to Fig. 4A, that the activation energy is proportional to the ionization potential of the hydrocarbons. Figure 4A clearly shows that the reaction with $O(^3p)$ divides the hydrocarbons into three different groups, while as far as the reaction with OH radicals is concerned (Fig. 4B), two groups can be distinguished. This shows that the reaction with $O(^3p)$ provides a much more selective characteristic by which the hydrocarbons can be distinguished than the reaction with OH radicals, which is most probably caused by the difference in electron affinity of $O(^3p)$ and $OH^{\cdot}$ (1.45 eV and 1.83 eV, respectively). This makes it understandable that the methods for measuring hydrocarbons based on the chemiluminescence reaction with ozone at elevated temperature [21] are less selective. In the reaction with ozone the active species are $O(^1d)$ atoms that arise from the thermal decomposition of ozone. The electron affinity of $O(^1d)$, 3.5 eV, considerably exceeds that of $O(^3p)$, and is therefore hardly selective in the reaction with hydrocarbons.

Analytical applications of the monitor

With the aid of an automatic gas diluting device, TELAB, the intensity of the chemiluminescence radiation was measured for a number of hydrocarbons in the range 0—2500 ppb (v/v). The relationship between intensity and concentration over the entire range of concentrations was linear. The detection limit was 3 ppb for butadiene and 5 ppb for butene. Additivity was checked by measuring two components separately a number of times, and comparing the sum of the signals with the response obtained with a mixture of the two components. In this way measurements were made for mixtures of 1,3-butadiene and butene-1, and of butene-1 and ethylene. The spread in results for the separate components on the one hand and for the mixture on the other, was less than 5% in all cases. Displacement on the column by gases adsorbed in succession is not to be expected, because the responses of 500 ppm of two components administered successively were not significantly different from the signals obtained after adsorption in the reverse order.

The monitor as a detector for gas chromatography

The possibility of using the monitor as a detector for a gas chromatograph was investigated. The reaction space (Fig. 2A) was coupled, by way of a restriction capillary, to the outlet of a gas chromatograph. The hydrocarbon fractions coming from a wetted aluminium oxide column were passed, by means of a splitter, to a flame ionization detector and to the hydrocarbon monitor. A mixture of 14 hydrocarbons was injected, containing 9 ng of each of the constituents. At the selected split ratio, 5 ng was passed to the ionization detector and 4 ng to the hydrocarbon monitor. The chromatograms thus obtained are shown in Fig. 5. It is clear that only the unsaturated (reactive) hydrocarbons are measured by the chemiluminescence monitor, whereas the ionization detector is unselective.

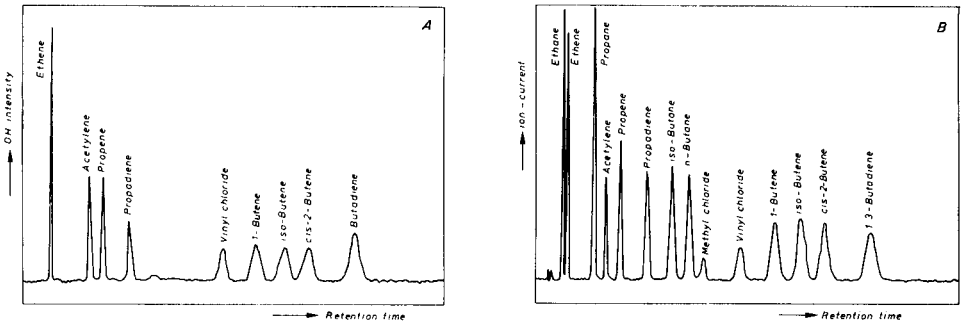

Fig. 5. Gas chromatograms of a mixture of 14 hydrocarbons using (A) the chemiluminescence detector (4 ng sample); (B) a flame ionization detector (5 ng sample).

Conclusions

The use of the specially-developed stable atomic oxygen source and an adsorption/desorption preconcentration system has made it possible to build a monitor which is sufficiently sensitive to detect reactive hydrocarbons in the atmosphere. Compared with the reactivity of hydrocarbons with hydroxyl radicals, the reaction with atomic oxygen, $O(^3p)$, is slightly too selective, but it is a good approximation to the reactions that occur in the atmosphere. The chemiluminescence intensity at 309.2 nm is a direct measure of both the concentration and the reactivity of the hydrocarbons measured. The instrument can be used not only to monitor the smog-forming potential of the atmosphere, but also for analytical measurements and for the detection of unsaturated hydrocarbons in gas chromatography.

This work has been supported by financial aid from the Dutch Ministry for Public Health and Environmental Hygiene.

REFERENCES

1 A. H. Falls and J. H. Seinfeld, Environ. Sci. Technol., 12 (1978) 1398.
2 H. Niki, E. E. Daby and B. Weinstock, Adv. Chem. Ser., 113 (1972) 16.
3 P. A. Leighton, Photochemistry of Air Pollution, Academic Press, New York, 1961.
4 C. J. Howard, J. Chem. Phys., 61 (1974) 1943.
5 K. Darnall, A. C. Lloyd, A. M. Winer and J. N. Pitts, Environ. Sci. Technol., 10 (1976) 692.
6 J. T. Herron and R. E. Huie, J. Phys. Chem. Ref. Data, 2 (1973) 467.
7 B. Krieger, M. Malki and R. Kummler, Environ. Sci. Technol., 6 (1972) 742.
8 A. Fontijn and R. Ellison, Environ. Sci. Technol., 9 (1975) 1157.
9 J. C. Greaves and J. W. Linnitt, Trans. Faraday Soc., 55 (1959) 1346.
10 A. M. Mearns and A. J. Morris, Nature, 225 (1970) 59.
11 F. K. McTaggert, Plasma Chemistry in Electrical Discharges, Elsevier, New York, 1967.
12 P. M. Houpt and G. H. W. Baalhuis, Appl. Spectrosc., 34 (1980) 89.
13 F. C. Fehsenfeld, K. M. Evenson and H. P. Broida, Rev. Sci. Instrum., 36 (1965) 294.
14 K. Sakodynskii, L. Panina and N. Klinskaya, Chromatographia, 7 (1974) 339.
15 R. H. Brown and C. J. Purnell, J. Chromatogr., 178 (1979) 79.
16 I. T. N. Jones and K. D. Bayes, J. Am. Chem. Soc., 94 (1972) 6869.

17 J. T. Herron and R. E. Huie, J. Phys. Chem., 73 (1969) 3327.
18 R. E. Huie and J. T. Herson, Prog. React. Kinet., 8 (1975) 1.
19 R. A. Bonanno, P. Kim, J. H. Lee and R. B. Timmoirs, J. Chem. Phys., 57 (1972) 1377.
20 A. G. Gaydon, The Spectroscopy of Flames, Chapman and Hall, London, 1974.
21 S. van Heusden and L. P. J. Hoogeveen, Fresenius Z. Anal. Chem., 282 (1976) 307.

Analytica Chimica Acta, 124 (1981) 23—30

DETERMINATION OF HUMIC ACID BY CHEMILUMINESCENCE

D. F. MARINO and J. D. INGLE, JR.*

Department of Chemistry, Oregon State University, Corvallis, OR 97331 (U.S.A.)

(Received 21st July 1980)

SUMMARY

The analytical utility of the chemiluminescence resulting from the reaction of humic acid with permanganate is investigated. The chemiluminescence response curve rises sharply to a peak value at about 0.5 s after mixing and decays somewhat more slowly. The peak signal for a fixed humic acid concentration is shown to pass through a maximum near a permanganate concentration of 17 μmol l^{-1} and to increase continuously with potassium hydroxide concentration up to 2.0 mol l^{-1}. Calibration plots of peak signal vs. humic acid concentration exhibit complex behaviour, being approximately linear up to about 20 mg l^{-1}, curving slightly toward the concentration axis up to about 40 mg l^{-1}, and then curving away from the concentration axis above 40 mg l^{-1}. The detection limit for humic acid is about 0.7 mg l^{-1}. No interference is observed for thirteen common inorganic species at typical levels in water samples. Substantial differences are observed for humic acid in selected samples determined by the chemiluminescence and visible absorption procedures.

The determination of humic acid has been investigated to a very minor extent [1, 2], in spite of the potential importance of this species as a vehicle for the mobilization, transportation, and immobilization of organic compounds and metals (some of which may be toxic pollutants), and as a proven natural complexation agent of toxic heavy metals [1, 3, 4]. This is due in part to the uncertain nature of this species and its inherently "operational definition" as the hydrophobic acid fraction of humus precipitating at pH 2.0 after extraction at pH 13—14 [1, 3, 4]. Two common analytical methods for humic acid are based on absorption at 430 nm [1] and fluorescence with excitation and emission wavelengths of 270 and 460 nm, respectively [2]. Both methods have detection limits of 0.25 mg l^{-1} with linear range to 50 mg l^{-1}. The accuracy of these methods is questionable when humic acid is determined by using "standard" humic acid from a different source than that of the unknown, because, molar absorptivities of humic acids from different sources differ by up to 273% [4]. Hence, a method for the determination of humic acid in natural waters that is relatively insensitive to differences in the make-up of humic acids from different sources would find broad application.

Because previous work by Slawinska and Slawinska had shown that humic acid could be made to chemiluminesce [5], and because work in this

laboratory had indicated the feasibility for the quantitative chemiluminescence determination of some polyphenols structurally similar to humic acid [6, 7], work was undertaken to develop a chemiluminescence system for the determination of humic acid in the hope that such a method would be less sensitive to the structural differences of humic acids from different sources than the current spectral methods were. After a method based on chemiluminescence resulting from the reaction of humic acid with permanganate had been developed, the responses of several organic model compounds were evaluated in an effort to relate relative chemiluminescence response to structural features in order to determine which functionalities on the humic acid molecule were responsible for the chemiluminescence, and to what extent. Finally, the humic acid—permanganate chemiluminescence system was evaluated in terms of response to humic acids from three different sources and to humic acid in a river water sample, and these results were compared with results obtained by molecular absorption.

EXPERIMENTAL

All chemiluminescence measurements were obtained with a discrete sampling chemiluminescence photometer system reported earlier [8] and with the modifications and similar experimental conditions previously described [9, 10]. The noise filter cut-off frequency was adjusted to 1.0 Hz to avoid attenuation of the fast chemiluminescence peaks from humic acids. All solutions were prepared with deionized water from a Millipore Milli-Q system fed by distilled water. Humic acid (Aldrich, technical grade H1-6752) was used without further purification. Dissolution of humic acid samples was accomplished with a minimum of 3 M KOH. There was no subsequent pH adjustment for chemiluminescence work, while adjustment to pH 10 was used for all molecular absorption studies. All other solutions were prepared from reagent-grade materials.

The chemiluminescence procedure consisted of addition with Eppendorf pipets of 1.0-ml portions of sample or blank and of KOH solution to the reaction cell followed by injection of 0.5 ml of permanganate solution or other oxidant with a mechanized dispensing syringe to initiate the reaction. A typical peak shape is shown in Fig. 1. Because there is no blank reaction in this method, the chemiluminescence signal is taken as the difference between the chemiluminescence peak height and the dark current level. After the chemiluminescence reaction was complete, the cell was evacuated and rinsed once with methanol and three times with deionized water.

Absorption work was conducted on a Cary model 118 spectrophotometer at a wavelength of 430 nm. All standards, samples, and blanks were adjusted to pH 10.0 with 0.5 M KOH solution prior to measurement.

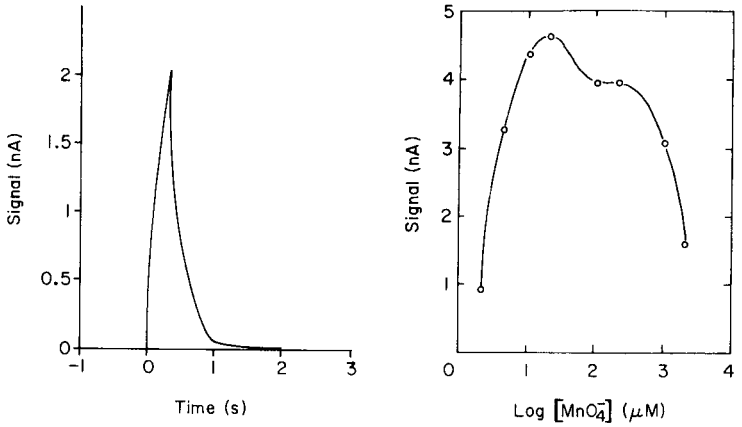

Fig. 1. Typical humic acid chemiluminescence response curve. C_{HA} = 10 mg/l; C_{KOH} = 2.0 M; $C_{MnO_4^-}$ = 17 μM.

Fig. 2. Influence of permanganate on chemiluminescence signal for humic acid. C_{KOH} = 1.5 M; C_{HA} = 100 mg/l.

RESULTS AND DISCUSSION

Choice of reagent

The choice of oxidant for this work was investigated by observing the action of several species on humic acid samples in 2 M KOH. Although Slawinska and Slawinska [5] used hydrogen peroxide, it was found that the chemiluminescence signal obtained with hydrogen peroxide was unacceptably small. Attempts at enhancement of this signal with common chemiluminescence activators (Co(II), Cu(II), etc.) show no improvement. Hexacyanoferrate(III) provided a more intense signal than peroxide but was accompanied by an equally blank reaction yielding a net chemiluminescence signal for humic acid of about the same magnitude as that obtained with peroxide. Permanganate provided a large chemiluminscence signal (ca. 20× greater than that with hydrogen peroxide) with no blank reaction and was chosen as the oxidant for this work. Addition of permanganate with the humic acid sample showed some small reaction prior to base addition; therefore, humic acid and 2 M KOH were added to the cell together followed by injection of permanganate to initiate the reaction.

Unless otherwise noted, all reagent concentrations are reported as final cell concentrations and all chemiluminescence signals are reported as photoanodic currents. Figure 2 illustrates the results of a study of the effects of permanganate concentration. Although a rather complex curve results, a clear maximum in the chemiluminescence signal intensity is observed at about 17 μM. The signal decreases at higher concentrations presumably resulting from absorption of the chemiluminescence by the permanganate.

The drop off at lower permanganate concentrations undoubtedly results from decreased reaction efficiency due to depletion of the reagent. Hence, the 17 μM level of permanganate was chosen as the cell concentration.

The results of the study of the effect of hydroxide concentration at a fixed permanganate concentration are shown in Fig. 3. In this case, no clear peak or plateau is evident, and the chemiluminescence signal continues to increase with the hydroxide concentration. Because 2 M KOH provided the greatest signal, this level was chosen for all further work.

Figure 4 presents a calibration curve for humic acid obtained under these conditions. The decreased sensitivity that occurs in the 30—80 mg l^{-1} region may be due to competing reactions of different functional groups on the humic acid molecule. The calibration curve exhibits moderate non-linearity from a detection limit of 0.7 mg l^{-1} up to 20 mg l^{-1}, but the determination of unknown humic acid concentrations is possible with fairly close standard bracketing. Although not shown on this figure, humic acid concentrations at the 200 and 500 mg l^{-1} level indicate a negative deviation in the signal at high humic acid concentrations, an effect directly analogous to the behavior exhibited by most of the phenolic model compounds to be discussed. Because humic acid absorbs over the visible region from <200 nm to ca. 600 nm, it is presumed that this is a self-absorption effect.

Interference studies

In this study, as in previous work [10] the detection limit (c_l) and interference level (c_l^*) are defined as the concentration of interfering species that produce a chemiluminescence signal equal to twice the standard deviation in the blank signal current (dark signal in this case) and the concentration of

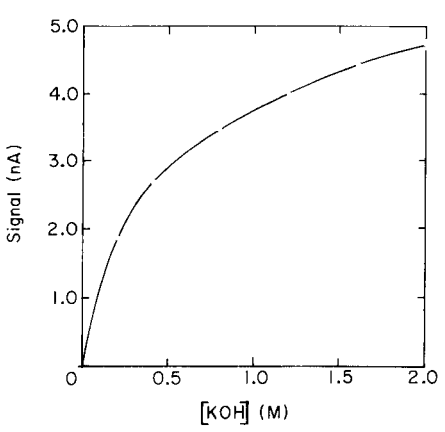

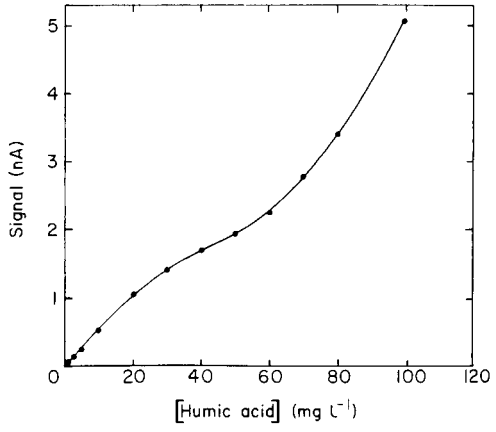

Fig. 3. Influence of potassium hydroxide on chemiluminescence signal for humic acid. C_{MnO_4} = 17 μM; C_{HA} = 100 mg/l.

Fig. 4. Calibration curve for humic acid. C_{KOH} = 2.0 M; C_{MnO_4} = 17 μM.

interfering species required to produce a change in the humic acid signal at the humic acid detection limit equal to twice the standard deviation of the blank signal, respectively. The calibration sensitivity (m) is the slope of the calibration curve for the interfering species while the calibration sensitivity (M) for the interfering species is the slope of the enhancement or depression curve, $\Delta I_{CL}/[INT]$, in the presence of a fixed amount of humic acid (5.0 mg l^{-1} in this case).

The detection limits and interference levels of several cationic and anionic species commonly found in natural waters are presented in Table 1. None of the species tested is normally present in sufficient concentration in surface waters to be above their interference or detection limits, and hence, should not interfere in determination of humic acid.

Model compound studies

A study of the chemiluminescence response of several organic model compounds similar to some of the proposed functional groupings of humic acid [1] was conducted in order to gain insight into those functionalities of the humic acid molecule that were responsible for chemiluminescence, and to what extent. Table 2 presents the results of this investigation. Several trends, particularly among the polyphenols, are evident. First, a dramatic lowering of the detection limit (increased chemiluminescence quantum and reaction efficiency) is achieved in progressing from simple phenol to catechol. Secondly, *meta* substitution of the hydroxyl groups (resorcinol) appears to provide a factor of 2 greater reactivity than *ortho* or *para* substitution. Strangely, the trisubstituted phenols (pyrogallol, phloroglucinol) appear slightly less reactive, even on a mole basis. Addition of an acid functionality (an electron-withdrawing, *meta*-directing group) appears to enhance reactivity (salicylic acid vs. phenol), while the acid functionality itself appears unreactive (benzoic acid). Increased size and rigidity also appear to enhance luminescence (tyrosine vs. phenol), while secondary amines by themselves

TABLE 1

Potential interferences for humic acid determined by chemiluminescence

Species	c_l (mg l^{-1})	c_l^* (mg l^{-1})	M (nA mg^{-1} l^{-1})	Species	c_l (mg l^{-1})	c_l^* (mg l^{-1})	M (nA mg^{-1} l^{-1})
Ca(II)	>500	>500	—	Br^-	>50	4.6	0.0052
Mg(II)	>500	>500	—	I^-	>50	14	−0.0023
Fe(III)[a]	>23	2.0	0.02	F^-	>50	>50	—
Co(II)	>500	>500	—	PO_4^{3-}	>500	600	5.2×10^{-5}
Al(III)	>10	>10	—	CO_3^{2-}	>5000	3500	9×10^{-6}
SO_4^{2-}	>50	>50	—	NO_3^-	>50	>50	—
Cl^-	>10 000	>10 000	—				

[a]Calibration slope for Fe(III) equals 0.0016 nA mg^{-1} l^{-1}.

TABLE 2

Chemiluminescence response of phenolic model compounds under the reaction conditions used for humic determination

Species		Detection limit (mg l^{-1})	Species		Detection limit (mg l^{-1})
Phenol		104	Salicylic acid	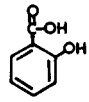	28.0
Catechol		0.16	Gallic acid	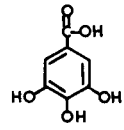	0.11
Resorcinol		0.09	Tyrosine	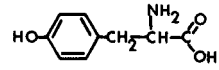	3.6
Hydroquinone	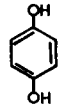	0.18	Cyclohexanol	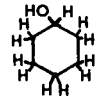	373
Pyrogallol		0.22	D-Glucose	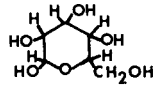	6.6
Phloroglucinol	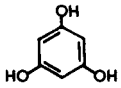	0.30	Lignin	–	0.44
Tannic acid	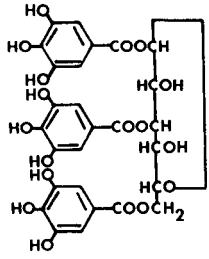	0.006	Fulvic acid	–	0.40
Benzoic acid	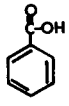	>500			

TABLE 3

Comparison of results for humic acid (HA) determined by chemiluminescence (CL) and absorption (A)

Humic acid sample	HA taken (mg l^{-1})		HA found (mg l^{-1})		Error (%)	
	CL	A	CL	A	CL	A
Chem. Proc. HA	11	5.0	11	8.0	0	58
North Carolina HA	10	5.0	9.9	3.7	1.0	35
Willamette River water	—	—	2.5	1.8	—	—

do not react (glycine, $c_l > 500$ mg l^{-1}). Finally, a combination of these effects, i.e., polyphenolic substitution with acid or ester ring substituents and a fairly large and rigid structure, produces the effect noted in tannic acid which has a detection limit a factor of 100 smaller than that of humic acid. Because these polyphenolic and acid-substituted phenolic groups are proposed to exist within the humic acid structure, those portions of the molecule are most likely the ones producing chemiluminescence. All of the polyphenols tested produced a negative deviation in the chemiluminescence signal at moderately high concentrations (10—20 mg l^{-1}), an effect also observed in the humic acid molecule.

Determination of humic acid

Humic acids from three different sources were compared using chemiluminescence and visible absorption (A) at 430 nm by constructing a calibration curve with one humic acid (Aldrich Chemical) and determining the concentration of another two humic acids (Chemicals Procurement Laboratories HS820, and humic acid isolated from water in North Carolina) as "unknowns" in order to evaluate the differences inherent in the two methods. The results are summarized in Table 3. It is apparent that the response of the three different humic acids is virtually identical when chemiluminescence is used. When absorption is used, 58% and 38% differences are incurred for the two samples treated as unknowns presumably because of the difference in molar absorptivities of the three samples [4].

Table 3 also presents the results of determination of humic acid in Willamette River water. As can be seen, depending on the method used, values for the humic acid content of the water differ by 39%. In this case, the humic acid value obtained by chemiluminescence was determined both by calibration curve and standard addition methods, with the humic acid concentration agreeing between the two methods, indicating virtually identical calibration sensitivity between the standard and the humic acid from the Willamette River. While it is not possible to confirm the accuracy of the chemiluminescence method, it is encouraging that the method yields consistent results among the different samples examined.

It is estimated that approximately 120 samples per hour can be processed. This method should find broad application in the determination of humic substances in natural water.

Acknowledgement is made to the NSF (grants CHE7617611 and CHE79-21243) for partial support of this research. We thank Rod Malcolm of the USGS in Denver, Colorado for providing the fulvic acid and North Carolina humic acid used in this work.

REFERENCES

1 E. T. Gjessing, Physical and Chemical Characteristics of Aquatic Humus, Ann Arbor Science, Michigan, 1976, pp. 27, 96.
2 G. L. Brun and D. L. D. Milburn, Anal. Lett., 10 (1977) 1209.
3 H. Thiele, H. Affeldt and G. Ryhiner, Sci. Proc. R. Dublin Soc., Ser. A, 1 (1960) 81.
4 M. Schnitzer and S. U. Khan, Humic Substances in the Environment, M. Dekker, New York, 1972, pp. 55—67.
5 D. Slawinska and J. Slawinska, Nature, March 213 (1967) 902.
6 R. J. Miller and J. D. Ingle, Jr., Determination of Polyphenols by Chemiluminescence, unpublished work, 1979.
7 R. J. Miller and J. D. Ingle, Jr., Trace Cobalt Determination via Pyrogallol and Lophine Chemiluminescence, 1979 Pittsburg Conference, Cleveland, OH.
8 S. Hoyt and J. D. Ingle, Jr., Anal. Chim. Acta, 87 (1976) 163.
9 L. A. Montano and J. D. Ingle, Jr., Anal Chem., 51 (1979) 919.
10 D. F. Marino and J. D. Ingle, Jr., Anal. Chem., in press.

Analytica Chimica Acta, 124 (1981) 31—38

COLLECTION OF ATMOSPHERIC POLYCHLORINATED BIPHENYLS ON AMBERLITE XAD-2 RESINS

GREGORY J. HOLLOD[a] and STEVEN J. EISENREICH*

Environmental Engineering Program, Department of Civil and Mineral Engineering, University of Minnesota, Minneapolis, MN 55455 (U.S.A.)

(Received 21st April 1980)

SUMMARY

The collection and retention capabilities of an Amberlite XAD-2 resin for polychlorinated biphenyl (p.c.b.) isomeric mixtures were investigated in a high-volume air sampling system. Collection efficiency studies, performed by spiking the glass fiber filters with Aroclor 1221, 1242 and 1254 isomeric standards, gave average recoveries of 93%. Polychlorinated biphenyl retention studies using ambient atmospheric p.c.b. and collection flow rates of 0.4 m^3 min^{-1} showed that the theoretical p.c.b. breakthrough occurred for a 600-ml XAD-2 resin bed at approximately 340 m^3 of air and for a 420-ml resin bed at approximately 115 m^3 of air. Results illustrate the need to evaluate breakthrough volumes when collecting volatile trace organics in the atmosphere.

An increasing interest in the role of the atmosphere as a pathway for global transport of toxic organics, such as polychlorinated biphenyls (p.c.b.), has generated a need to determine atmospheric concentrations of these compounds [1—3]. Since the concentration of atmospheric p.c.b. is low (i.e. 10^{-9} g/m^3), determination requires a preconcentration/isolation step.

Different types of solid adsorbents have been utilized in the collection of atmospheric p.c.b. with polyurethane foam plugs (p.f.p.) [4, 5], coated p.f.p. [6, 7], and florisil [8, 9] being the most popular choices. Recently a divinylbenzene copolymer resin (XAD-2) has been shown to be efficient at collecting atmospheric organics when compared to florisil, and a higher collection efficiency for some p.c.b. isomers when compared to the p.f.p. systems [10].

The efficiency of an air sampling system for the collection of atmospheric p.c.b. can be evaluated using elution chromatography, where the spike is introduced to the adsorbent column as a single plug and eluted as a band [11]. However, during an air sampling event, the collection system behaves similarly to a frontal gas—solid chromatographic system, continuously introducing atmospheric p.c.b. to the adsorbent column [12]. This study investigates the movement of p.c.b. through an XAD-2 resin bed as a function of the total ambient air volume sampled.

---

[a]Present address: E. I. du Pont de Nemours & Co., Environmental Transport Division, Savannah River Laboratory, Aiken, SC 29801, U.S.A.

The efficiency of the XAD-2 resins for retaining collected atmospheric p.c.b. was tested by measuring the mass of ambient atmospheric p.c.b. that was present in each layer of a fractionated XAD-2 resin bed after various air sampling periods. The collection efficiency of the XAD-2 resin air sampling system was evaluated using elution chromatography in the laboratory.

EXPERIMENTAL

Sampling system

A Universal High Volume Air Sampler System (BGI, Inc., Waltham, MA, USA) was modified for collection of atmospheric p.c.b. using XAD-2 resins as shown in Fig. 1. An aluminum standpipe (24 cm long, 9.5 cm i.d.) was attached to the motor housing, and the end of the standpipe was threaded to accommodate the filter holder. An aluminum basket with a 60-mesh brass screen soldered at one end with an XAD-2 resin capacity of 600 ml (78 mm depth) was used. A removable stainless steel screen served as the top of the basket and also as a support for the filter. A Gelman glass fiber filter (10 cm) was placed on the top of the sampler between two teflon gaskets and held in place by a screw-on metal cap assembly. The glass fiber filter was used to prevent airborne particulates from fouling the XAD-2 resins and also to collect particulate p.c.b. Some of the air filter samples were extracted for 24 h with petroleum ether in a Soxhlet extractor, the ether solution then being concentrated to 0.5 ml. Polychlorinated biphenyls were never detected in the air filter sample extracts because they either desorbed from the particulates during the sampling event, or the relatively low air sample volumes did not provide sufficient particulate matter containing p.c.b. for detection. However, the majority of atmospheric p.c.b. is thought to be in the gas phase [2, 5, 6].

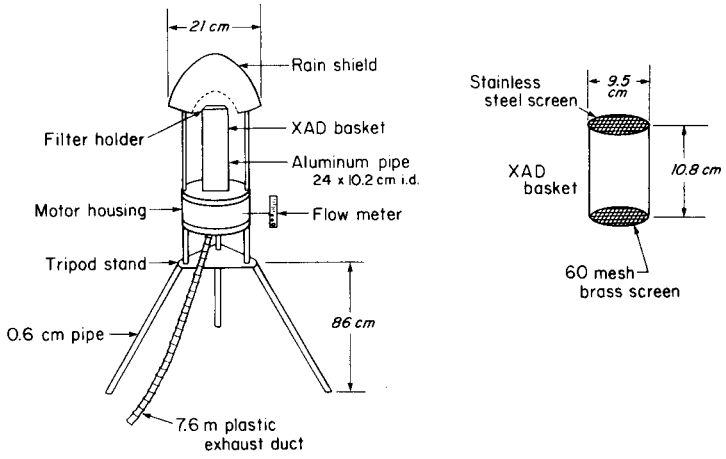

Fig. 1. Organic microcontaminant air sampling system.

The air flow through the sampler was monitored by a rotameter-type flow meter, which had been calibrated in the laboratory using a Dwyer Slack-Tube Manometer and standard calibrating plates supplied and calibrated at BGI, Inc. The pressure drop across the air sampler was plotted versus flow of air for each of the five plates.

Materials

Anhydrous sodium sulfate (granular, Mallinckrodt), florisil (60/100 PR grade, Floridin Chemical Comp.), and alumina (80/100, Mallinckrodt) were extracted with a hexane–acetone mixture (1 + 1) for 24 h in a Soxhlet extractor. These materials were then dried at 60°C with a purified stream of nitrogen and then activated at 500°C in a muffle furnace for 12 h.

The Amberlite XAD-2 resin (Rohm and Haas, 20-50 mesh) was first rinsed for 15 min with distilled water, then transferred to a Soxhlet extractor and extracted for 24 h with nanograde acetone (Mallinckrodt). This was followed by a 48-h extraction, with nanograde petroleum ether being added every 24 h. The XAD-2 resins were then dried at 60°C for 24 h and stored in a sealed, teflon-lined screw-cap 3.9-l glass bottle.

Collection and treatment of air samples

Air samples were collected using either 420 or 600 ml of XAD-2 resin, and sample collection volumes ranged from 72 to 924 m^3 of air. The sample collection rate was typically 0.4 m^3 min^{-1}, which corresponds to a flow velocity through the resin bed of 95 cm s^{-1}. After the air sampling event, the XAD-2 resins were Soxhlet-extracted for 24 h using petroleum ether. The sample extract was concentrated to 5 ml in a Kuderna-Danish apparatus and then concentrated to 0.5 ml with a gentle stream of purified nitrogen.

The extraction of clean XAD-2 resins revealed the presence of sufficient material sensitive to electron capture detection to prevent quantification of any Aroclor p.c.b. present in the sample extracts. These interfering substances were removed from the extracts using a micro-column containing 0.5 g of alumina (3% H_2O, w/w), 0.25 g of florisil, and 0.25 g of anhydrous sodium sulfate. Recovery studies showed that a 2:1 alumina/florisil mixture with 2 ml of hexane as the eluent gave 98% recovery and a reproducibility of ±0.001 μg (n = 8) for Aroclor p.c.b. standard mixtures (Analabs, Inc., North Haven, CT). After sample clean-up, the sample was again concentrated to 0.5 ml with purified nitrogen, with the sides of the sample vial being periodically rinsed with hexane to minimize surface adsorption onto the glass walls. There was no material detectable by electron capture in the blank samples after using the described sample clean-up procedure.

The accuracy and precision of the analytical procedure were determined by spiking 420 ml and 600 ml portions of clean XAD-2 resins with a known mixture of Aroclor 1242 and 1254 standards. The two standard mixtures of 0.5 μg and 10 μg of total p.c.b. were prepared in acetone and applied to the XAD-2 resins with a Hamilton syringe. Following the extraction and clean-up

procedures as described above, the analytical recoveries for duplicate trials at each concentration for both resin volumes were 90% with a standard deviation of ±0.02 μg.

Each sample extract was chromatographed on at least two different columns using a Hewlett-Packard 5840 gas chromatograph (g.c.), equipped with a ^{63}Ni (15 mCi) electron capture detector and a Hewlett-Packard 5840A integrating recorder. The dimensions of the packed columns were 2.4 m × 2 mm i.d., and the liquid phases used, both coated on 80/100 Chromasorb W, were either 1.5% OV-17 + 1.95% QF-1 or 4% SE-30 + 6% OV-210. The chromatographic conditions were: column temperature 190°C, injector temperature 225°C, detector temperature 350°C, nitrogen flow ml min^{-1}, and chart speed 1 cm min^{-1}.

The collection efficiencies of the XAD-2 resins for gaseous Aroclor 1221, 1242 and 1254 were tested by spotting a glass fiber filter in several locations with a known amount of p.c.b. standard. After the air sampler ran for 20 min (8 m^3), the filter paper and the XAD-2 resins were extracted separately to determine the collection efficiency of the XAD-2 resins.

The retention efficiency of the XAD-2 resin bed for p.c.b. was determined using ambient air and atmospheric p.c.b. as the "spike". The aluminum basket containing XAD-2 resins was sectioned into three equal layers with two stainless steel screens. One retention study was performed using a 600-ml total resin bed (273 g of resin) and to provide a comparison of mass loading of p.c.b. per volume of XAD-2 resins; a second study was performed using a total of 420 ml of XAD-2 resins (191 g).

Air samples were collected for various time periods on the roof of the Space Science Center about 30 m above ground on the University of Minnesota campus in Minneapolis. Each layer of the XAD-2 resin bed was collected, stored, extracted and processed separately. The sample chromatograms were compared to chromatograms of known Aroclor standards, and regions in the sample chromatograms were defined as Aroclor 1242 and 1254 type p.c.b., according to the classification used by Webb and McCall [13]. The percent distribution of Aroclor 1242 and 1252 mixtures was determined for each layer using the following procedure. Eight to ten peaks common to all three of the chromatograms resulting from one fractioned air sample and representative of Aroclor 1242 and 1254 mixtures were selected. The distribution of either Aroclor 1242 or 1254 in each section was determined by summing the area of a common peak and calculating percent of total. The Aroclor p.c.b. distribution was computed as the average of all the determinations. The absolute mass of p.c.b. material in the XAD-2 resin bed was found by combining all three extracts and quantifying its chromatogram.

The same air sampling unit was used to collect all the atmospheric p.c.b. samples. Three air samples were collected over a 48-h period, with the sample volume of 188 m^3. The standard deviation for the entire procedure was calculated for Aroclor 1242 and 1254 as 0.9 ng m^{-3} and 0.7 ng m^{-3}, respectively.

RESULTS AND DISCUSSION

The collection efficiency studies, based on direct spiking of Aroclor 1221, 1242, 1254 p.c.b. onto the glass fiber filter, were done to determine if the system was capable of collecting known amounts of p.c.b. The results showed that an average of less than 7% of the applied p.c.b. mixtures stayed on the filter and the remaining p.c.b. (93%) volatilized and were all collected on the XAD-2 resin bed. In this recovery experiment, the XAD-2 resin bed was fractionated into two equal parts, and p.c.b. were not detected in the bottom half of the resin bed after 8 m^3 of sampled air.

From preliminary air sampling experiments, it was found that p.c.b. were detected in the bottom half of a fractionated 600-ml XAD-2 resin bed after 6 h (150 m^3) of air sampling. This finding led to the study of the retention of p.c.b. on two different volumes of XAD-2 resins over various sampling time periods and using natural background levels of p.c.b. as the "spike".

The results of the percent mass distribution of Aroclor 1242 and 1254 in the 600- and 420-ml fractionated resin bed are shown in Figs. 2 and 3. Though the results may be biased because of the assumption that no p.c.b. breakthrough occurred in the air volumes sampled, the percent mass distribution of p.c.b. on the resin bed was calculated in order to compare the relative distributions. Plotting the percent mass distribution instead of the actual mass of p.c.b. served to normalize the sampling variables such as temperature (15—32°C), humidity (50—80%), and atmospheric p.c.b. concentrations (1—20 ng m^{-3}). The changes in atmospheric p.c.b. concentrations prevented sample-to-sample comparisons of absolute area counts for individual Aroclor 1242 and 1254 p.c.b. isomers. However, a comparison of the relative distribution of Aroclor 1242 and 1254 p.c.b. mixtures within each layer from sample-to-sample was made. The total mass of p.c.b. collected for all the samples ranged from 0.9 to 1.7 μg. Based on the volume of p.c.b. collected and the surface area of the XAD-2 resins used, it was calculated that if only p.c.b. were collected by the XAD-2 resins, this would not exceed the capacity of the XAD-2 resins.

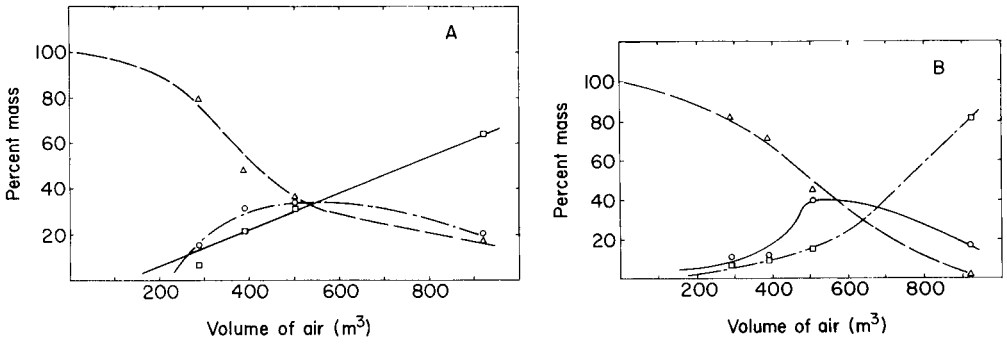

Fig. 2. Distribution of Aroclor 1242 and 1254 in a 600-ml XAD-2 resin bed fractionated into 200-ml sections: (△) top; (○) middle; (□) bottom. (A) Aroclor 1242; (B) Aroclor 1254.

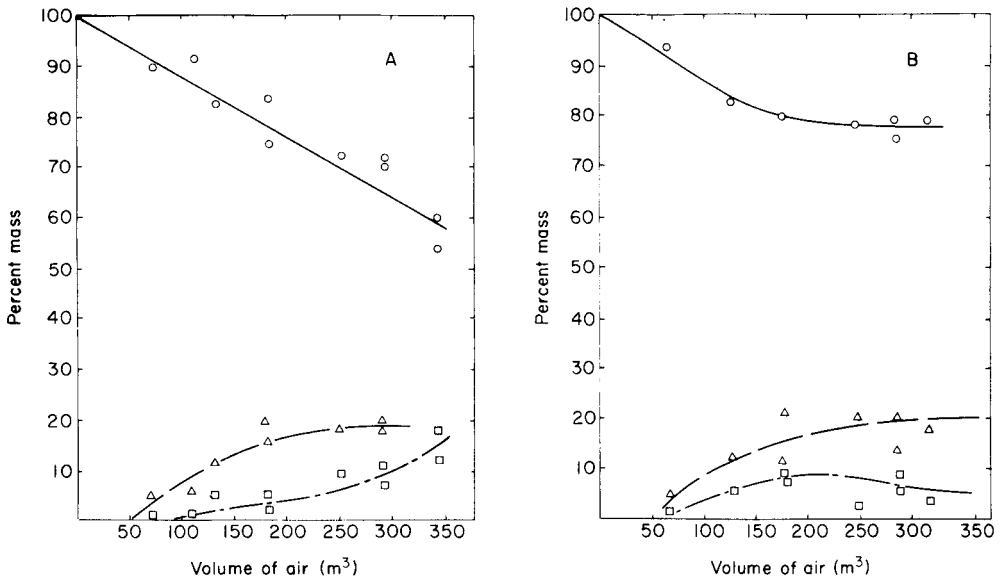

Fig. 3. Distribution of Aroclor 1242 and 1254 in a 420-ml XAD-2 resin bed fractionated into 140-ml sections: (○) top; (△) middle; (□) bottom. (A) Aroclor 1242; (B) Aroclor 1254.

Figure 2 shows a decreasing trend in the top section for the percent Aroclor 1242 and 1254 p.c.b. mixtures at short sampling times, while the middle and bottom curves showed increasing concentrations with increasing sample volumes. This phenomenon would be expected in frontal chromatography where the p.c.b. are continually introduced to the column and partition with the air flow [12]. As collection time increases, the mass distribution in the bed would reach an equilibrium loading in each fraction of the bed. For a three-layered bed, the steady state condition would be reached when 33% of the mass was present in each layer. In this experiment, after this condition was achieved, a continuous decrease in percentage of Aroclor 1242 and 1254 in both the top and middle sections of the resin bed (Fig. 2) was observed. The bottom section of the 600-ml XAD-2 resin bed did not show a decrease in percentage of Aroclor 1242 and 1254 with increasing air volumes, but this trend would most likely be observed at larger air sample volumes.

The decrease in percentage of p.c.b. in the top and middle sections of the XAD-2 resin bed could be due to volatilization of the Aroclor 1242 and 1254 from the XAD-2 resins and/or to displacement of the p.c.b. from the XAD-2 resins. Since the ratio of the percentage of Aroclor 1242/1254 in the top sections of the 600- and 420-ml beds remained constant with air sample volume from sample-to-sample except for the 924 m^3 sample in the 600-ml resin bed, volatilization is not likely the principal mechanism for loss of p.c.b. contributing to the isomeric distribution of Aroclor 1242 and 1254. The consistency of this ratio indicates that both Aroclor 1242 and

1254 are displaced at approximately the same rate from the top section of the resin bed. If volatization were occurring, the more volatile Aroclor 1242 isomeric mixture would be removed preferentially [14].

The decrease in percentage of p.c.b. in the top and middle sections could also be due to displacement or competition for sites on the XAD-2 resins by other organic compounds (e.g. hydrocarbons, acids, esters) in air. Evidence of this was the presence of a yellow substance in the XAD-2 resin extract of the sample. The yellow color increased in intensity on the alumina/florisil columns with samples of increasing air volumes. The yellow material in sample extracts collected in urban air has also been observed by others [5, 14].

Another explanation for the displacement of p.c.b. from the XAD-2 resins may be a strong diurnal variation in ambient levels of p.c.b. in Minneapolis air. For example, large quantities of p.c.b. may be collected by the XAD-2 resins during the day and "eluted" through the column by the cleaner air at night. This phenomenon could be investigated by performing an integrated air sampling procedure over a 24-h period, or by passing p.c.b.-free air through XAD-2 resins that were loaded with p.c.b.

The steady state distribution of p.c.b. in the 420-ml resin bed was not reached because of the low air sample volumes collected (Fig. 3). The results shown in Fig. 3 do give more detail for the type of retention efficiency the XAD-2 resin bed has with the collection of atmospheric p.c.b. in the initial 400 m^3 of sampled air. The difference in the results for these two resin beds may be explained by difference in volume loading of p.c.b. per mass of XAD-2 resin.

Assuming that the collection of p.c.b. in each of the three sections of the XAD-2 resin bed is equal, the theoretical breakthrough volume can be determined by extrapolating the curve for the bottom section of the resin bed back to the abscissa and multiplying by 1.5. The breakthrough for the 600-ml bed was calculated as about 340 m^3 of air, while breakthrough for the 420-ml resin bed was about 115 m^3 of air. The results suggest that when XAD-2 resins are used for collection of volatile trace organics in the atmosphere, special consideration should be given to breakthrough of the compounds of interest, especially when large sampling volumes are used (> 100 m^3). Perusal of the literature [15] suggests that examples of trace organic breakthrough which results in an underestimation of reported atmospheric concentrations are numerous.

REFERENCES

1 G. E. Harvey and W. G. Steinhauer, Atmos. Environ., 8 (1974) 777.
2 The Tropospheric Transport of Pollutants and Other Substances to the Oceans; National Academy of Sciences, Washington, DC, 1978.
3 R. W. Risebrough, P. Rieche, D. B. Peakall, S. G. Herman and N. M. Kirven, Nature, 232 (1968) 50.
4 Environmental Science and Engineering, Inc., EPA-600/4-78-048 (1978) p. 103.
5 T. F. Bidleman and C. E. Olney, Bull. Environ. Contam. Toxicol., 11 (1974) 44.

6 T. J. Murphy and C. P. Rzeszutko, J. Great Lakes Res., 3 (1977) 305.
7 C. G. Simon and T. F. Bidleman, Anal. Chem., 51 (1979) 1110.
8 Midwest Research Institute, EPA-68-02-1780, Task no. 2, 1977.
9 C. S. Giam, H. S. Chan and O. S. Neff, Anal. Chem., 47 (1975) 2320.
10 P. V. Doskey and A. W. Andren, Anal. Chim. Acta, 110 (1979) 129.
11 C. N. Reilley, G. P. Hildebrand and P. Ashley, Anal. Chem., 34 (1962) 349.
12 F. R. Cropper and R. Kaminsky, Anal. Chem., 35 (1963) 735.
13 R. O. Webb and A. C. McCall, J. Chromatogr. Sci., 11 (1973) 366.
14 P. V. Doskey, Master's Thesis, University of Wisconsin—Madison, 1978.
15 G. J. Hollod, PhD Thesis, University of Minnesota—Minneapolis, 1979.

Analytica Chimica Acta, 124 (1981) 39—63

KINETIC TREATMENT OF UNSEGMENTED FLOW SYSTEMS
Part 1. Subjective and Semiquantitative Evaluations of Flow-Injection Systems with Gradient Chamber

HARRY L. PARDUE* and BERNARD FIELDS**

Department of Chemistry, Purdue University, West Lafayette, IN 47907 (U.S.A.)

(Received 30th June 1980)

SUMMARY

A variable-time kinetic model is used to evaluate a single-channel flow-injection system with gradient chamber that has been identified as a continuous-flow titration. A physical model, mathematical equations, computed concentration vs. time profiles, experimental data, and formal definitions are used to identify qualitative and quantitative features of the method that have not been apparent from the titration model for the system. It is shown that determinations can be performed with and without reactant in the flow stream and when reactant is in the flow stream, with and without reactant in the gradient chamber when the sample is introduced. It is shown that lowest concentrations with shortest cycle times can be achieved when determinations are performed without reagent in the gradient chamber initially. Characteristics unique to each of three different data processing options are used to evaluate the validity of equations presented. It is suggested that some methods previously identified as continuous-flow titrations are most accurately identified as variable-time kinetic methods, and it is shown that this semantic differentiation can provide improved insight into the methods and can expand the scope of the methods by suggesting new experimental approaches with potential advantages relative to previously described procedures.

Although the analytical literature contains many reports of unsegmented-flow sample-processing systems, it is only during the last few years that these systems have begun to receive the widespread recognition long given to segmented-flow systems. Much of the current success can be attributed to the early work of Růžička and Hansen [1] and Stewart et al. [2], and the continuing work of many [3, 4] who have recognized the potential of flow-injection approaches for mechanized sample processing. Although progress in the area has been rapid, one feature of the systems, namely the kinetic character, has received relatively little explicit attention. Mottola and Hanna [5] and Růžička and Hansen [6] have noted the analogies between these systems and chemical kinetic processes and Mottola and his colleagues have addressed several aspects of the issue quantitatively [5, 7]. There remain many aspects of the kinetic character of methods based on unsegmented-flow sample-processing systems that merit attention.

**Present address: I.C.I. Petrochemicals Division, Wilton, Gt. Britain.

This and a related paper [8] focus attention on one aspect, namely procedures that have been identified as continuous-flow titrations. Three procedures are discussed, two briefly [9, 10] and one in detail [11]. Equations developed in a subsequent paper [8] for a single-channel flow-injection system with a gradient chamber [11] are used in this paper to evaluate that system qualitatively and semiquantitatively. The other methods [9, 10] are discussed later in the paper to illustrate the generality of the kinetic concepts and to permit comparisons of conceptual similarities and differences. It is concluded that one of the methods [9] is most accurately identified as a kinetic titration, and that two procedures [10, 11] are most accurately identified as variable-time kinetic methods. It is shown that the semantic differentiation between titration and variable-time kinetic procedures is significant because the kinetic view leads to the suggestion of alternative experimental approaches with potential advantages for two methods [10, 11] and provides insight into the quantitative characteristics of one method [11] that has not been provided by the titration model initially used. Rather than being restrictive, the variable-time kinetic view of the two methods should expand their scope to include species that cannot be determined by titrimetric methods. Titrimetric methods require stoichiometric chemical reactions; it is shown that a chemical reaction is not an essential component in two of the processes [10, 11], so that these processes become applicable to some components for which no suitable titrants are available.

Rationale for the kinetic view

In any quantitative chemical determination, the property of the system that is finally measured will exhibit time-dependent character until all processes in the system that influence the property are at equilibrium. Methods based on measurements of time-dependent properties are identified as kinetic determinations while methods based on measurements of time-independent properties are identified as equilibrium determinations. Because equilibrium and kinetic concepts are equally valid for both chemical and physical processes, these statements are equally valid for both chemical and physical processes. It is common practice to identify as kinetic methods those procedures in which chemical kinetic processes are monitored in solutions in which physical processes such as mixing or dilution are at equilibrium; it is equally valid to identify as kinetic methods procedures in which physical kinetic processes are monitored in solutions in which chemical reactions are at equilibrium. Considering the self-evident facts that no system can be at equilibrium until all processes in the system are at equilibrium, that the kinetic and equilibrium regions of any property of a system are mutually exclusive, and that the kinetic and equilibrium regions for any property of a system are all inclusive, it follows that every quantitative chemical determination must have either kinetic character or equilibrium character; there is no other possibility. While it is possible to have a kinetic determination in which some processes are at equilibrium, it is not possible to have an equilibrium determination

in which any processes that influence the measured property are not at equilibrium.

Although determinations with kinetic character can be traced back at least 100 years [12], kinetic determinations have not been acknowledged explicitly to an extent comparable to equilibrium methods [13]. It is only during the last two decades that kinetic methods have received any substantial recognition [5, 7, 13—15], and during this period emphasis has been focused on chemical kinetics. These are surprising facts to some because physical processes such as mixing and mass transport impart kinetic character to measurements just as surely as chemical processes, and it is highly probable that the number of modern determinations involving measurements made on transient processes is much greater than the number based on systems at equilibrium. Kinetic aspects of chemical, physical, and physico-chemical processes play important roles in many types of quantitative determinations [13, 14] and these kinetic processes need to be given more extensive and explicit attention than has been the case in the past.

In the context of this paper, there are these two emerging concepts, kinetic measurement approaches and unsegmented-flow sample processing systems, that are quite naturally compatible with each other. Except in the special cases when there is no mixing at all, or when mixing is complete, mixing during the flow process will impart kinetic character to the measurement process in the presence or absence of chemical kinetic processes. Because it is quite probable that measurement and data processing methods that have been developed in recent years [7, 14, 15] for chemical kinetic processes are equally applicable to physical kinetic processes, it seems appropriate that there should be effective communication and interaction among persons specializing in these areas.

The single-channel flow-injection system with a gradient chamber has been selected for detailed discussion in this paper because it offers attractive features in terms of sample size and simplicity of design and operation, because it is amenable to mathematical treatment, and because the kinetic treatment offers new insight into some characteristics of the method.

EXPERIMENTAL

Equations developed [8] for the single channel flow-injection system are evaluated via the determination of hydrochloric acid. Concentration changes in the gradient chamber are monitored photometrically with color indicators and data were obtained from response curves on a strip-chart recorder. Basic forms of bromothymol blue and bromophenol blue with pH transition ranges of 6.0—7.6 and 3.0—4.6, respectively, were monitored at 620 and 590 nm, respectively. All solutions were prepared and handled with usual care; there are no special features that merit comment.

Symbols

The symbols used are identified in terms of the flow diagrams in Fig. 1 and the following general reaction $A + zB \rightarrow P$ where A is the species to be

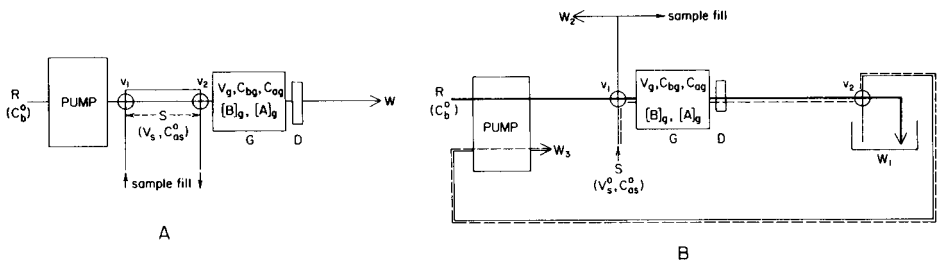

Fig. 1. Block diagrams of series (A) and parallel (B) sample introduction systems. R, reagent; S, sample; G, gradient chamber; D, detector; W, waste; v_1, v_2, 3-way valves. See Table 1 for other symbols.

determined and is identified as the determinant, and B is a reactant with reaction ratio z. For the determinant (A), C_{as}° represents the initial concentration in the undiluted sample and C_{ag} represents the concentration in the gradient chamber. For the reactant (B), C_b° is the initial concentration in the reagent flow stream, C_{bg}° is the initial concentration in the gradient chamber when the first increment of sample begins to enter the chamber, and C_{bg} is the instantaneous concentration in the gradient chamber at any time. In all of this discussion, the term reagent refers to the solution in the flow stream before the sample injection point (v_1 in Fig. 1) and, while the reagent in this case always contains an acid—base indicator, it may or may not contain the reactant (KOH).

For situations involving rapid changes that produce discontinuities in response curves, the symbol $[A]^p$ or $[B]^p$ represents the instantaneous concentration that takes full account of all reaction and dilution processes prior to point p, but does not account for processes that follow point p. Subscripts a, b, s, r and g represent determinant, reactant, sample, reagent, and gradient chamber, respectively. Symbols V, n, and f are used to represent volume, moles, and volume flow rate, respectively. The symbol t represents instantaneous elapsed time from a particular reference point, and Δt represents a time interval between two reference points. All symbols used are summarized in Table 1 with equivalents from other papers.

General procedures

Results are reported for three general operating procedures. In one, the flow stream contains reactant, B, at concentration $C_b^\circ > 0$ and the gradient chamber is filled initially with undiluted reagent ($C_{bg}^\circ = C_b^\circ$) when sample is introduced. In a second case, the flow stream contains reactant ($C_b^\circ > 0$) but the gradient chamber contains only diluent ($C_{bg}^\circ = 0$) when sample is introduced. In the third case, no reactant is used in either the flow stream or the gradient chamber ($C_b^\circ = 0$ and $C_{bg}^\circ = 0$). In the second case, the desired initial condition in the gradient chamber ($C_{bg}^\circ = 0$) is approximated by injecting each successive sample at the end-point of the previous sample when reactant concentration in the chamber is very low.

TABLE 1

List of symbols used

Parameter or variable	Symbols		Parameter or variable	Symbols	
	This paper[a]	Ref. 11		This paper[a]	Ref. 11
Determinant concentration (mol l^{-1})[a]			Flow rate (ml s^{-1})	f	ν
Initial	C°_{as}	C'_o	Time		
Time dependent in gradient chamber	C_{ag}		To clear reagent from gradient chamber	t_1	
At end-point	C^{ep}_{ag}; $[A]^{ep}_g$		For all sample to enter gradient chamber	t_2	
Reagent concentration (mol l^{-1})			For end-point to be reached	t_3	
Undiluted in flow stream	C°_b		Time intervals		
Initial in gradient chamber	C°_{bg}		$t-t_o$	Δt_o	
Time dependent in gradient chamber	C_{bg}		$t-t_1$	Δt_1	
Volume (ml)			$t-t_2$	Δt_2	
Gradient chamber	V_g	V	t_3-t_1	Δt_{ep}	t_{eq}
Sample	V_s	S_v			

[a] C_x represents analytical concentration (before reaction) and [X] represents actual concentration (after reaction).

Flow systems

Two flow systems used in the flow-injection studies are illustrated in Fig. 1. Figure 1A is a series sample introduction system similar to the single-channel system described earlier [11] and Fig. 1B is a parallel sample introduction system that is described briefly here. The valves, v_1 and v_2, are operated synchronously. When valves v_1 and v_2 are in the reagent position, reagent is pumped along the heavy line through the gradient chamber, the detection flow cell, and to waste, W_1. Solution from W_1 is pumped along the thin solid line to W_3. The "sample fill" line permits the line between S and v_1 to be filled with sample while reagent is being pumped through the gradient chamber. When valves v_1 and v_2 are in the sample position, reagent is pumped along the heavy line to v_1 where it is diverted to W_2, and sample, S, is drawn along the dashed line through v_1 to the gradient chamber while solution from the gradient chamber is drawn along the dashed line through v_2 to W_3. After an accurately measured time, the valves are switched so that reagent is again pumped to the gradient chamber. This system permits a closer approach to plug flow to be achieved during sample introduction but makes sample volume more dependent upon flow rates and sampling time.

Reagents

All solutions were prepared in distilled water. In all cases, the reagent flow stream included an acid—base indicator (bromothymol blue or bromophenol blue) and either potassium hydroxide as reactant or sodium chloride for ionic strength control.

Hydrochloric acid samples. Stock 0.200 mol l^{-1} hydrochloric acid was prepared from concentrated reagent (analytical grade, Mallinckrodt) by dilution and standardization against Titrisol potassium hydroxide solution. Solutions of desired concentration (4—200 mmol l^{-1}) were prepared by dilution.

Potassium hydroxide solution. A stock solution of 1.00 mol l^{-1} potassium hydroxide solution was prepared from a vial of Titrisol potassium hydroxide solution (MCB reagent). Solutions of 1.0 and 5.0 mmol l^{-1} potassium hydroxide were used.

Indicators. Bromothymol blue (MCB) at 0.016 mmol l^{-1} (10^{-3}%) was used in experiments with base in the flow stream. Bromophenol blue (MCB) at 0.015 mmol l^{-1} (10^{-3}%) was used in experiments with no base in the flow stream. Indicators were included in the reagent solution.

Sodium chloride. A solution of 0.2 mol l^{-1} sodium chloride (Fisher) was used in the reagent stream to control ionic strength in the experiment with no base.

Apparatus

Pump tubing and valves. A Gilson Minipuls 2 peristaltic pump was used to pump the streams. All sample loops and flow streams consisted of appropriate lengths of 0.8 mm i.d. teflon tubing, except as noted below. Between points S and G (Fig. 1A) the dead volume was 13.5 μl consisting of an outlet port in the chromatography valve (0.35 cm length, 1 mm i.d.), teflon connecting tubing (3 cm length, 0.5 mm i.d.), and a bore drilled into the gradient chamber (0.5 cm length, 0.75 mm i.d.). Between points S and D, the tubing volume was 7.5 μl consisting of a bore in the chamber (0.6 cm length, 0.75 mm i.d.) and a connecting tube (2.4 cm length, 0.5 mm i.d.). The slide valves (v_1, v_2) were eight-port Unimetrics chromatography slide valves used in both series and parallel modes.

Detection system. A colorimeter based on a red light emitting diode (Dialco) and a silicon phototransistor (Texas Instruments, TIL 78) was used to monitor transmittance. A current-to-voltage converter consisting of a field effect transistor operational amplifier (Farnell NE 536H) with a gain resistor of 10 megohms was used to convert the phototransistor current to voltage with a transfer function of 10 V μA^{-1}. The cell path length was 1 mm.

In the experiment without base in the flow stream, a yellow LED was substituted for the red one.

Gradient chamber. The chamber was machined from plexiglas. The upper section was an accurately machined hemispherical depression (19.7 mm base diameter) in a flat polished surface and contained an output port at the top of the dome. When clamped against a second polished block containing an input port, the seal was watertight.

Teflon covered magnets were used as stirrers. The chamber volume, V_g, may be varied by using magnets of different size or by clamping a plexiglas cylinder between the upper and lower blocks.

Procedures

All reported data represent the mean of two results.

Series sample introduction ($C^{\circ}_{bg} = C^{\circ}_{b}$). The sample loop is external and is filled by aspirating sample into the loop with a syringe. When the valve is switched to the sampling position, sample enters the system and is automatically flushed through with reagent. After the second "end-point", sufficient time is allowed for $C^{\circ}_{bg} \geqslant 99\%\ C^{\circ}_{b}$ before the next sample is introduced.

Series sample introduction ($C^{\circ}_{bg} = 0$). Sample loop filling and sample injection are the same as above. A preliminary sample is injected to clear reagent from the chamber and the result of that sample is discarded. After the first color change, the sample loop is refilled and this and subsequent samples are injected at the instant of the end-point of the previous sample. Time intervals are measured in the usual way [11]. For most cases, there is sufficient time during each run for the sample loop to be cleared of the current sample and refilled with the next sample before the end-point for the current sample is reached. In this way, samples can be processed continuously without discarding results.

Parallel sample injection ($C^{\circ}_{bg} = C^{\circ}_{b}$). Sample is aspirated with a syringe sufficiently to fill the input tube between S and the valve before the gradient chamber (Fig. 1B). When the valve is switched for sample injection, reagent from the reservoir is diverted to external waste and sample is aspirated into the system for a carefully controlled time via the tube which returns to the pump. When the valve is changed to the run position, reagent is pumped through the system from the reservoir to continue the determination and the line returning to the pump is disconnected from the system. The flow rates in the sampling and run positions should be as close as possible for best results. Sufficient time elapses between samples for $C_{bg} \geqslant 99\%\ C^{\circ}_{b}$.

Parallel sample injection ($C^{\circ}_{bg} = 0$). Sample that has been drawn into the sample line during the current run is injected at the instant of the end-point of the previous sample.

Determination of parameters

Gradient chamber volume (V_g). Gradient chamber volume was determined by timing the filling of the chamber at a known slow flow rate from the peristaltic pump.

Sample volume. For series injection, sample volume was determined by filling the sample loop with 1.00 M Titrisol potassium hydroxide, injecting the sample into a stream of distilled water, collecting all the effluent, and titrating the effluent with standard hydrochloric acid.

For parallel injection, the sample volume was determined by measuring the mass of distilled water delivered at the same flow rate and sampling time used for samples. The mean of at least five injections is used.

Flow rate (f). Flow rate was determined by weighing the volume of distilled water pumped in a fixed time.

Time. Time intervals were determined from the midpoint of the transmittance changes at the "end-points". For large transmittances, these points

will be very close to the midpoint of the absorbance changes. In any case, the transition times are very short compared to the measurement times, Δt_{ep}.

ASSUMPTIONS AND KINETIC MODEL

The principal assumptions made in this and the related paper are that (a) all chemical reactions proceed to completion rapidly, (b) sample introduction involves plug flow, (c) mixing in the gradient chamber is instantaneous, and (d) there is no mixing between the gradient chamber and the detector. It is probable that the weakest of these assumptions is that involving plug flow during sample introduction; experimental results related to this assumption are presented and discussed later [8].

Figure 2 illustrates the physical model on which this treatment is based. As the first increment of sample enters the gradient chamber at t_0, determinant in the sample will react with any reactant in the chamber. Therefore, determinant concentration in the chamber will not increase until time t_1 when all reactant has been cleared from the chamber; after t_1, determinant concentration will increase until time t_2 when all sample has entered the chamber. Between times t_2 and the end-point at t_3, determinant concentration in the gradient chamber will be reduced by the combined processes of mass flow out of the chamber (a first-order process) and reaction with any reactant in the reagent stream (a zero-order process because flow rate is constant). The quantity that has been identified [11] as t_{eq} and related to concentration is the interval $\Delta t = t_3 - t_1$. To the extent that the assumption of plug flow holds, the total time required for all sample to enter the gradient chamber is $t_2 = V_s/f$ where V_s and f are sample volume and volume flow rate, respectively.

The physical model in Fig. 2 is used in the related paper [8] to develop a mathematical description of the system within assumptions stated above. Selected equations from that treatment are used in the present paper to discuss some important characteristics of the system.

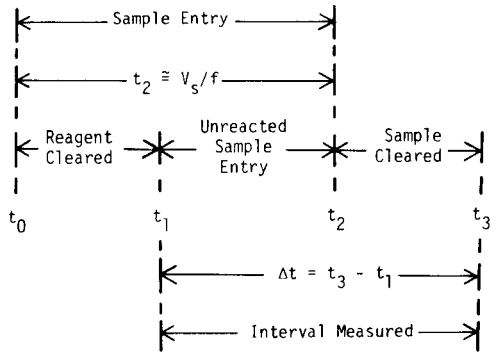

Fig. 2. Physical model for the single-channel flow-injection system with gradient chamber.

CONCENTRATION VS. TIME DEPENDENCIES

Whatever the nature of the method, an important factor in being able to use it to its fullest advantage is a detailed knowledge of how different experimental parameters and procedural options influence concentration vs. time relationships. Some equations needed to discuss these dependencies are presented below; the proofs are given in the related paper [8].

Mathematical equations

The time interval, t_1, required for all reactant to be cleared from the gradient chamber is given by

$$t_1 = (V_g/f)\ln\,(1 + zC^\circ_{bg}/C^\circ_{as}) \tag{1}$$

where V_g is the volume of the gradient chamber, f is the volume flow rate, z is the reaction ratio, C°_{bg} is the reactant concentration in the gradient chamber when sample first begins to enter the chamber, and C°_{as} is the determinant concentration in the injected sample. Between times t_0 and t_1, determinant concentration in the gradient chamber remains near zero; between times t_1 and t_2 determinant concentration in the gradient chamber increases as follows

$$C_{ag} = C^\circ_{as}\,\{1 - \exp[-(f/V_g)(t - t_1)]\}\quad (\text{for } t_1 \ll t \ll t_2) \tag{2}$$

where all symbols are defined above and in Table 1. Determinant concentration reaches a maximum value at $t_2 = V_s/f$; the maximum concentration is given by

$$[A]^{max}_g = C^\circ_{as}\,\{1 - \exp[-(f/V_g)(t_2 - t_1)]\}\quad (\text{at } t_2) \tag{3}$$

After t_2, determinant concentration in the gradient chamber decreases as follows

$$C_{ag} = [A]^{max}_g \exp[-(f/V_g)(t - t_2)] - zC^\circ_b\,\{1 - \exp[-(f/V_g)(t - t_2)]\}$$
$$(\text{for } t_2 \ll t \ll t_3) \tag{4}$$

where C°_b is the reactant concentration in the flow stream. The first term on the right represents loss of determinant via mass flow when there is no reactant in the flow stream; the second term on the right represents the influence of reactant on the loss of determinant. It should be noted that a pure exponential decay will result only when $zC^\circ_b = 0$.

Mass flow and reaction components

Solid curves in Fig. 3(A and B) represent computed concentration vs. time profiles for two values of determinant concentration for which $C^\circ_{as} \cong C^\circ_b$ and $C^\circ_{as} \gg C^\circ_b$, respectively. The dashed plots represent the contributions to the total by the reaction (curve a) and the mass flow (curve b) processes. In these plots, t_1 was computed with eqn. (1), t_2 was computed as V_s/f, C_{ag} between t_1 and t_2 was computed with eqn. (2), C^{max}_{ag} at t_2 was computed with

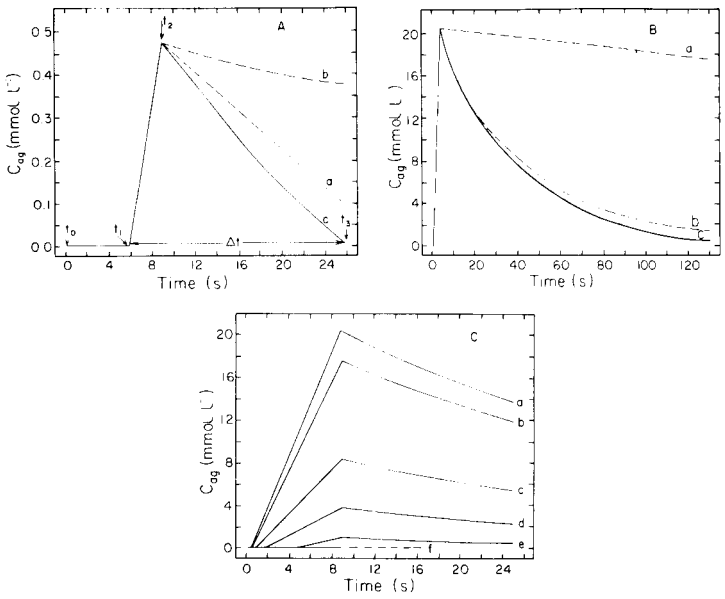

Fig. 3. Effects of determinant concentration on concentration vs. time profiles with reactant in flow stream and gradient chamber. All frames: V_g = 0.98 ml; V_s = 0.20 ml; f = 0.0225 ml s^{-1}; $C_b^\circ = C_{bg}^\circ$ = 1.00 mmol l^{-1}. In A and B, (a) reaction contribution; (b) mass flow contribution; (c) total contribution; determinant concentration (C_{as}°) is (A) 7 and (B) 100 mmol l^{-1}. In C, C_{as}° values are: (a) 110; (b) 100; (c) 50; (d) 25; (e) 10; (f) $\leqslant$ 4.4 mmol l^{-1}.

eqn. (3), and C_{ag} between t_2 and t_3 was computed with eqn. (4). To keep these and other similar data in perspective with indicator response curves reported previously [11], it should be noted that although these processes are taking place, all changes except those near t_1 and t_3 are obscured by the indicator as was noted earlier [11].

At the lower concentration (Fig. 3A), the reaction process consumes about twice as much determinant as is lost via mass flow; at the higher concentration, the mass flow process accounts for a large percentage of the total change and the reaction process is relatively unimportant until the latter stages of the process. The principal role of the reactant at the higher concentration is to produce an abrupt change at t_3 and that is its most useful function at the lower concentration. The significance of these observations is discussed in more detail in a later subsection. At this point, it is noted that the zero-order process (curve a) predominates when $C_{as}^\circ \cong C_b^\circ$ and that the first-order process predominates when $C_{as}^\circ \gg C_b^\circ$.

Figure 3C shows concentration vs. time data for a series of concentrations plotted on the same scales so that relative effects are more easily visualized. As sample concentration decreases, the peak value decreases and t_1 increases. Eventually, a point is reached at which the amount of determinant in the sample is inadequate to clear all reactant from the gradient chamber, and

determinant concentration remains at zero (curve f). The concentration at which this occurs represents the minimum that can be determined for any set of conditions, and is the value obtained by extrapolating t vs. ln C plots to $t = 0$ [11]. This point is treated quantitatively in a later subsection.

Effects of reactant concentration

It was noted earlier [11] that concentration in the flow stream can be selected to suit the determinant concentration best. Figure 4A shows the effect of reactant concentration on the expected responses for a single determinant concentration for the situation when the gradient chamber contains undiluted reagent when sample is introduced. It is observed that the response decreases as reagent concentration increases, and that eventually a point is reached (curve f) at which no response is observed.

The loss in response with increasing reactant concentration results from the fact that some sample must be consumed to clear reactant from the gradient chamber before determinant concentration can increase above zero. This suggests that the sensitivity loss shown in Fig. 4A could be avoided by initiating experiments without any reactant in the gradient chamber. Figure 4B shows concentration vs. time profiles expected for the same conditions as in Fig. 4A except that the gradient chamber contains no reactant when sample is introduced ($C^{\circ}_{bg} = 0$). It is noted that the expected sensitivity for this situation remains unchanged even for reagent concentration in the flow stream (C°_{b}) that exceeds the value of 2.27 mmol l^{-1} for which zero response is predicted in Fig. 4A (curve f). This option of initiating each experiment without any reactant in the gradient chamber could permit more flexible variation of reagent concentration in the flow stream to control other features such as measurement time and sample throughput [11] without sacrificing performance at lower concentrations.

Minimum concentration

If experiments are done with reactant in the gradient chamber when sample is introduced ($C^{\circ}_{bg} > 0$), then some minimum sample concentrations, $C^{\circ}_{as,\,min}$,

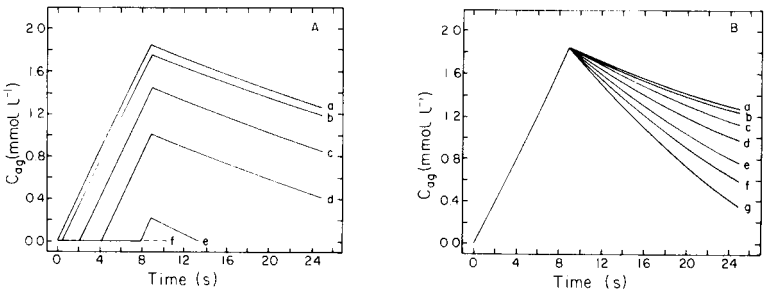

Fig. 4. Effects of reactant concentration on concentration vs. time profiles. Both frames: $V_g = 0.98$ ml; $V_s = 0.20$; $f = 0.0225$ ml s^{-1}; $C^{\circ}_{as} = 10$ mmol l^{-1}. For A, $C^{\circ}_{bg} = C^{\circ}_{b}$ = (a) 0.0; (b) 0.1; (c) 0.5; (d) 1.0; (e) 2.0; (f) $\geq$ 2.27 mmol l^{-1}. For B, $C^{\circ}_{bg} = 0$; C°_{b} = (a) 0.0; (b) 0.1; (c) 0.5; (d) 1.0; (e) 2.0; (f) 2.27 and (g) 3.0 mmol l^{-1}.

will be required to clear reactant from the chamber (curves f in Fig. 3C and 4A) and sample concentrations at and below that value cannot be determined with the method as described to date [11]. This situation, which develops when the amount of determinant in the sample is just equal to or less than the amount required to clear reactant from the gradient chamber, can be expressed mathematically as $t_1 \geqslant t_2$. This characteristic of the method can be quantified with eqn. (1) by substituting $t_1 \geqslant t_2$ when $C^\circ_{ag} = C^\circ_{as,\,min}$ and substituting $t_2 = V_s/f$. The result after rearrangement is

$$C^\circ_{as,\,min} \leqslant zC^\circ_{bg}/[\exp(V_s/V_g) - 1] \tag{5a}$$

Figure 5 includes plots of $C^\circ_{as,\,min}$ vs. C°_{bg} for different values of V_s/V_g. The points and solid line encompass conditions that have been evaluated experimentally [11]; the dashed lines represent other viable options. The dependence upon V_s/V_g can be visualized more directly by using the approximation, $e^x \approxeq x + 1$ for small x to simplify eqn. (5a) as follows

$$C^\circ_{as,\,min} \lesssim zC^\circ_{bg}V_g/V_s \tag{5b}$$

The most important conclusion drawn from the equations and Fig. 5 is that the minimum concentration can be reduced to a lower limit imposed by the indicator system by performing experiments without any reactant in the gradient chamber when sample is introduced.

The quantity identified above as $C^\circ_{as,\,min}$ is the same quantity obtained by extrapolating t_{eq} vs. ln C plots to $t_{eq} = 0$ [11]. It is important to note that this quantity would represent a detection limit only in the ideal situation of zero noise and infinite sensitivity in the detection system. Because all detectors have finite noise and sensitivity, the actual detection limit would be somewhat larger than $C^\circ_{as,\,min}$. The difference would be small for conditions used to date, but would be substantial for some other viable conditions (e.g., $C^\circ_{bg} \ll C^\circ_{as}$).

Proposed experimental options

Equations and graphical results presented above permit some interesting and potentially useful conclusions to be drawn concerning this general approach. Perhaps the most obvious conclusion is that inclusion of reactant in the gradient chamber when sample is introduced causes both a loss of sensitivity and an increase in the minimum concentration (or amount) of determinant that can be determined. There is one other less obvious but conceptually important conclusion to be drawn from the results.

Růžička et al. [11] made the point that reactant concentration in the flow stream can be adjusted to suit determinant concentration. To take maximal advantage of this suggestion, it is important to know what range of reactant concentrations is possible; to establish that, it is important to identify as precisely as possible the principal role of the reactant. When the relative contributions of the reaction and mass flow processes to the total process in Fig. 3B are compared, it becomes apparent that the relative

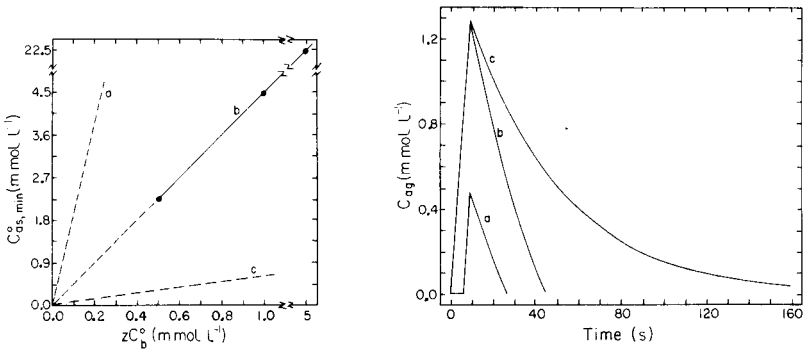

Fig. 5. Effects of flow parameters on minimum concentration that can be determined. V_s/V_g ratio is: (a) 0.05; (b) 0.20; (c) 0.50.

Fig. 6. Effects of reactant concentration in flow stream and gradient chamber on concentration vs. time profiles. $V_g = 0.98$ ml; $V_s = 0.20$ ml; $f = 0.0225$ ml s^{-1}; $C^\circ_{as} = 7$ mmol l^{-1}. (a) $C^\circ_b = C^\circ_{bg} = 1.00$ mmol l^{-1}; (b) $C^\circ_b = 1.00$, $C^\circ_{bg} = 0.0$ mmol l^{-1}; (c) $C^\circ_b = C^\circ_{bg} = 0.00$ mmol l^{-1}.

contribution of the reaction is significant only in the latter stages of the process. The principal difference between experiments conducted with and without reactant in the flow stream for this situation is that the rate of concentration change near the end of the process would be much greater with reactant than without it. Given sufficient time, curve b would drop to the lowest levels shown for curve c. Given these facts, it is difficult to avoid the conclusion that the principal role of the reactant in the flow stream in this case is to produce a more abrupt concentration change at some point in the process than would be observed without it. Although the reaction process contributes a larger fraction of the total change in Fig. 3A, the fact remains that in the absence of reactant in the flow stream, the mass flow process represented by curve b would eventually reduce determinant concentration to a level suitable for measurement of Δt. Therefore, although reactant in the flow stream aids in the detection of reference points between which Δt is measured, it is concluded that similar experiments could be performed without reactant; and because it is shown later that some advantages could accrue from such a procedure, it is suggested that potential users of this general approach should include $C^\circ_b = 0$ as a viable choice in the range of reactant concentrations used to best-suit determinant concentrations.

In summary, this preliminary treatment of the flow-injection experiment with a gradient chamber leads to three combinations of reactant concentrations in the flow-stream and gradient chamber; the combinations are: (a) $C^\circ_b = C^\circ_{bg} > 0$; (b) $C^\circ_b > 0$, $C^\circ_{bg} = 0$; and (c) $C^\circ_b = C^\circ_{bg} = 0$. Concentration vs. time plots for a single low determinant concentration under each of these three sets of conditions are presented in Fig. 6. Of these three options, that with $C^\circ_b > 0$ and $C^\circ_{bg} = 0$ (curve b) would appear to be the most attractive. Its most attractive features are that: (a) the minimum concentration is limited only by detector characteristics rather than by a combination of

detector characteristics and reactant in the gradient chamber; (b) changes at the end-point are abrupt; (c) reactant concentration in the flow stream can be used to adjust measurement time and other characteristics without sacrificing performance at low concentrations; and (d) the throughput rate can be faster than the situation when $C_{bg}^{\circ} = C_{b}^{\circ}$ because it is not necessary to wait between determinations for this condition ($C_{bg}^{\circ} = C_{b}^{\circ}$) to be re-established.

Other characteristics of these three general situations are discussed in the next section.

RESPONSE CURVES

When hydrochloric acid was determined with 1.0 mmol l^{-1} potassium hydroxide and 0.016 mmol l^{-1} bromothymol blue in the reagent flow stream as described earlier [11], response curves were virtually identical to those reported (Fig. 10 [11]) when our experiments were performed with and without reagent in the gradient chamber initially. The curves exhibited abruptly increasing and decreasing signals when the first and last traces of unreacted acid entered and disappeared from the gradient chamber. Time intervals, Δt, for these types of experiments were measured at 50% of the full height of the signal changes.

While these response curves are well suited for quantitative determinations with visual detection of the reference points between which time intervals are measured, they are not useful for monitoring the time-dependent processes that occur away from the abrupt changes [11]. Because these processes involve acid concentration changes in the range of 10^{-3}—10^{-4} mol l^{-1}, an indicator with a transition interval in this range is more useful for continuous monitoring of the time-dependent changes. Bromophenol blue with a transition range of 3.0—4.6 was selected for this study. Buffer solutions were used to evaluate $pK_{HIn} = 3.77$ for the indicator and a molar absorptivity—path length product (ϵb) of 7.15×10^{3} l mol^{-1} for the basic form of the indicator monitored at 590 nm in the flow cell.

Figure 7A is a response curve for 160 mmol l^{-1} hydrochloric acid run with the basic form of bromophenol blue monitored at 590 nm without any potassium hydroxide in the flow stream ($C_{b}^{\circ} = 0$). Although the recorded signal is approximately linear in the concentration of the basic form of the indicator ($\Delta[In^{-}] \cong 1.5 \times 10^{-5}$ mol l^{-1} full scale), indicator response is not linear with change in acid concentration; the plot is much less sensitive to changes in H^{+} at the top than at the bottom. The open circles on the plot were computed with eqn. (4) with $C_{b}^{\circ} = 0$ and using the values of ϵb and pK_{HIn} given above. There is good agreement between theory and experiment for this high acid concentration.

The dashed curve is computed with eqn. (4) for the situation with potassium hydroxide in the flow stream ($C_{b}^{\circ} = 1.00$ mmol l^{-1}). It is observed that the presence of base in the flow stream has little effect on the response curve for more than 70 s. Given that the half-life for the gradient chamber/

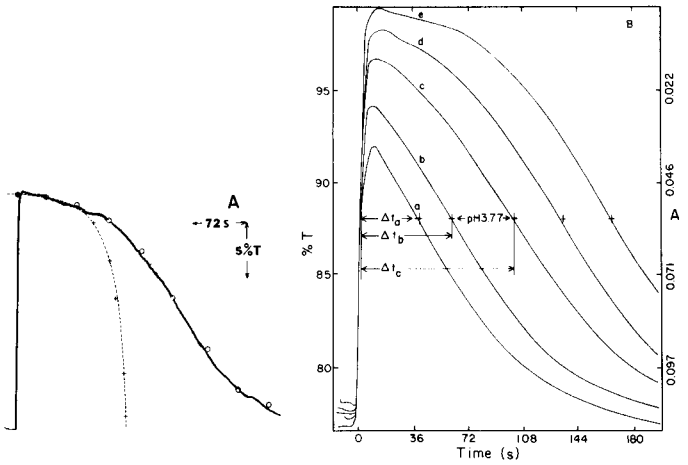

Fig. 7. Response curves for hydrochloric acid determination without potassium hydroxide in flow stream. For A and B, the parallel system (Fig. 1B) was used with V_g = 1.644 ml; V_s = 0.1933 ml; f = 0.0406 ml s^{-1}; $C^\circ_{bg} = C^\circ_b$ = 0.0; bromophenol blue = 0.015 mmol l^{-1}; λ = 590 nm; scale, 75% T to 100% T bottom to top. (A) Solid curve is the detector response; (○) computed response (see text); (+) computed response for C°_b = 1.00 mmol l^{-1} and C°_{bg} = 0.00 mmol l^{-1}. (B) Detector response for C°_{ag} values of: (a) 4; (b) 8; (c) 20; (d) 40; (e) 80 mmol l^{-1}.

flow system is 28 s ($t_{1/2}$ = 0.693 V_g/f), this means that the process has gone through almost three half-lives (ca. 88% complete) before the reagent in the flow stream has any substantial influence on the process. (At 72 s, the HCl concentration would have decreased from its maximum value near 17.6 mmol l^{-1} to about 2.6 mol l^{-1}, with 94% of that change resulting from mass flow and 6% resulting from reaction if 1.0 mmol l^{-1} KOH were included in the flow stream.) In contrast, base in the flow stream accounts for more than 60% of the change between 72 and 124 s. The facts are that potassium hydroxide in the flow stream contributes a relatively small percentage to the total process but produces an abrupt change when the mass-flow process approaches completion. These observations support the earlier conclusion that the principal role of reactant is to enhance the sensitivity of the detection system as the mass-flow process approaches completion. While the percentage contribution of the reaction to the total process increases as the C°_{as}/C°_b ratio decreases (see Fig. 3), the fact remains that the principal function of the reaction is to accelerate a process (decrease in determinant concentration) that would take place in the absence of any reactant in the flow stream.

If the above argument is valid, and if one is willing to forego the potential advantage of the abrupt change to mark the point at which t_3 is measured, then it should be possible to select some fixed reference point on response curves such as that in Fig. 7A, and measure the time interval required for the process to reach that point without any reactant. Figure 7B shows a series of such response curves on which the reference point at 88% T corresponding

to $[In^-]/[HIn] = 1$ has been selected. It is shown later that Δt vs. ln C°_{as} plots are linear with slopes identical to those obtained with reagent in the flow stream.

Some aspects of the curves in Fig. 7B merit discussion. The different shapes for different concentrations result primarily from the nonlinear character of the indicator system. For the higher concentrations ($\geqslant$ 20 mmol l^{-1}), the indicator is forced most of the way into the acid form where it loses sensitivity, and the plots tend to curve toward the time axis as acidity decreases and sensitivity increases. For the lower concentrations, the indicator is in the more nearly linear range near the peaks, but then moves into a low sensitivity region at longer times. Despite this latter problem, plots a and b more accurately reflect the first-order character of the process than do the others. All curves approach the peak values more slowly than expected (V_s/f = 4.7 s), and peak heights for curves (a—d) are not as large as expected (eqn. 3). Both effects reflect deviations from plug flow. This point is treated in more detail in a related paper [8].

The kinetic processes made apparent by these response curves are operative in all applications of this general approach; they are not observed in some cases because indicator conditions are selected to emphasize only the start and end points of the processes between t_1 and t_3 in Fig. 2.

If 1.0 mmol l^{-1} potassium hydroxide had been included in the flow stream and gradient chamber for these experiments, then the minimum concentration predicted with eqn. (5a) would be 8 mmol l^{-1}. The plots in Fig. 7B show well formed response curves down to 4 mmol l^{-1} and could perhaps have been extended to lower levels. This is judged to be convincing evidence for one advantage of initiating experiments with minimal reactant in the gradient chamber, whether it is or is not included in the flow stream.

CALIBRATION PROCEDURES

The concentration vs. time and kinetic response curves presented in earlier sections lend themselves to a variety of data acquisition and data processing options. This discussion is limited to the measurement approach suggested earlier in which the time interval, $\Delta t = t_3 - t_1$ (Fig. 2), is measured, but it includes three different calibration options for the time interval.

Plotting options

Figure 8 (A—C) illustrates three different plotting options for each of the three sets of operating conditions discussed earlier. It should be noted that curves c and c′ in Fig. 8A represent the same data set; curve c is plotted on the same scale as curves a and b to facilitate visualization of relative responses whereas curve c′ is plotted on a compacted scale to show behavior at higher concentrations. These linear coordinate plots all show the same general behavior, namely a continuous decrease in sensitivity as concentration increases. This point, and the associated loss in reliability that can accompany

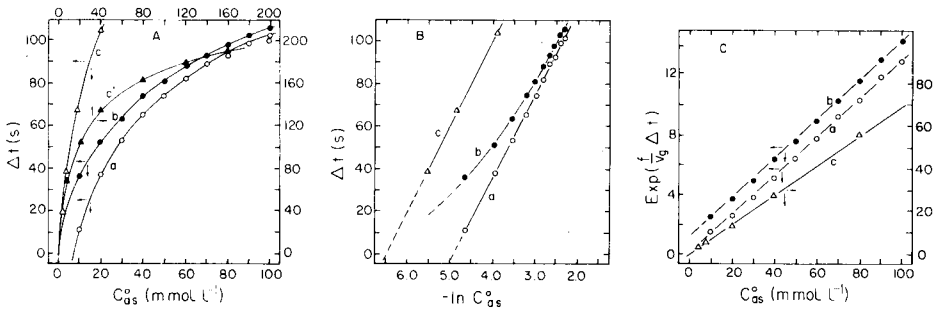

Fig. 8. Calibration plots for hydrochloric acid determined with and without potassium hydroxide in flow stream and gradient chamber, with the parallel system. (A) C°_{as} vs. Δt; (B) $-\ln C^{\circ}_{as}$ vs. Δt; (C) C°_{as} vs. exp ($f\Delta t/V_g$). Conditions as in Fig. 7 with the following exceptions: curves a and b, f = 0.0413 ml s^{-1}, bromothymol blue = 0.016 mmol l^{-1}, λ = 620 nm. Curve a, $C^{\circ}_{b} = C^{\circ}_{bg}$ = 1.00 mmol l^{-1}; curve b, C°_{b} = 1.00 mmol l^{-1}, C°_{bg} = 0.00 mmol l^{-1}; curve c, $C^{\circ}_{b} = C^{\circ}_{bg}$ = 0.0.

the decrease in sensitivity, should be kept fully in mind when other plotting options are used to obtain linear plots. In addition to differences in detailed shapes, the plots also exhibit other differences including the different intercepts and slopes. Curve a has a nonzero intercept because some sample is required to clear reactant from the gradient chamber initially; curves b and c have zero intercepts because there is no reactant in the gradient chamber to be cleared when sample is introduced.

The Δt vs. ln C plots in Fig. 8B show interesting behavior in that plots a and c are linear while curve b exhibits curvature. The common feature between curves a and c is that the reactant concentration in the gradient chamber when sample is introduced is equal to that in the flow stream ($C^{\circ}_{bg} = C^{\circ}_{b}$); the unique feature of curve *b* is that the above equality does not exist ($C^{\circ}_{bg} \neq C^{\circ}_{b}$).

The plotting option in Fig. 8C produces linear plots for all three experimental options. Again, curves a and c share a common feature, namely a zero—zero intercept while curve b is unique in that it has a nonzero intercept. On the other hand, curves a and b have similar slopes while curve c has a much greater slope (note different ordinates).

The plotting format in Fig. 8C would appear to have at least three attractive features. The features are that it produces linear plots for all these experimental options, it is linear in concentration, and it permits more direct visualization of scatter or uncertainty in concentration data than is apparent from ln C plots that tend to compact and obscure uncertainties.

A useful feature of the plots in Fig. 8 is that they exhibit some characteristics that can be used to test any mathematical description proposed for the system. These data are used in the next subsection for a semiquantitative evaluation of equations based on a variable-time kinetic model. The approach is to use the equations to rationalize the shapes, slopes, and intercepts of curves in Fig. 8 (B, C).

Mathematical equations

The variable-time kinetic model applied to this system yields [8] the relationship

$$C^{\circ}_{as} = [A]^{ep}_{g} + zC^{\circ}_{b}\{1 - \exp[-(f/V_g)(t_3 - t_2)]\} \div \{1 - \exp[-(f/V_g)(t_2 - t_1)]\}\exp[-(f/V_g)(t_3 - t_2)] \quad (6)$$

where $[A]^{ep}_{g}$ is the determinant concentration in the gradient chamber at t_3, and other symbols are defined in Table 1. Because this equation is much too complex to visualize dependencies, some simplified forms [8] are used to rationalize the behavior observed in Fig. 8. It will be apparent that the simplified equations involve approximations that make them less reliable than the more rigorous forms discussed later [8]; nevertheless, the simplified forms are very useful for present purposes.

Logarithmic plots. For the situation when $C^{\circ}_{bg} = C^{\circ}_{b}$ (reactant in gradient chamber initially), eqn. (4) can be simplified and rearranged to

$$\Delta t_{ep} = (V_g/f)\ln[\exp(V_s/V_g) - 1]\, C^{\circ}_{as} - (V_g/f)\ln(C^{\circ}_{b} + [A]^{ep}_{g}) \quad (7a)$$

where $\Delta t_{ep} = t_3 - t_1$ and $[A]^{ep}_{g}$ is the determinant concentration in the gradient chamber at the end point. This equation correctly predicts the linear relationships observed for curves a and c in Fig. 8B. For curve a, $C^{\circ}_{b} = 1.00$ mmol l^{-1}, and since the indicator range for bromothymol blue used for that determination is between pH 6.0 and 7.6, $[A]^{ep}_{g}$ is less than 1×10^{-6} mol l^{-1}. Clearly, $C^{\circ}_{b} \gg [A]^{ep}_{g}$ and the last term simplifies to $(V_g/f)\ln C^{\circ}_{b}$. For curve c, $C^{\circ}_{b} = 0$ so that the last term simplifies to $(V_g/f)\ln [A]^{ep}_{g}$. As noted in Fig. 7B, the end point was selected at pH 3.77 corresponding to $[H^+]^{ep}_{g} = 0.17$ mmol l^{-1}. From these observations, it is expected that intercepts on the time axis for curves a and c should differ by $(V_g/f)\ln(C^{\circ}_{b}/[A^+]^{ep}_{g}) = 71$ s. Intercept values in Table 2 for these curves differ by 66 s. The comparison, 66 vs. 71 s, is quite reasonable considering that the extrapolation to $\ln C^{\circ}_{as} = 0$ is an order of magnitude or more beyond the highest concentration value.

TABLE 2

Comparison of experimental results with predictions using simplified equations

Fig. No.	Plot	Situation		Least-squares results[a]			Predicted results		
		C°_{b}	C°_{bg}	Slope	Intercept	Std. error	Slope	Intercept	Eqn. no.
8B	a	>0	C°_{b}	41.7 ± 0.2	201 ± 0.4	0.51	39.8	195	7a
8B	c	0	0	41.5 ± 0.3	267 ± 1	0.9	40.5	269	7a
8C	a	>0	C°_{b}	131 ± 8	−0.07 ± 0.03	0.03	124	0.02	8b
8C	b	>0	0	132 ± 1	1.04 ± 0.04	0.05	118	1.12	8e
8C	c	0	0	694 ± 9.9	−0.6 ± 0.8	1.4	692	0	8c

[a] All correlation coefficients are greater than 0.999.

It is reasonable to compare eqn. (7a) for the case when $C_b^\circ > 0$ with the equation based on a titration model (eqn. 8 [11]). Noting from above that $C_b^\circ \gg [A]_g^{ep}$ and using the approximation, $\exp(V_s/V_g) - 1 \approx V_s/V_g$, eqn. (7a) can be simplified to

$$\Delta t_{ep} \approx (V_g/f) \ln (V_s/V_g)\, C_{as}^\circ - (V_g/f) \ln C_b^\circ \tag{7b}$$

which is equivalent to the expression based on a titration model. In judging the validity of the titration model from this result, the reader should consider several points. Equation (7b) is an approximation based on the two assumptions stated above. For values of V_s and V_g = 0.20 and 0.98 ml used earlier, $\exp(V_s/V_g) - 1 = 0.226$ while $V_s/V_g = 0.204$, corresponding to a 10% difference between the C_{as}° multipliers in eqns. (7a) and (7b). Equation (7b) is valid only for small values of V_s/V_g; eqn. (7a) is valid for any practical value of V_s/V_g. Equation (7a) accounts for any indicator choice while eqn. (7b) is valid only for an indicator system for which $[A]_g^{ep} \ll C_b^\circ$. Equation (7a) is valid for all values of C_b° including $C_b^\circ = 0$ while eqn. (7b) is valid only for $C_b^\circ > 0$. Finally both eqns. (7a) and (7b) are valid only for the situation in which $C_b^\circ = C_{bg}^\circ$; it is shown below that eqn. 4 from which these equations were developed is valid for situations in which $C_b^\circ \neq C_{bg}^\circ$.

Curve b in Fig. 8B shows that when $C_b^\circ \neq C_{bg}^\circ$, plots of Δt vs. $\ln C^\circ$ are not linear and neither eqn. (7a) nor (7b) includes the dependency to account for this. The nonlinear calibration plots can be rationalized with an approximate form of eqn. (4) [8] as follows

$$\Delta t_{ep} \approx (V_g/f) \ln [(V_s/V_g)\, C_{as}^\circ + z(C_b^\circ - C_{bg}^\circ)] - (V_g/f) \ln [[A]_g^{ep} + zC_b^\circ] + (V_s/f) \tag{7c}$$

For the special case in curve b of Fig. 8B, $C_{bg}^\circ = 0$ and $C_b^\circ \gg [A]_g^{ep}$ so that eqn. (7c) reduces to

$$\Delta t_{ep} \approx (V_g/f) \ln [V_s\, C_{as}^\circ/V_g + zC_b^\circ] - (V_g/f)\, z \ln C_b^\circ + V_s/f \tag{7d}$$

As C_{as}° approaches zero, the first logarithmic term will approach the fixed value of $\ln zC_b$, and the slope of the plot is expected to decrease as shown in curve b of Fig. 8B. It is satisfying that this behavior was predicted before any experimental work was begun and in fact suggested the experiments used to verify it. This ability to predict this unusual behavior is judged to be rather convincing evidence for the viability of the variable time kinetic model.

While it is easy to understand why curve c in Fig. 8B is linear and why curve b is nonlinear, it is not so easy to understand precisely why curve a is linear. For the situation in curve c, there is no reactant, and the mass flow process should give the pure first-order decay needed for linear Δt vs. $\ln C_{as}^\circ$ plots. For the situation in curve b, the net process is a combination of zero- and first-order processes that are not expected to give linear Δt vs. $\ln C$ plots. The discussion associated with Fig. 3 (A and B) showed that the zero-order process predominates when $C_{as}^\circ \cong C_b^\circ$, and that the first-order process predominates when $C_{as}^\circ \gg C_b^\circ$. Accordingly, the slopes of Δt vs. $\ln C$ plots are expected to increase from unity at low determinant concentrations to V_g/f

at high concentrations. That is the reason for the curvature in curve b and similar curvature noted for other such curves later [8]. Similarly, data in curve a result from a combination of zero- and first-order processes; however, the presence of reactant in the gradient chamber equivalent to that in the flow stream causes the system to behave mathematically as if it were first-order. Reasons for this behavior are discussed in detail in the related paper; for the present it is simply stated that the amount of determinant that reacts between t_0 and t_1 exactly compensates for that portion of the zero-order process that contributes nonlinearity in curve b in Fig. 8B.

Least-squares slopes and intercepts for data in curves a and c are compared in Table 2 with values computed with eqns. (7b) and (7d) above. Agreement between experimental and predicted slopes is 5% or better and agreement between intercepts is 3% or better. Also, agreement between experimental slopes (41.7 vs. 41.5) is excellent. The standard error of estimate is 1.5% or less of the mean Δt, suggesting a high degree of linearity for the plots.

Exponential plots. For the situation when $C^\circ_{bg} = C^\circ_b$, eqn. (7a) is applicable and can be arranged to

$$\exp[(f/V_g)\Delta t_{ep}] = C^\circ_{as}[\exp(V_s/V_g) - 1]/(C^\circ_b + [A]^{ep}_g) \tag{8a}$$

This equation predicts a proportional relationship between the exponential term and determinant concentration; that relationship is confirmed by experimental data in curves a and c of Fig. 8C and entries for these data in Table 2 that show intercepts of -0.07 and -0.7, respectively.

For experiments with $C^\circ_b = 1.0$ mmol l^{-1} and bromothymol blue indicator, C°_b is much larger than $[A]^{ep}_g$ and eqn. (8a) simplifies to

$$\exp[(f/V_g)\Delta t_{ep}] = C^\circ_{as}[\exp(V_s/V_g) - 1]/C^\circ_b \tag{8b}$$

For curve a in Fig. 8C, the least-squares slope is 131 l mol^{-1} compared with a computed value (eqn. 8b) of 124 l mol^{-1} corresponding to a difference of less than 6%.

For experiments with $C^\circ_b = 0$, eqn. (8a) simplifies to

$$\exp[(f/V_g)\Delta t_{ep}] = C^\circ_{as}[\exp(V_s/V_g) - 1)/[A]^{ep}_g \tag{8c}$$

Curve c in Fig. 8C represents this situation with $[A]^{ep}_g = 0.17$ mmol l^{-1}. The experimental slope (Table 2) of 694 compared with a computed value (eqn. 8c) of 734 l mol^{-1}, corresponding to a difference of 5%.

For the situation when reactant concentration in the flow stream and gradient chamber are not equal when sample is introduced ($C^\circ_{bg} \neq C^\circ_b > 0$), an alternative approximate form of the equation [8] is

$$\exp[(f/V_g)\Delta t_{ep}] \approx V_s C^\circ_{as}/V_g z C^\circ_b + V_s/V_g + 1 - C^\circ_{bg}/C^\circ_b - zC^\circ_{bg}/C^\circ_{as} \tag{8d}$$

For the special case in curve b of Fig. 8C when $C^\circ_b > 0$ and $C^\circ_{bg} = 0$, eqn. (8d) simplifies to

$$\exp[(f/V_g)\Delta t_{ep}] \approx V_s C^\circ_{as}/V_g z C^\circ_b + V_s/V_g + 1 \tag{8e}$$

Slope and intercept computed with this equation for conditions in curve b are 118 l mol^{-1} and 1.12, respectively, compared with experimental values of 132 and 1.04 in Table 2.

While there are differences between experiment and theory that exceed experimental uncertainty at the 95% confidence level, all of these equations account quite reasonably for gross differences among characteristics of different operating procedures. Some key points to note are the accurately predicted curvature of curve b in Fig. 8B, the substantially greater sensitivity of the situation when $C_b^\circ = 0$ relative to when $C_b^\circ > 0$ (curves c and a in Fig. 8C), and the nonzero intercept for curve b in Fig. 8C. All of these features and others were predicted quantitatively before any experiments were conducted. All these points are judged to lend strong support to the validity of these equations within the limitations of assumptions stated earlier.

SUBJECTIVE COMPARISONS

Because the method discussed above is one of many (see references in [11]) identified as continuous-flow titrations, and because the model used to identify a method can influence the manner in which it is treated and implemented, it is desirable to generalize the above presentation somewhat. Some reference to common practice and two formal definitions will be useful in this discussion.

Titration procedures in present analytical textbooks involve detection of the point of more or less complete reaction between two species with associated measurement of the amount of one species required to react with a measured amount of a solution of the other. Titration has been defined [16] as "... the process of determining a substance A by adding increments of substance B (almost always a standardized solution) with provision for some means of recognizing the point at which all A has reacted, thus allowing the amount of A to be found from the known amount of B added up to this point, the reacting ratio of A and B being known from stoichiometry or otherwise". Because some reagent or sample must be flushed out of the gradient chamber when sample or reagent flows into it, it is clear that the procedures discussed above and in [11] cannot satisfy the criterion of a titration that all of determinant (A) must react. Figure 3 (A, B) shows the relative amounts of determinant that react and that are "lost" via mass flow for two sets of conditions. This equivalence criterion is a critical one in determining some of the most significant advantages and limitations of titration methods. Furthermore, response curves in Fig. 7B show that very similar experiments can be conducted without reactant in the flow stream, and those determinations clearly are not titrations. Calibration results in Fig. 8 (A—C) as well as the equations presented above strongly suggest that all of these experiments are part of the same general group; experiments with and without reagent are special cases of the same general approach.

While the equation based on a titration model has proven useful, it is substantially less complete than equations based on a kinetic model. In our view, it is in the best interest of this methodology to use more accurately descriptive terminology to represent it.

Although some colorimetric indicators used to date [11] tend to obscure the time-dependent processes that take place in this flow injection procedure, the potentiometric response curves [11], specially selected indicator conditions used above (Fig. 7), and computed concentration vs. time curves presented above emphasize time-dependent changes during the process. Given the formal definition of kinetics [17] as "a branch of physical science that deals with the rate of change in a physical or chemical system" (the universality should be noted), and the fact that the measurement objective (Δt) in these experiments depends upon the rates of physical processes (mass flow), it is difficult to avoid the conclusion that this approach is most accurately identified as some type of kinetic method.

A key feature of this method is that what is measured and related to concentration is the time required for a process to pass between two predetermined reference points. Such procedures have been identified for many years as variable-time kinetic methods [14, 15, 18]. Because this method satisfies all the criteria of a variable-time kinetic method, because it does not satisfy all the criteria of titrations [16], and because the variable-time kinetic model leads to a more complete mathematical treatment of the system than the titration model, it appears that the kinetic terminology is the most accurately descriptive of method concepts and characteristics.

These ideas are not limited to this flow injection procedure. Figure 9A shows dot tracings of response curves for a procedure [10] in which a sample stream at constant flow rate is mixed with a reagent stream in which the amount of reactant per unit of time mixing with the sample stream increases linearly with time for a period and then decreases linearly with time. The descending plot in Fig. 9B is the calibration curve obtained when the quantity, $\Delta t = t_n' - t_n$ (identified as Q_c [10]) is plotted vs. concentration. It is apparent from the experimental procedure that total amounts of reactant and determinant are not equivalent during the measurement interval; there-

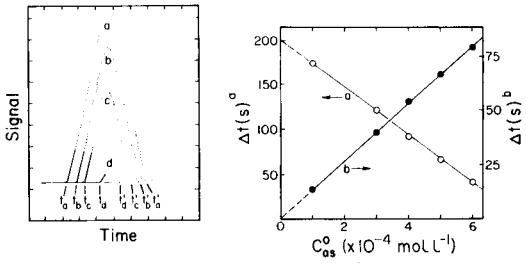

Fig. 9. Dot tracings of response curves and calibration plots for ascorbic determinations [10]. A, Dot tracings for (a) 0.0; (b) 0.25; (c) 0.55; (d) 1.1 mmol l^{-1}. B, Calibration plots Δt^a is Q_c from [10]; Δt^b is $t_b - t_a$, $t_c - t_a$, and $t_d - t_a$.

fore this method does not satisfy the equivalency criterion of a titration [16]. The procedure meets all the criteria of a variable-time kinetic method, and viewing it as such, it became apparent that the information needed to complete a determination could be obtained from that portion of the response curves represented by solid lines in Fig. 9A. The ascending plot in Fig. 9B is a calibration plot obtained by plotting $\Delta t = t_b - t_a$, $t_c - t_a$, $t_d - t_a$, etc. vs. concentration. It is easily shown that the relationship for these plots is

$$C_{as}^{\circ} = [z(dI/dt)/f_s mF]\,\Delta t \qquad (9)$$

where dI/dt is the rate of change of electrolysis current, f_s is the sample flow rate, m is the electrons per molecule in the electrolysis process, F is the Faraday constant, and other symbols are defined in Table 1. Because dI/dt (or df_b/dt for variable flow rates) increases linearly, what is measured is the time required for the reactant concentration in the flow stream to become equivalent to the determinant concentration; the procedure is analogous to a zero-order chemical kinetic process.

The alternative revised procedure suggested by the variable-time kinetic model has the advantages of a proportional relationship between concentration and the measurement objective and that the current (or flow) gradient need not be reversed and can therefore be extended to higher levels for higher sample concentrations. The reduction in measurement time (Δt vs. 2τ [10]) might influence the throughput rate substantially.

It should not be concluded from these examples that none of the continuous-flow procedures satisfy the equivalency criterion of a titration. In an earlier method [9], reagent flow rate is adjusted until it is chemically equivalent to the sample stream. Because the quantity measured and related to concentration is the flow rate needed to maintain the condition of chemical equivalency, amounts of reagent and sample are equivalent throughout the measurement period. Because the method satisfies the criterion of chemical equivalency between determinant and reactant, it is accurately identified as a titration; because the equivalency condition involves a steady state between two rate processes, the procedure is most accurately identified as a kinetic titration. Care should be exercised to differentiate between this kinetic titration and equilibrium titrations with kinetic end-point detection [19].

The relative merits of direct measurement methods and titrimetric methods were compared briefly in the flow injection paper [11]. It is important to note that titrimetric methods represent just one example of a group of methods that can be identified as indirect methods in the sense that what is measured and related to concentration is not detector signal, but rather some other variable such as volume, time, electrolysis current, etc. The variable-time kinetic method, like a titration, is a part of the indirect measurement category; the fixed-time kinetic method [14, 15, 18], like direct measurements of absorbance or electrode potential at equilibrium, is part of the direct measurement category. All the indirect methods have the

common feature that it is not essential to know the mathematical relationship between detector signal and determinant concentration as is the case with direct measurement methods.

CONCLUSIONS

The kinetic view of this general procedure has added to its scope by suggesting alternatives to procedures reported to date. The procedure that appears most attractive involves the use of reactant in the flow stream with introduction of the sample into a gradient chamber containing little or no reactant. Two potential advantages of this procedure are the lower concentrations to which it should be applicable and the shorter time between samples; two potential disadvantages are that this procedure is more sensitive to variations in the initial reactant concentration in the chamber than those for which $C^{\circ}_{bg} \approx C^{\circ}_{b}$, and the nonlinear Δt vs. ln C°_{as} plots that result when $C^{\circ}_{bg} \neq C^{\circ}_{b}$ (Fig. 8B). The latter point is not judged too significant because our preference is for the exponential plots (Fig. 8C) that are linear for all situations.

In addition to offering new insight into the quantitative characteristics of this approach, and suggesting different experimental procedures, the variable-time kinetic view has other implications. Because chemical reactions are an inherent part of titration procedures, they are limited to species for which suitable reactants are available. Because the reactant is not an essential part of these flow injection methods, they are not limited to species for which suitable titrants are available. Also, it is suggested that the triangular gradient method [10] could be implemented with a second reference flow stream containing determinant by noting the time required for determinant flow rate in the reference stream to become equivalent to that in the sample stream. No reaction would be required and the end result would be essentially the same. Whether these features have real analytical utility remains to be seen; however, it is a feature common to null-point methods [20] that have found some utility, and should be recognized so that any potential value can be exploited.

Finally, it should be noted that the acid/base reaction with color indicator used above served only as an illustrative example; conclusions drawn are general and should apply for a wide variety of different combinations of species and detectors with and without chemical reactions. In fact, it is probable that some conclusions related to minimum concentrations can be exploited more effectively with other systems that are not complicated by buffering effects, dissolved carbon dioxide, lower limits imposed by acid–base properties of water, and complex indicator behavior. In particular, it should be noted that when no alkali is used in the flow stream for the determination of acids, then the acid–base indicator is the principal reactant and imposes a lower limit on the acid concentration that could be determined even in the absence of other complicating features.

It is re-emphasized that the variable-time kinetic view of these methods [10, 11] does not restrict their applications but rather broadens their scope to determinations of many species for which suitable titrants are not available. Data processing methods adapted over the years for chemical kinetic methods [14, 15] are almost certainly applicable to these physical kinetic methods.

This investigation was supported by Research Grant No. GM 13326-13 from the NIH, USPHS.

REFERENCES

1 J. Růžička and E. H. Hansen, Anal. Chim. Acta, 78 (1975) 145.
2 K. K. Stewart, G. R. Beecher and P. E. Hare, Anal. Biochem., 70 (1976) 167.
3 D. Betteridge, Anal. Chem., 50 (1978) 833A.
4 Proceedings of an International Conference on Flow Analysis, Anal. Chim. Acta, 114 (1979).
5 H. A. Mottola and A. Hanna, Anal. Chim. Acta, 100 (1978) 167.
6 J. Růžička and E. H. Hansen, Anal. Chim. Acta, 99 (1978) 37.
7 H. A. Mottola, CRC Crit. Rev. Anal. Chem., 4 (1975) 229.
8 H. L. Pardue and B. Fields, Anal. Chim. Acta, 124 (1981) 65.
9 W. J. Blaedel and R. H. Laessig, Anal. Chem., 36 (1964) 1617.
10 G. Nagy, Zs. Feher, K. Toth and E. Pungor, Anal. Chim. Acta, 100 (1978) 181.
11 J. Růžička, E. H. Hansen and H. Mosbaek, Anal. Chim. Acta, 92 (1977) 235.
12 W. Roberts, Proc. R. Soc. London, 32 (1881) 145.
13 H. A. Mottola, J. Chem. Educ., in press.
14 H. L. Pardue, Clin. Chem., 23 (1977) 2189.
15 H. V. Malmstadt, E. A. Cordos and C. J. Delaney, L. Meites (Ed.), in CRC Reviews in Analytical Chemistry, CRC Press, Cleveland, OH, 1972, p. 559.
16 H. M. N. H. Irving, H. Freiser and T. S. West, IUPAC Compendium of Analytical Nomenclature, Definitive Rules 1977, Pergamon, Oxford, 1978, p. 41.
17 Webster Third New International Dictionary of the English Language, Unabridged, G. and G. Merriam, Springfield, MA, 1961.
18 W. J. Blaedel and G. P. Hicks, in C. N. Reilley (Ed.) Advances in Analytical Chemistry and Instrumentation, Vol. 3, J. Wiley, New York, 1964, pp. 105.
19 H. A. Mottola and H. Freiser, Anal. Chem., 40 (1968) 1266.
20 R. A. Durst and J. K. Taylor, Anal. Chem., 39 (1967) 1374.

Analytica Chimica Acta, 124 (1981) 65—79

KINETIC TREATMENT OF UNSEGMENTED FLOW SYSTEMS
Part 2. Detailed Treatment of Flow-Injection Systems with Gradient Chamber

HARRY L. PARDUE* and BERNARD FIELDS**

Department of Chemistry, Purdue University, West Lafayette, IN 47907 (U.S.A.)

(Received 30th June 1980)

SUMMARY

A kinetic model is utilized for a detailed mathematical treatment and experimental evaluation of single-channel and dual-channel flow injection systems that include a gradient chamber. The kinetic model includes three distinct stages in the process, namely clearing reactant from the gradient chamber by first portions of sample, continued entry of sample into the gradient chamber, and decrease of determinant concentration in the gradient chamber via dilution and reaction with reagent. Equations predict entirely different behavioral patterns for different conditions and these predictions are verified experimentally for a wide range of conditions. The data show that the variable-time kinetic model is superior to the titration models previously utilized to describe these flow systems. The principal limitation of the kinetic equations involves an assumption of plug flow that is not completely valid. The extent of deviations from ideal behavior depend on conditions, but are negligible at low concentrations (0—50 mmol l^{-1}) and can be 10% or larger at higher concentrations (>100 mmol l^{-1}). While equations are not exact, they are useful in predicting performance characteristics for a variety of conditions and experimental approaches.

A related paper [1] has discussed subjectively and semiquantitatively the kinetic character of three procedures [2—4] that use unsegmented-flow sample processing. It was concluded that one procedure [2] is best identified as a kinetic titration and that two procedures [3, 4] are best identified as variable-time kinetic methods. A kinetic approach to one procedure [3] results in modest procedural and data processing improvements while the kinetic approach to another procedure [4] results in substantial improvements in the quantitative description of the method. Simplified equations based on a kinetic model of the flow injection system [4] correctly predicted complex behavior patterns that are quite different for different operating conditions and that were verified experimentally.

This paper discusses the kinetic model and detailed equations resulting from it in more detail for both single-channel and dual-channel flow-injection systems that include gradient chambers [4]. The model involves a three-step process in which (a) some of the species to be determined (the determinant) reacts with the reagent in the gradient chamber as the first portions of sample

**Present address: I.C.I. Petrochemicals Division, Wilton, Gt. Britain.

enter the chamber, (b) the determinant concentration in the gradient chamber increases to a maximum value as that portion of the sample not required to clear reactant enters the chamber, and (c) the determinant concentration in the chamber decreases toward a predetermined reference point as a result of dilution and reaction with reagent in the flow stream. Differential equations describing these processes are formulated and integrated using appropriate boundary conditions. The resulting equations take account of parameter dependencies that both have and have not been considered in the past.

It is shown that kinetic-model equations give substantially better agreement with experimental observations than do the titration-model equations reported previously. It is also shown that some deviations from ideal behavior that tend to be most significant at highest determinant concentration probably result from failure of the plug-flow assumption made to simplify the derivations. Despite these deviations, the kinetic equations give substantially better insight into parameter dependencies than has been available, and they can be used to identify and test the relative merits of different operating procedures.

EXPERIMENTAL

General

Hydrochloric acid was determined using potassium hydroxide as reactant. Basic forms of bromothymol blue and bromophenol blue were monitored at 620 and 590 nm, respectively. Ascorbic acid at pH 2.3 used as a tracer in some experiments was monitored at 254 nm. All solutions were prepared and handled with usual care; there are no special features that merit comment.

Symbols used in this paper are identical to those tabulated earlier [1] and details are not repeated here except to note that C_A° and C_B° refer to the initial analytical concentration of determinant and reactant, respectively, C_a and C_b refer to the instantaneous concentrations of determinant and reactant, $[A]^p$ and $[B]^p$ refer to the instantaneous concentrations at some point, p, corresponding to a discontinuity in a response curve or a preselected reference point, z is the reaction ratio between determinant A, and reactant B, and subscripts a, b, s, r, and g refer to determinant, reactant, sample, reagent, and gradient chamber, respectively. Some typical examples are C_{as}°, C_{bg}°, and $[A]_g^{ep}$ which represent the determinant concentration in the unmodified sample, the reagent concentration present initially in the gradient chamber, and the determinant concentration at an end-point. The symbol t represents the elapsed time relative to the point when sample first begins to enter the gradient chamber, and Δt represents a time interval between any two selected reference points.

The series and parallel sample introduction systems used in this work were described earlier [1]. Parameter values are presented in figure legends.

Reagents, apparatus, and procedures

Reagents, apparatus, and procedures were as described earlier [1] except for the ascorbic acid tracer experiments. A 2.5×10^{-4} mol l^{-1} solution of ascorbic acid (J. T. Baker, reagent grade) in 0.005 mol l^{-1} hydrochloric acid was used in the tracer studies. The carrier stream was 0.005 mol l^{-1} hydrochloric acid.

An Altex analytical u.v. detector 153, was used in conjunction with a filter at 254 mm and a cell path length of 0.5 mm in the tracer studies.

KINETIC TREATMENT

This treatment is presented for a single-channel system with and without reagent in the flow stream, and for a dual-channel system.

Models

The physical model on which the treatment of the single-channel system is based was presented earlier (Fig. 2 [1]). Figure 1 illustrates important differences among the different systems to be discussed below. Figure 1A represents a typical concentration vs. time profile in the gradient chamber for a low determinant concentration in a single-channel system with reactant present initially in the flow stream and gradient chamber. Figure 1B represents the concentration vs. time profile in the gradient chamber for the same determinant concentration in the single-channel system without reactant in the flow stream and for the dual-channel system.

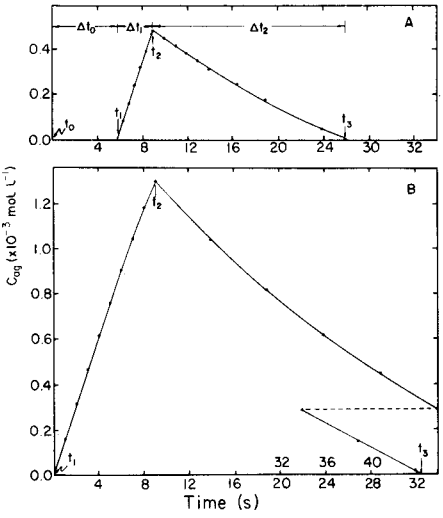

Fig. 1. Computed concentration vs. time profiles for determinant in gradient chamber. Equations (4b) for A and (6a) for B, and related equations, were used in the calculations. V_g = 0.98 ml; V_s = 0.20 ml; f = 0.0225 ml s^{-1}; C°_{as} = 7 mmol l^{-1}. (A) $C^{\circ}_{bg} = C^{\circ}_{b}$ = 1.00 mmol l^{-1}; (B) $C^{\circ}_{bg} = C^{\circ}_{b}$ = 0.00 mmol l^{-1}.

For the single-channel system with reactant, sample begins to enter the gradient chamber and to react with reactant at t_0. At t_1, all reactant in the chamber is removed and the determinant concentration increases as sample continues to enter the chamber. At t_2, all sample will have entered the chamber, the concentration will have reached a maximum value, and the concentration begins to decrease toward zero as a result of dilution and reaction with reactant in the flow stream. The point at t_3 is identified as the time at which the concentration decreases to a preselected reference point as determined by a suitable detection system. The measurement objective in experiments reported to date is the interval, Δt, between t_1 and t_3.

For the single-channel system without reactant and the dual-channel system, there is no reactant to be cleared from the gradient chamber, and the determinant concentration begins to increase when the first increment of sample enters the gradient chamber so that $t_0 = t_1 = 0$. Because the sample does not react as it enters the chamber, the maximum concentration is higher in Fig. 1B than in Fig. 1A; because there is no reactant in the flow stream, the effective rate constant for the decay process is smaller in Fig. 1B than in Fig. 1A.

Concentration vs. time profiles monitored at the detector will be similar to that in Fig. 1A for the single-channel system with reactant and the dual-channel system, and will be that in Fig. 1B for the single-channel system without reactant.

Concentration vs. time profiles for the single-channel system with reactant in the flow stream but no reactant in the gradient chamber initially will be a composite of Fig. 1B between t_1 and t_2 and Fig. 1A beyond t_2.

Assumptions. The principal assumptions made in this treatment are that: (a) the chemical reactions proceed to completion rapidly; (b) sample introduction involves plug flow; (c) mixing in the gradient chamber is instantaneous; and (d) there is no mixing between the gradient chamber and the detector. Deviations from this ideal behavior are discussed later.

Single-channel system with reactant

The single-channel system with reactant is treated first because equations for this system are easily modified to be applicable to the other systems. This system is treated in the three stages represented in Fig. 1A.

First stage ($t_0 \leqslant t \leqslant t_1$). During the first stage when reagent is being cleared from the gradient chamber, the determinant concentration in the chamber is zero, and it is most convenient to discuss the time dependence of the reagent concentration. The rate of change of reagent concentration is given by

$$-\mathrm{d}C_{bg}/\mathrm{d}t = f\,C^{\circ}_{as}/z\;V_g + f\,C_{bg}/V_g \qquad (1a)$$

where the first term on the right accounts for reaction with determinant and the second term accounts for dilution. Integration, substitution of $C_{bg} = C^{\circ}_{bg}$ at $t = 0$, and rearrangement yields

$$C_{bg} = (C^{\circ}_{as}/z + C^{\circ}_{bg}) \exp(-ft/V_g) - C^{\circ}_{as}/z \quad (\text{for } 0 \leqslant t \leqslant t_1) \tag{1b}$$

At the end of this stage, $C_{bg} = 0$ at t_1 so that eqn. (1b) rearranges to

$$t_1 = (V_g/f)\ \ln(1 + zC^{\circ}_{bg}/C^{\circ}_{as}) \tag{1c}$$

which shows the dependence of the length of this process on the initial sample and reagent concentrations.

Second stage ($t_1 \leqslant t \leqslant t_2$). During this stage, the rate of increase in determinant concentration is given by

$$dC_{ag}/dt = (f/V_g)\ C^{\circ}_{as} - (f/V_g)\ [A]_g \quad (\text{for } t_1 \leqslant t \leqslant t_2) \tag{2a}$$

which upon integration and substitution of $C_{ag} = 0$ at $t = t_1$, yields

$$C_{ag} = C^{\circ}_{as}\ (1 - \exp[-(f/V_g)\ (t - t_1)])\ \ (\text{for } t_1 \leqslant t \leqslant t_2) \tag{2b}$$

which confirms first-order behavior, but in the time interval, $\Delta t_1 = t - t_1$ rather than total elapsed time. Determinant concentration will reach its maximum value in the gradient chamber when $t = t_2$ so that eqn. (2b) yields

$$[A]^{max}_g = C^{\circ}_{as}\ (1 - \exp\ [-(f/V_g)(t_2 - t_1)])\ \tag{2c}$$

where, for plug flow, $t_2 = V_s/f$.

Third stage ($t_2 \leqslant t \leqslant t_3$). During this stage, the rate of decrease in determinant concentration is given by

$$-dC_{ag}/dt = f\ C_{ag}/V_g + z\ f\ C^{\circ}_b/V_g \quad (\text{for } t \geqslant t_2) \tag{3a}$$

which upon integration and substitution $C_{ag} = [A]^{max}_g$ (eqn. 2c) at $t = t_2$ yields

$$C_{ag} = C^{\circ}_{as}\ \{1 - \exp\ [-(f/V_g)(t_2 - t_1)]\} \exp\ [-(f/V_g)(t - t_2)]$$
$$- zC^{\circ}_b\ \{1 - \exp\ [-(f/V_g)(t - t_2)]\}\ \ (\text{for } t \geqslant t_2) \tag{3b}$$

which emphasizes the relationships among the different time intervals in Fig. 1A.

Single-channel system without reactant

Equations for this system can be obtained by setting $C^{\circ}_b = 0$ and $C^{\circ}_{bg} = 0$ in eqns. (1–3) above.

First stage. Setting $C^{\circ}_{bg} = 0$ in eqn. (1c) confirms the expected result that $t_1 = 0$ (see Fig. 1B) because there is no reactant to be cleared from the gradient chamber.

Second stage ($t_1 \leqslant t \leqslant t_2$). Equations (2b) and (2c) with $t_1 = 0$ and $t_2 = V_s/f$ reduce to

$$C_{ag} = C^{\circ}_{as}\ [1 - \exp\ (-ft/V_g)]\ \ (\text{for } t_1 \leqslant t \leqslant t_2) \tag{4a}$$

and

$$[A]^{max}_g = C^{\circ}_{as}\ [1 - \exp\ (-ft_2/V_g)]\ \ (\text{at } t = t_2) \tag{4b}$$

which confirm the expected pure exponential rise in concentration when $C^{\circ}_{bg} = 0$.

Third stage ($t_2 \leqslant t \leqslant t_3$). Equation (3b) with $t_1 = 0$ and $C^{\circ}_{b} = 0$ simplifies to

$$C_{ag} = C^{\circ}_{as} \{1 - \exp [-ft_2/V_g]\} \exp [-(f/V_g)(t - t_2)] \quad (\text{for } t > t_2) \tag{5}$$

where the term in brackets on the right is $[A]^{max}_{g}$ from eqn. (2c). This equation predicts the expected first-order decay, but in terms of $[A]^{max}_{g}$ which is a fixed fraction of C°_{as}.

Dual-channel system

Because no reactant flows through the gradient chamber in the dual-channel system [4], all points and equations presented in the previous section apply for concentrations in the gradient chamber. However, concentrations monitored by the detector are substantially different from those in the gradient chamber because of reaction and dilution at the mixing point. These concentrations must be treated in the same three stages described for the single-channel system.

First stage ($t_0 \leqslant t \leqslant t_1$). During this stage, determinant concentration at the detector is zero ($C_{ad} = 0$) and reactant concentration varies with time as follows

$$C_{bd} = \{zf_r C^{\circ}_{b} - f_s C^{\circ}_{as} [1 - \exp (-ft/V_g)]\}/(f_s + f_r) \quad (\text{for } t_0 \leqslant t \leqslant t_1) \tag{6a}$$

Substituting $[B]_d = 0$ at t_1, into eqn. (6a) and rearranging yields

$$t_1 = (V_g/f) \ln [f_s C^{\circ}_{as}/(f_s C^{\circ}_{as} - zf_r C^{\circ}_{b})] \tag{6b}$$

Second stage ($t_1 \leqslant t \leqslant t_2$). After t_1, determinant from the gradient chamber chemically exceeds reactant in the flow stream ($f_s C_{ag} \geqslant zf_r C^{\circ}_{b}$), and determinant concentration at the detector increases:

$$C_{ad} = \{f_s C^{\circ}_{as} [1 - \exp (-ft/V_g)] - zf_r C^{\circ}_{b}\}/(f_s + f_r) \quad (\text{for } t_1 \leqslant t \leqslant t_2) \tag{7}$$

The maximum determinant concentration monitored at the detector, $[A]^{max}_{d}$, can be computed by substituting $t = t_2 = V_s/f_s$ into eqn. (7).

Third stage ($t_2 \leqslant t \leqslant t_3$). During this stage, the determinant concentration decreases according to

$$C_{ad} = \{f_s C^{\circ}_{as} [1 - \exp [-f(t_2 - t_1)/V_g]] \exp [-f(t - t_2)/V_g] - zf_r C^{\circ}_{b}\}/(f_s + f_r) \quad (\text{for } t > t_2) \tag{8}$$

where t_1 is computed with eqn. (6b) and $t_2 = V_s/f_s$.

These equations are evaluated and discussed below.

RESULTS AND DISCUSSION

Tracer experiments

Ascorbic acid monitored at 254 nm was used as a tracer to evaluate the extent to which deviations from the ideal assumptions influenced concen-

trations monitored at the detector in the single-channel system with series and parallel sample introduction (Fig. 1 [1]). Figure 2 presents experimental data along with results (solid lines) computed with eqns. (4a), (4b), and (5). Ordinates are plotted on log scales so that regions corresponding to and deviating from expected first-order behavior are visualized more readily. Good agreement between experimental and predicted response is observed at all points except regions near $t = 0$ and $t = t_2$. Deviations in these regions almost certainly result from deviations from plug flow during sample entry into the gradient chamber.

Because the flow at the center of a tube is greater than the average flow rate, f, it is expected that some tracer will reach the gradient chamber before the time predicted assuming plug flow, and because flow near the tube walls is slower than the average flow rate, it is expected that a time greater than V_s/f will be required for all tracer to enter the chamber, and it is expected that the observed maximum concentration will be less than predicted on the basis of plug flow. The estimated time difference ($t_{0,\,\mathrm{exp}} - t_{0,\,\mathrm{calc}} \approx -2$s) is expected to be the same for both systems because flow rates are similar and line lengths between sampling point and the gradient chamber are the same. The maximum concentration ratios ($[A]^{max}_{exp}/[A]^{max}_{calc}$) obtained by extrapolating theoretical lines for $t > t_2$ to t_2 are 0.76 for the series system and 0.86 for the parallel system. Not only does the parallel system give a maximum concentration closer to the value expected for ideal behavior, but the peak value also occurs closer to the expected time, $t_2 = V_s/f$.

While both systems deviate from ideality, the parallel system is expected to give better agreement with equations developed above than the series

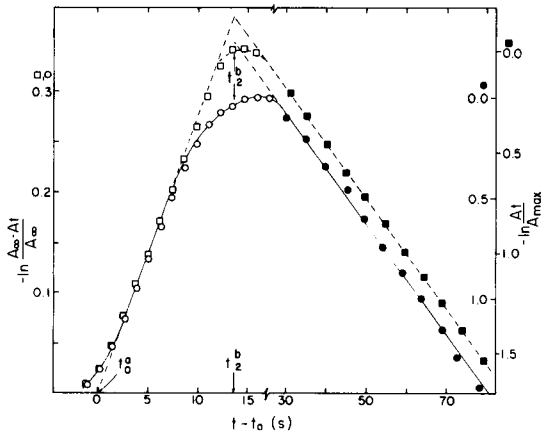

Fig. 2. Results for ascorbic acid used as tracer in the flow systems. V_g = 1.191 ml; V_s = 0.456 ml; C°_{as} = 0.25 mmol l^{-1}; wavelength = 254 nm. (○, ●) Series sample introduction [1], f = 0.0339 ml s^{-1}. (□, ■) Parallel sample introduction [1], f_r = 0.0329, f_s = 0.0338 ml s^{-1}.

system. The deviations should be kept in mind during subsequent discussions in this paper and in applications of these methods.

Single-channel system with reactant

Because the single-channel system with reactant is the most complex of the three systems, it offers the opportunity for the most rigorous testing of equations.

Alternative forms of equations. Some alternative forms of equations presented earlier [1] will be useful for this discussion. After substituting $C_{ag} = [A]_g^{ep}$ at t_3 and $t_3 = \Delta t_{ep} + t_1$ into eqn. (3b), it can be arranged to

$$\exp(f\,\Delta t_{ep}/V_g) = \{C_{as}^\circ\,[\exp[f(t_2 - t_1)/V_g] - 1] + zC_b^\circ \exp[f(t_2 - t_1)/V_g]\}/([A]_g^{ep} + zC_b^\circ) \quad (9a)$$

For computer processing of $\exp(\Delta tf/V_g)$ vs. C_{as}° data, this equation can be expressed in terms of experimental parameters by substituting $t_2 = V_s/f$ and $t_1 = (V_g/f)\ln(1 + C_{bg}^\circ/C_{as}^\circ)$ from eqn. (1c) above. The result is

$$\exp(f\Delta t_{ep}/V_g) = C_{as}^\circ\,\{C_{as}^\circ\,[\exp(V_s/V_g)]\,(zC_b^\circ + 1) - C_{as}^\circ - C_{bg}^\circ\}/(C_{as}^\circ + C_{bg}^\circ)([A]_g^{ep} + zC_b^\circ) \quad (9b)$$

For hand calculator processing, the approximate form (eqn. 8d [1])

$$\exp(f\Delta t_{ep}/V_g) \approx V_sC_{as}^\circ/V_gzC_b^\circ + V_s/V_g + 1 - C_{bg}^\circ/C_b^\circ - zC_{bg}^\circ/C_{as}^\circ \quad (9c)$$

is easier to use and is obtained from eqn. (9a) by applying the approximation $\ln(1 + x) \cong x$ to eqn. (1c) for t_1, substituting $t_2 = V_s/f$, applying the approximation $e^x \approx (1 + x)$ to the exponential terms, and assuming $[A]_g^{ep} \ll zC_b^\circ$.

Equation (9a) is easily rearranged into the form

$$\Delta t_{ep} = (V_g/f)\ln\{C_{as}^\circ\,[\exp[f(t_2 - t_1)/V_g] - 1] + zC_b^\circ \exp[f(t_2 - t_1)/\,V_g]\} - (V_g/f)\ln\{[A]_g^{ep} + zC_b^\circ\} \quad (9d)$$

For computer data processing, this equation can be used in the form

$$\Delta t_{ep} = (V_g/f)\ln\left\{C_{as}^\circ\,\frac{C_{as}^\circ\,[\exp(V_s/V_g)]\,(zC_b^\circ + 1) - C_{as}^\circ - C_{bg}^\circ}{(C_{as}^\circ + zC_{bg}^\circ)}\right\} - (V_g/f)\ln\{[A]_g^{ep} + zC_b^\circ\} \quad (9e)$$

For hand calculator data processing, the approximation (eqn. 7c [1])

$$\Delta t_{ep} \approx (V_g/f)\ln[(V_sC_{as}^\circ/V_g) + z(C_b^\circ - C_{bg}^\circ)] - (V_g/f)\ln[[A]_g^{ep} + zC_b^\circ] + V_s/f \quad (9f)$$

is obtained by applying the $\ln(1 + x) \cong x$ and $e^x \cong 1 + x$ approximations to the first bracketed term in eqn. (9c).

Quantitative results. Figures 3—5 include quantitative data obtained with the series and parallel sample introduction systems [1] for a variety of

conditions. Experimental data are represented by open and closed circles and results computed with eqn. (8) from ref. 4 and eqn. (3b) above are plotted as solid and dashed curves respectively. As an aid in comparing plots of Δt_{ep} vs. ln C, it should be noted that the spacing along the ln C axis (Δln C) multiplied by 100 is almost identical to percentage difference between concentrations for any two plots being compared as long as the difference is small ($\Delta \ln C \leqslant 0.2$). For example, if one were comparing concentration computed with the titration model (C_T°) versus that with the kinetic model (C_K°), then the difference, $\Delta \ln C^\circ = \ln C_T^\circ - \ln C_K^\circ$ is equal to $\ln (C_K^\circ / C_T^\circ)$, and the concentration ratio is $C_K^\circ / C_T^\circ = \exp(\Delta \ln C) \cong 1 + \Delta \ln C$ (since $e^x \approx (1 + x)$ for $x \ll 1$). The difference between plots 1 and 2 in Fig. 3B is $\Delta \ln C \approx 0.2$ and corresponds to a concentration ratio of $C_T / C_K \cong 1.20$, representing a 20% difference. Thus, equal slopes in these plots is a necessary but not a sufficient criterion for agreement.

Figures 3A, 3B, and 4 represent data obtained with the series sample introduction system. While there are slight deviations from theory in all cases, especially at higher determinant concentrations, the kinetic-model

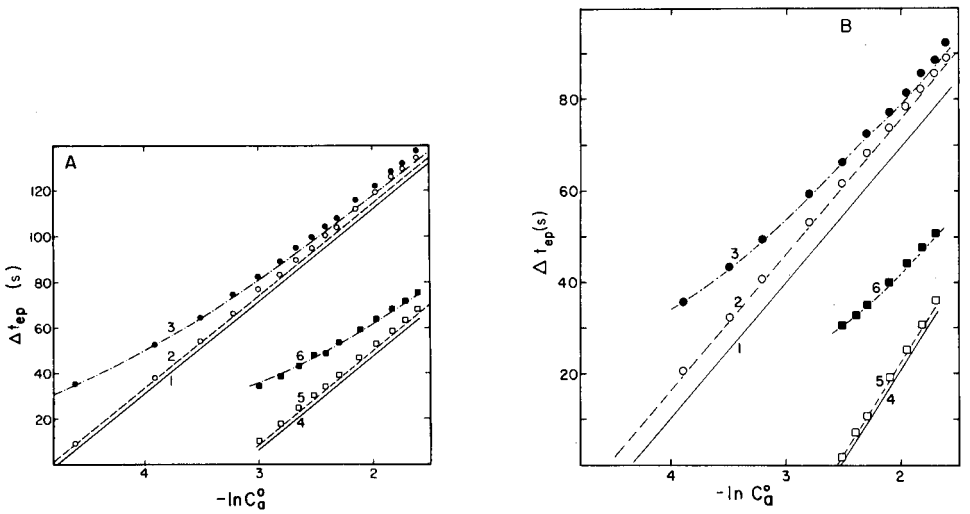

Fig. 3. Comparison of experimental and computed results for determination of HCl with and without KOH in gradient chamber initially, with series sample introduction. Experimental results (all plots): (○, □) $C_{bg}^\circ = C_b^\circ$; (●, ■) $C_{bg}^\circ = 0$. Computed results (all plots): (——) eqn. 8 [4]; (— — —) and (— · —) eqn. (9d) (this paper) and related equations.
(A) All plots: $V_g = 1.644$ ml; $V_s = 0.1933$ ml; $f = 0.0413$ ml s^{-1}. Curves 1—3, $C_b^\circ = 1$ mmol l^{-1}; curves 4—6, $C_b^\circ = 5$ mmol l^{-1}. (○) y = (41.7 ± 0.2)x + (201 ± 0.4)s; $s_{yx} = 0.51$; $r = 0.9999$. (□) y = (41.7 ± 0.3)x + (135 ± 0.6)s; $s_{yx} = 0.40$; $r = 0.9998$.
(B) Curves 1—3, $V_g = 1.191$ ml; $V_s = 0.456$ ml; $f = 0.040$ ml s^{-1}; $C_b^\circ = 5$ mmol l^{-1}. Curves 4—5, $V_g = 1.644$ ml; $V_s = 0.1015$ ml; $f = 0.0397$; $C_b^\circ = 5$ mmol l^{-1}. (○) y = (29.8 ± 0.07)x + (137 ± 0.2)s; $s_{yx} = 0.16$; $r = 0.99998$ (□) y = (42.1 ± 0.6)x + (108 ± 1.2)s; $s_{yx} = 0.42$; $r = 0.9995$.

equations follow the general trends of the experimental observations for a rather wide range of operating conditions. This is judged to be convincing evidence of the viability of the kinetic model used to develop these equations. It is also observed that the kinetic-model equations agree more closely with experimental observations in all cases than does the titration-model equation; the latter equation fails badly for cases in which $C^{\circ}_{bg} = 0$, but it was not intended to cover such situations. Curvature of experimental results observed at higher concentrations almost certainly results from deviations from plug flow during sample introduction. Although this problem has not been addressed quantitatively, it appears logical that small amounts of sample entering the gradient chamber earlier and later than expected for plug flow would have a greater effect on the measured time interval for higher concentrations than for lower concentrations.

Figure 5 represents data obtained with the parallel sample introduction system. The substantially better agreement of kinetic-equation predictions with experimental observations tends to support the conclusion that deviations from predicted behavior with the series system results from failure of the plug-flow model. Results in Fig. 5 also suggest that parallel sample introduction may be preferred when it is a viable option.

It is suggested that the exp $(\Delta tf/V_g)$ vs. C plotting scheme illustrated in these plots has some substantial advantages in comparison with the Δt vs.

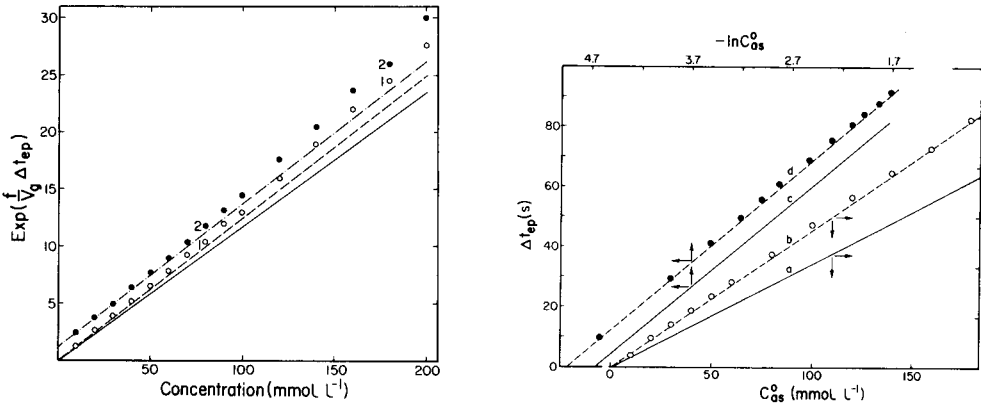

Fig. 4. Comparison of results for flow-injection determination of HCl with and without KOH present initially in gradient chamber. Conditions and plot identifications as in Fig. 3A, plots 1—3. (○) (first 6 points): y = (131 ± 8)x — (0.07 ± 0.03); $s_{yx} = 0.03$; $r = 0.9999$ (●) (first 6 points): y = (132 ± 1)x + (1.04 ± 0.04); $s_{yx} = 0.05$; $r = 0.9999$.

Fig. 5. Comparison of results for flow-injection determination of HCl with KOH in flow stream with parallel sample introduction. $V_g = 1.644$ ml; $V_s = 0.613$ ml; $f = 0.0418$ ml s^{-1}; $C^{\circ}_b = C^{\circ}_{bg} = 4.94$ mmol l^{-1}. (○, ●) Experimental; (— — —) computed with eqn. 4b; (——) computed with eqn. 8 [4]. (○) y = (132 ± 1)x + (1.04 ± 0.04); $s_{yx} = 0.047$; $r = 0.9998$ (●) y = (28.4 ± 0.03)x + (140 ± 0.1); $s_{yx} = 0.097$; $r = 0.99999$.

ln C scheme for analytical applications. In addition to being linear in concentration, and requiring only one nonlinear data transformation, it is more responsive to non-ideal behavior and variability in parameter values. The plotting scheme also linearizes data for the situation when $C^{\circ}_{bg} \neq C^{\circ}_{b}$. These characteristics are apparent from a comparison of the data in Fig. 4 with plots 2 and 3 in Fig. 3A. While the logarithmic plots will usually appear to have less scatter, any scatter masked by the log scale is retrieved in the concentration result when the exponential is computed. The exponential plotting scheme should represent the more useful performance indicator for the critical analyst.

Data presented for situations in which $C^{\circ}_{bg} = 0$ and $C^{\circ}_{bg} = C^{\circ}_{b}$ represent two extremes, and it should be clear that results for other situations in which $0 \leqslant C^{\circ}_{bg} \leqslant C^{\circ}_{b}$ will fall between plots such as 1 and 2 in Figs. 3A and 4. These results demonstrate the importance of careful control of reactant concentration in the gradient chamber, C°_{bg}, when sample is introduced. Poor control will result in substantial scatter about calibration plots. This point is discussed in more detail below.

Special features

Several selected features of this method merit additional comment.

Effects of C°_{b} and C°_{bg}. The nonlinear Δt_{ep} vs. ln C°_{as} plots obtained when $C^{\circ}_{bg} \neq C^{\circ}_{b}$ are the expected result for mixed zero- and first-order processes; linear plots obtained when $C^{\circ}_{bg} = C^{\circ}_{b}$ are somewhat unexpected for the mixed-order processes, and it is instructive to consider reasons for this behavior. Simply stated, the reason for the linear relationship between Δt and ln C when $C^{\circ}_{bg} = C^{\circ}_{b}$ is that the amount of determinant that reacts with reactant during the time period between t_0 and t_1 compensates exactly for the complicating effect of the zero-order process (mass flow with reaction) superimposed on the first-order process (mass flow alone). While this conclusion can be proven rigorously by appropriate manipulations of eqn. (3b) above into eqn. (7a) presented earlier [1], the effect is more easily visualized with a simplified form of eqn. (3b).

The first term in eqn. (3b) includes the expression from $[A]^{max}_{g}$ in eqn. (2c), and the equation can be simplified by using a simplified expression for the maximum determinant concentration in the gradient chamber. Because the time, t_1, required for all reactant to be cleared from the chamber is short compared with the half-life for the chamber, the amount of reactant lost via mass flow will be small, and most of the reactant present initially will react with determinant. Therefore, the maximum determinant concentration can be estimated as

$$[A]^{max}_{g} \approx C^{\circ}_{as} V_s / V_g - C^{\circ}_{bg} \qquad (10a)$$

When the first term in eqn. (3b) is replaced by this simplified term, the result can be expanded and rearranged as follows

$$[A]_g + C_b^\circ \approx C_{as}^\circ V_s/V_g \exp[-f(t-t_2)/V_g] - C_{bg}^\circ \exp[-f(t-t_2)/V_g] + C_b^\circ \exp[-f(t-t_2)/V_g] \quad (10b)$$

In the special case when $C_{bg}^\circ = C_b^\circ$, the last two terms cancel each other, leaving a pure exponential involving C_{as}° which is a requirement for linear Δt vs. ln C_{as}° plots; in the more general case when $C_{bg}^\circ \neq C_b^\circ$, the two terms do not cancel and the linear relationship is not expected. That the titration model predicted a nearly correct form for the Δt vs. ln C relationship is somewhat fortuitous because that model did not include the true origin of the linearizing feature, namely the reaction of reactant in the gradient chamber initially with determinant.

The compensating feature described above will be exact only when C_{bg}° is exactly equal to C_b°; however, the degree of nonlinearity can be reduced by making $C_{bg}^\circ \approx C_b^\circ$. Because the half-life ($t_{1/2} = 0.693\ V_g/f$) for most systems described to date is about 30 s, it will be necessary to wait at least 120 s (four half-lives) between determinations to ensure that $C_{bg}^\circ \geqslant 0.94\ C_b^\circ$ and that Δt vs. ln C plots are linear or that exp ($f\Delta t/V_g$) vs. C plots have zero intercepts. The alternative procedure of working with $C_{bg}^\circ \approx 0$ can permit throughput approaching 60 samples/hour [4] to be achieved.

Minimum concentrations. Concentration data in Table 1 show that the minimum concentration that can be determined with that set of conditions is near 4.4 mmol l^{-1}. That result has been generalized (eqn. 5a [1]). As examples, conditions used to obtain data in Fig. 4 predict a minimum concentration near $C_{as,\,min}^\circ = 4.94/(e^{0.613/1.191} - 1) = 7.3$ mmol l^{-1}, while conditions used for data in Fig. 3 with $C_{bg}^\circ = 0$ predict a minimum concentration of zero. All of these predictions assume ideal behavior (zero measurement uncertainty, infinite detector sensitivity, and no interferences); detection limits will be somewhat higher than these values of $C_{as(min)}^\circ$.

Amounts reacting. Mass information in Table 1 show that total amounts of determinant, n_{aT}, and reagent that react, n_{bR}, in these flow-injection determinations are different for all concentrations. In fact, the ratio of the moles of determinant to the moles of reactant (n_{aT}/zn_{bR}) increases linearly with determinant concentration. For data in Table 1, $n_{aT}/n_{bR} \cong 4.3 \times 10^3\ C_{as}^\circ$. This result can also be generalized as follows

$$n_{aT}/zn_{bR} = V_s C_{as}^\circ/[fC_{as}^\circ t_1 + fC_b^\circ(t_3 - t_2)] \quad (11)$$

For a titration, the ration is unity [5].

Time periods. Time information in Table 1 shows that for the situation when $C_{bg}^\circ = C_b^\circ$, t_1 is a significant fraction of t_3 for all concentrations up to 25 mmol l^{-1} and that t_2 is significant at all concentrations. Processes occurring during these periods were not considered in the earlier treatment [4].

End-point detection. All procedures that relate measured time intervals to determinant concentration include the end-point determinant concentration explicitly or implicitly. For dual-channel systems, the end-point concentration is $[A]_g^{ep} = zf_r C_b^\circ/f_s$; for the single channel system executed as illustrated earlier

TABLE 1

Performance data computed[a] with equations based on kinetic model

Concentration information			Mass information			Time information				
Conc. ($\times 10^{-3}$ mol l^{-1})		Ratio $[A]_g^{max}/C_{as}^{\circ}$	Amount of substance (μmol)		Ratio[c] n_{aT}/n_{bR}	Time (s)				Ratio $\Delta t_1/\Delta t_{ep}$
C_{as}°	$[A]_g^{max}$		Determinant	Reagent		t_1	t_2	t_3	Δt_{ep}	
$C_{bg}^{\circ} = C_b^{\circ} = 1 \times 10^{-3}$ mol l^{-1}										
4.4[b]	0.0	0.0	0.8	0.8	1.00	8.9	8.9	0	0	∞
7	0.48	0.07	1.4	1.35	1.04	5.8	8.9	25.3	19.5	0.29
10	1.03	0.10	2.0	1.7	1.18	4.1	8.9	39.2	35.0	0.12
25	3.79	0.15	5.0	2.6	1.92	1.7	8.9	76.6	74.9	0.02
50	8.40	0.17	10.0	3.4	2.94	0.9	8.9	106	105	0.01
100	17.6	0.18	20.0	3.9	5.13	0.4	8.9	136	135	0.00
$C_{bg}^{\circ} = 0$; $C_b^{\circ} = 1 \times 10^{-3}$ mol l^{-1}										
0	0.0	0.0	0.0	0.0	—	0	—	0	0	—
2.5	0.46	0.18	0.5	0.36	1.39	0	8.9	24.9	24.9	—
7	1.29	0.18	1.4	0.80	1.75	0	8.9	44.5	44.5	—
10	1.85	0.18	2.0	1.01	1.98	0	8.9	53.9	53.9	—
25	4.62	0.18	5.0	1.68	2.98	0	8.9	83.5	83.5	—
50	9.24	0.18	10.0	2.27	4.41	0	8.9	109	109	—
100	18.5	0.18	20.0	2.90	6.91	0	8.9	138	138	—

[a]Computed with parameters in ref. [4] (V_g = 0.98 ml, V_s = 0.20 ml, f = 0.0225 ml s^{-1}, $C_b^{\circ} = 1 \times 10^{-3}$ mol l^{-1}). [b]To be detected, determinant concentration must be somewhat larger than 4.4×10^{-3} mol l^{-1}. [c]Ratio of total moles of determinant (n_{aT}) to the moles of reactant (n_{bR}) that react with determinant.

in Fig. 3A [1], the reference point is obtained from a calibration plot of detector signal vs. determinant concentration; for single-channel systems with reactant in the flow stream, estimation of determinant concentration at the end-point is more complex. Two points are certain: determinant concentration at the end-point will be much less than reactant concentration in the flow stream ($[A]_g^{ep} \ll C_b^{\circ}$), and the pertinent value is that consistent with the kinetic process in the gradient chamber that determines t_3. Although an exact quantitative treatment is not possible, the instantaneous equivalency relationship at the end-point is

$$[A]_g^{ep} = z[B]_g^{ep} = z(fC_b^{\circ}/V_g)\delta t \qquad (12)$$

where δt is a finite increment of time following the onset of the end-point during which sufficient reactant enters the gradient chamber to react completely with all determinant remaining in the chamber. The interval, δt, is dependent on stirring efficiency; it will be small for good stirring efficiency and large for poor stirring efficiency. If it is assumed that the transition period is one second or less ($\delta t \leqslant 1$ s), then substituting typical values of

$z = 1$, $f = 0.02$ ml s^{-1}, and $V_g = 1$ ml, it follows that $[A]_g^{ep} = z[B]_g^{ep} \ll 0.02$ C_b°. This approximate treatment helps to quantify the assumption ($[A]_g^{ep} \ll C_b^\circ$) used to simplify eqn. (3a) to (3b) in ref. [1], and shows that while the assumption [4] that $[A]_g^{ep} = zC_b^\circ$ for $f_a = f_b$ is valid for a dual-channel system, it is not valid for a single-channel system.

Relative magnitudes of C_b° *and* C_{as}°. Data presented above and earlier [1, 4] have shown that the concentration of reactant in the flow stream relative to determinant concentration has significant influences on the characteristics of the method. For example, the maximum sensitivity and minimum deviation from first-order behavior is achieved for the smallest reactant concentration ($C_b^\circ = 0$) [1]. Because all experiments reported to date have involved reactant concentrations substantially less than determinant concentrations ($C_b^\circ \leqslant 0.15\ C_{as}^\circ$), it is useful to consider potential effects of the other alternative, namely when reactant concentration is substantially larger than determinant concentration. Such experiments, if at all feasible, would likely need to be conducted with $C_{bg}^\circ = 0$, and this condition is assumed for the following discussion. For the situation when $C_b^\circ \gg [A]_g$, the zero-order process resulting from reagent mass flow would predominate and the first-order process resulting from determinant mass flow would be minimized, and this would have two potentially important consequences.

One consequence is that the predominantly zero-order process would result in a linear relationship between Δt and C_{as}°; the other is that the procedure would more nearly satisfy the equivalency criterion of a titration [1, 5] because a relatively small percentage of determinant would be lost via mass flow. While such conditions would require a substantially larger gradient chamber or smaller flow rate to give reasonable time intervals, the potential advantages may merit the effort.

Titration option. While it has been noted [1] that procedures implemented to date do not satisfy the equivalency criterion of a titration, it is worthy of note that the part of the process between t_0 and t_1 (Fig. 1A) does indeed satisfy that requirement because all determinant that enters the chamber during that period is reacted. If conditions and procedures were altered to emphasize that process, then eqn. (1c) could be used to relate C_{as}° and t_1.

Conclusions

Equations developed above are not exact; the most significant limitation is likely that resulting from the assumption of plug flow. Data in Fig. 2 give some direct indication of the extent of the deviations, and also show that the parallel sample introduction system improves the performance. Despite these limitations, the equations presented above have given additional insight into influences of experimental parameters on method characteristics and should be useful to any who wish to design procedures to satisfy particular conditions. For example, if one wishes to maximize sample throughput rate by injecting each subsequent sample rapidly after the end-point of the previous sample, one must accept nonlinear Δt_{ep} vs. ln C plots (see Fig. 3) or

nonzero intercepts for exp ($\Delta tf/V_g$) vs. C plots. If one wishes to minimize dependence on the time between samples, one must wait several half-lives between samples for reactant concentration to be restored in the gradient chamber. Thus, the kinetic treatment gives the user the ability to predict method characteristics more effectively than has been possible to date, and that is one of the major goals of a mathematical treatment of any system. It is probable that analogous kinetic treatments will be comparably effective for other methods that use unsegmented-flow sample processing.

This investigation was supported by Research Grant No. GM 13326-13 from the NIH, USPHS.

REFERENCES

1 H. L. Pardue and B. Fields, Anal. Chim. Acta, 124 (1981) 39.
2 W. J. Blaedel and R. H. Laessig, Anal. Chem., 36 (1964) 1617.
3 G. Nagy, Zs. Feher, K. Toth and E. Pungor, Anal. Chim. Acta, 100 (1978) 181.
4 J. Růžička, E. H. Hansen and H. Mosbaek, Anal. Chim. Acta, 92 (1977) 235.
5 H. M. N. H. Irving, H. Freiser and T. S. West, IUPAC Compendium of Analytical Nomenclature, Definitive Rules 1977, Pergamon, Oxford, 1978, p. 41.

Analytica Chimica Acta, 124 (1981) 81—84

SINGLE-DROP METHOD FOR DETERMINATION OF CYANIDE IN SOLUTION WITH A PIEZOELECTRIC QUARTZ CRYSTAL

T. NOMURA

Department of Chemistry, Faculty of Science, Shinshu University, Asahi, Matsumoto 390 (Japan)

(Received 1st September 1980)

SUMMARY

The change in frequency of a horizontal quartz crystal in contact with a single drop of solution is measured. When the gold electrode of the crystal is dissolved by reaction with cyanide in alkaline solution, the further change of frequency is linearly related to cyanide concentration in the range 10^{-3}—10^{-4} M at pH 10.4. Only silver(I) and mercury(II) interfere if EDTA is added.

A piezoelectric quartz crystal has been used as a sensor for determinations of several substances in air [1] but only of a very few substances in water [2] because the frequency of the crystal is changed by the weight of material adsorbed on the electrode. When the crystal becomes wet it does not oscillate, so that the determination of dissolved substances in a solution is carried out with a dried crystal after the solution has been removed. Therefore, the determination is time-consuming.

It has been found that if the crystal is wetted only on one side, it still oscillates. A cell has been built for passing a liquid over one side of the crystal, and the behavior of the crystal in contact with the liquid has been discussed [3]. The difference (ΔF) between the frequency shift of the crystal in contact with the solution and that with water depends on the density (d, g cm^{-3}) and the specific conductivity (κ, Ω^{-1} cm^{-1}) of the solution as described by eqn. (1) (the numerical values change with the shape of the cell):

$$\Delta F = \Delta F_\kappa - \Delta F_d = 2.87 \times 10^3 \kappa^{0.611} - 8.69 \times 10^3 (d - 1)^{1.02} \quad (1)$$

where ΔF_κ and ΔF_d are the frequency shifts, compared to the shift caused by water, dependent on the specific conductivity and density, respectively. It was shown [3] to be possible to determine cyanide, which reacts with the silver electrode and decreases its weight, and thus increases the frequency of the crystal in the solution.

In this paper, it is shown that a single drop of liquid placed on a horizontal electrode allows the crystal to oscillate. The frequency is changed by the liquid and by ions which react with the electrode. However, the frequency

shift is variable because the drop on the electrode spreads out and the area of the electrode in contact with the liquid changes. A constant area can be obtained if the crystal is treated with teflon so as to restrict the spreading of the drop. This system is applied for the determination of cyanide in solution.

EXPERIMENTAL

Apparatus

The piezoelectric quartz crystal, oscillator, thermostatted air bath, digital counter and recorder were as described previously [2].

The crystal was coated with teflon (Scotchgard, Sumitomo 3M Co.) by the following method. One drop of water (5 μl) was placed on the centre of the gold electrode of the horizontal crystal. Teflon solution was sprayed as an aerosol onto the remainder of the crystal. After several minutes, when the solvent had evaporated and the resin adhered to the electrode around the drop of water, the teflon on the drop of water was washed away with water and the crystal was dried for a few hours in air in order that the resin should adhere strongly to the electrode. The teflon treatment decreased the frequency by about 3 kHz in air.

When the frequency of the crystal had increased by about 5 kHz, owing to continued dissolution of the electrode by reaction with cyanide, the electrode was plated with gold in 0.02 M sodium dicyanoaurate(I) solution at 0.33 V for 5 min.

Procedure for determination of cyanide ($0.1—4.0 \times 10^{-3}$ M)

Place one drop (5 μl) of the sample solution adjusted to pH 10.4 on the electrode of the horizontal crystal in an air bath. Measure the frequency difference (ΔF_c) of the crystal in contact with the sample solution between just after placing the drop and 4 min later. Determine the concentration of cyanide from a calibration curve of ΔF_c against cyanide concentration.

Remove the crystal and the holder from the oscillator and wash the crystal with water and then with acetone. Set the crystal into the oscillator for the next measurement after drying.

RESULTS AND DISCUSSION

Behavior of the crystal

When one drop (5 μl) of liquid was placed on the gold electrode, the frequency of the crystal decreased as shown in Fig. 1. There was only a small difference (100 Hz) between the frequency shift of the crystal in contact with water and that in contact with 1 M sodium chloride or sodium hydroxide solution. This arises because, from eqn. (1), the frequency shift caused by the change in density of the solution is nearly equal but opposite to that caused by the change in specific conductivity. However, for solutes

with smaller activity coefficients, a larger difference in frequency shift is obtained. Thus, for 1 M sodium sulfate, the difference was −360 Hz compared with water. Accordingly, it is convenient for determinations of a material in solution to use electrolytes which cause little difference in frequency shift with the components of the solution.

The frequency of the crystal in contact with a concentrated solution decreased because of the absorption of moisture from the air; thus 1 M sodium hydroxide changed the frequency by −120 Hz over 4 min, and 1 M sodium chloride caused a −50 Hz change over 4 min, as shown in Fig. 1(b).

The frequency of the crystal in contact with cyanide solution changed as shown in Fig. 1(c). The frequency difference (ΔF_c), i.e., the difference between the frequency of the dry crystal just before the addition of the cyanide solution and that of the dried crystal just after the reaction, was proportional to the concentration of cyanide. The change results from a decrease in the weight of the electrode owing to the dissolution of gold as its cyanide complex, similar to the reaction between cyanide and silver [3]. The difference was the same for solutions at 20 or 30°C. Therefore, it was unnecessary to leave the sample solution in a thermostat. Several minutes were required for drying a crystal washed with water and acetone at room temperature (about 20°C), but only 2 min were needed at 30°C.

Determination of cyanide

The reaction time of cyanide with the gold electrode was 2—3 min (Fig. 1c) and was independent of cyanide concentration, at least up to 4×10^{-3} M.

Cyanide solutions of 2×10^{-3} M final concentration were prepared using sodium borate—sodium hydroxide buffer solutions of various pH values (or

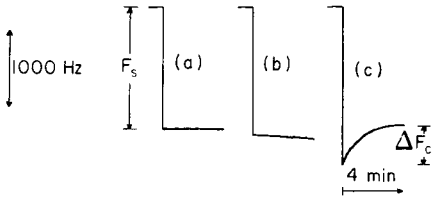

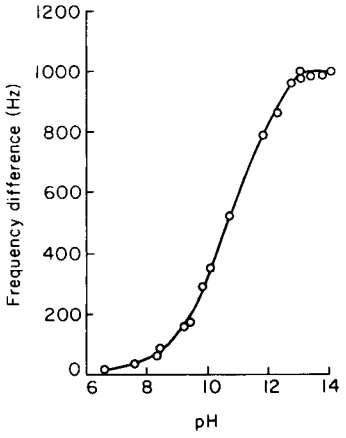

Fig. 1. Typical frequency shifts (F_s) and frequency differences (ΔF_c) of the crystal recorded when (a) 1 drop of water, (b) 1 M sodium chloride, and (c) 2×10^{-3} M cyanide in sodium borate buffer (pH 10.4), were placed on the dry crystal.

Fig. 2. Dependence of frequency difference on pH for 5 μl of 2×10^{-3} M cyanide.

sodium hydroxide solutions above pH 13), and their cyanide concentrations were measured by the recommended procedure. The response increased with increasing pH up to pH 13, as shown in Fig. 2, and then became constant. Note that these values are corrected for frequency changes caused by water absorption by the concentrated sodium hydroxide solutions, but no frequency change was observed in the buffer solutions. All further experiments were carried out at pH 10.4 because of the buffer capacity and reproducibility.

The calibration graph prepared from results obtained by using the recommended procedure was linear over the range 1.0×10^{-4}–4.0×10^{-3} M, and can be described by the equation $[CN^-] = (\Delta F_c/235) \times 10^{-3}$ M, where ΔF_c is the frequency difference (in Hz) measured. The standard deviation was 13.0 Hz (2.8%) for 5 determinations of 2×10^{-3} M cyanide with the same crystal. When five different crystals were used, the standard deviation was 16.8 Hz (3.6%).

The effects of several ions were investigated for the determination of 2×10^{-3} M cyanide; changes in frequency exceeding ±5% were considered to result from interferences. Anions which would react with the gold [4], such as chloride, bromide and thiocyanate, had no effect even when present in a 10-fold molar excess. Mercury(II) and silver(I) interfered because they formed stable complexes when present in equivalent molar concentrations. Other cations which interfered by forming cyanide complexes or hydroxide precipitates (cadmium(II), cobalt(II), copper(II), iron(III), lead(II), nickel(II) and zinc(II)) could be completely masked by adding EDTA to the sample solution to give a 1×10^{-2} M solution.

REFERENCES

1 J. Hlavay and G. G. Guilbault, Anal. Chem., 49 (1977) 1890.
2 T. Nomura and O. Hattori, Anal. Chim. Acta, 115 (1980) 323.
3 T. Nomura and A. Minemura, Nippon Kagaku Kaishi, 1980 (1980) 1621.
4 L. G. Sillen and A. E. Martell, Stability Constants of Metal—Ion Complexes, The Chemical Society, London, 1964, pp. 123, 288, 324.

Analytica Chimica Acta, 124 (1981) 85—90

AN ELECTRONICALLY CONTROLLED DUAL-INTERMEDIATE COULOMETRIC TITRATOR WITH END-POINT ANTICIPATION

JOHN T. STOCK

Department of Chemistry, University of Connecticut, Storrs, CT 06268 (U.S.A.)

(Received 18th August 1980)

SUMMARY

An electronically controlled dual-intermediate coulometric titrator that is constructed from readily-available components and a simple semimicro titration cell are described. The circuitry of the titrator permits most of the titration to be run rapidly, but provides gradual approach to the changeover and end-points. The device was tested by the determination of 4—385 μg of aniline by generation of excess of bromine, followed by back-titration with copper(I). Standard deviations ranged from ±0.5 μg with small amounts of aniline to ±3.7 μg with large amounts.

A common titrimetric procedure for substances that react slowly involves the addition of a known amount of reactant, waiting for the reaction to proceed to completion, and back-titration of the excess of reactant with a second reagent that reacts quite rapidly with the first one. Buck and Swift [1] determined submillimolar amounts of aniline by coulometric addition of excess of bromine followed by coulometric back-titration with copper(I). These workers used a NaBr—$CuSO_4$—HCl medium in which bromine generation can be changed to back-titration by mere reversal of the generating current. The equilibria involved in this dual-intermediate process [2, 3] and the optimum conditions for the determination of aniline [4] have been further studied. The dual-intermediate approach has been used for a variety of other species [5—12].

These titrations were performed manually. Mechanized coulometric titrators began to appear approximately 30 years ago [13] and recent reviews [14] indicate that the development of these devices is continuing. The present account describes an electronically controlled dual-intermediate coulometric titrator by which the major portions of the titrants are generated rapidly. However, the termination points of the forward addition of reactant and the back-titration are approached by brief generations that alternate with waiting periods. The principle applied here to generation of excess of bromine and back-titration with copper(I) can obviously be modified for cases where the first reactant has reducing action. Modification of the switching system should allow the device to be used for cases that require the use of externally-generated reagents.

EXPERIMENTAL

Titration cells

A 100-ml tall beaker was used as the larger of the two titration cells. A rubber stopper, with an opening for sample introduction, supports the working electrode, isolation chamber for the auxiliary electrode, and indicator system [15]. Working and auxiliary electrodes are each 13-mm squares of platinum foil. The biamperometric indicator electrodes are two parallel 28-gauge platinum wires fixed 3 mm apart by a glass bead that is sealed across the free ends [16]. Each wire has a 15-mm exposed length. The smaller cell shown in Fig. 1 was made by cutting down a weighing bottle and supporting it in a spring clamp [16].

The electrode systems are cemented to a rectangle (A) of unclad electronic circuit board. To allow this assembly to be held on a ring stand, the board is screwed to a 70-mm length of hardwood rod (B). The 9 mm × 5 mm platinum foil working electrode is pinch-sealed into one end of 4-mm diameter soft glass tube (C). A little mercury serves as contact intermediate and is introduced before the upper end of the tube is plugged. The electrode is mounted edge-on to the motion of the solution in the cell.

A spiral (E) of platinum wire forms the auxiliary electrode. The upper end of the wire has a connecting lead of subminiature PVC-covered flexible wire with a 10-cm loop as shown. This allows ready removal of (E) from isolation chamber (D). This is made from 8-mm diameter tubing by drawing out to yield an orifice that is approximately 1.5 mm in diameter. The orifice is closed by a short plug (G) of filter paper that has been soaked in the appropriate chamber solution and then well tamped down [17]. With 1 M

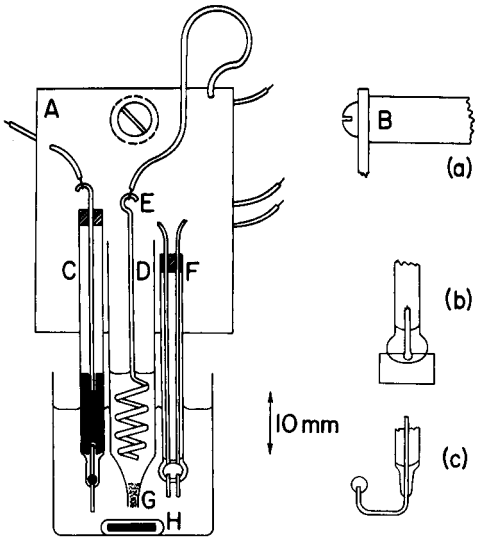

Fig. 1. Small titration cell.

H_2SO_4 in both cell and chamber, the resistance between working and auxiliary electrodes was in the range 300—400 Ω.

Pinch-sealing is used to secure the platinum wire biamperometric electrode pair in a 4-mm diameter tube (F). After sealing on the glass separator bead, the pair is bent twice at right angles, as shown at (c). This allows the exposed wires to be completely submerged when the depth of solution in the cell is small. The upper ends of the wires are threaded through holes in the board and soldered to flexible connecting leads. The stirring-bar (H) is a glass-enclosed, 7-mm length of sewing needle [16].

Samples were introduced into the cells by 2-ml and 0.2-ml Gilmont microburettes.

Reagents

Standard aniline solution, 0.385 g l^{-1} in 1 M HCl, was made by direct weighing of freshly-distilled aniline. The concentration was checked by manually-controlled coulometric titration [1]. The titration medium was made in the cell by introducing equal volumes of 0.25 M NaBr and 0.05 M $CuSO_4$ in 2.7 M HCl. The electrolyte used in the isolation chamber was 1 M H_2SO_4.

Operating principles of the titrator

Only the main controls are mounted on the front panel of the titrator. Subsidiary controls and all other components are mounted on a baseboard that is secured to the panel. The sides of the lift-off cabinet have small labelled openings for screwdriver adjustment of the controls that set the operating parameters of the instrument. Power supplies are mounted on the well-ventilated rear of the baseboard.

Operating principles are illustrated in Fig. 2. High and low coulometric constant currents, set at 9.65 mA and 0.965 mA respectively, are selected by a switch that also controls the lighting of the appropriate decimal point of a 3-digit, 7-segment light emitting diode (LED) readout. The constant current lines go to a relay that allows the polarity of the generating system

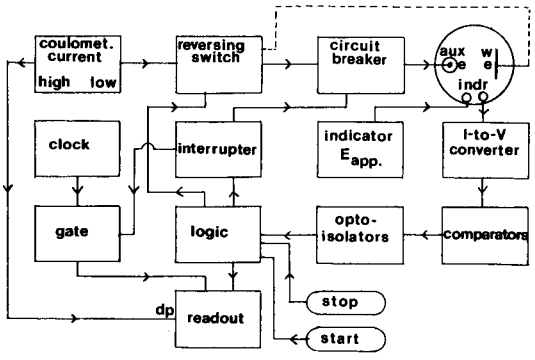

Fig. 2. Block diagram of titrator system.

to be reversed. However, the current can flow only when permitted by the circuit breaker, which is a second relay. When ready for titration, the readout is at zero and a red LED is lit to show that the working electrode is the anode (generation of oxidant) and the generating current is cut off.

When the gate is open, the quartz crystal clock feeds 1.000-Hz pulses to the readout, which counts up during oxidant generation and down during back-titration. The choice of frequency and of coulometric current enables the readout to indicate directly in microequivalents. Gate and circuit breaker are controlled by the interrupter, which has three states, ON, OFF, and MARK-SPACE. The latter is adjustable and was set at approximately 1.1 s on, 3 s off, in the present application.

Pressing the START button of the logic system causes the interrupter to start the titration and to open the gate. The lighting of a yellow LED along with the red one indicates that generation of an oxidant is proceeding. Eventually, the current in the biamperometric indicator circuit begins to rise and this current is proportionately converted to a voltage that is continuously monitored by a set of four comparators. Two comparators are active during the forward generation, while the responses of the other two control the back-titration. The comparator outputs are coupled to the logic system by four opto-isolators.

Suppose that the forward generation is to be stopped when the indicator current is 10 μA. When this current reaches a presettable value such as 9 μA, the first comparator causes the interrupter to go to the MARK-SPACE state. The yellow LED goes on and off, the readout increases intermittently, and the 10-μA point is approached slowly. The triggering of a second comparator at this point causes reversal of the polarity of the generating system, return of the interrupter to the ON state, and change of readout response to "count down". The red LED goes out and a green one lights to indicate that back-titration is proceeding. When the indicator current has fallen to a low preset value such as 4 μA, the triggering of the third comparator again brings on the MARK-SPACE action. Finally, the indicator current sinks to the chosen end-point value, which must of course be greater than the residual current value. Titration then ceases and the readout is recorded manually before the STOP button is pressed to prepare the system for the next titration. A new titration can be initiated by merely pressing the START button.

Complete circuit details will be provided to interested readers.

RESULTS AND DISCUSSION

The well-established Br_2—Cu(I) system [1, 5—8] was chosen to test the titrator, with aniline as the titrand [1]. Current-to-voltage conversion was adjusted so that an input of 10 μA (the desired maximum indicator current) gave an output of 2.28 V. An output of this magnitude triggers the change from forward to back titration. Response settings for the other comparators were (a) forward continuous-to-intermittent, 2.04 V; (b) back continuous-to-

intermittent, 0.90 V; (c) stop, 0.22 V. Because of the comparative slowness of the bromination of low concentrations of aniline, the forward titration termination requires less "anticipation" than that of the rapid back-titration. Changes in cell parameters may necessitate alteration of the continuous-to-intermittent points. In the present experiments, it was found that setting (b) could be reduced to approximately 0.6 V without causing overshoot of the stop potential. The forward and back "intermittent" stages should involve approximately equal numbers of microequivalents.

A useful effect that was not foreseen in the design stage concerns the switches from continuous to intermittent titration. An arrest of approximately 5 s occurs before the regular MARK-SPACE action ensues. This provides additional time for the equilibration of the solution in the cell.

Blank runs were made at 9.65 mA with 50 ml of mixed NaBr—$CuSO_4$ solution in the larger cell. The average readout and standard deviation for 6 runs were -0.05 ± 0.06 μeq. Corresponding data at 0.965 mA with 5 ml of solution in the smaller cell were $+0.05 \pm 0.03$ μeq. Actual runs were corrected for these average blanks.

Unless otherwise indicated, the results listed in Table 1 were obtained by the successive addition to the cell of equal amounts of aniline solution. A pretitration run with approximately 0.05 ml of this solution was performed each time the cell was emptied and refilled. The total time per run with the largest (385 μg) amount of aniline was approximately 450 s.

Conclusions

Using their high-precision manual technique on amounts of aniline similar to those taken in the present work, Buck and Swift [1] obtained average errors ranging from +1.1 to −0.2 μg: corresponding standard deviations were

TABLE 1

Results for determination of aniline in standard samples
(Regression equation (found (y) vs. taken (x)); $y = (1.000 \pm 0.002)x - 0.7 \pm 0.4$; $s_{yx} = 0.9$; $r = 0.99998$)

Number of determinations	Aniline (μg)[a]		Error (μg)	Std. dev. (μg)
	Taken	Found		
6[b]	385	385	0	3.7
6[b]	231	230	−1	3.7
6[b]	116	114	−2	3.6
6[c]	38.5	36.9	−1.6	0.5
5[c]	26.8	26.1	−0.7	0.6
11[c,d]	19.2	18.5	−0.7	0.8
11[c,d]	11.5	11.6	+0.1	0.6
7[c]	3.9_0	4.1_9	+0.3	0.3

[a]1 mole of aniline reacts with 3 moles of bromine. [b]50 ml of cell solution, 9.65 mA. [c]5 ml of solution in smaller cell, 0.965 mA, [d]7 runs, then 4 runs with refilled cell.

±1.2 μg and ±0.27 μg. The reasonably accurate results that are rapidly obtainable with the present automatic titrator could probably be improved by modifications such as provision of a 4-digit readout and of an anticipation system that senses the rate of change of signal from the indicator electrodes.

REFERENCES

1 R. P. Buck and E. H. Swift, Anal. Chem., 24 (1952) 499.
2 P. S. Farrington, D. J. Meier and E. H. Swift, Anal. Chem., 25 (1953) 591.
3 J. J. Lingane and F. C. Anson, Anal. Chem., 28 (1956) 1871.
4 L. A. Chazova, B. A. Lopatin, G. L. Loshkarev and E. V. Rubanova, Fiz. Khim. Metody Anal. Kontrolya Proizvod., Mezhvus, Sb., 2 (1976) 33.
5 A. P. Zozulya and E. V. Novikova, Zavod. Lab., 29 (1963) 543.
6 F. Kawamura, K. Momoki and S. Suzuki, Bunseki Kagaku, 3 (1954) 29.
7 F. Magno, Farmaco Ed. Prat., 22 (1967) 677.
8 F. Magno and M. Fiorani, Ric. Sci., 38 (1968) 119.
9 A. J. Bard and J. J. Lingane, Anal. Chim. Acta, 20 (1959) 463.
10 A. J. Bard, Anal. Chem., 32 (1960) 623.
11 Hui-yu Yen, Chao-Pin Chang and Yu-Hsien Li, K'o Hsueh T'ung Pao, 23 (1978) 740.
12 Z. Slovak and J. Borak, Chem. Prum., 18 (1968) 82.
13 J. J. Lingane, Electroanalytical Chemistry, 2nd edn., Interscience, New York, 1958, p. 528.
14 J. T. Stock, Anal. Chem., 48 (1976) 1R; 50 (1978) 1R; 52 (1980) 1R.
15 D. T. Sawyer and J. L. Roberts, Experimental Electrochemistry for Chemists, J. Wiley, New York, 1974, p. 425.
16 J. T. Stock and M. A. Fill, Mikrochim. Acta, (1—2) (1953) 89.
17 N. H. Furman and R. N. Adams, Anal. Chem., 25 (1953) 1564.

Analytica Chimica Acta, 124 (1981) 91—98

COATED-WIRE ORGANIC ION-SELECTIVE ELECTRODES IN TITRATIONS BASED ON ION-PAIR FORMATION
Determination of Arenediazonium Salts with Sodium Tetraphenylborate

K. VYTŘAS*, M. REMEŠ[a] and H. KUBEŠOVÁ-SVOBODOVÁ[b]

Department of Analytical Chemistry, College of Chemical Technology, 532 10 Pardubice (Czechoslovakia)

(Received 29th July 1980)

SUMMARY

Titrimetric determinations of arenediazonium salts can be based on ion-pair formation between the diazonium cation and tetraphenylborate. Titrations are done under cooling with ice and are followed potentiometrically with organic ion-selective electrodes comprising PVC membranes plasticized with polar solvents and coated on aluminium wires. The method was tested in determinations of arenediazonium salts derived from 20 aromatic amines, including aniline, toluidines, naphthylamines and their derivatives. Except for compounds containing hydrophylic groups such as —COOH and —OH, the potentiometric titration curves have well defined end-points. The results are reproducible, with relative standard deviations in the range 0.4—1.4% at the millimolar level. The method can be used for reliable determinations of arenediazonium salts in analytical control of azo dyestuff production.

Most methods of the classical type for the determination of arenediazonium salts are based either on their oxidation properties or on azo-coupling reactions; all these methods include some tedious procedures. For example, titrimetric azo-coupling with 0.1 M solutions of 1-phenyl-3-methyl-5-pyrazolone, *m*-phenylenediamine [1], or secondary aliphatic amines [2] is time-consuming because of the external end-point detection by spot testing. Titrations with titanium(III) solutions [3] must be done under an inert atmosphere (carbon dioxide or nitrogen). Decomposition of diazonium salts catalyzed by copper(I) chloride in hydrochloric acid and accompanied by evolution of nitrogen [1] is characterized by all the troubles of gasometric methods. Titrations with perchloric acid in a dioxane medium [4] are very unselective

In the work reported here, conditions for the determination of arenediazonium salts were studied by means of organic ion-selective electrodes,

---

[a]Present address: Department of Research Management and Technical information, UNICHEM, General Directorate of Chemical Industry, 532 06 Pardubice, Czechoslovakia.
[b]Present address: Analytical Department of Plant Research, East-Bohemian Chemical Plants Synthesia, 532 17 Pardubice-Semtín, Czechoslovakia.

which can be applied generally for precipitation titrations of univalent organic cations with sodium tetraphenylborate (see [5]).

EXPERIMENTAL

Solutions and methods of measurements

Sodium tetraphenylborate solution ($NaBPh_4$, 2.5%) was prepared by dissolving 25 g of the substance (p.a., Lachema) in 500 ml of water; about 5 g of alumina was added, and the bottle was shaken occasionally for about 16 h. Then the solution was filtered, adjusted with sodium hydroxide to pH 9, and diluted to 1 l with water. The solution was standardized potentiometrically against recrystallized thallium(I) nitrate [5, 6].

Aromatic amines were converted to hydrochlorides by additions of hydrochloric acid, and solutions were prepared containing 0.2—0.01 mol of the substance per liter. Solutions of arenediazonium salts were prepared by titration of precisely measured volumes of the respective amine solutions with sodium nitrite under cooling to 0°C with ice; the end-point of the diazotization was checked both potentiometrically (with a Pt electrode vs. SCE) and with iodide—starch papers. Some of amines were diazotized in suspension. Specific conditions required for the diazotization of each of the amines [7] are summarized in Table 1. The solutions of the arenediazonium salts were kept in an ice-box, for not longer than 8 h.

For the potentiometric measurements, OP-204/1, OP-205, and OP-208 pH meters (Radelkis, Budapest) were used. The electrochemical cell consisted of the appropriate ion-selective electrode (see below) and a saturated calomel electrode (SCE) with a 0.01 M $NaNO_3$ salt bridge to avoid contamination of the titrated solution with potassium ions. Titrations were made in the usual way: the solution of the diazonium salt was transferred to a beaker (100 or 150 ml), the volume was adjusted to 50—75 ml (to obtain a ca. 0.005 mol l^{-1} solution of the titrated substance), and the $NaBPh_4$ titrant (2.5%) was added from an automatic burette (10 ml). The titration vessel was cooled with ice to 0°C externally, or an ice cube was dropped directly into the solution. If necessary, the pH value of the titrated solution was adjusted by addition of concentrated Britton—Robinson buffer (a 0.4 M H_3PO_4—0.4 M CH_3COOH—0.4 M H_3BO_3 stock solution mixed with desired amount of 2 M NaOH), and was checked potentiometrically with calibrated glass and saturated calomel electrodes.

Ion-selective electrodes

Coated-wire ion-selective electrodes were prepared by using an isolated aluminium conductor. The bare wire was dipped into a solution of poly(vinyl chloride) (PVC, 0.09 g) and plasticizer (0.2 ml) in tetrahydrofuran (3 ml) and the solvent was allowed to evaporate. Ion-exchangers were not added to the membranes. Electrodes were preconditioned by using them in titrations of thallium(I) nitrate or the particular organic cation with

TABLE 1

List of titrated solutions and characterization of titration curves

Arenediazonium cation titrated	Preparation	Titration conditions			Titration curve	
		Conc. (mol l^{-1})	pH	Electrode used	Steepness (mV/0.1 ml)	Overall potential change (mV)
Benzene-	0.2 M aniline (50 ml) 1 M $NaNO_2$[a]	0.006	HCl	878C	10—14	200—210
				878D	5—8	140—160
				878I	5—7	120—130
3-Chlorobenzene-	0.2 M 3-chloroaniline 1 M $NaNO_2$[a]	0.006	HCl	878C	18—24	200—205
			4		20—34	220
			6		48—50	230
			8		44—47	240
			10		38	230
4-Chlorobenzene-	0.2 M 4-chloroaniline 1 M $NaNO_2$[a]	0.004	HCl	878A	5	115—135
				878C	6	155—170
4-Bromobenzene-	0.2 M 4-bromoaniline 1 M $NaNO_2$[a]	0.004	HCl	878A	6	130—135
			HCl	878C	24—26	230
			4		30—32	260—280
			6		34—38	270—290
			8		33—36	260
			10		30—34	260
			HCl	20—15	18--20	190
2,5-Dichlorobenzene-	0.04 M 2,5-dichloroaniline 0.5 M $NaNO_2$[b]	0.006	HCl[c]	878C	20—30	180—215
2-Nitrobenzene-	0.2 M 2-nitroaniline 1 M $NaNO_2$[a]	0.006	HCl	878C	8—12	180—190
			4		14—15	250
			6		30	240
			8[c]		8—10	245
3-Nitrobenzene-	0.2 M 3-nitroaniline 1 M $NaNO_2$[a]	0.006	HCl	878C	8—10	210—220
				878D	7—8	130—160
				878I	5—8	160
4-Nitrobenzene	0.2 M 4-nitroaniline 1 M $NaNO_2$[a]	0.006	HCl	878C	15—17	230
				878D	7—8	110—115
				878I	7—10	125—145
3-Methoxybenzene-	0.1 M 3-methoxyaniline 0.5 M $NaNO_2$[d]	0.005	HCl	878C	12—16	190—205
			4		17	195
			6		14—17	200
			8		15—18	220
			10		18—22	215
4-Methoxybenzene-	0.1 M 4-methoxyaniline 0.5 $NaNO_2$[d]	0.005	HCl	878C	15—18	175—200
			4		20—25	210
			6		23—25	235
			8		26	235
			10		28	235
3-Hydroxybenzene-	0.2 M 3-aminophenol 1 M $NaNO_2$[a]	0.006	HCl	878C	4--6	110—120
4-Carboxybenzene-	0.1 M 4-aminobenzoic acid 1 M $NaNO_2$[d]	0.005	HCl	878C	1	50—70
3-Methylbenzene-	0.2 M 3-toluidine 1 M $NaNO_2$[a]	0.006	HCl	878C	10—12	205
			4		19—20	205
			6		20—25	225
			8		25—35	240
4-Methylbenzene-	0.2 M 4-toluidine 1 M $NaNO_2$[a]	0.006	HCl	878C	23—25	205—220
				878D	12—17	160
				878I	14—16	170—180
3-Nitro-4-methyl-benzene-	0.2 M 3-nitro-4-methyl-aniline, 0.5 M $NaNO_2$[a]	0.005	HCl	878C	5—6	140—155
			4		12—14	185
			6		14—16	195
N-Acetyl-3-amino-benzene-	0.1 M N-acetyl-3-phenylene-diamine, 1 M $NaNO_2$[d]	0.01	HCl	878C	6—8	180—205
			3		8—11	175

TABLE 1 (continued)

Arenediazonium cation titrated	Preparation	Titration conditions			Titration curve	
		Conc. (mol l^{-1})	pH	Electrode used	Steepness (mV/0.1 ml)	Overa poten chang (mV)
			5		10—11	175
			7[c]		10—17	180
	0.1 M N-acetyl-3-phenylene-diaminehydrosulphate, 0.5 M $NaNO_2$[d]	0.005	HCl 4	878C	20—30	220—
					20—25	220
			6		30—39	195
			8[c]		17—30	190
1-Naphthalene-	0.025 M 1-naphthylamine 0.25 M $NaNO_2$[e]	0.003	HCl	878A	14—17	170—
				878B	17—20	170—
				878C	22—25	200—
				878D	17—20	160
				878I	15—20	190
				878J	9—10	100—
				878M	15—17	190—
				878N	17—20	170—
				878P	8—12	135—
					20—15	20—26	215—
4-Bromo-1-naphthalene-	4-bromo-1-naphthylamine[f] 0.25 M $NaNO_2$[e]	0.005	HCl	878C	30—37	215—
4-Nitro-1-naphthalene-	4-nitro-1-naphthylamine[g] 0.25 M $NaNO_2$[e]	0.003	HCl	878C	15—18	230
2-Naphthalene-	0.025 M 2-naphthylamine 0.25 M $NaNO_2$[e]	0.003	HCl 4	878C	30—35	260—
					46—50	290—
			6		58—62	295—
			8		63—67	305—

[a]The stock solution was 0.1 M. [b]0.02 M stock solution. [c]Lower results at given pH. [d]0.05 M stock solution. [e]0.01 M stock solution. [f]0.55 g diazotized in suspension in 40 ml of 11 M HCl and 20 ml of water. [g]0.47 g diazotized in suspension, as in footnote f.

$NaBPh_4$ solution; within a few conditioning titrations, the organic solvent (plasticizer) in the membrane became gradually saturated with precipitated tetraphenylborate [8], and the titration curves were usually reproducible after the second titration.

Different plasticizers were used (electrode working code numbers are given in parentheses): dioctylphthalate (878A), diamylphthalate (878B), 2-nitrophenyl 2-ethylhexyl ether (878C), diamyloxalate (878D), didecylphthalate (878I), dioctylsebacate (878J), tricresylphosphate (technical, 878M, or with gas chromatographic purity, 878N), and dimethoxybenzene (878P). A commercial Ca^{2+}-selective electrode (Crytur 20-15; PVC membrane containing a Ca^{2+}-selective ligand and a trace of sodium tetraphenylborate, plasticized with 2-nitrophenyl n-octyl ether) with internal electrolyte ($CaCl_2$) and internal reference (Ag/AgCl) electrode was used for comparison.

RESULTS AND DISCUSSION

Titration curves

The titrimetric determination of arenediazonium salts is based on ion-pair formation of the cation with tetraphenylborate

$$Ar{-}N^{+}{\equiv}N + BPh_4^- \rightleftharpoons [Ar{-}N_2^+, BPh_4^-]$$

The ion-pair compound is practically insoluble in water. Both the steepness of the break in the potentiometric titration curve and the overall size of the potential break are governed by the solubility product of the precipitate formed. However, the shape of the titration curve can also be significantly influenced by the plasticizer in the electrode membrane. This influence was studied in titrations of benzene-, 4-chlorobenzene-, 4-bromobenzene-, 3- and 4-nitrobenzene-, 4-toluene-, and 1-naphthalenediazonium salts. In all cases, the most advantageous shapes of the potentiometric titration curves were observed when 2-nitrophenyl 2-ethylhexyl ether was used to plasticize the electrode membrane. This electrode (code number 878C) was then preferred in most further studies.

The role of the membrane plasticizer can be seen from Fig. 1, where 10 titration curves recorded for the determination of 1-naphthalenediazonium chloride are shown. The probability of extraction of the precipitated 1-naphthalenediazonium tetraphenylborate into a membrane plasticizer increases with its increasing polarity and, consequently, both the steepness and size of the potential break increase. It should be mentioned that electrode selectivity towards organic ions is generally directly proportional to the distribution ratio of the ion-pairs formed, as shown by Scholer and Simon [9] and Freiser et al. [10].

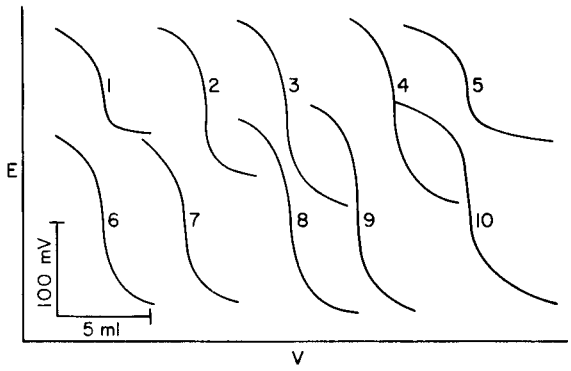

Fig. 1. Influence of the electrode membrane plasticizer on the shape of the potentiometric titration curves of 1-naphthalenediazonium chloride (0.0025 M) with $NaBPh_4$ (0.063 M). The indicating electrodes used were: (1) 878J; (2) 878D; (3) 878N; (4) 878M; (5) 878P; (6) 878A; (7) 878B; (8) 878I; (9) 878C; (10) Crytur 20-15.

Accuracy, reproducibility, and interferences

When the results of the determinations with tetraphenylborate solutions which are summarized in Table 1 were compared with the amounts of the amines weighed originally, statistically insignificant differences were obtained only in titrations of the 4-methoxybenzene- and 2-naphthalenediazonium salts. In other determinations, somewhat lower results were obtained. It should be mentioned that most of the amines used here were not completely pure and that reliable check determinations depend largely on the choice and availability of a suitable standard substance. When the results were compared with the consumptions of sodium nitrite solution obtained when the diazonium salts were prepared from the corresponding amines, differences were usually not observed.

When interferences in the titrated solutions were avoided, the results were readily reproducible, with relative standard deviations lying in the range 0.4—1.4%. The first two titration curves for each salt usually had an atypical shape but subsequent curves were practically identical. Both the accuracy and reproducibility of the determinations can be influenced by interferences as outlined below.

Since the stabilities of the arenediazonium salts are different with regard to temperature and light, particular conditions are required for the determination of each compound. The main decomposition reaction in acidic aqueous medium can be described by the scheme

$$Ar{-}N_2^+ \xrightarrow{k_1} Ar^+ + N_2;\ Ar^+ + \begin{cases} H_2O \\ X^- \end{cases} \xrightarrow{k_2} \begin{cases} Ar{-}OH + H^+ \\ Ar{-}X \end{cases}$$

From the kinetic point of view, the decomposition is limited by the rate of the first reaction; the carbonium cation formed then reacts with a nucleophilic agent (e.g., water or halide) to form the respective derivative.

In nearly neutral medium, the decomposition of arenediazonium salts is complicated by other reactions, e.g., azo coupling of the salt with the phenol formed, Bamberger's hydrolytic reaction, etc. In alkaline solutions, the arenediazonium ion decomposes according to the scheme

$$Ar{-}N_2^+ + H_2O \rightleftharpoons Ar{-}N_2{-}OH + H^+ \rightleftharpoons Ar{-}N_2{-}O^- + 2\,H^+.$$

In all cases, when old solutions of arenediazonium salts were titrated with sodium tetraphenylborate, low results were obtained. Decomposition of the salt in acidic medium is retarded by electronegative substituents, but the same substituents accelerate the diazotate formation in alkaline medium.

Diazonium salts containing hydrophilic groups such as hydroxyl and carboxyl tend to form zwitterions. The potentiometric titration curves of these salts showed only slight curvature and the end-point readings were ambiguous. Salts containing a sulphonic acid group could not be determined titrimetrically.

Decomposition of the precipitated arenediazonium tetraphenylborate

was observed in some cases; this was accompanied by evolution of gas bubbles. The reaction was not studied in detail but it probably involves formation of nitrogen, triphenylboron and an Ar—Ph compound. The decomposition does not influence the arenediazonium ion concentration in solution, and so titration curves can be recorded as usual.

Erroneous results were obtained when the diazonium salts prepared contain an excess of either amine or sodium nitrite. Aromatic amines, converted to substituted ammonium salts in mineral acid medium, are also precipitated and titrated with tetraphenylborate [11]. Excess of nitrite decomposes tetraphenylborate by oxidation. Small excesses of both amine and nitrite cause high end-point readings. If the excess is large, two potential breaks appear in the titration curve; the first is due to precipitation of the arenediazonium ion but the end-point is again erroneous. Interference of nitrite ion can be suppressed if the titrated solution is buffered to pH > 4, the titration error then being less than ±3% (see Table 2).

This titrimetric method for the determination of arenediazonium salts

TABLE 2

Influence of the excess of amine or sodium nitrite on the end-point reading in titrations of 75-ml volumes

Diazonium salt	Amount taken	Interference	Amount added (ml)	pH	Error in end-point (%)
4-Bromobenzene	3 ml 0.1 M	$NaNO_2$ (0.1 M)	1	HCl	+28
			3	HCl	−23
			2	HCl	+9.5
				4	+7.0
				6	+0.6
				8	+0.6
				10	+1.9
		4-Bromoaniline (0.1 M)	1	HCl	+11
			3	HCl	+39
			2	HCl	+37
				4	+13
				6	−21[a]
				8	−23[a]
2-Naphthalene	25 ml 0.01 M	$NaNO_2$ (0.1 M)	1.5	HCl	+9.6
				4	−2.7
				6	−2.5
				8	−2.7
		2-Naphthylamine (0.25 M)	5	HCl	+19.3
				3	+3.7
				5	−51.7[b]
				7	−51.7[b]
				9	−51.7[b]

[a]Partial azo coupling. [b]Quantitative azo-coupling with an amine added.

with sodium tetraphenylborate solution has been tested on some technical samples [12]. It proved to be quick, simple, and sufficiently reliable. The main applications of the method will probably arise in the analytical control of azo dyestuffs production.

REFERENCES

1 M. Jureček, Organická Analysa, Vol. II, p. 405, Nakladatelství ČSAV, Prague, 1957.
2 A. P. Terentev and I. S. Tubina, Zh. Anal. Khim., 18 (1963) 113.
3 E. Knecht and L. Thompson, J. Soc. Dyers Colour., 36 (1920) 215; 41 (1925) 94.
4 C. W. Pifer and E. G. Wollish, Anal. Chem., 24 (1952) 300.
5 K. Vytřas, Am. Lab., 11 (1979) No. 2, 93; Int. Lab., 9 (1979) No. 2, 35.
6 K. Vytřas, V. Říha and S. Kotrlý, Sb. Ved. Pr., Vys. Sk. Chemickotechnol., Pardubice, 35 (1976) 41.
7 R. P. Lastovskii and Yu. I. Vainshtein, Tekhnicheskii analiz v proizvodstve promezhutochnykh produktov i krasitelei, 3rd. edn; pp. 142—165, Goskhimizdat, Moscow, 1958.
8 K. Vytřas, M. Dajková and M. Remeš, Cesk. Farm., in press.
9 R. Scholer and W. Simon, Helv. Chim. Acta, 55 (1972) 1801.
10 H. J. James, G. D. Carmack and H. Freiser, Anal. Chem., 44 (1972) 856.
11 K. Vytřas, Collect. Czech. Chem. Commun., 42 (1977) 3168.
12 K. Vytřas, T. Čapoun, H. Svobodová and J. Latinák, unpublished results.

Analytica Chimica Acta, 124 (1981) 99—105

DIFFERENTIAL PULSE POLAROGRAPHIC DETERMINATION OF TRACES OF PHOSPHORUS IN SEMICONDUCTOR SILICON†

PIER LUIGI BULDINI*

C.N.R.-Istituto LAMEL, Via de' Castagnoli 1, 40126 Bologna (Italy)

DONATELLA FERRI

Istituto Chimico, Facoltà di Ingegneria, Università di Bologna, 40136 Bologna (Italy)

(Received 6th March 1980)

SUMMARY

A method for the indirect determination of phosphorus in semiconductor silicon is presented. After silicon dissolution with hydrofluoric and nitric acids and matrix volatilization, molybdophosphoric acid is formed in 0.25 M hydrochloric acid and then extracted into n-butyl acetate. Back-extraction with 2 M ammonium nitrate—1 M ammonia solution and addition of nitric acid gives a suitable supporting electrolyte for measurement of the catalytic molybdenum wave. Differential pulse polarography provides a detection limit of ca. 5 ng g^{-1} with a precision of about ±2%, with linear calibration curves up to at least 0.1 μg P ml^{-1}.

Traces of phosphorus have a strong effect on the electrical properties of silicon used in semiconductor devices [1]. These traces are usually determined by neutron activation [2—4]; among the chemical methods, which are cheaper and more convenient, only fluorimetry [5] and spectrophotometry [6] have been considered for application to semiconductor silicon. It seemed of interest to examine the possibilities of voltammetric techniques for phosphorus determinations. After the usual heteropoly complex formation, molybdophosphoric acid may be determined directly in ethanolic lithium chloride supporting electrolyte in the presence of acetic acid [7, 8], or indirectly by evaluating the molybdenum content of the heteropoly acid [9, 10].

It proved to be very difficult to obtain reliable results when molybdophosphoric acid was determined in non-aqueous solvent, and so the indirect method was considered. The indirect determination of phosphorus via molybdenum evaluation by atomic absorption spectrometry has been studied extensively [11], but only Bazzi and Boltz [9] and Fogg and Yoo [10] seem to have applied voltammetry for this purpose. It must be noted that the citrate or tartrate buffers used as the supporting electrolyte in the earlier work give diffusion currents that are far smaller than those produced when the catalytic molybdate wave in nitrate medium is used.

†Presented at Heyrovsky Memorial Congress on Polarography, Prague, August 1980.

The proposed method couples the advantage derived from the amplification factor inherent in the heteropoly acid formation (a P:Mo ratio of 1:12) with the high sensitivity of the well-shaped molybdate wave in nitrate supporting electrolyte. In acidic solutions, molybdophosphoric acid is readily formed when an excess of molybdate is present. After removal of the excess of molybdate, the heteropoly acid can be decomposed with a basic nitrate buffer. After acidification, molybdate ion is easily determined by differential pulse polarography.

PRELIMINARY STUDIES

Acidity and molybdate concentration

The condensation of orthophosphate and molybdate ions in acidic solution to give molybdophosphoric acid ($H_3PMo_{12}O_{40}$) is used very extensively. The optimum conditions of formation for spectrophotometric purposes consist of having a final molybdate concentration of approximately 0.04 M and a final acidity of about 0.25 M in hydrochloric acid [12, 13]. Lower molybdate concentrations have been reported satisfactory. Under the conditions used here, the final molybdenum wave obtained for 4 ng P ml^{-1} was unaffected by changes in the molybdate concentration in the range 0.01—0.04 M. The blank increased only very slightly over this range, but a concentration of 0.01 M was preferred in order to reduce as far as possible the number of washes needed to remove excess of molybdate completely before the polarographic determination.

Molybdophosphoric acid extraction

Simon and Boltz [11] extensively studied the extraction of heteropoly acids, and found n-butyl acetate to be the most selective and efficient

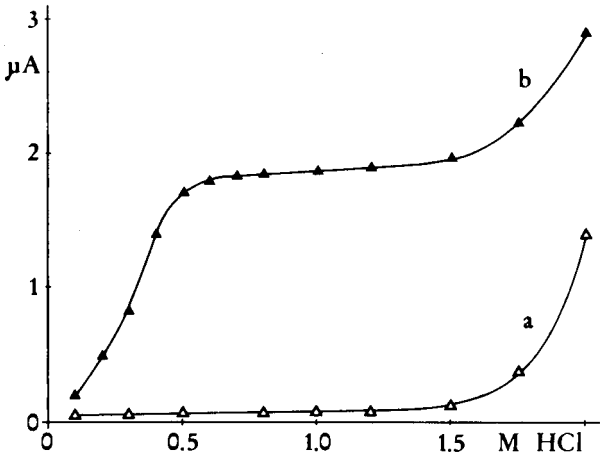

Fig. 1. The influence of the acidity of the wash solution on extraction of molybdate and molybdophosphate. Final molybdenum(VI) concentration, 0.01 M. Operating features as reported in the Procedure. (a) Blank; (b) 4 ng P ml^{-1}.

solvent for the extraction of molybdophosphoric acid. The best acidity range for this extraction was 0.1—1.0 M hydrochloric acid. Simon and Boltz [11] also stated that co-extraction of molybdosilicic and molybdogermanic acids can be avoided by using an acidity less than 0.5 M hydrochloric acid. Accordingly, the formation of molybdophosphoric acid and its extraction into n-butyl acetate can be done in 0.25 M hydrochloric acid.

Under the conditions recommended here, a single 10-ml aliquot of n-butyl acetate was proved to extract molybdophosphoric acid completely. Further extractions showed no evidence of the heteropoly complex. Blank experiments were done to determine the amount of molybdate ions extracted into n-butyl acetate. It was found that a considerable amount of molybdenum was recovered on back-extraction, and so it became very important to ensure correct washing of the n-butyl acetate extracts. It is necessary to shake the organic phase with dilute hydrochloric acid to remove traces of molybdate. It was proved that the acidity of the wash solution influenced both the molybdate and molybdophosphate acid extraction. Figure 1 shows that the best acidity range is 0.8—1.3 M hydrochloric acid, and so a (1 + 9) hydrochloric acid wash solution was adopted. Three washes with 10-ml portions of (1 + 9) hydrochloric acid assured complete removal of the excess of molybdate. Four washes did not further affect the levels of the blank or the molybdenum wave whereas two washes were inadequate to reduce the blank to a constant value. A single wash left a considerable amount of the excess of molybdate in the organic phase.

This washing step may be considered the most important of the entire procedure and great care must be taken to avoid erratic results. The use of separating funnels in this step was not satisfactory because the aqueous solution containing the excess of molybdate may infiltrate the cone and socket of the stopcock. Accordingly the molybdophosphoric acid extraction and washing steps were done in centrifuge tubes, the exhausted aqueous layers being sucked out. Only for the back-extraction of the heteropoly acid was the organic layer transferred to a separating funnel.

Molybdophosphoric acid decomposition and supporting electrolyte

The molybdophosphoric acid extract is decomposed if the n-butyl acetate is contacted with an aqueous alkaline buffer solution. The molybdenum of the heteropoly acid is then transferred to the aqueous phase. This decomposition takes place within the 1-min shaking time specified in the procedure.

Experiments were done in which the n-butyl acetate phase was shaken with successive aliquots of alkaline buffer solution and the molybdenum content of each portion was determined. It was found that equilibration for 1 min with a single 2-ml portion of alkaline buffer effected destruction of the molybdophosphoric acid and gave quantitative recovery of the molybdenum from the n-butyl acetate phase. Routinely, it proved useful to wash the socket and plug of the separating funnel with a second 1-ml portion, extract this, and combine the two aqueous portions.

A buffer solution was sought which could be used to decompose the complex and also serve as a suitable supporting electrolyte in the subsequent polarographic determination.

Previous studies [14] had shown that the molybdenum diffusion current remains constant when the polarographic determination is done at a total nitrate concentration greater than 1.5 M. The effect of nitric acid concentration on the diffusion current does not seem to be critical; it has a small influence only on the half-wave potential value. Thus it seemed convenient to decompose the heteropoly complex and to extract molybdenum with an ammonium nitrate—ammonia buffer, and then add nitric acid to acidify the mixture.

The best results were obtained by using a 2 M NH_4NO_3—1 M NH_3 buffer for the extraction, and then adding nitric acid to give a final 1.8 M NH_4NO_3—0.2 M HNO_3 solution for the supporting electrolyte.

During the extraction step, the layers are readily separated without centrifugation in a few seconds, but after the nitric acid addition, the n-butyl acetate saturating the aqueous phase must be removed before the polarographic analysis. If not removed, n-butyl acetate in the 1.8 M NH_4NO_3—0.2 M HNO_3 supporting electrolyte causes a sudden drop of current at −0.25 V (vs. SCE) that interferes with the molybdenum peak measurement ($E_{1/2}$ = −0.21 V). A benzene wash of the aqueous solution removes n-butyl acetate completely, so that further steps before the polarographic analysis can be avoided.

EXPERIMENTAL

Reagents

Erbatron electronic-grade chemicals were used. Their maximum certified phosphorus contents were: 50% HF, 0.00003% P; 65% HNO_3, 0.000003% P; 37% HCl, 0.000003% P; 32% NH_3, 0.000006% P; n-butyl acetate, 0.00003% P; $(NH_4)_6Mo_7O_{24}\cdot 4H_2O$, 0.00015% P. In order to determine the effective contribution of the reagents, blank determinations were done under the conditions reported in the Procedure. The maximum phosphorus content never exceeded 5 ng P.

Normal precautions for trace analysis were taken throughout the work. Reagents and solutions were stored in polyethylene bottles; polyethylene volumetric ware was used throughout, in order to prevent adsorption/desorption phenomena.

All plastic ware and PTFE vessels were cleaned by filling with concentrated hydrochloric acid, washing in running distilled water, then filling with 8 M ammonia solution, leaving overnight and finally rinsing thoroughly with twice-distilled water. Preferably a set of equipment should be kept only for phosphorus determinations; if this is done, it can be washed after use with running distilled water, and the acid/ammonia treatment is required only occasionally.

Working standards were prepared daily by diluting stock phosphorus solution (1000 $\mu g\ ml^{-1}$) obtained from primary standard-grade KH_2PO_4 with twice-distilled water.

Apparatus

The silicon samples were dissolved in PTFE test tubes fitted with 29/32 sockets in a dissolution device (Berghof, Tubingen, Germany), as described elsewhere [15]. Solvent extraction was done in 100-ml polyethylene centrifuge tubes, while the final back-extraction is carried out in separating funnels.

The AMEL (Milan) Model 472 Multipolarograph was used with a Model 460 stand, a 5-ml microcell, a dropping mercury electrode ($m^{2/3}$ = 1.79), a saturated calomel reference electrode and a platinum ring auxiliary electrode [15]. Instrumental conditions were: pulse height 100 mV, drop time 2 s and scan rate 2 mV s^{-1}. Solutions were deaerated with pure nitrogen for 2—3 min before measurement and thermostatted at 25.0 ± 0.1°C.

Procedure

The preliminary sample treatment based on matrix elimination was as reported previously [16]. Briefly, the samples (generally in slice form) are cleaned by ultrasonic washing with trichloroethylene—acetone—methanol [17], etched with a hydrofluoric—nitric acid (1 + 1) mixture, washed in running twice-distilled water, dried in a nitrogen flow, and powdered finely in an agate mill.

Place 10—100 mg of sample in a PTFE test tube, add 2 ml of 65% HNO_3 and 5 ml of 12 M HF, and heat at 50°C for 1 h [15]. Then heat at 110°C for 2 h while passing filtered air through the tube. Phosphorus remains quantitatively in the small residue as phosphate [6]. Then add 5 ml of 0.5 M hydrochloric acid, shake well in order to dissolve any residue, transfer to a polyethylene centrifuge tube, wash the PTFE test tube with 4 ml of twice-distilled water, and add the wash to the centrifuge tube. Add 1 ml of 0.015 M ammonium heptamolybdate (0.1 M Mo(VI)) and 10 ml of n-butyl acetate. Wait for 5 min, shake for 2 min, centrifuge, and discard the aqueous layer containing the excess of molybdenum. Wash three times with 10-ml portions of (1 + 9) hydrochloric acid to remove any trace of the excess of molybdenum present in the organic layer. Transfer an n-butyl acetate aliquot to a separating funnel and decompose the molybdophosphoric acid and extract molybdate with 2 ml of 2 M NH_4NO_3—1 M NH_3 buffer solution, by shaking for 1 min. Repeat the extraction with another 1-ml portion of the alkaline buffer, taking care that the plug of the separating funnel is well washed. Run the two alkaline extracts into a second separating funnel, add 2 ml of 2 M HNO_3, and wash the aqueous layer with a few milliliters of benzene in order to remove any n-butyl acetate that may have saturated the aqueous phase.

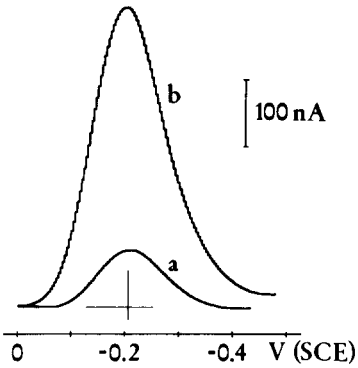

Fig. 2. Typical polarograms showing the method of peak measurement. Operating features as reported in the Procedure. (a) Blank; (b) 4 ng P ml^{-1}.

Transfer the solution to a polarographic cell, deaerate for 3 min, and record the polarogram from 0 to −0.4 V (vs. SCE). Measure the peak height at −0.21 V and compare it with a calibration curve obtained in the same manner. A typical polarogram with the method of measurement is reported in Fig. 2. The calibration curve obtained under the recommended conditions is nearly linear up to 0.1 μg P ml^{-1}; the relative standard deviation (n = 10) for 0.001 μg P ml^{-1} taken through the whole procedure was ±4%.

RESULTS AND DISCUSSION

Table 1 reports the results obtained for some silicon samples, with a comparison of results obtained by electrical [1] and fluorimetric measurements [5]. The results indicate that the proposed method allows satisfactory determinations and is suitable for routine analysis. The precision and sensitivity of the polarographic method are better than those of the fluorimetric method. When the described conditions are used, the proposed method

TABLE 1

Determination of phosphorus in silicon samples

Sample[a]	Resistivity (ohm × cm)	P[b] ($\mu g\ g^{-1}$)	Fluorimetric[c]		Polarographic[d]	
			P ($\mu g\ g^{-1}$)	s_r (%)	P ($\mu g\ g^{-1}$)	s_r (%)
W.Ch.	4.2×10^{-2}	8.1	7.8	4.0	7.94	1.7
W.Ch.	6.4×10^{-2}	4.0	4.4	9.0	4.32	1.8
M.	9.0×10^{-2}	2.2	2.4	9.5	2.38	2.1
M.	4.1×10^{-1}	0.33	—	—	0.32	2.1

[a]W. Ch., Waker Chemitronic GmbH, Burghausen (FRG); M., Montedison SpA, Milan (Italy). [b]Phosphorus content derived from electrical measurements [1]. [c]Fluorimetric determinations (n = 5) [5]. [d]n = 10.

permits determinations of phosphorus levels as low as 5 ng g^{-1}, with a relative standard deviation of ±4—5%.

No cations were found that cause interference on the catalytic wave of molybdate. Those species that have reduction potentials near the wave of molybdate would be potential interferences, but the n-butyl acetate extraction of molybdophosphoric acid is highly selective, thus eliminating all interferences. This same extraction eliminates any interference from the silicate residue because molybdosilicic acid is not extracted.

The authors thank Prof. P. Lanza and D. Nobili for their helpful suggestions.

REFERENCES

1 J. C. Irvin, The Bell System Tech. J., 41 (1962) 387.
2 J. S. Makris and B. J. Masters, J. Electrochem. Soc., 120 (1973) 1252.
3 E. Ligeon, M. Bruel, A. Bontemps, G. Chambert and J. Monnier, J. Radioanal. Chem., 16 (1973) 537.
4 G. Restelli, F. Girardi, F. Mousty and A. Ostidich, Nucl. Instrum. Methods, 112 (1973) 581.
5 P. L. Buldini and D. Sandrini, Anal. Chim. Acta, 98 (1978) 401.
6 F. A. Pohl and W. Bonsels, Mikrochim. Acta, (1962) 97.
7 F. Pottkamp and F. Umland, Angew. Chem., 83 (1971) 809; Fresenius Z. Anal. Chem., 255 (1971) 367; 260 (1972) 185.
8 F. Pottkamp, F. Umland and H. Reimann, Fresenius Z. Anal. Chem., 261 (1972) 102.
9 A. Bazzi and D. F. Boltz, Anal. Lett., 9 (1976) 1111.
10 A. G. Fogg and K. S. Yoo, Anal. Lett., 9 (1976) 1035.
11 See S. J. Simon and D. F. Boltz, Anal. Chem., 47 (1975) 1758 (and references therein).
12 D. F. Boltz and M. G. Mellon, Anal. Chem., 20 (1948) 749.
13 D. F. Boltz and J. A. Howell (Eds.) Colorimetric Determination of Non-metals, J. Wiley, New York, 1978, p. 343.
14 P. Lanza, D. Ferri and P. L. Buldini, Analyst (London), 105 (1980) 379.
15 P. L. Buldini, Q. Zini and D. Ferri, Anal. Chim. Acta, 124 (1981) 233.
16 P. L. Buldini, D. Ferri and P. Lanza, Anal. Chim. Acta, 113 (1980) 171.
17 P. Lanza and P. L. Buldini, Anal. Chim. Acta, 85 (1976) 69.

Analytica Chimica Acta, 124 (1981) 107—112

DETERMINATION OF SELENIUM(IV) BY ANODIC STRIPPING VOLTAMMETRY WITH AN IN SITU GOLD-PLATED ROTATING GLASSY CARBON DISK ELECTRODE

ROBERT S. POSEY and RICHARD W. ANDREWS*

Department of Chemistry, University of Alabama in Birmingham, University Station, Birmingham, AL 35294 (U.S.A.)

(Received 26th February 1980)

SUMMARY

The application of an in situ gold-plated glassy carbon disk electrode to the determination of selenium(IV) by anodic stripping voltammetry is described. A single anodic stripping peak is obtained for solutions containing less than 1×10^{-6} M Se(IV). The minimum concentration detected was 2×10^{-9} M Se(IV). The determination of selenium in NBS SRM 1577 (Bovine Liver) by anodic stripping voltammetry with an in situ gold-plated rotating glassy carbon electrode yielded a value of 1.14 ± 0.07 μg Se g^{-1} compared with a certificate value of 1.1 ± 0.1 μg Se g^{-1}.

A recent paper described the determination of tellurium(IV) by anodic stripping voltammetry (a.s.v.) with the use of an in situ gold-plated rotating glassy carbon disk electrode (RAuGCDE) [1]. In the case of the determination of Te(IV) by a.s.v. with glassy carbon electrodes, a substantial enhancement of sensitivity was observed when Au(III) was also present in the sample solution and codeposition of gold and tellurium occurred [1]. When solid gold electrodes are used for a.s.v., there is evidence of poor reproducibility of current—voltage curves and extraneous stripping peaks in the stripping voltammograms recorded for the supporting electrolyte solutions [2]. Mechanical pretreatment (polishing) usually removes these effects, but such pretreatment is neither convenient nor simple.

A gold-plated glassy carbon electrode offers an opportunity to circumvent such difficulties insofar as the gold surface is continuously renewable. No decrease in the detection limits for the determination of Te(IV) by a.s.v. was observed when externally gold-plated glassy carbon electrodes were compared to solid gold electrodes [1]. When Au(III) was added to test solutions containing Te(IV) and allowed to codeposit, detection limits similar to the solid gold electrode were also obtained. Such electrodes were described as in situ gold-plated glassy carbon electrodes; they should not be regarded as gold analogs of mercury thin film electrodes in which a very concentrated amalgam is formed that enhances the sensitivity of the a.s.v. determination [3]. Advantages of the gold-plated glassy carbon electrodes

are those of experimental simplicity (the gold film can be removed by wiping the electrode surface with a tissue) and an enhancement of the sensitivity of the a.s.v. determination in which a glassy carbon electrode is used as the working electrode.

The voltammetry of selenium(IV) in 0.1 M $HClO_4$ at RAuDE's has been described [4]. In that report, the use of externally gold-plated glassy carbon electrodes for the determination of selenium(IV) was suggested. In this report, the determination of selenium(IV) by a.s.v. with in situ RAuGCDE's is described.

EXPERIMENTAL

Apparatus and instrumentation

A model RDE3 bipotentiostat (Pine Instrument Co., Grove City, PA) was used as a 3-electrode potentiostat. A model PIR Analytical Rotator and glassy carbon disk electrode (Pine Instrument Co.), were used in all experiments. The projected surface area of the glassy carbon disk electrode was 0.452 cm^2. A model 2000 Omnigraph X-Y recorder (Houston Instruments, Belaire, TX) was used to record current—potential curves. A Keithley model 168 digital multimeter was used to measure all voltages, and a Keuffel and Esser compensating planimeter was used to integrate peak areas. The electrolysis cell was a Metrohm titration cell modified to accommodate the RAuGCDE by enlarging the center hole of the cap. The reference and auxiliary electrodes were separated from the main chamber by fine glass frits. All glass parts of the electrolysis vessel were soaked in concentrated nitric acid for at least 3 h before use. The reference electrode was a Ag/AgCl electrode filled with 4 M NaCl; a spiral of Pt wire served as the auxiliary electrode.

The RGCDE was polished with 1.0 μm, and 0.05 μm Buehler alumina on Buehler microcloth lubricated with deionized distilled water. The potential of the RGCDE was cycled between +1.0 V and —0.40 V during deaeration; following deaeration the working electrode was cycled between the previous limits until a reproducible current—voltage curve was recorded. The solution was then made 1×10^{-6} M in gold(III) for the in situ RAuGCDE experiments.

Reagents

The Se(IV) stock solution was prepared from selenium (99.999%; Alpha Ventron). The gold(III) plating solution was prepared by dissolving gold (99.999%; Alpha Ventron) in a minimum of aqua regia and dilution with 0.1 M HNO_3. All other solutions were prepared from Baker Analyzed Reagents. The water used was demineralized, distilled from alkaline permanganate, and redistilled; distillations were done under nitrogen. Stock solutions were stored in polyethylene bottles; all subsequent solutions were prepared by dilution of appropriate quantities of the stock solutions dispensed with Eppendorf micropipets.

Procedure for the determination of selenium in NBS SRM 1577 (Bovine Liver)

Weigh the lyophilized sample into the dissolution flask and attach the reflux head. Add 25 ml of a 1:1 HNO_3:$HClO_4$ mixture per gram of liver. Heat until the sample dissolves and dense fumes of perchloric acid are evolved. Cool the solution, transfer it to a 100-ml volumetric flask, and dilute to volume. Transfer the diluted solution to the electrolysis cell, deaerate, and add a volume of gold(III) stock solution to make the sample solution 1×10^{-6} M in Au(III). Set the potential of the RAuGCDE to −0.400 V, deposit for 10 min, sweep the potential to +1.4 V and record the stripping voltammogram. Add two 0.80-μg aliquots of Se(IV) and repeat the deposition and stripping steps after each addition.

RESULTS AND DISCUSSION

Figure 1 shows current—voltage curves recorded following a 4-min deposition at −0.40 V for a solution containing no Se(IV), 3×10^{-7} M Se(IV), and 3×10^{-7} M Se(IV) with 1.0×10^{-6} M Au(III). The residual current—voltage curve with no deposition is also shown. The enhancement in the magnitude of the Se(IV) stripping peak by Au(III) is substantial, and clearly indicates that Se(0) is stabilized by an Au—Se interaction on the electrode. Figure 2 shows a series of current—voltage curves recorded with the in situ RAuGCDE for several concentrations of Se(IV). The behaviour is similar to that previously reported for the voltammetry of Se(IV) at RAuDE's [4]. The quantity of charge consumed in the oxidation of deposited selenium in the peak at +1.1 V never exceeds a monolayer equivalent. Additionally, it should be noted that a single anodic stripping peak is observed when the concentration of Se(IV) is less than 5×10^{-5} M when the potential is held at a value less than +0.05 V. For Se(IV) concentrations less than 1×10^{-5} M and for deposition times less than 5 min with E = −0.40 V, a single anodic stripping peak was observed.

Stripping voltammetry of Se(IV) with in situ RAuGCDE

The utility of the single anodic stripping peak at +1.1 V observed for less than 1×10^{-6} M Se(IV) at deposition times less than 5 min was assessed. The influences of deposition potential (E_{dep}), deposition time (t_{dep}), sweep rate (v), rotational velocity (ω), Au(III) concentration, and Se(IV) concentration were examined. Finally, the method was applied to the determination of selenium in NBS Bovine Liver (SRM 1577). Figure 3 shows a plot of the absolute value of the charge consumed vs. deposition potential; the apparent $E_{1/2}$ is −0.07 V vs. Ag/AgCl which is comparable to the −0.10 V vs. SCE value previously reported for the reduction of Se(IV) on RAuDE's [2]. Plots of charge vs. deposition time were linear for deposition periods as long as 10 min. Plots of charge vs. $\omega^{1/2}$ and peak current vs. v were also linear. Table 1 summarizes the regression analysis of the plots. The Levich equation implies that a plot of charge vs. $\omega^{1/2}$ will be linear for a convective diffusion-

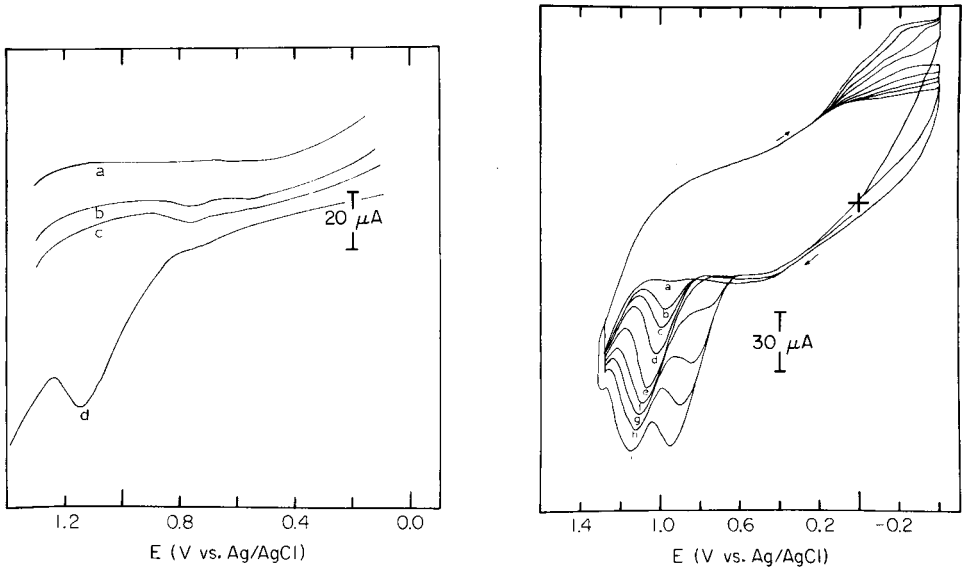

Fig. 1. Stripping voltammograms for Se(IV) at glassy carbon RDE's. RGCDE; 1600 rpm; 5 V min^{-1}; 0.1 M $HClO_4$; E_{dep} = —0.40 V. (a) Residual, no deposition; (b) residual, 4-min deposition; (c) 3 × 10^{-7} M Se(IV), 4-min deposition; (d) 3 × 10^{-7} M Se(IV) + 1 × 10^{-6} M Au(III), 4-min deposition.

Fig. 2. Current—potential curves for several Se(IV) concentrations. RAuGCDE; 1600 rpm; 5 V min^{-1} 0.1 M $HClO_4$; 1 × 10^{-6} M Au(III). Selenium(IV) molarity: (a) 0; (b) 5 × 10^{-6}; (c) 1 × 10^{-5}; (d) 2 × 10^{-5}; (e) 3 × 10^{-5}; (f) 5 × 10^{-5}; (g) 7 × 10^{-5}; (h) 1 × 10^{-4}; (i) 2 × 10^{-4}.

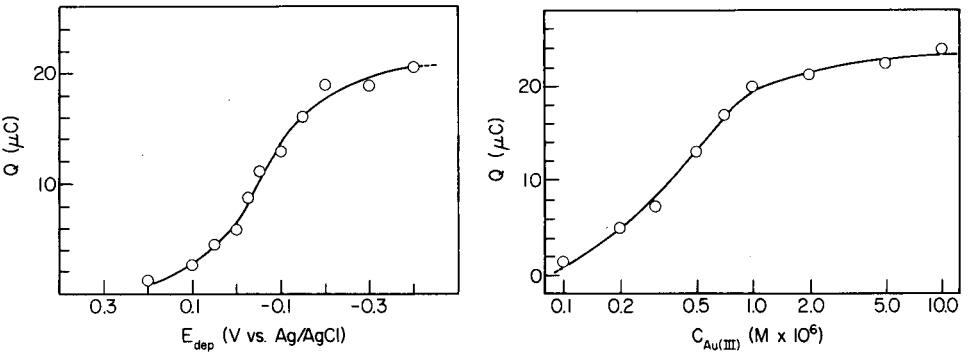

Fig. 3. Deposition potential study. RGCDE; 2500 rpm; 5 V min^{-1}; T_{dep} = 2 min; 0.1 M $HClO_4$; 2 × 10^{-7} M Se(IV); 1 × 10^{-6} M Au(III).

Fig. 4. Gold(III) concentration study. RGCDE: 2500 rpm; 5 V min^{-1}; E_{dep} = —0.40 V; t_{dep} = 2 min; 0.1 M $HClO_4$; 2 × 10^{-7} M Se(IV).

TABLE 1

Regression analysis of characteristic plots[a]

Regression equation	Range	s_{yx}	S_b	S_a
$Q(\mu C) = 0.63\ t_{dep}$ (s) + 0.009	$0 \leqslant t_{dep} \leqslant 10$	0.58	0.4	0.0017
$Q(\mu C) = 2.07\ \omega^{1/2}$ (rad $s^{-1})^{1/2}$ + 0.8	$42 \leqslant \omega \leqslant 513$	1.13	1.3	0.08
$i_p(\mu A) = 0.112\ v$ (mV s^{-1}) + 6.9	$10 \leqslant v \leqslant 150$	0.29	0.49	0.005
Q/t_{dep} ($C\ min^{-1}$) = $2.54 \times 10^8 C_{Se(IV)}$ (M) + 0.9	$2 \times 10^{-9} \leqslant C_{se} \leqslant 2 \times 10^{-6}$	0.48	0.19	1.0×10^6

[a]Regression equation is taken to be linear with $y = ax + b$. S_{yx}, S_a, and S_b are standard deviations of regression, slope, and intercept, respectively.

controlled deposition process [5] while Branina's equation predicts a linear relationship between the peak stripping current observed for RDE's and the applied sweep rate [6]. The influence of the Au(III) concentration on the absolute value of the quantity of charge consumed during the oxidation of the deposited selenium was investigated and the results are shown in Fig. 4. At Au(III) concentrations less than 1×10^{-7} M, little enhancement is observed while further increase in the quantity of charge is not observed for Au(III) concentrations greater than 5×10^{-6} M.

A calibration curve was prepared to determine the detection limits and linear dynamic range of the determination of Se(IV) by a.s.v. with in situ RAuGCDE's. A plot of charge normalized by deposition time was linear from 2×10^{-9} M to 2×10^{-6} M. The regression analysis of that curve is also summarized in Table 1. The 2×10^{-9} M detection limit is four times larger than the 5×10^{-10} M value previously obtained with a RAuDE [4]. This is a consequence of the larger residual currents associated with glassy carbon electrodes. Recent experience with the determination of tellurium(IV) by a.s.v. demonstrated only a factor of two difference in detection limits obtained with in situ RAuGCDE's and RAuDE's [1]. The in situ RAuGCDE was chosen for use here because of its greater experimental simplicity. It should be noted that in situ gold-plated electrodes are less costly than solid gold electrodes.

Determination of selenium(IV) in NBS SRM 1577 (Bovine Liver)

The Bovine Liver standard (NBS SRM 1577) has a certificate value of 1.1 ± 0.1 μg Se g^{-1}. Selenium was determined in several samples of the bovine liver by the procedure detailed above. Stripping voltammograms from a typical determination and the standard addition curve are shown in Fig. 5. The dashed line in Fig. 5 indicates the baseline chosen for the integration of the selenium stripping peak shown in curve a. The values obtained in four determinations were 1.13, 1.22, 1.07 and 1.15 μg Se g^{-1}. Four blank determinations yielded values of 0.022, 0.030, 0.020 and 0.025 μg Se g^{-1}. The average value corrected for the blank is 1.12 ± 0.10 μg Se g^{-1} (mean ±95% confidence limits). The agreement with the certificate value is excellent.

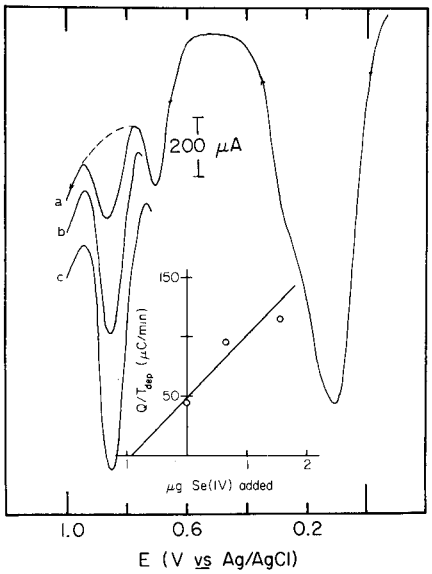

Fig. 5. Determination of selenium in bovine liver. RAuGCDE; 1600 r.p.m.; 5 V min^{-1}; E_{dep} = −0.40 V; 0.7998 g of sample dissolved in HNO_3:$HClO_4$ + 1 × 10^{-6} M Au(III). (a) Sample with 10-min deposition; (b) sample + 0.79 μg Se(IV) with 11-min deposition; (c) sample + 1.58 μg Se(IV) with 12-min deposition.

The stripping peak at +0.10 V is due to the presence of copper in the bovine liver while the peak at +0.75 V is most likely due to the presence of Te(IV). Addition of tellurium(IV) to the test solution resulted in an increase in the magnitude of the peak; the certificate for SRM 1577 contains no information regarding the tellurium content; the present experiments indicate that the liver contains between 0.1 and 0.5 μg Te g^{-1}.

The support of the Faculty Research Council of the University of Alabama in Birmingham is gratefully acknowledged.

REFERENCES

1 R. S. Posey and R. W. Andrews, Anal. Chim. Acta, 119 (1980) 55.
2 R. W. Andrews, Ph.D. Dissertation, Iowa State University, Ames, IA, 1975.
3 T. M. Florence, J. Electroanal. Chem., 27 (1970) 273.
4 R. W. Andrews and D. C. Johnson, Anal. Chem., 47 (1975) 294.
5 V. G. Levich, Physiochemical Hydrodynamics, Prentice-Hall, Englewood Cliffs, NJ, 1962.
6 Kh. Z. Branina, Electrokhimyia, 2 (1966) 1006.

Analytica Chimica Acta, 124 (1981) 113—119

DOSAGE DIRECT DU PARACETAMOL DANS LES MILIEUX BIOLOGIQUES PAR POLAROGRAPHIE SINUSOIDALE

M. ALKAYER, J. J. VALLON*, Y. PEGON et C. BICHON

Laboratoire Pharmaceutique de Biochimie, Toxicologie et Analyse des Traces, Hopital E. Herriot et Département de Chimie Analytique, Faculté de Pharmacie, Lyon (France)

(Reçu le 4 août 1980)

SUMMARY

(The direct determination of paracetamol in biological fluids by a.c. polarography.) Paracetamol can be determined rapidly in biological fluids (blood serum and urine) by a.c. polarography. After elimination of protein by perchloric acid, followed by reaction with nitrous acid in acidic medium, the nitro derivative is measured at pH 10. As little as 4×10^{-6} M paracetamol (0.6 $\mu g\ ml^{-1}$) in serum can be determined.

RESUME

Les auteurs proposent un dosage direct du paracétamol dans les milieux biologiques en particulier le sérum sanguin, par polarographie à tension sinsoïdale surimposée. Après défécation à l'acide perchlorique suivie de réaction en milieu acide avec l'acide nitreux, le dérivé nitré formé est mesuré par polarographie à pH 10. Des quantités aussi faibles que 4×10^{-6} M, soit 0,6 $\mu g\ ml^{-1}$ dans le sérum, peuvent être dosées.

Le paracétamol (acétaminophène, N-acétyl-*p*-aminophénol) constitue chez l'homme le métabolite principal (80%) de la phénacétine (ethoxy-*p*-acétanilide) dont il permet d'expliquer les propriétés analgésiques et antipyrétiques. Le paracétamol entre dans la composition de nombreuses spécialités (48 recensées en France en 1980).

Bien que la paracétamol soit beaucoup moins toxique que la phénacétine (action méthémoglobinisante en particulier) son utilisation thérapeutique doit rester limitée dans le temps, car même à doses usuelles, on note la possibilité d'atteinte hépatique chronique [1]. L'intoxication aigüe se caractérise par une nécrose hépatique tardive proportionnelle à la dose. Le responsable est un métabolite hydroxylé formé sous l'action du cytochrome P450 hépatique; ce métabolite hautement réactif, est normalement inactivé dans le foie par conjugaison avec le glutathion. En cas de surdosage la réserve hépatique de glutathion s'épuise et le métabolite hydroxylé se lie par covalence à des macromolécules essentielles à la survie le l'hépatocyte et entraîne la nécrose hépatique centrolobulaire. Les barbituriques et l'alcool, activateurs du cytochrome P450, aggravent ce phénomène. En cas d'intoxication aigüe, la nécrose hépatique survient après 24—48 h. Il est donc possible

de se faire une idée de la gravité de l'intoxication en dosant le paracétamol sanguin dont la demi-vie, normalement de 1,5—2 h, est considérablement augmentée.

Les méthodes de dosage du paracétamol sont, soit des méthodes avec séparation chromatographique, soit des méthodes spectrophotométriques. Bien qu'une méthode directe de chromatographie en phase gazeuse ait été proposée [2], il est préférable de former un dérivé silylé [3—6] ou acétyle [7, 8] du paracétamol avant la séparation. En chromatographie liquide haute performance la détection est réalisée par spectrophotométrie dans l'ultraviolet [9—11] ou par électrochimie [12]. Les méthodes spectrophotométriques sont moins spécifiques. Par spectrophotométrie dans l'ultraviolet, le dosage est fait, soit par lecture différentielle à deux pH [13], soit par lecture à une longueur d'onde où les interférences sont moins importantes [14]. On trouve aussi des techniques utilisant la réduction du complexe tripyridyl-s-triazine-fer(III) [15, 16], la décoloration du diphénylpicrylhydrazyl [14], et la formation de 2-nitro-4-aminophénol avec l'acide nitreux [17], ou d'un indophenol [18] ou d'un azoïque après hydrolyse, diazotation et copulation [19, 20].

Nous présentons ici une méthodes de dosage dans le sang et les urines fondée sur la nitrosation de la molécule suivie de la détection du dérivé formé par polarographie à tension sinusoïdale surimposée. La méthode montre une bonne sélectivité liée à la réaction de nitrosation et une sensibilité élevée permettant d'évaluer des taux sanguins thérapeutiques.

PARTIE EXPERIMENTALE

Matériel et réactif

Le polarographe est un modèle Tacussel PRG 3. Les solutions aqueuses sont les suivantes: nitrite de sodium (Prolabo; 0,1 à 1 M), acide perchlorique (Prolabo; 10%, voisin de 0,65 M), tampon de Britton—Robinson (mélanges à parties égales d'acide phosphorique, acide acétique, acide orthoborique, chacun 0,04 M) et tampon borate 0,3 M à pH 10.

Etude de la réaction entre l'acide nitreux et le paracétamol

Cette réaction a déjà été l'objet de nombreux travaux [21—24] en vue de la mise au point du dosage colorimétrique du médicament. Des avis contradictoires ont été émis en ce qui concerne la structure du chromophore obtenu. Un premier travail de Le Perdriel et al. [21] apporta la preuve de la formation d'un dérivé *ortho*-nitré (et non pas nitrosé comme certains le pensaient) par action en milieu chlorhydrique d'un excès de nitrite de sodium. La réaction est complète après 15 min et après alcalinisation à pH 10 le chromophore présente un maximum d'absorption à 440—450 nm. Le mécanisme de la réaction fut ensuite élucidé par Challis et Higgins [24] étudiant le nitrosation des phénols *para*-substitués: la première étape consiste en une nitrosation en *ortho* du groupe phénol suivie immédiatement et

rapidement d'une oxydation en dérivé nitré en milieu acide. La vitesse de la nitrosation est constante pour les concentrations d'acide perchlorique inférieure à 0,5 M [24]. Nous avons étudié sur du paracétamol 10^{-4} M l'influence de la concentration en nitrite sur la vitesse de formation du dérivé nitré à pH 0 dans l'acide perchlorique à 10%. La Fig. 1 montre que la nitration est complète en 30 min ou moins dès que la concentration en nitrite est supérieure ou égale a 0,1 M. Le dérivé formé reste stable pendant plus de 3h: après 24 h on note une perte d'intensité de 10%. L'intensité maximum n'est jamais obtenue avec du nitrite 0,01 M.

En fonction de ces résultats, nous avons adopté pour la suite des essais le protocole suivant pour l'étape de nitration: contact de 30 min avec le nitrile de sodium 0,1 M en milieu acide perchlorique à 5%.

Etude du comportement polarographique du dérivé nitré

La réduction polarographique des groupements nitrés procède généralement selon deux étapes successives: la première donne une vague polarographique à 4 électrons et conduit au dérivé hydroxylaminé qui, dans une deuxième étape à deux électrons, conduit à l'amine. Toutefois pour les phénols *ortho* ou *para* nitrés la réduction passe par une structure quinonique intermédiaire de sorte que l'on n'observe qu'une vague unique très intense à 6 électrons [25].

Influence du pH. Nous avons étudié successivement les variations des potentiels de pic (E_p) et celles des intensités (i_p) en fonction du pH (Fig. 2). On constate une diminution linéaire de Ep avec le pH dans le tampon de Britton—Robinson 0,04 M; la variation est de 0,06 volt par unité pH. L'étude de l'intensité de pic montre que i_p est presque constante aux pH acides et jusqu'à pH 6. Elle augmente alors brutalement pour atteindre une valeur double à partir de pH 9 et jusqu'à pH 11 où les valeurs diminuent de nouveau.

Influence de la fréquence du signal surimposé. Dans le tampon de Britton—Robinson l'étude a été faite sur 10 ml de paracétamol 10^{-5} M à pH 10. La

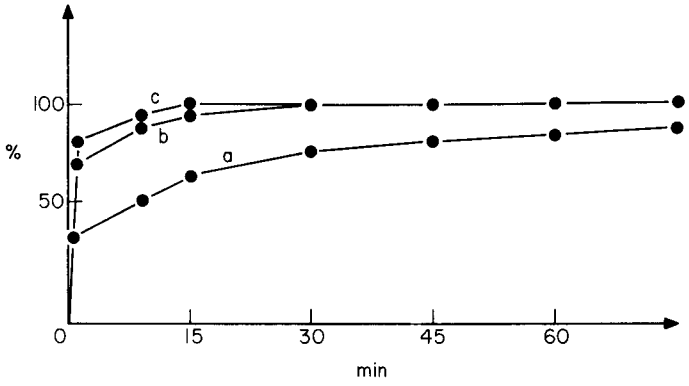

Fig. 1. Cinétique de la nitrosation du paracétamol dans $HClO_4$ 10%.

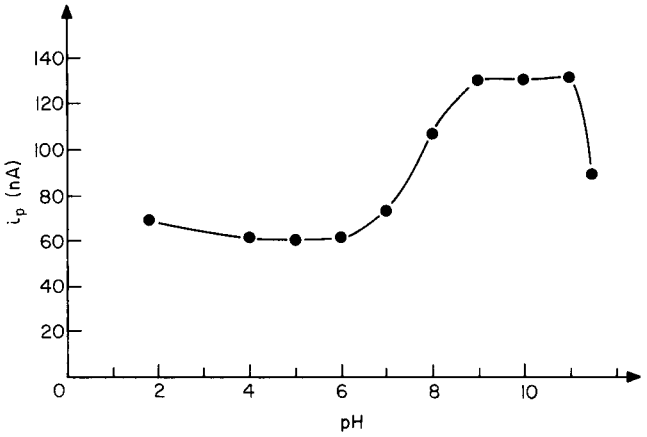

Fig. 2. Influence du pH sur l'intensité du pic (i_p).

nitration préalable était obtenue par action du nitrite de sodium 0,1 M pendant 30 min. Les réglages de l'appareil étaient: ΔE = 10 mV; ϕ = 0 gr; ϵ = 125 nA/25 cm; h = 60 cm; m = 1 coup/s. Nous avons constaté que de 3 Hz à 300 Hz le courant de base augmente régulièrement tandis que l'intensité faradaïque passe par un maximum à 15 Hz. Au delà de 100 Hz le pic se déforme et n'est plus mesurable (Tableau 1).

Influence de l'angle de phase de détection (ϕ). A la fréquence choise de 15 Hz, la zone de —50 à + 150 grades a été explorée avec les mèmes réglages que précédement. La sensibilité maximum de détection est obtenue pour un angle de phase voisin de 0 gr (Tableau 1).

Influence de l'amplitude du signal alternatif (ΔE) surimposé (ω). L'intensité alternative enregistrée est en principe proportionnelle à l'amplitude de la

TABLEAU 1

Variations de l'intensité de pic avec la fréquence (ω), l'angle (ϕ), l'amplitude (ΔE) de la tension surimposée. Etude de la largeur de pic à mi-hauteur (ΔE, $i_{p/2}$).

$i = f(\omega)$		$i = f(\phi)$		$i = f(\Delta E)$		
ω(Hz)	i_p(nA)	ϕ(grades)	i_p(nA)	ΔE(mV)	i_p(nA)	$\Delta E\ i_{p/2}$
3	23	—50	17,5	1	2,5	0,08
6	24	—25	23	2	5	0,08
9	25	0	25	5	13	0,08
12	25	+25	24	10	25	0,08
15	25	+50	22	20	41	0,09
30	25	+100	20	50	50	0,13
60	21,5					
120	17,5	+150	12	100	—	—
180—	—			200	—	—
300						

tension surimposée, au moins pour les faibles valeurs de celle-ci. L'intensité maximum est obtenue pour une tension de —50 mV, mais au delà de —50 mV l'accroissement d'intensité n'est plus proportionnel à ΔE et le pic polarographique s'élargit rapidement $\Delta E\ i_{p/2}$ = 0,13 V (Tableau 1). Le gain de sensibilité n'est que de 13% environ entre 20 et 50 mV de sorte que nous avons choisi une tension alternative surimposé de 20 mV pour les mesures.

Dosage polarographique du paracétamol sérique

Les critères de qualité de la méthode ont été déterminés à partir d'un pool de sérums humains auquel on a ajouté du paracétamol. Les dosages ont été faits sur 1 ml de surnageant résultant de la défécation de 1 ml de sérum par 1 ml d'acide perchlorique à 10%. A cette prise d'essai du surnageant on ajoute 0,1 ml de nitrite de sodium 1 M; après 30 min on dilue dans 8,9 ml de tampon borique à pH 10 et en enregistre le polarogramme.

Pour l'enregistrement de la courbe d'étalonnage, les essais ont été pratiqués sur six points de la courbe (0—1 × 10^{-4} M de paracétamol dans le sérum soit 0—5 × 10^{-6} M dans la solution finale) réalisés sur six échantillons du même sérum. La ligne de base, fournie par l'enregistrement du tampon Britton—Robinson pH 10 en l'absence de sérum, a servi comme valeur de zéro des intensités (Fig. 3, Tableau 2). La sensibilité, correspondant à la pente de la courbe d'étalonnage est égale à 4,3 nA environ pour une concentration de 10^{-6} M. Pour mesurer la limite de détection, nous avons

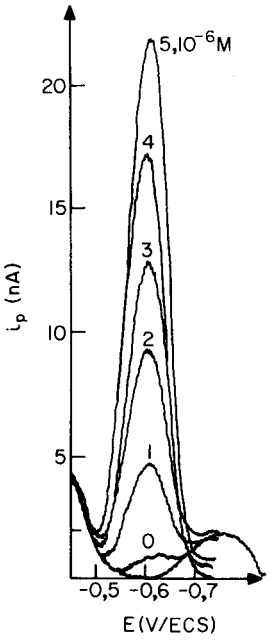

Fig. 3. Etalonnage dans le sérum.

TABLEAU 2

Courbe d'étalonnage du paracétamol (0—10^{-4} M dans le sérum soit 0—5 × 10^{-6} M dans la solution analysée)

Paracétamol (× 10^{-6} M)	i_p [a] (nA)	Ecart-type (s)	Coefficient de variation (%)	Paracétamol (× 10^{-6} M)	i_p [a] (nA)	Ecart-type (s)	Coefficient de variation (%)
0	0,800	0,0175	2,18	3	12,708	0,0684	0,53
1	4,557	0,0568	1,25	4	16,771	0,0684	0,41
2	8,736	0,0983	1,12	5	21,833	0,0819	0,37

[a] $n = 7$.

enregistré sept polarogrammes d'un sérum dépourvu de paracétamol. Les intensités dues au sérum, mesurées au potentiel de pic et par rapport au tampon Britton—Robinson, nous ont servi à calculer la limite de détection (i_p + 3s) pour une probabilité de 99,8%. Compte tenu de la sensibilité de la méthode, la limite de détection correspond à une concentration en paracétamol de 1,99 × 10^{-7} M dans la solution finale soit environ 4 × 10^{-6} M dans le sérum (0,60 μg ml^{-1}).

Nous avons recherché la répétabilité en enregistrant sept fois au cours de la journée un même surnageant de défécation d'un sérum chargé avec 10^{-4} mol l^{-1} de paracétamol. Le coefficient de variation était de 0,25%. Pour établir la reproductibilité, plusieurs sérums ont été chargés 7 jours de suite en paracétamol et enregistrés en répétant chaque jour la défécation et la nitrosation. Le coefficient de variation est de 2,80%.

Plusieurs médicaments susceptibles d'être associés au paracétamol dans des formes médicamenteuses ou leurs métabolites ont été testés: acide acétyl salicylique, acide salicylique, phénacétine, antipyrine, amidopyrine. Aucun de ces produits en solution 10^{-4} M n'a donné de pic polarographique dans la zone de potentiel dans les conditions du dosage. Mélangés au paracétamol, aucun n'a provoqué de modification du pic de celui-ci.

DISCUSSION

L'étude du comportement polarographique du dérivé nitré a montré l'existence d'une seule vague ce qui prouve, s'il en est besoin, que comme l'ont montré Le Perdriel et al. [21] c'est le dérivé *ortho*-nitré qui se forme. Le potentiel de réduction diminue linéairement quand le pH augmente ce qui est en accord avec une réduction par hydrogénation en amine primaire. L'intensité maximum obtenue en milieu alcalin tend à prouver l'existence de phénomènes électrostatiques surajoutés qui seraient liés à l'existence de la forme anionique du paracétamol. L'application au dosage direct dans le sérum, sans extraction préalable a été possible grâce à la double sélectivité apportée par le nitration et par la détection polarographique. Certains auteurs [21] avaient déjà montré l'absence d'interférence par des médic-

aments de structure voisine comme la phénacétine ou l'acétanilide. Le dosage polarographique s'est avéré très sensible puisque des taux sériques de 4×10^{-6} M sont décelables, alors que les concentrations au cours d'une thérapeutique sont de l'ordre de 10^{-3} M et que les méthodes colorimétriques ont une limite de détection vers 10^{-4} M.

La même méthode est applicable à d'autres milieux biologiques, en particulier les urines. Sa sélectivité, sa sensibilité et sa simplicité la rendent particulièrement utile pour la surveillance thérapeutique des malades.

BIBLIOGRAPHIE

1 P. Lechat, G. Lagier et J. Boiteau, Thérapie, 33 (1978) 551.
2 J. Grove, J. Chromatogr., 59 (1971) 289.
3 R. P. Miller et L. J. Fischer, J. Pharm. Sci., 63 (1974) 969.
4 G. Ramachander, F. D. Williams et J. F. Emele, J. Pharm. Sci., 62 (1973) 1498.
5 H. V. Street, J. Chromatogr., 109 (1975) 29.
6 B. H. Thomas et B. B. Coldmell, J. Pharm. Pharmacol., 24 (1972) 243.
7 L. P. Hackett et L. J. Dusci, Clin. Chim. Acta, 74 (1977) 187.
8 L. F. Prescott, J. Pharm. Pharmacol., 23 (1971) 807.
9 D. Blair et B. H. Rumack, Clin. Chem., 23/4 (1977) 743.
10 T. Buchanan, P. Adriaenssens and M. J. Stewart, Clin. Chim. Acta, 99/2 (1979) 161.
11 L. T. Wony, G. Solomonray et B. H. Thomas, J. Pharm. Sci., 65 (1976) 1064.
12 R. M. Riggin, A. L. Schmidt et P. T. Kissinger, J. Pharm. Sci., 64 (1975) 680.
13 J. Knepil, Clin. Chim. Acta, 52 (1974) 369.
14 J. I. Routh, N. A. Shane, E. G. Arrendondo et W. D. Paul, Clin. Chem., 14 (1968) 882.
15 T. Z. Liu et H. K. Oka, Clin. Chem., 25/6 (1979) 1143.
16 T. Z. Liu et H. K. Oka, Clin. Chem., 26/1 (1980) 69.
17 L. Chafetz, R. E. Daly, H. Schriftman et J. J. Lomner, J. Pharm. Sci., 60 (1971) 463.
18 R. M. Welch et A. H. Conney, Clin. Chem., 11 (1965) 1064.
19 B. B. Brodie et J. Axelrod, J. Pharmacol. Exp. Therap., 94 (1948) 22.
20 J. R. Gixelt, A. Robertson et E. W. Chesney, J. Pharm. Pharmacol., 15 (1963) 440.
21 F. Le Perdriel, C. Hanegraaff, N. Chastagner et E. De Montety, Ann. Pharm. Franc., 26 (1968) 227.
22 M. C. Inamdar et N. N. Kaji, Ind. J. Pharm., 31 (1969) 79.
23 L. Chafetz, R. E. Daly, H. Schriftman et J. J. Lomner, J. Pharm. Sci., 60 (1971) 463.
24 B. C. Challis et R. J. Higgins, J. Chem. Soc. Perkin Trans. 2, (1972) 2365.
25 R. Pointeau et J. Bonastre, Elements de Polarographie, Masson, Paris, 1970, p. 304.

Analytica Chimica Acta, 124 (1981) 121—129

IN SITU ELECTRODEPOSITION FOR THE DETERMINATION OF LEAD AND CADMIUM IN SEA WATER

G. E. BATLEY

Analytical Chemistry Section, Australian Atomic Energy Commission Research Establishment, Lucas Heights, N.S.W. 2234 (Australia)

(Received 19th August 1980)

SUMMARY

Electrodeposition techniques for the direct determination of lead and cadmium in sea water at the natural pH and in the presence of dissolved oxygen are examined. Anodic stripping voltammetry, at either the hanging mercury drop electrode or glassy carbon thin film electrode, is suitable for the determination of labile lead and cadmium. The presence of dissolved oxygen increases the height of the lead wave with a shift to more negative potentials. A more versatile technique is in situ deposition of labile metals on a mercury-coated graphite tube electrode. The mercury film, deposited in the laboratory, is stable on the dried tubes which are used later for field electrodeposition. The deposited metals are determined by electrothermal atomic absorption spectrometry.

A major problem in the determination of trace concentrations of heavy metals in natural waters is the ease with which sample contamination can occur during the analysis. Recent years have seen a proliferation of data in this area, many of which are patently in error because of contamination problems. For sea water, the absolute concentrations of metals such as lead and zinc are the subject of a continuing debate [1, 2], with recent publications [3, 4] reporting only nanogram per litre concentrations of these metals in open ocean waters. Techniques which require sample handling and multiple reagent additions are more prone to errors, which can be satisfactorily eliminated only by the use of in situ preconcentration or monitoring methods. An example is the submersible, chelating resin preconcentration procedures of Davey and Soper [5].

Anodic stripping voltammetry (a.s.v.) is one of the few techniques suitable for the direct determination of heavy metals in natural waters; however, it is not readily adaptable to in situ measurements. Lieberman and Zirino [6] examined a continuous flow system for the a.s.v. determination of zinc in sea water, using a tubular graphite electrode predeposited with mercury. A limitation of the approach was the need to pump sea water to the measurement cell, while the method required the removal of oxygen, with nitrogen, before measurements.

Recently, Batley and Matousek [7, 8] examined the electrodeposition of the irreversibly-reduced metals, Co, Ni and Cr, on graphite tubes for measure-

ment by electrothermal atomization. This method offered considerable potential for contamination-free preconcentration of heavy metals from sea water. Although only labile metal species will electrodeposit, it is likely that, at the natural pH, this fraction of the total metal could yet prove to be the most biologically important [9]. This paper examines techniques for the in situ electrodeposition and determination of lead and cadmium in natural waters.

EXPERIMENTAL

Apparatus and reagents

A PAR model 174 Polarographic Analyzer was used with either a hanging mercury drop electrode (HMDE) or a glassy carbon electrode (GCE) for a.s.v. studies. Measurements were made in the differential pulse mode using a pulse modulation amplitude of 25 mV.

The same unit was used in the laboratory for controlled potential electrodeposition, utilizing the cell and pump system described previously [8]. For field electrodeposition, a battery-powered, controlled potential electrolysis unit (AAEC Type 611) was used in conjunction with the electrode probe shown in Fig. 1. This consisted of a 60 × 3 cm Perspex cylinder having at one end, a teflon electrode holder, a platinum anode and a silver–silver chloride reference electrode. Pyrolytic-coated graphite tubes, supplied by Varian for use in their CRA-90 furnace unit, were used as cathodes. The sample was drawn through the electrode using a Masterflex peristaltic pump [8].

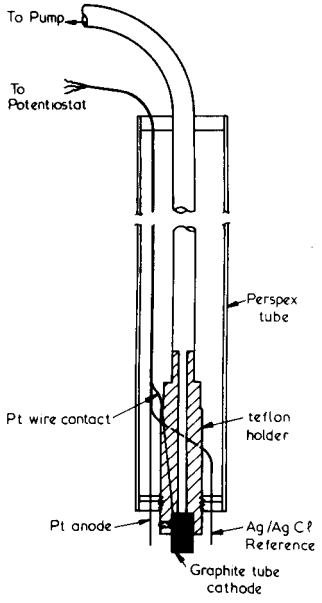

Fig. 1. Electrode probe used for in situ graphite tube electrodepositions.

Atomic absorption measurements were made with a Varian CRA-90 carbon furnace accessory on a Varian Techtron AA5 spectrometer. The furnace power supply was used in the atomization mode, programmed for a 500°C s^{-1} ramp to 1800°C for lead (1500°C for cadmium) with a 2 s hold. The lead line at 217.0 nm was monitored; the 228.8 nm line was used for cadmium.

Mercury(II) nitrate solution (3×10^{-2} M) was prepared by dissolution of the appropriate quantity of Merck Suprapur mercury in Suprapur nitric acid.

Method for graphite tube electrodeposition

Preclean the pyrolytic graphite tubes by firing several times at the atomization temperature, using the CRA-90 unit. Transfer a tube to the laboratory electrodeposition unit and plate with mercury, for 3 min, from a deaerated solution (25 ml) of distilled water containing mercury(II) nitrate (0.6 ml, 3×10^{-2} M) using a controlled potential of −0.3 V vs. Ag/AgCl. With the potential still applied, rinse the tube well with distilled water, dry the external faces with a filter paper and store in a polypropylene pill-pack until ready for use. At the sampling site, load the mercury-coated tube in the electrode probe with the aid of plastic-coated tweezers. Tighten the Perspex screw so that the tube touches the platinum contact. Immerse the probe in the water to a depth of about 10 cm, start the pump and apply the desired control potential (−0.85 V vs. Ag/AgCl for lead and cadmium). After the necessary deposition time (15—30 min for sea water), withdraw the probe, immerse it in distilled water for 5 s, then dry the external face of the tube, and place the tube in a pill-pack for transportation to the laboratory.

Atomic absorption determinations are done using the conditions outlined above. Determine reagent blanks by electrodeposition in the sampled water for comparable times at potentials where the metals of interest do not deposit (−0.3 V vs. Ag/AgCl for lead and cadmium).

RESULTS AND DISCUSSION

Voltammetry in the presence of oxygen

The determination of heavy metals by stripping voltammetry is usually done in the absence of oxygen. The reduction of oxygen is a two-step process giving rise, in sea water at the natural pH, to waves at −0.05 V and −0.9 V vs. SCE, because of the well-known reduction to hydrogen peroxide and hydroxide ion, respectively. In unbuffered solutions, hydroxide ions will increase the pH in the diffusion layer, with possible precipitation of metal species and a reduction in peak heights. Bond [10] showed that in buffered solutions, oxygen did not interfere with the pulse polarographic determination of cadmium, lead and copper, at concentrations above 5×10^{-6} M, apart from increasing the base current as a result of the oxygen reduction waves.

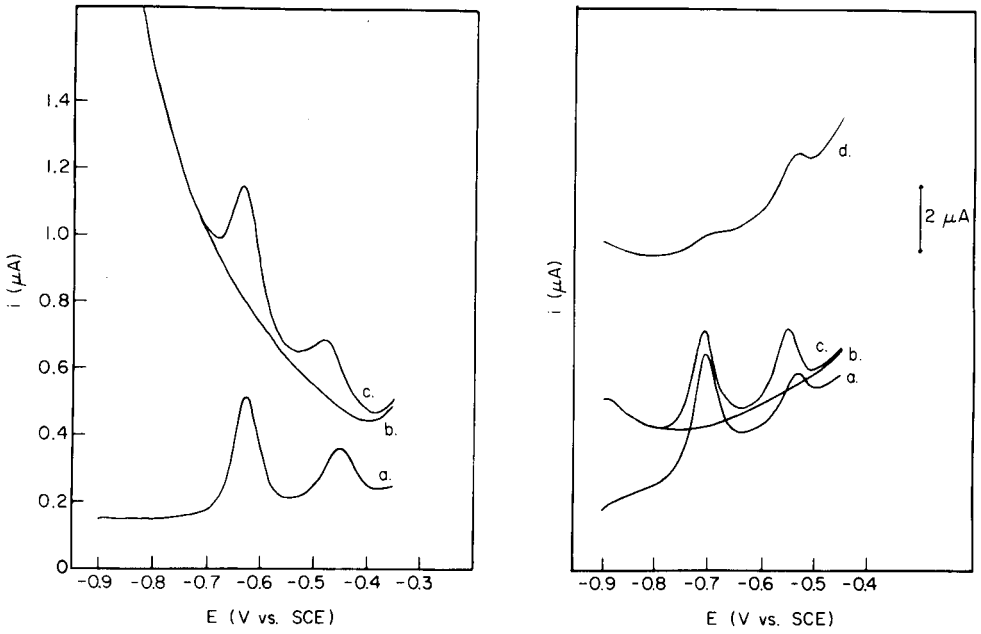

Fig. 2. Stripping peaks for cadmium and lead in sea water, pH 7.8, at HMDE. Differential pulse mode, 25-mV modulation, 3-min deposition at −0.9 V vs. SCE. (a) Deoxygenated solution containing 2.2 μg Cd l^{-1} and 4.1 μg Pb l^{-1}; (b) blank containing dissolved oxygen; (c) blank containing dissolved oxygen 2.2 μg Cd l^{-1} and 4.1 μg Pb l^{-1}.

Fig. 3. Stripping peaks for cadmium and lead in sea water, pH 7.8, at a performed mercury film on GCE. Differential pulse mode, 25-mV modulation, deposition at −0.9 V vs. SCE. (a) Deoxygenated solution, 2.2 μg Cd l^{-1}, 4.1 μg Pb l^{-1}, 3-min deposition; (b) in presence of dissolved oxygen, blank, 3-min deposition; (c) as for (b) plus 2.2 μg Cd l^{-1}, 4.1 μg Pb l^{-1}; (d) as for (b), 30-min deposition.

TABLE 1

Effect of oxygen and pH on a.s.v. calibration plots for Cd and Pb in sea water[a]

Metal	pH	Electrode	Slope of calibration plot (μA l^{-1})	
			O_2 present	O_2 absent
Cd	4.8	HMDE	0.133 ± 0.015	0.139 ± 0.009
Cd	7.8	HMDE	0.140 ± 0.011	0.147 ± 0.005
Pb	4.8	HMDE	0.072 ± 0.007	0.068 ± 0.005
Pb	7.8	HMDE	0.040 ± 0.004	0.033 ± 0.002
Cd	4.8	GCE[b]	1.50 ± 0.08	1.50 ± 0.07
Cd	7.8	GCE[b]	1.24 ± 0.06	1.36 ± 0.08
Pb	4.8	GCE[b]	0.710 ± 0.021	0.762 ± 0.034
Pb	7.8	GCE[b]	0.382 ± 0.013	0.234 ± 0.032

[a]Differential pulse mode, 25-mV modulation amplitude, 3 min deposition at −0.9 V vs. SCE. [b]Preformed film by 3-min deposition at −0.3 V vs. SCE, from 7.2 × 10^{-4} M Hg^{2+} in 0.016 M acetate, pH 4.8.

Studies with spiked sea water showed that low concentrations of cadmium and lead could be measured in the presence of oxygen by using differential pulse a.s.v. at the HMDE. The presence of oxygen resulted in a highly sloping baseline (Fig. 2) giving rise to greater analytical errors. In samples buffered to pH 4.8, peak heights and peak potentials did not differ significantly, before and after oxygen removal (Table 1). For samples at the natural pH 7.8, although the cadmium wave was unchanged, the lead wave in the presence of oxygen was greater in height by 21% and shifted by 15 mV to a more negative potential (Fig. 2, Table 1).

At the glassy carbon electrode, using both in situ and preformed mercury films, similar results were obtained, but the sloping baseline interference observed at the HMDE was less evident because of the higher stripping currents. Preformed film data are shown in Table 1 and illustrated in Fig. 3. At the natural pH, the lead wave was increased in height in the presence of oxygen by more than 60% (Table 1) with a negative potential shift of 17 mV. The peak heights showed good linear relationships with solution lead concentration up to 10 $\mu g\ l^{-1}$ and with deposition times up to 24 min.

It was notable that in unbuffered salt solutions, such as 0.5 M NaCl and 0.5 M $NaClO_4$, the behaviour in the presence of oxygen was less reproducible. Stripping peaks for both lead and cadmium were significantly broader and tended to increase in height for successive depositions and strippings: potential shifts were also greater. In 0.5 M NaCl, the cadmium and lead waves shifted by 45 and 105 mV more negative respectively. This difference in potential shift is related to the greater insolubility of lead hydroxide versus cadmium hydroxide [11]. In the carbonate-buffered sea water sample, any pH increase in the diffusion layer was so small that only a 5-mV shift in the cadmium peak potential could be detected (Table 2). Studies of the effect of pH on the lead peak potential in deaerated sea water agree with those of Petrie and Baier [12]; however, measurements in solutions of pH higher than

TABLE 2

Comparison of electrode parameters

	HMDE	TE[a]	GCE
Surface area, cm^2	0.029	0.85	0.066
Diffusion layer thickness δ, cm	5×10^{-3}	2.5×10^{-3}[b]	8×10^{-4}
Relative rates of diffusion of O_2 to electrode, mol s^{-1}	1	58	14
Relative rates of formation of OH^-, H_2O_2 per unit area, mol $cm^{-2}\ s^{-1}$	1	2	6
% Enhancement of Pb wave with O_2 present	20	48	63
% Enhancement of Cd wave with O_2 present	−9	n.d.[c]	−7
Potential shift for Pb wave, mV	−15	—	−19
Potential shift for Cd wave, mV	−5	—	−5

[a]Graphite-tube electrode. [b]Estimated according to Schieffer and Blaedel [16]. [c]Not determined.

those reported by these authors showed that the measured lead peak potential in the presence of oxygen at pH 7.8 is equivalent to the peak obtained in the absence of oxygen in sea water at pH 9.4.

As has been shown previously [12, 13], there is also a reduction in the a.s.v. response to cadmium and lead with increasing pH, because of the formation of electrochemically inactive species. Petrie and Baier [12] reported a decrease in the height of the lead a.s.v. wave at pH 7.8 in organic-free sea water to 31% of its value at pH 4.8; at pH 8.1 the wave was only 20% of its height at pH 4.8, although this may alter in the presence of dissolved organic matter. It is important, therefore, that calibrations by standard addition do not alter the pH of the samples or large errors can be introduced.

For the analysis of sea water at the natural pH and in the presence of dissolved oxygen, the limits of detection for lead and cadmium were estimated at 18 and 10 ng l^{-1}, respectively, using a 30-min deposition at the GCE. In the absence of oxygen these limits were reduced to 14 and 7 ng l^{-1}, respectively. For these metals at least, the a.s.v. technique is a suitable direct measurement technique and analyses could conveniently be performed on sea water pumped directly through the a.s.v. cell at the sampling site.

Graphite tube electrodeposition

A more versatile technique than stripping voltammetry for the in situ measurement of labile metal species in sea water is to electrodeposit them in the presence of dissolved oxygen onto mercury-coated graphite tubes, which can then function as furnaces for atomic absorption analysis with electrothermal atomization [7, 8]. This technique can be applied to metals, other than lead and cadmium, whose peaks in an a.s.v. determination may have been obscured by the oxygen reduction peaks.

Although a.s.v. studies have shown that the presence of oxygen has no detrimental effects on the deposition of labile metal species from sea water, a further requirement for graphite-tube electrodeposition is that the predeposited mercury film be stable. It would be desirable to be able to deposit this film on the tubes in the laboratory for subsequent transportation to the field for metal electrodepositions. A series of tubes was therefore precoated with mercury by 3-min depositions from 7.2×10^{-4} M mercury(II) nitrate solution in 0.016 M acetate buffer (pH 4.6). The coated tubes were washed with distilled water and then stored for four days exposed to the air, during which time the surfaces were allowed to dry. Lead electrodepositions were then carried out from sea water spiked with 2.1 μg Pb l^{-1}, and the deposits were determined by electrothermal atomic absorption spectrometry. Results for 12 tubes showed a standard deviation of ±14% which was within the precision of the technique.

Calibration graphs obtained for lead in sea water at pH 7.8 showed a 48% increase in slope in the presence of oxygen (Fig. 4). This increase, though less than that for the GCE, is greater than that observed at the HMDE.

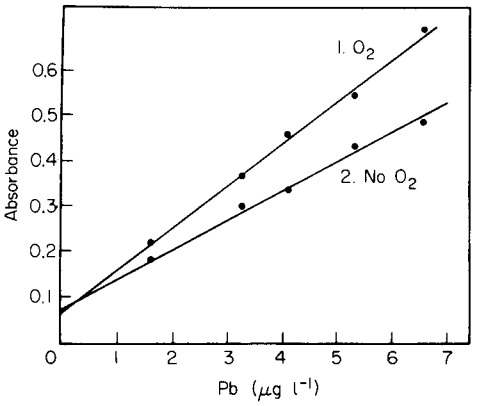

Fig. 4. Calibration graphs for atomization of lead electrodeposited from sea water, pH 7.8, at a mercury-coated graphite tube electrode, in the presence and absence of oxygen; 3-min deposition at −0.9 V vs. SCE.

The behaviour may be explained in terms of the differences in areas and diffusion layer thicknesses of the three electrode types. Table 2 lists surface areas and calculated diffusion layer thicknesses for the electrodes used [14—16]. On the basis of Fick's Law, using the known diffusion coefficient for oxygen [17] and a calculated concentration of 2.2×10^{-4} M in sea water [18], it was possible to calculate the relative rates of diffusion of oxygen to the three electrodes and also relative rates of formation per unit electrode area of the hydrogen peroxide and hydroxide. These rates are in the order of the observed lead peak enhancement.

While the potential shifts may be accounted for by the differing rates of hydroxide ion production, it is necessary to explain the varying enhancement of the lead peak height in the presence of oxygen at the three electrodes. These are not brought about by hydroxide ion; for it was observed that the lead wave, although shifted to more negative potentials, continued to diminish in height in more alkaline solutions up to pH 13. The phenomenon is most likely to be associated with hydrogen peroxide formation, but during the deposition rather than any stripping step, because the wave height increased also at the graphite tube where only deposited metal was measured. Strnad [19] showed that lead catalysed the polarographic reduction of oxygen, a behaviour he attributed to the oxidation of Pb(II) to Pb(IV) by hydrogen peroxide. It is likely that a similar reaction is involved in these studies, with some of the divalent lead diffusing to the electrode being oxidised to the tetravalent state, which must diffuse to the electrode at a faster rate than Pb^{2+}.

The in situ electrodeposition technique was applied to the determination of lead in saline waters of the Port Hacking Estuary near Sydney. Graphite tubes precoated with mercury were used in the immersible Perspex electrode probe. For natural lead concentrations, depositions in excess of 15 min were required to give absorbance values greater than 0.1 during atomization

TABLE 3

Determination of lead in sea water (Port Hacking Estuary) by in situ graphite tube electrodeposition[a]

Deposition time (min)	Deposition potential (V vs. Ag/AgCl)	Absorbance	Deposition time (min)	Deposition potential (V vs. Ag/AgCl)	Absorbance
15	−0.85	0.162	15	−0.30	0.115
15	−0.85	0.178	15	−0.30	0.060
15	−0.85	0.150	30	−0.30	0.095
30	−0.85	0.273	30	−0.30	0.090
30	−0.85	0.354	0	—	0.025
30	−0.85	0.305	0	—	0.054
			0	—	0.018

Calculated labile Pb concentration = 0.15 $\mu g\ l^{-1}$
Measured a.s.v.-labile Pb concentration = 0.13 $\mu g\ l^{-1}$

[a]See footnote (a), Table 1.

(Table 3). Blank values for the coated-tubes were low, but increased for tubes immersed in the sampled water at a controlled potential below that required for lead deposition (−0.3 V vs. Ag/AgCl), for deposition times similar to those used for lead determinations. Results for lead showed good agreement with those for labile lead determined independently by stripping voltammetry (Table 3).

The limits of detection for metals in sea water using in situ graphite tube electrodeposition will be governed by the deposition time. Unlike laboratory analyses, there will be no depletion of metals from the solution when lengthy deposition times are used, since fresh sample is being continuously pumped through the electrode. It should therefore be possible to detect the extremely low metal concentrations in open ocean water. For lead it was found, for example, that a 2-h deposition in the presence of oxygen gave a measured lead atomization absorbance equivalent to twice the blank value, for sea water containing 10 ng Pb l^{-1}.

It should be noted that stripping analyses in the presence of dissolved oxygen have been reported previously by Jagner [20]. In his potentiometric stripping technique, metals deposited at a glassy carbon electrode can be re-oxidized by dissolved oxygen on removal of the controlled potential. This oxidation occurs rapidly, but the precision is low for the determination of metals at the natural levels in seawater, and mercury(II) ion is the preferred oxidant [20, 21]. The possibility of spontaneous oxidation of deposited metal, in both the a.s.v. and graphite-tube electrodeposition methods used in these studies, was avoided by not removing the controlled potential while the working electrode was in contact with an oxygenated solution.

Conclusion

These studies make it clear that electrodeposition techniques offer considerable potential for contamination-free in situ preconcentration of metals from sea water at the natural pH and in the presence of oxygen. Anodic stripping voltammetry is suitable for continuous monitoring of lead and cadmium, using 30-min depositions at a preformed mercury film on a glassy carbon electrode, with stripping in the differential pulse mode.

As an alternative, for these metals and also for metals whose a.s.v. suffers interference from the presence of oxygen reduction waves, in situ field electrodeposition on mercury-coated graphite tubes is a suitable preconcentration method, with the final measurements being performed later in the laboratory by atomic absorption spectrometry.

Labile metal measured in sea water at the natural pH will be a considerably lower fraction of the total metal than that measured in more acidic solutions and the significance of these data in both biological and metal transport studies has yet to be adequately demonstrated. In situ techniques will, however, provide a rapid method for pollution monitoring and the detection of metals at concentrations below those where biological effects have been observed.

REFERENCES

1 U. Forstner and G. T. W. Wittman, Metal Pollution in the Aquatic Environment, Springer-Verlag, Berlin, 1979.
2 T. M. Florence, in J. O. Nriagu (Ed.), Zinc in the Environment, Part 1: Ecological Cycling, J. Wiley, New York, 1980, p. 199.
3 C. Patterson, D. Settle and B. Glover, Mar. Chem., 4 (1976) 305.
4 K. W. Bruland, R. P. Franks, G. A. Knauer and J. H. Martin, Anal. Chim. Acta, 105 (1979) 233.
5 E. W. Davey and A. E. Soper, Limnol. Oceanogr., 20 (1975) 1019.
6 S. H. Lieberman and A. Zirino, Anal. Chem., 46 (1974) 20.
7 G. E. Batley and J. P. Matousek, Anal. Chem., 49 (1977) 2031.
8 G. E. Batley and J. P. Matousek, Anal. Chem., 52 (1980) 1570.
9 J. Young, J. M. Gurtisen, C. W. Apts and E. A. Crecelius., Mar. Environ. Res., 2 (1979) 265.
10 A. M. Bond, Talanta, 20 (1973) 1139.
11 L. G. Sillen and A. E. Martell, Stability Constants, Special Publication No. 17, Chemical Society, London, 1964.
12 L. M. Petrie and R. W. Baier, Anal. Chem., 50 (1978) 351.
13 T. M. Florence and G. E. Batley, Talanta, 23 (1976) 179.
14 G. E. Batley and T. M. Florence, J. Electroanal. Chem., 55 (1974) 23.
15 W. Davison, J. Electroanal. Chem., 87 (1978) 395.
16 G. W. Schieffer and W. J. Blaedel, Anal. Chem., 49 (1977) 49.
17 J. Buffle, M. Pelletier and D. Monnier, J. Electroanal. Chem., 43 (1973) 185.
18 R. A. Horne, Marine Chemistry, Wiley—Interscience, New York, 1969.
19 F. Strnad, Collect. Czech. Chem. Commun., 11 (1939) 391.
20 D. Jagner, Anal. Chem., 51 (1979) 342.
21 D. Jagner and K. Aren, Anal. Chim. Acta, 107 (1979) 29.

Analytica Chimica Acta, 124 (1981) 131—142

DETERMINATION OF ARSENIC(III), ARSENIC(V), ANTIMONY(III), ANTIMONY(V), SELENIUM(IV) AND SELENIUM(VI) BY EXTRACTION WITH AMMONIUM PYRROLIDINEDITHIOCARBAMATE—METHYL ISOBUTYL KETONE AND ELECTROTHERMAL ATOMIC ABSORPTION SPECTROMETRY

KUNNATH S. SUBRAMANIAN and JEAN C. MERANGER*

Environmental Health Centre, Health Protection Branch, Health and Welfare Canada, Tunney's Pasture, Ottawa, Ontario K1A 0L2 (Canada)

(Received 3rd July 1980)

SUMMARY

The solution conditions and other parameters affecting the ammonium pyrrolidinedithiocarbamate—methyl isobutyl ketone extraction system for graphite-furnace atomic absorption spectrometric determination of As(III), As(V), Sb(III), Sb(V), Se(IV) and Se(VI) were studied in detail. The solution conditions for the single or simultaneous extraction of As(III), Sb(III) and Se(IV) were not critical. Arsenic(V) and Se(VI) were not extracted over the entire range of pH and acidity studied. Antimony(V) was extracted only in the acidity range 0.3—1.0 M HCl. Simultaneous extraction of total arsenic and total antimony was possible after reduction of As(V) with thiosulphate. Interference studies are also reported.

The determination of arsenic, selenium and antimony in the environment is of considerable current interest. For example, the arsenic contamination of public water supplies in several parts of the world is known to cause skin pigmentation changes, keratoses and carcinoma [1]. Arsenic is also recognized as a cumulative poison and carcinogen [2]. Although definitive evidence is lacking, the presence of selenium in water has also been linked to a number of human diseases, notably cancer and dental caries [3], although selenium in trace amounts is found to be essential for both man and animals and its deficiency has been linked to some types of muscular degeneration [4—6]. The soluble salts of antimony are also known to be toxic [7]. Furthermore, the toxicity and physiological behaviour of arsenic [8], selenium [9], and possibly antimony are dependent on their oxidation states. Therefore, it is desirable to develop methods for the determination of arsenic, antimony and selenium in their different oxidation states. The predominant valencies of As, Sb and Se are probably +3 and +5, +3 and +5, and +4 and +6, respectively [10].

In addition to their existence in different chemical forms, these elements occur in the environment at such low concentrations (usually $\leqslant 1.0$ ng ml^{-1})

that they cannot be determined reliably even by the most sensitive hydride evolution—electrothermal atomic absorption spectrometric technique. In addition, the method is subject to serious interferences [11, 12]. Solvent extraction appears to be an effective way to concentrate these elements from aqueous samples. Enhancement factors as high as 100 can easily be obtained. Also, the technique eliminates matrix effects, provides matrix normalization (i.e., making the matrix of all the samples the same as that of the standard), is simple, fast, easy to manipulate, and is probably amenable to automated on-line analysis. Ammonium pyrrolidinedithiocarbamate (APDC) forms complexes with a number of metals under the same conditions, which can be extracted into solvents such as methyl isobutyl ketone, MIBK [13]. Although APDC is known to complex As(III), Sb(III) and Se(IV) selectively [13], few comprehensive studies have been published on the APDC—MIBK system for these elements, and studies [14—16] that have been done in aqueous solution deal with only some aspects of the overall problems involved.

In this paper, a detailed study of the APDC—MIBK system for arsenic, antimony and selenium is described. The aspects studied included the effect of pH on extraction efficiency, the time stability of the chelates following extraction at different pH values, the optimum APDC concentration, the optimum solution conditions for reduction, and the minimum time required for quantitative extraction.

EXPERIMENTAL

Apparatus

A Perkin-Elmer Model 603 atomic absorption spectrometer equipped with an HGA-2100 graphite furnace and a deuterium arc background corrector was used. Perkin-Elmer electrodeless discharge lamps were used as narrow line sources for the three elements to enhance sensitivity. Nitrogen served as purge gas. The internal gas interrupt mode was used during atomization.

An Orion Model 901 Microprocessor Ionalyzer equipped with a sleeve-type Ag/AgCl single junction reference electrode and a low "sodium-ion error" glass electrode (Orion Models 90-01 and 91-01, respectively) was used for pH measurement. The time stability of the aqueous solutions of APDC, and the solubility of MIBK in water and ammonium citrate solutions were determined with a Pye-Unicam SP1800 double-beam spectrophotometer using a pair of matched 1-cm Hellma quartz cells.

All extraction studies were done in 125-ml Pyrex glass separatory funnels fitted with polytetrafluorethylene stopcocks and polyethylene stoppers. Nalgene linear polyethylene screw-cap bottles of 1-l capacity were used as containers for raw, treated and distributed drinking water samples.

Reagents

High-purity water, obtained by distilling double-deionized water in a Corning all-glass distillation unit, was used throughout the present study.

Ammonium citrate buffer (20%, w/v) was prepared by dissolving 200 g of ammonium citrate, dibasic (ACS grade, Fisher Scientific) in 500 ml of water, adjusting the pH to 7.2 with concentrated ammonia, and making up to 1 l with water. It was extracted for 3 min with 10 ml of a 5% solution of purified APDC and 50 ml of MIBK, and the extraction was repeated until the aqueous layer was virtually free of any trace element impurities as determined by g.f.a.a.s. The aqueous phase was stored in a 1-l pre-cleaned polyethylene bottle.

An APDC solution (2% w/v) was prepared by dissolving 20 g of the compound (Baker Analyzed) in 1 l of water, extracting for 3 min with 50 ml of MIBK, discarding the ketone layer, and repeating the extraction until the organic phase was colourless. The aqueous phase, when stored in a pre-cleaned polyethylene bottle at room temperature, was stable for at least one month.

Methyl isobutyl ketone (4-methyl-2-pentanone, ACS grade, Fisher Scientific) was used without further purification.

Certified atomic absorption standards containing 1000 mg l^{-1} of As(V), Sb(III) or Se(IV) were obtained from Fisher Scientific.

An arsenic(III) stock solution (1000 mg l^{-1}) was prepared by dissolving 0.1320 g of high-purity arsenic(III) oxide (N.B.S. Standard Reference Material 83c, dried at 105°C for 2 h) in 2 ml of 1 M NaOH; 25 ml of water was added, and the solution was made acidic with 4 ml of 1 M HCl, diluted to 100 ml with water and stored in a pre-cleaned polyethylene bottle. Antimony(V) and selenium(VI) stock solutions (1000 mg l^{-1}) were prepared by dissolving separately 2.168 g of potassium antimonate and 2.393 g of sodium selenate (both B.D.H. AnalaR) in water, making up to 1 l in 0.1% HNO_3 and stored in clean polyethylene bottles. In all cases, working standards of lower concentrations were prepared fresh daily by serial dilution of the stock solutions with 0.1% HCl for As(III) and Sb(III), and with 0.1% HNO_3 for As(V), Sb(V), Se(IV) and Se(VI).

All other reagents and solutions used were of the highest purity available.

Analytical procedure

Prior to use, all the containers were cleaned sequentially with a detergent wash, tap water rinse, a 24-h soak in 1% HNO_3 (Baker Ultrex), and several rinses with high-purity water [17].

Time stability of APDC solutions. Initially, spectra of 10^{-3} M (0.01%, pH = 6.46) and 10^{-4} M solutions (pH 6.72) of APDC were obtained from 200—300 nm using water as the reference. Subsequent measurements were made during a one-month period by recording absorbance values at 300 nm and 290 nm for the 10^{-3} M and 10^{-4} M solutions, respectively.

Solubility of MIBK in water and ammonium citrate. Aliquots of 0.5, 1.0, 2.0 and 5.0 ml of MIBK were pipetted into 25-ml Pyrex volumetric flasks, and diluted to the mark with water. The absorbance of each aqueous phase was measured at 256 nm with water as reference after vigorous shaking of

each flask for 2 min. The procedure for ammonium citrate solutions was basically the same. Measurements were done using 1.0, 2.0, 3.0, 4.0, 6.0 and 10.0% ammonium citrate at 304 nm with the corresponding ammonium citrate solution as the reference.

Effect of pH on the extractions. Citrate buffer (5 ml) was added to 10 ml of standard solution (25 ng ml^{-1} for As(III) or As(V), 30 ng ml^{-1} for Sb(III) or Sb(V), 50 ng ml^{-1} for Se(IV) or Se(VI)). The pH was adjusted to a value between 1.0 and 9.0 with 1 M HCl or 1 M NaOH. (At pH values below 2.5, no buffer was added because the addition of APDC to the solution altered the pH only by 0.1—0.2. At pH values above 2.5, the addition of APDC changed the pH by 1.0—2.0 and therefore the addition of a buffer was necessary to maintain the pH.) Studies were also done in the acidity range 0.1—4.0 M HCl. The solutions were transferred to separatory funnels, 5 ml of 2% APDC was added and the complex was extracted for 3 min with 5 ml of water-saturated MIBK.

The concentration of arsenic, antimony or selenium was determined by injecting 20 μl of the MIBK phase into the pyrolytically coated graphite tube using an Eppendorf pipette fitted with disposable polypropylene tips. Decontamination of the tips from traces of the analytes was achieved by soaking them overnight in 1% HCl followed by several rinses with water. The optimum "dry", "char", and "atomize" HGA-2100 program developed in this laboratory (Table 1) was followed and the peak absorbance was measured. The results of triplicate determinations of each test solution were then averaged to obtain plots of extraction vs. pH for each element. Tests for completeness of extraction were made by multiple extractions of the same aqueous phase and monitoring the levels of As, Sb or Se in each organic phase. Blanks were run regularly and their values were subtracted from the gross values to obtain the net values reported.

Optimum extraction time and APDC concentration. The procedures were the same as in the study of the effect of pH except that the separatory funnels were shaken for different time intervals (5—900 s), or different amounts of APDC (0.001—50%) were added.

TABLE 1

Optimized graphite-furnace atomic absorption spectrometric parameters for As, Sb and Se in MIBK

Parameters	As(III)	Sb(III)[a]	Se(IV)	Parameters	As(III)	Sb(III)[a]	Se(IV)
Line (nm)	193.7	217.6	196.0	Atom. temp.[b](°C)	2600	2600	2600
Slit (nm)	0.7	0.2	0.7	Atom. time (s)	7	8	7
Char temp.[b] (°C)	200	500	200	Integration time (s)	5	5	5
Char time (s)	60	30	60	E.d.l. power (W)	8	7	6

[a]Parameters for Sb(V) are identical. [b]Temperatures represent the meter settings on the control panel of the HGA-2100 temperature programmer.

Time stability of the chelates in MIBK. The studies were done at various pH values under the following conditions. After extraction as in the pH effect experiments, the MIBK phase was left in contact with the aqueous phase at 25°C in a lit room. Similar experiments were carried out with the two phases kept in the dark. Other sets of experiments were carried out in which, after extraction, the aqueous layer was drained off and the organic layer was shaken with 10 ml of water. The MIBK phase was left in contact with the water phase at 25°C in a lit or a dark room. In a further set of experiments, after extraction, one portion of the organic phase was transferred to a clean, dry Pyrex glass centrifuge tube which was kept in a lit room. Another portion of the organic phase was transferred to similar centrifuge tubes but kept in the dark. The experiment was repeated using a 10-ml water wash as described above. In all cases, the As, Sb and Se concentrations were monitored at various time intervals by injecting 20 μl of the MIBK phase into the graphite furnace as described above. Any temporal variations in the sensitivity of the graphite furnace were accounted for by injecting a freshly extracted MIBK solution of each element once every 2 h.

Calibration. The range of linear calibration was determined by preparing a series of aqueous standards and extracting them under the optimum solution conditions and with aqueous to organic phase volume ratios (i.e., V_w/V_o) of 1, 5 and 10. The calibration was done in triplicate for As(III), As(V), Sb(III), Sb(V), Se(IV), and Se(VI) by extracting the element in each oxidation state singly, and also simultaneously in various combinations.

Since APDC forms complexes only with As(III) and Se(IV), reduction of As(V) to As(III), and Se(VI) to Se(IV) was necessary before calibration could be effected for these species, and also for total arsenic and total selenium. Optimum solution conditions for the reduction of As(V) to As(III) were studied by investigating the suitability of reductants such as potassium iodide (10—40%), sodium thiosulphate (0.5—10%), or a mixture of iodide and thiosulphate at various acidities (0.01—0.50 M HCl), as well as at different reduction times (1—60 min), and APDC concentrations (0.01—5.0%). Reduction of Se(VI) to Se(IV) was effected in warm 4 M HCl [18].

Precision and accuracy. The precision was evaluated at concentrations corresponding to 5 and 10 times the detection limit of each element. The extraction was done for single species as well as for mixtures by preparing 10 solutions, each containing the same concentration of a given element.

The reliability of the extraction procedure, applied to some water samples, was investigated as follows. Ten samples each of raw, treated and distributed water were freed from any As, Sb or Se by extraction with APDC—MIBK. Known aliquots of each sample were then spiked with amounts of As(III), As(V), Sb(III), Sb(V), Se(IV) or Se(VI) corresponding to 5, 10, 20 and 40 times the detection limits, and recovery studies were made by extracting the elements with APDC—MIBK either singly or simultaneously.

Effect of other ions. Optimum solution conditions were also used for all the elements. The studies were done at levels corresponding to 10 and 20

times the detection limit for each oxidation state. The initial concentration of each additional ion was significantly higher than is usually found in fresh or potable waters, and was progressively lowered until the response corresponded to 100 ± 10% of the metal recovery. The ions tested are listed later.

Analysis of aqueous samples

Determination of As(III), Sb(III) and Se(IV). Aqueous solutions (25 ml) which had been neutralized with sodium hydroxide were transferred to 125 ml separatory funnels. Ammonium citrate buffer (10 ml) was added, the pH was adjusted to 3.5—5.0, and 5 ml of 2% APDC and 5 ml of water-saturated MIBK were added. The solution was extracted for 1 min. The aqueous layer was drained off. The organic phase was washed twice with 10 ml of high-purity water. The amounts of As(III), Sb(III) and Se(IV) were determined by g.f.a.a.s. by injecting 20 μl of the MIBK phase into the graphite tube under the optimum instrumental conditions for each element (Table 1).

Determination of total arsenic and total antimony. A 25-ml sample was acidified to 0.3—0.4 M with 6 M HCl, and 3 ml of 2% sodium thiosulphate solution was added with swirling. After 5 min, 5 ml of water-saturated MIBK and 5 ml of 5% APDC were added. The solution was extracted for 5 min and the arsenic and antimony contents in the organic layer were measured as described above.

Determination of total selenium. A 100-ml beaker containing 25 ml of sample was heated on a boiling water bath for 15—20 min after the acidity had been adjusted to 4 M with hydrochloric acid. The solution was cooled to 25°C and neutralized with sodium hydroxide, 10 ml of citrate buffer was added to adjust the pH to 3.5—5.0, and the solution was transferred to a 125-ml separatory funnel, using a few ml of 10^{-4} M HCl to rinse the beaker. A 5-ml portion of water-saturated MIBK and 10 ml of 2% APDC were added, the mixture was extracted for 1 min, and the selenium content of the organic phase measured by g.f.a.a.s. as described above.

The concentrations of As(V), Sb(V) and Se(VI) in the samples were obtained by subtracting the values of As(III), Sb(III) and Se(IV) from the total arsenic, antimony and selenium, respectively.

RESULTS AND DISCUSSION

Investigation of experimental variables

The complexation efficiency of APDC is considerably influenced by its hydrolytic stability. The decomposition of APDC in aqueous media is pH-dependent and proceeds by the following mechanism [19]. From the

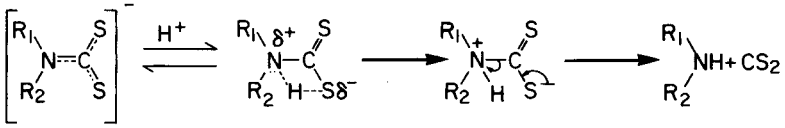

apparent rate constant data [20], the half-life values for APDC were calculated to be 32 min, 59 min, 2 h, 20 h, 9 days, 90 days and 170 days at pH $\leqslant$2, 3, 4, 5, 6, 7, and 7.3, respectively. In the present case, the APDC solutions corresponding to 10^{-1} M (1%; pH 7.55), 10^{-3} M (pH 6.46), and 10^{-4} M (pH 6.72) were found to be stable for at least one month, consistent with the above data.

The solubility of MIBK in water and in 1.0, 2.0, 3.0, 4.0, 6.0, and 10.0% ammonium citrate solution was 2.6, 2.4, 2.0, 1.7, 1.5, 1.3, 1.2 and 0.5%, respectively, at 25°C. These values are comparable to those reported by Everson and Parker [21]. The data show the need either to extract standards and samples at the same aqueous to organic phase volume ratio or to pre-equilibrate the MIBK with water (or citrate buffer of the appropriate concentration) if precision and accuracy are not to be lost.

The relationship between the pH or acidity of the aqueous solution, prior to the addition of APDC, and % extraction is shown in Fig. 1. Complete transfer from aqueous to organic phase occurs in a single extraction over the pH range 1.0—6.8 for As(III), 0.0—9.0 for Sb(III) and 1.0—5.5 for Se(IV). There was virtually no extraction of As(V) and Se(VI) at pH 1.0—10.0, and of Sb(V) at pH 2.5—10.0. Arsenic(III) and selenium(IV) were quantitatively extracted from 0.3—0.5 M HCl; but As(V) was incompletely extracted from 0.3—1.0 M HCl, Sb(V) was quantitatively extracted and Se(VI) was not extracted.

As can be seen from Fig. 1, As(III), Sb(III), and Se(IV) were quantitatively extracted over a wide pH range. However, simultaneous extraction of As(III), Sb(III) and Se(IV) was possible only in the pH range 3.0—5.5 because of interference from Sb(V) which was extractable up to pH 2.5, and because Se(IV) could not be quantitatively extracted beyond pH 5.5. Total antimony could be easily determined because both Sb(III) and Sb(V) were simultaneously extracted in the acidity range 0.3—1.0 M HCl. Determination of total arsenic and total selenium necessitated reduction of As(V) to As(III) and Se(VI) to Se(IV) prior to APDC—MIBK extraction, because both As(V) and Se(VI) were practically unextracted over the entire range of pH and acidity studied.

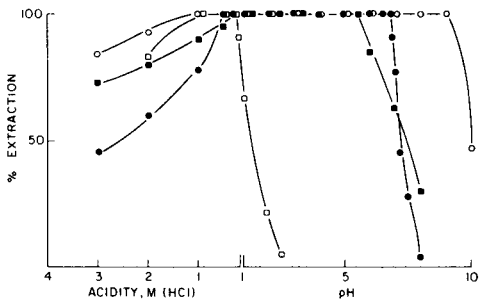

Fig. 1. Effect of pH on the extraction efficiency of the APDC—MIBK procedure (V_w/V_o = 5): (•) As(III), 25 ng ml^{-1}; (○) Sb(III), 30 ng ml^{-1}; (▪) Se(IV), 50 ng ml^{-1}; (□) Sb(V), 30 ng ml^{-1}.

For the reduction of As(V) to As(III), potassium iodide and sodium thiosulphate were tested. A solution of 50 ng As(V) ml^{-1} was quantitatively reduced by as little as 0.5% KI in $\geqslant$0.3 M HCl. However, even with 5.0% KI, it took nearly 35 min for complete reduction to As(III); at 0.5% KI, 70 min was required. When the solution contained 0.05% sodium thiosulphate in addition to 0.5% KI, the reduction was complete in 1 min. Subsequent studies showed that quantitative reduction could be effected by thiosulphate alone. The reduction was complete in 1 min with a 0.1% sodium thiosulphate solution in 0.1 M HCl. However, with more than 0.5 M HCl even the 0.5% solution of thiosulphate began to decompose; when the concentration of thiosulphate exceeded 0.4% it started to decompose even in 0.1 M HCl. For these reasons, the reduction of As(V) to As(III) was best effected by using a 0.1—0.4% sodium thiosulphate solution in 0.1—0.4 M HCl as in the procedure described under Experimental.

Both Sb(III) and Sb(V) were extracted from 0.3—1.0 M HCl. Therefore, reduction of Sb(V) was not required prior to extraction for the determination of Sb(V) and total antimony. The thiosulphate reduction of As(V) and the subsequent extraction of As(III) could be effected quantitatively in the above acidity range, and thiosulphate did not interfere with the extraction of Sb(III) and Sb(V), so that it was possible to extract and determine total arsenic and total antimony simultaneously.

Selenium(VI) had to be reduced to Se(IV) before total selenium could be determined. The use of thiosulphate or potassium iodide did not prove effective. Therefore, the conventional procedure of reduction with boiling 4 M HCl was adopted [18]. As the reduction was somewhat involved, requiring heating of the solution and a high acid concentration, total selenium was determined separately.

Extraction was complete on shaking for 5 s for Sb(III), 10 s for Se(IV) and 20 s for As(III) in the pH range 1.0—2.0 at 25°C. In the case of Sb(V) at least 5.0 min shaking was required for quantitative extraction from 0.5 M HCl at 25°C. When a 0.5 M HCl solution containing Sb(V) and 1% APDC was boiled for 1 min, cooled to 25°C and then extracted, complete transfer of the Sb(V) chelate occurred on shaking for 30 s. Thus the complexation of Sb(V) with APDC appears to be slow, probably because of the high stability of the oxo anion in aqueous acid.

Quantitative extraction of As(III), Sb(III), Se(IV) and Sb(V) occurred when the APDC to metal concentration ratio (w/v) was $\geqslant 2.5 \times 10^{-2}$, 1.7×10^{4}, 2.5×10^{2} and 1.3×10^{5}, respectively. At an APDC to metal ratio of 50, 9% of As(III) and 52% of Se(IV) were extracted. For Sb(III), the extraction was 45, 21 and 0% at APDC to Sb(III) ratios of 1.2×10^{4}, 8.7×10^{3} and 1.8×10^{3}, respectively. About 20% of Sb(V) was extracted at an APDC to Sb(V) ratio of 2.5×10^{4}. In general, a final APDC concentration of 0.05—0.10% should be sufficient to extract As(III), Sb(III) and Se(IV) quantitatively and simultaneously from aqueous solution.

Stability of the extracted chelates

During the processing of a large number of samples, it is extremely important that the extracted chelates remain stable in the MIBK phase for a sufficient length of time to permit reliable determination. In this study, time stability is arbitrarily defined as the period during which the absorbances of the extracted APDC chelates are at least 95% of the absorbances obtained from a freshly extracted sample.

When the metal complexes in the MIBK phase were left in contact with the aqueous phase at 25°C and were kept in the light or dark, the As(III), Sb(III) and Se(IV) complexes were stable for 3 days, 8 days and 6 h, respectively, at pH 1—5, so that the order of stability appears to be Sb(III) > As(III) ≫ Se(IV). The complexes did not seem to be photosensitive since there was no significant difference in the results obtained between solutions kept in the light or dark. The stability of the chelates of As(III), Sb(III) and Se(IV) increased to 9 days, 21 days and 28 h when the acidic aqueous phase was replaced with high-purity water (pH 7.0). The As(III) and Sb(III) chelates were stable for at least 2 months when the MIBK phase was transferred to dry centrifuge tubes. The Se(IV) chelate, however, was stable for only 2 days when stored in this way, but was stable at least for a week if the MIBK solution was first washed with high-purity water before transfer to a dry centrifuge tube. The greater instability of the Se(IV) complex may be attributed to its decomposition by the small amount of aqueous acid dissolved in the MIBK phase.

In summary, the best way to stabilize the metal—APDC chelates is to drain off the original aqueous acidic phase, rinse the MIBK phase with high-purity water at least twice and then transfer the rinsed MIBK phase into clean, dry centrifuge tubes. The instability of the complexes may also be improved by other methods. For example, the highly unstable Mn—APDC chelate has been stabilized for 3 days, 1 week and 2 weeks using aqueous 20% acetone [22], aqueous 95% ethanol [23], and a 1:1 acetone—hydrochloric acid mixture [24], respectively. These procedures may also work for the complexes of As(III), Sb(III), Sb(V) and Se(IV). In addition, both the stability and sensitivity may be improved by back-extraction of the chelates from the MIBK into a smaller volume of acidified (pH 1.0) aqueous solution and determination of the metals by direct injection of the aqueous solution into the graphite tube.

The conditions required for the quantitative extraction of As(III), Sb(III), Se(IV) and Sb(V) are summarized in Table 2. It can be seen that As(III), Sb(III) and Se(IV) can be simultaneously extracted at pH 3.0—5.5 at an APDC to metal concentration ratio exceeding 1.7×10^4 with an extraction time of 20 s.

Calibration, precision and accuracy

The linear working range, detection limit, and sensitivity for the three elements in MIBK are given in Table 3. The values for these parameters in

TABLE 2

Optimum solution conditions for the quantitative extraction of As, Sb and Se from aqueous solution into MIBK

Parameters	As(III)[a]	Sb(III)	Se(IV)[a]	Sb(V)
pH	1.0—6.8	1.0—9.0	1.0—5.5	—
Acidity (M)[b]	0.3—0.5	0.3—1.0	0.3—0.5	0.3—1.0
[APDC]/[Metal][c]	2.5×10^2	1.7×10^4	2.5×10^2	1.3×10^5
Extraction time (s)[d]	⩾20	⩾5	⩾10	⩾300
Chelate stability (days)[e]	166 (1—5)	62 (1—5)	8 (1—5)	10 (0.3—1.0)

[a]As(V) and Se(VI) were not extracted over the entire range of pH and acidity studied. [b]Molarity of aqueous HCl. [c]Concentrations in w/v. [d]Time required for shaking the separatory funnels manually. [e]As defined in text. The numbers in parentheses denote the pH range prior to extraction for As(III), Sb(III) and Se(IV), and acidity range for Sb(V).

TABLE 3

Analytical parameters for As, Sb and Se in the MIBK phase with g.f.a.a.s.

Parameters	As(III)	Sb(III)[d]	Se(IV)
Sensitivity (pg)[a]	25	6	100
Detection limit (ng ml^{-1})[b]	0.7	1.0	3.0
Linear working range (ng ml^{-1})	0—90	0—70	0—100
Precision (%)[c] at 5 × d.l.	17	12	21
10 × d.l.	9	5	14

[a]Mass for 0.0044 absorbance units with the nitrogen flow in the interrupt mode during atomization. [b]Twice the standard deviation of the blank. [c]Coefficient of variation (95% confidence, 10 determinations). [d]Values are identical for Sb(V).

the organic phase remain unchanged at V_w/V_o ratios of 1, 5, and 10, for the single or simultaneous extraction of metals. The detection limit quoted refers to the organic phase. In the aqueous phase, its value will depend upon the phase volume ratio; when it is 10, the detection limits in ng ml^{-1} would be 0.07, 0.10 and 0.30 for As(III), Sb(III) and Se(IV), respectively. Table 3 also gives the precision obtained for measurements at 5 and 10 times the detection limit for each element. Considering the levels measured, the range of precision (3—10%) seems to be satisfactory.

Standard additions were used to illustrate the reliability of the proposed methods, as suitable standard reference samples are not available. The average percentage recovery of each element in each oxidation state from various water samples is summarized in Table 4. The average recovery is within 100 ± 10% for arsenic and antimony, and 100 ± 15% for selenium by single as well as simultaneous extractions. Similar recoveries were also obtained on the pre-extracted samples by using single or simultaneous extractions.

TABLE 4

Recovery of arsenic, antimony and selenium from spiked samples of raw, treated and distributed drinking water by the APDC—MIBK g.f.a.a.s. method

Concentration of spike (ng ml^{-1})	Recovery (%)[a]					
	As(III)	As(V)	Sb(III)	Sb(V)	Se(IV)	Se(VI)
5.0	92 ± 3	94 ± 3	97 ± 3	97 ± 2	—	—
10.0	95 ± 4	96 ± 2	97 ± 2	96 ± 3	—	—
20.0	95 ± 2	93 ± 3	96 ± 3	93 ± 4	88 ± 3	84 ± 4
40.0	97 ± 3	97 ± 2	96 ± 2	95 ± 3	90 ± 4	89 ± 5
60.0	—	—	—	—	93 ± 4	94 ± 3
80.0	—	—	—	—	92 ± 3	91 ± 4

[a]Values given represent the average ± standard deviation of triplicate results each for 10 raw, treated and drinking water samples ranging in hardness from 1 to 554 mg $CaCO_3$ l^{-1}. The values are similar for single as well as simultaneous extractions. The values for As(V), Sb(V) and Se(VI) are obtained by subtracting the values of As(III), Sb(III) and Se(VI) from total As, total Sb and total Se, respectively.

Effect of diverse ions

Extractions of As(III), Sb(III) and Se(IV) at concentrations 10 and 20 times above the detection limit showed no interference from Ca^{2+}, Mg^{2+}, Na^+, and K^+ at levels up to 300 mg l^{-1}; NO_3^-, $H_2PO_4^-$, SO_4^{2-}, F^-, Cl^-, Br^- and I^- up to 200 mg l^{-1}; EDTA and humic acid as the sodium salt up to 25 mg l^{-1}, and Ag, Al, Cd, Co, Cu, Hg, Ni, Pb and Zn up to 1 mg l^{-1}. Iron(III), Mn(II) and Cr(VI) could be tolerated up to 10, 20 and 1 mg l^{-1} respectively, for As(III) and Se(IV), but only up to 1.0, 5.0 and 0.1 mg l^{-1}, respectively, for Sb(III). Nitrite at 75 ng ml^{-1} completely suppressed the extraction of all three elements. Fortunately, nitrite is not usually found in drinking waters and its effect may therefore be ignored. The mutual interference effects among As(III), Sb(III) and Se(IV) do not appear to be serious. The following concentration ratios can be tolerated: Sb(III)/As(III) = 3 and Se(IV)/As(III) = 100 in the extraction of As(III); As(III)/Sb(III) = 25 and Se(IV)/Sb(III) = 200 in the extraction of Sb(III); As(III)/Se(IV) = 15 and Sb(III)/Se(IV) = 10 in the extraction of Se(IV).

Conclusion

The procedures outlined can be used for the simultaneous determination of: As(III), Sb(III) and Se(IV); total arsenic and total antimony, and hence As(V) and Sb(V); and total selenium and Se(VI) from the difference between total selenium and Se(IV). The method is not sufficiently sensitive to permit its use for determining the background levels of these elements in natural waters. However, it should be applicable to polluted waters and work along these lines is now in progress.

REFERENCES

1 J. M. Harrington, J. P. Middaugh, D. L. Morse and J. Houseworth, Am. J. Epidemiol., 108 (1978) 377.
2 S. Hernberg, in H. H. Hiatt (Ed.), Origins of Human Cancer, Vol. 4, Cold Spring Harbour Laboratories, New York, 1977, pp. 147—157.
3 C. D. Rail and W. M. Hadley, J. Environ. Health, 39 (1976) 173.
4 L. Fishbein, in R. A. Goyer and M. A. Mehlman (Ed.), Toxicology of Trace Elements, J. Wiley, New York, 1977, p. 228.
5 M. G. Lansford and E. J. Calabrese, Med. Hypotheses, 5 (1979) 877.
6 I. Hoffman, K. J. Jenkins, J. C. Meranger and W. J. Pigden, Can. J. Anim. Sci., 53 (1973) 61.
7 T. D. Luckey and B. Venugopal, Metal Toxicity in Mammals, Vol. 1, Plenum Press, New York, 1977, p. 139.
8 H. A. Schroeder and J. J. Balassa, J. Chronic Dis., 19 (1966) 85.
9 I. S. Palmer and O. E. Olsen, J. Nutr., 104 (1974) 306.
10 A Report of the Safe Drinking Water Committee, Drinking Water and Health, Part I, Ch. V, National Research Council, Washington, DC, 1977.
11 F. D. Pierce and H. R. Brown, Anal. Chem., 49 (1977) 1417.
12 M. Verlinden and H. Deelstra, Fresenius Z. Anal. Chem., 296 (1979) 253.
13 See, e.g., A. Hulanicki, Talanta, 14 (1967) 1371.
14 T. Kamada, Talanta, 23 (1976) 835.
15 T. Kamada and Y. Yamamoto, Talanta, 24 (1977) 330.
16 T. Kamada, T. Shiraishi and Y. Yamamoto, Talanta, 25 (1978) 15.
17 J. C. Meranger, K. S. Subramanian and C. Chalifoux, Environ. Sci. Technol., 13 (1979) 707.
18 APHA-AWWA-WPCF, Standard Methods for the Examination of Water and Wastewater, 14th edn., APHA, Washington, DC, 1975, pp. 238—239.
19 S. J. Joris, K. I. Aspila and C. L. Chakrabarti, J. Phys. Chem., 74 (1970) 860.
20 K. I. Aspila, V. S. Sastri and C. L. Chakrabarti, Talanta, 16 (1969) 1066.
21 R. J. Everson and C. J. Parker, Anal. Chem., 46 (1974) 2040.
22 E. A. Jenne and J. W. Ball, At. Absorpt. Newsl., 11 (1972) 90.
23 R. F. Roberts, Anal. Chem., 49 (1977) 1862.
24 R. D. Olsen and M. R. Sommerfeld, At. Absorpt. Newsl., 12 (1973) 115.

Analytica Chimica Acta, 124 (1981) 143—154

DETERMINATION OF LEAD IN SEA WATER BY ELECTROTHERMAL ATOMIC ABSORPTION SPECTROMETRY AFTER ELECTROLYTIC ACCUMULATION ON A GLASSY CARBON FURNACE

G. TORSI*, E. DESIMONI, F. PALMISANO and L. SABBATINI

Istituto di Chimica Analitica, Università degli Studi, Via Amendola 173, 70126 Bari (Italy)

(Received 17th July 1980)

SUMMARY

Lead in sea water is determined by combining in situ preconcentration of the analyte on a proper glassy carbon furnace from flowing solutions, with electrothermal atomic absorption spectrometry. The apparatus is a modified version of a prototype previously tested for lead determination in different salt solutions and for mercury determination in sea water. The effects of experimental parameters such as pH, flow rate, electrolysis current, electrolysis time, etc., are described and the optimum conditions for determination of lead are given. The relative standard deviation at 1.5 ng Pb ml^{-1} is ±1%, and the detection limit (twice the standard deviation of the blank) is 0.03 ng ml^{-1}.

Despite its sensitivity, electrothermal atomic absorption spectrometry (e.a.a.s.) has not found wide application for direct determinations of trace elements in sea water. The large amount of sodium chloride in sea-water samples causes non-specific absorption [1—5] which can be only partially compensated by background correction. In addition, the sea-water matrix may give rise to chemical as well as physical interferences related to the complex physico-chemical phenomena [6—8] associated with vaporization of metals and of the matrix itself.

Several matrix modifiers, which alter the drying or charring properties of the sample matrix, have been tested [9—13] in order to reduce non-specific absorption. However, the matrix modification methods do not permit determinations of the indigenous lead in sea water because of the relatively high detection limit and poor precision. Yet, gross chemical manipulations of the samples should be avoided in order to prevent contaminations which can be dramatic when the analyte is present at ppb or sub-ppb level.

With the temperature-controlled heating method described by Lundgren et al. [14], the heating rate can be chosen independently of the final temperature, thus permitting a selective volatilization. However, this method cannot be used successfully for the determination of lead in strong sodium chloride solutions like sea water, because the temperature at which atomization of lead is rapid coincides with the volatilization temperature of sodium chloride. Ashing of sea-water samples by a hydrogen diffusion flame [15]

was successful in the direct determination of Fe, Ni, and Cu but cannot be applied for lead because hydrogen is not sufficiently effective as a suppressor for the Pb—NaCl system.

In order to overcome the problem of the high non-specific absorption, alternative procedures have been tested, which involve prior separation of the trace metals from the salt matrix. Examples of extraction of trace metals from sea water as chelates with subsequent determination by e.a.a.s. have been described [16, 17] but these, and similar methods, are seldom effective and satisfactory when the matrix is very complex and the analyte concentration very low.

In contrast, the coupling of electrochemical and spectroscopic techniques, i.e., electrodeposition of a metal followed by detection by atomic absorption spectrometry, has received limited attention. Wire filaments, graphite rods, pyrolytic graphite tubes and hanging drop mercury electrodes have been tested [18—29] for electrochemical preconcentration of the analyte to be determined by a.a.s. However, these ex situ preconcentration methods are often characterized by unavoidable irreproducibility, contaminations arising from handling of the support and detection limits unsuitable for lead detection at sub-ppb levels.

These drawbacks could be certainly avoided by performing in situ deposition. The sole attempt in this direction was made by Torsi [30] who set up an apparatus which permitted both in situ electrochemical preconcentration of the analyte from a flowing solution and almost complete suppression of matrix effects because the matrix could be removed by suitable washing. The feasibility of this approach was successfully tested with respect to lead determinations in different salt solutions (mainly ammonium acetate), and some preliminary results were reported for real samples, such as sea water and urine [30]. Later [31] the possibility of determining mercury in sea water was also tested.

In the work described here, a systematic investigation was carried out to establish fully the potentialities of such an apparatus; the technique offers distinct possibilities in solving complex analytical problems with comparatively cheap instrumentation. The determination of lead in sea water was chosen as the analytical problem. The effects of experimental parameters such as pH, flow rate, electrolysis time, etc. were studied in order to establish the optimum conditions.

Since the apparatus used here is a modified, more versatile and functional version of the original prototype [30], it is described in some detail with emphasis on the improvements.

EXPERIMENTAL

Apparatus

The apparatus is basically an electrothermal device in which the furnace (or the rod) is replaced by a small crucible made of glassy carbon. Figure 1

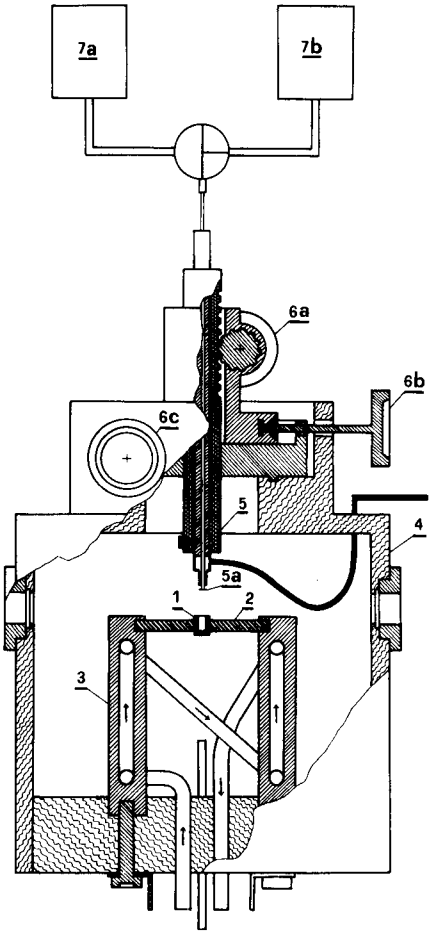

Fig. 1. Overall view of the apparatus. (1) Vitreous carbon crucible; (2) graphite rod; (3) water-cooled, steel column electrical leads; (4) plexiglas cover; (5) feeder; (5a) feeder tip; (6a–c) slide knobs; (7a, b) washing and sample solution reservoirs.

represents an overall view of the apparatus whose main components, marked by numbers, are briefly described. The glassy carbon crucible (1) was 8 mm high, 5 mm outer diameter, 3 mm internal diameter, 6 mm deep (Le Carbon Lorraine, Paris). These crucibles worked better than those house-machined from a cylindrical rod [30] of glassy carbon, probably because of superior homogeneity and more mirror-like form of the internal surface. With regard to the graphite rods (2) which keep the crucible firmly in position, improvements were made in the shape and dimensions to maximize the contact area with the crucible walls and so to obtain uniform heating of the crucible itself. The water-cooled stainless steel columns (3) press the graphite rods against the crucible by two screws hidden inside and act also as electrical leads. The plexiglas box (4) made it possible to use the controlled inert atmosphere

necessary to avoid drastic reduction of the absorption signal caused by oxygen. The solution feeder (5) is completely different from the prototype described earlier [30]; it consists of a cylinder which can be moved up and down by means of a knob (6a) into a metal block attached to the upper part of the plexiglas box. A three-way stopcock at the cylinder top connects, by teflon tubing (1.5 mm o.d., 0.8 mm i.d.), the feeder tip (5a) to the washing and sample solution reservoirs (see below). Other knobs (6b and c) enable the feeder to be moved in the horizontal plane. The three knobs permit a micrometric spatial adjustment of the feeder tip.

Figure 2 represents a cross-section of the feeder tip which is fixed to the metal cylinder by a screw. As can be seen, the solution is forced to follow a definite path. The level of the liquid inside the crucible is determined by the dynamic equilibrium between the solution flow and the applied suction. A slight excess of suction allows partial aspiration of the surrounding inert

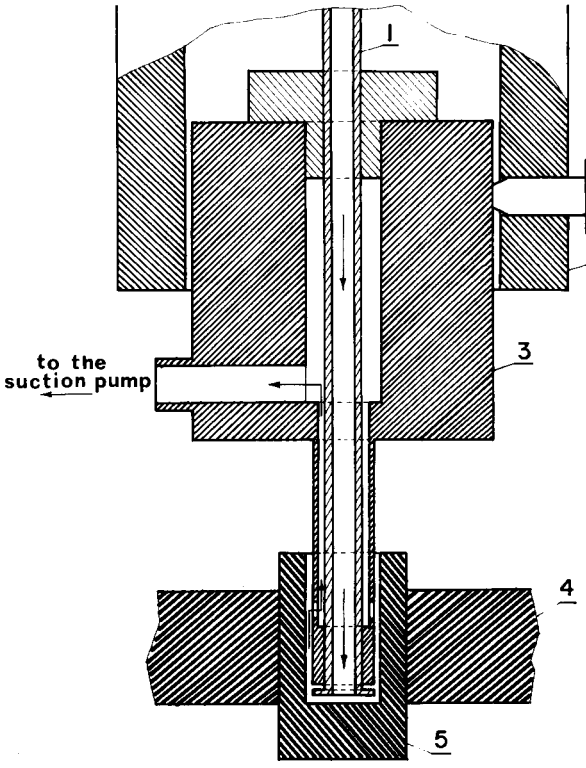

Fig. 2. Cutaway of the feeder tip and solution path. (1) Teflon tubing; (2) cylinder; (3) feeder tip; (4) graphite rods; (5) vitreous carbon crucible.

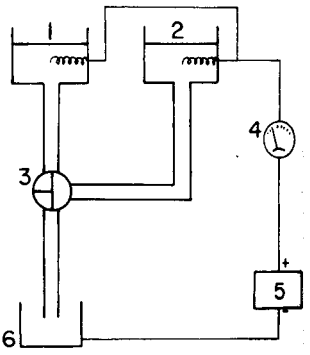

Fig. 3. Electrolysis circuit layout. (1, 2) Sample and washing solution compartments; (3) three-way stopcock; (4) ammeter; (5) 500V d.c. variable power supply; (6) crucible.

atmosphere (together with the solution). In this way, provided that the teflon tip is less than 1 mm above the bottom of the crucible, all the solution is sucked away (probably by capillarity) when the flow is stopped.

The apparatus described above has been in operation for over one year. The crucible is the only piece that must be replaced from time to time, as a consequence of irreversible changes in its surface caused by the repeated thermal treatments. It has been found that after 500 measurements the analytical response decreases by about 30%.

Figure 3 shows a block diagram of the electrolysis circuit; the crucible (6) acts as a cathode while the anode is a platinum foil dipped into either the sample solution reservoir (1) or the washing solution reservoir (2). A two-electrode system was chosen instead of a three-electrode configuration for the sake of simplicity. The pre-electrolysis was performed at constant current by a 500-V d.c. variable power supply (5). Under these conditions, the cathode potential is not controlled so that other metals can be codeposited with lead. There is no great need to control the deposition potential, because the spectral selectivity is sufficiently good to prevent interferences by other metals during the atomic absorption step.

All the results reported here were obtained with a research spectrometer described elsewhere [32, 33]. Comparable results can be obtained by combining the apparatus with any good commercial spectrometer suitable for e.a.a.s. The peak heights were measured, and the peaks were directly displayed on a Gould Advance OS4000 memory oscilloscope. A hard copy was obtained on a strip-chart recorder through a Gould Advance 4001 Option Unit.

Samples and solutions

Sea-water samples were collected from the Adriatic Sea about 8 km south of Bari. Polyethylene containers, previously cleaned by the procedure recommended earlier (Table 8 [34]) were used for collection and storage. The sea water was acidified to pH 2, just after collection, with high-purity nitric acid to release lead as free ion [35] and minimize adsorption losses.

A stock solution of lead ions (10 μg ml^{-1}) was prepared from reagent-grade lead nitrate and twice-distilled water and acidified to pH 1 with concentrated nitric acid. More dilute solutions used for standard additions were prepared daily just before use. Memory effects were avoided by using each bottle or container only for a solution of a particular concentration.

The 2 mol l^{-1} KNO_3 and 0.2 mol l^{-1} ammonium acetate washing solutions (see below) were prepared from the reagent-grade salts and pre-purified by exhaustive (potential-controlled) electrolysis at a platinum or mercury pool cathode [36].

Argon or nitrogen (UPP grade, Matheson) was further deoxygenated on a BASF catalyst column for use as the inert atmosphere.

Procedure

A typical measurement was performed in the following way. The feeder was lowered into the crucible and the sample solution (sea water) was allowed

to flow under an inert atmosphere with the suction on. A constant current was applied for a predetermined time. When the pre-electrolysis was over, the flow was changed from the sample to the ammonium acetate washing solution, while the deposited metals were maintained under cathodic protection. Ammonium acetate was selected for its low decomposition temperature, and a 0.2 mol l^{-1} concentration was used to ensure sufficient conductivity. The washing was improved by gently raising the feeder tip two or three times in order to wet the rim of the crucible. It was considered complete after about 1 min. At this point, the feeder tip was raised to the highest position and the usual steps for an e.a.a.s. measurement were followed: drying for 30 s at 90°C, ashing for 30 s at 700°C, and atomization for 8 s at 1700°C with measurement at 283.3 nm.

A typical atomization signal obtained in this way is shown in Fig. 4. As can be seen, the baseline increases smoothly with time as a consequence of an upward lift of the crucible caused by thermal expansion of the material. A first check of the baseline, to see if the signal was due only to the electrodeposited lead from the sample solution, was done by following the above-described procedure without electrolysis of the sea water. A second check of the baseline, to detect any non-specific signal from broad-band absorption, was done by following the above procedure exactly, except that the wavelength used was 287.3 nm, which is a non-analytical line, available with the lead hollow-cathode lamp, sufficiently close to the analytical line (283.3 nm). When no signal was detected, except for the slow slight increase of the baseline, the experimental conditions were considered satisfactory.

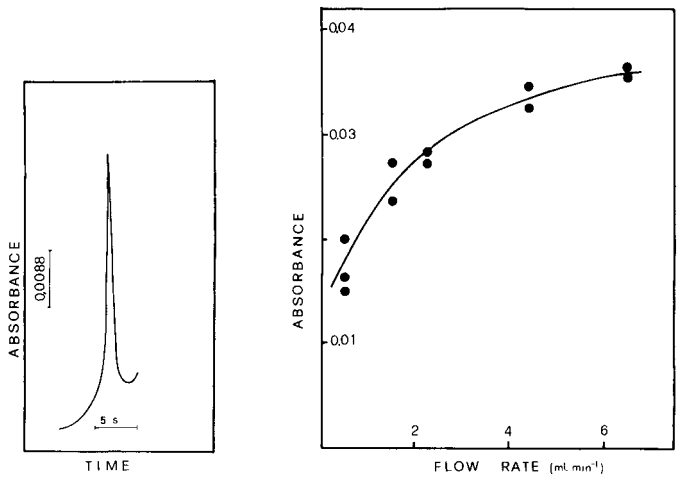

Fig. 4. Typical recorder trace of sea water containing 2.8 ng Pb^{2+} ml^{-1} after a 2 min electrolysis time.

Fig. 5. Plot of absorbance vs. flow rate. Distance of the tip from the bottom, 0.05 cm; electrolysis current 2 mA; pH 1.9; electrolysis time 2 min; $[Pb^{2+}]$ = 1.5 ng ml^{-1}.

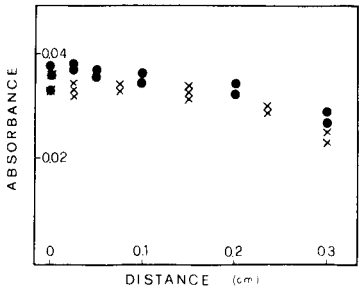

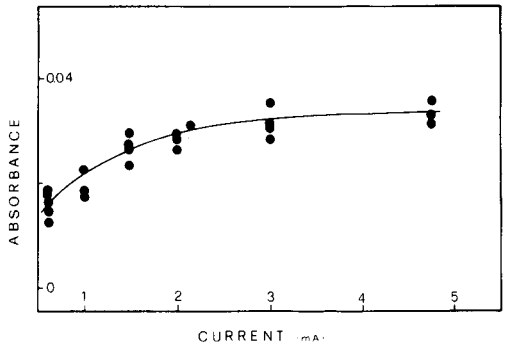

Fig. 6. Plot of absorbance vs. the distance of the feeder tip from the crucible bottom. Flow rate 4 ml min^{-1}; pH 1.9; electrolysis current 2 mA; electrolysis time 2 min; $[Pb^{2+}]$ = 1.5 ng ml^{-1}. Two independent series of measurements are plotted (•, ×).

Fig. 7. Plot of absorbance vs. electrolysis current. Flow rate 4 ml min^{-1}; distance of the tip from the bottom, 0.05 cm; pH 1.9; electrolysis time 2 min; $[Pb^{2+}]$ = 1.5 ng ml^{-1}.

RESULTS AND DISCUSSION

Optimization of the procedure

Flow rate and feeder position. Figures 5 and 6 show that the absorbance increases with increasing flow rate and decreasing distance of the feeder tip from the crucible bottom. These results can be explained by considering that reduction of the thickness of the diffusion layer increases the mass transfer.

Influence of current. Figure 7 shows the signal variation with the electrolysis current. A constant maximum absorbance value is reached, as would be expected. However, the current seems rather high even taking into account that the surface roughness can be high. Deaeration of the solutions had no appreciable influence on the constant maximum absorbance value. The high value of the current, the absence of large concentrations of reducible species in sea water and the small influence of the oxygen content, suggest that hydrogen ion is predominantly reduced.

Influence of pH. The role of hydrogen ions in the electrodeposition step is further emphasized by the data shown in Fig. 8. The maximum efficiency for the electrodeposition step is around pH 2 because of the presence of more available lead. In fact, the available lead depends on the stability of the lead complexes in sea water and on the rate constants for their formation. Decreasing pH causes more lead to become available for deposition because of preferential protonation of organic and inorganic ligands and dissolution of gelatinous precipitates (e.g. $Fe(OH)_3$, $Mg(OH)_2$, etc.) which may adsorb or occlude the metal ion and inactivate the electrode surface. At pH values lower than 2, the signals decrease because of the increasing proportion of the reduction current consumed by hydrogen evolution and partial inactivation of the electrode surface by gas bubbles. Figure 9 shows the results obtained in a simpler matrix such as 1.5 mol l^{-1} KNO_3 containing 20.5 ng Pb^{2+} ml^{-1}.

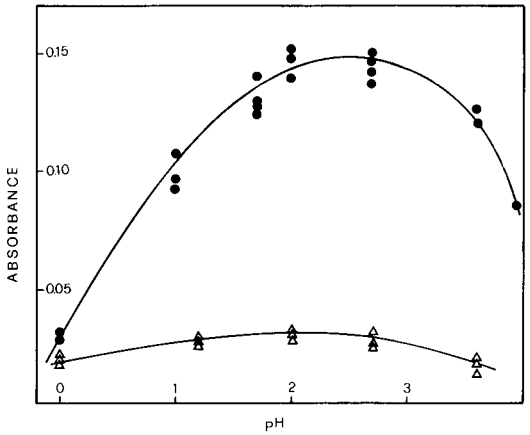

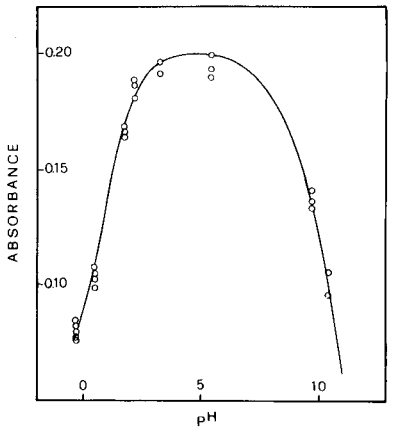

Fig. 8. Influence of pH on the absorbance peak of lead in sea water for lead contents of: (•) 20.5 ng ml^{-1}; (△) 2.5 ng ml^{-1}. Flow rate 4 ml min^{-1}; distance of the tip from the bottom, 0.05 cm; electrolysis current 2 mA; electrolysis time 2 min.

Fig. 9. Influence of pH on the absorbance of lead (20.5 ng ml^{-1}) in KNO_3—HNO_3 solution at a final constant ionic strength of 1.5 mol l^{-1}. Other conditions as in Fig. 8.

Similar behavior was found in sodium chloride. As expected, the maximum signal response is shifted towards neutral pH; in basic media the signal decreases again, probably because lead is present in an electroinactive form. Comparison of Fig. 9 with Fig. 8 (upper curve) indicates that the same amount of lead gives rise to a signal which is 30% lower in sea water than in KNO_3. This may be attributed to a matrix effect during the deposition step, and indicates that for quantitative purposes the use of the standard addition method is imperative (see below).

Electrolysis yield

In order to evaluate the yield of the electrodeposition step, the following procedure was used. First, 5 μl of an acidified lead nitrate solution containing 1 μg Pb^{2+} ml^{-1} was placed in the crucible of the apparatus and the relevant absorption signal was recorded by the e.a.a.s. procedure. Then a sea-water solution with 2.5 ng Pb^{2+} ml^{-1} added was passed through the apparatus and electrolyzed and analyzed as described in the procedure. The volume of flowing solution necessary to give the same signal obtained for the acidified lead nitrate solution was determined. The same crucible was, of course, used in both measurements and it was assumed that the peak height is independent of the form or the distribution of the analyte on the crucible walls. This procedure was set up in order to avoid gross errors from the imperfect linearity of the plots of absorbance vs. concentration (see below) and absorbance vs. electrolysis time [30]. The yield calculated in this way ranged between 1.2 and 1.7%. It should be pointed out that these values are in the usual range for electrochemical flow systems. For example,

for tubular graphite electrodes [37], plating efficiencies ranging between 4.3 and 0.55% were found, depending on the flow rate, though the solution was recirculated by a peristaltic pump. The plating efficiency found by Batley and Matousek [25] for lead in sea water by using e.a.a.s. coupled with electrodeposition on a tubular graphite electrode in a flow-through cell is again in a similar range. The low plating efficiency observed in such systems is offset by the high sensitivity of the e.a.a.s. step.

Analytical results

A calibration curve for lead in sea water obtained by the standard addition method is shown in Fig. 10. A deviation from linearity is observed at higher lead concentrations; a similar deviation was observed in plots of peak height vs. electrolysis time. The entire set of data may be fitted: i) by choosing a regression line of appropriate order; ii) by using equations which correct for non-linearity [38]; iii) by using sophisticated algorithms [39]. However, since the extrapolated blank value is of interest here, a simpler procedure may be adopted. In fact, when the first two standards are used (12 measurements) the experimental data are fitted very well by a straight line obtained by the usual (unweighted) least-squares procedure. The following equation was obtained Abs = (0.0064 ± 0.0005) + (0.01247 ± 0.0004)C where C is the lead concentration (ng ml^{-1}) and the confidence limits on the slope and intercept values are calculated at a 95% confidence level. The correlation coefficient was found to be 0.9983 and the estimated value for the original sample was found to be 0.51 $\mu g\ l^{-1}$ with confidence limits [40] at the 95% confidence level, of ±0.036 $\mu g\ l^{-1}$. This value is well within the normal range reported in the literature [41, 42] for the natural lead content of unpolluted sea water. Four replicate measurements gave a mean value of 0.52 ± 0.06 ng ml^{-1}. Accuracy was tested by analyzing the same sea-water sample by d.p.a.s.v.

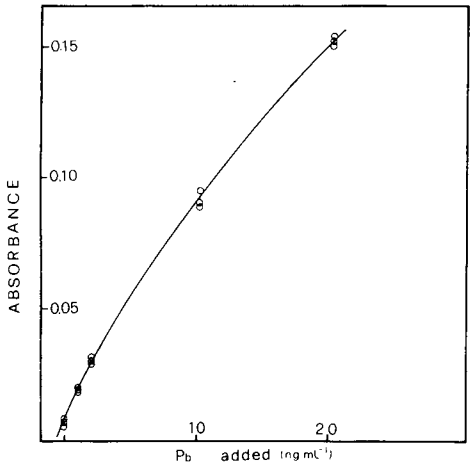

Fig. 10. Calibration curve for lead in sea water, pH 1.9. Other conditions as in Fig. 8.

TABLE 1

Detection limits (signal:noise = 2:1) expressed in ng ml^{-1} for some elements in sea water by different techniques

Metal \ Technique	E.a.a.s. in situ deposition	Flame a.a.s. ex situ deposition on Pt filament	E.a.a.s. ex situ deposition on W filament	E.a.a.s. ex situ deposition on Hg drop	E.a.a.s. ex situ deposition on graphite tubular electrode
Cd		0.1[c]	0.1; 0.01[d]	14[e]	
Cu				0.2[f]	
Pb	0.1; 0.03[a]	5[c]		42[e]	0.14[g]
Hg	0.8[b]	100[c]			

[a]Present work, 2 min and 10 min deposition, respectively. [b]10 min deposition [31]. [c]2 min deposition [22]. [d]2 min and 20 min deposition, respectively, in 0.1 mol l^{-1} KCl [19]; the method was applied to Cd determination in sea water [20]. The detection limits, however, were not directly addressed. [e]These values represent the metal content found in sea water. The detection limits are not mentioned [26]. [f]30 min deposition time [23]. [g]10 min deposition time [25].

at a rotating glassy carbon mercury film electrode [43]. This procedure gave a value of 0.65 ± 0.08 ng ml^{-1} (n = 5) which is not significantly different from the previous one according to a t test at a 95% confidence level.

These values are close to the upper limit of the normal range for lead in sea water; this is not surprising because the analyzed water was from a surface sample collected in a shoal near an urban area.

Detection limit and reproducibility

The detection limit of the proposed technique is clearly dependent on the electrolysis time, the other parameters (solution flow, pH, electrolysis current, etc.) being constant. However, the electrolysis time cannot be increased indefinitely because over a long time scale other factors can introduce errors or influence the reproducibility of measurement. A pre-electrolysis time of 10 min is considered as an acceptable value for many practical purposes. On this basis, a detection limit (signal:noise = 2:1) of 0.03 ng ml^{-1} (or 2.4×10^{-11} g) was found for ten replicate measurements performed on a sea-water sample spiked with 1 ng Pb^{2+} ml^{-1}.

Table 1 reports the detection limits for some elements in sea water found by different authors using different techniques coupling electrochemical preconcentration and atomic absorption spectrometry. As can be seen, the present technique gives the lowest detection limits for lead and mercury. For lead, this detection limit is of the same order of magnitude as those offered by a.s.v. which is considered at present to be the most suitable routine technique for the determination of lead in sea water.

The reproducibility of the method is influenced by many experimental parameters which are related to the deposition and atomization steps, and

depends on the analyte concentration. Normally a standard deviation of about 10% was obtained. A relative standard deviation of this order of magnitude appears acceptable, considering the complexity of the matrix and the very low level (sub-ppb) of the metal determined.

Thanks are due to Prof. P. G. Zambonin for his interest in this work and for reading the manuscript and to V. Sacchetti and G. Cosmai of the mechanical shop for their skilled help. This work was carried out with the financial assistance of the Italian National Research Council (C.N.R. Rome).

REFERENCES

1 J. W. McLaren and R. C. Wheeler, Analyst (London), 102 (1977) 542.
2 M. J. Adams, G. F. Kirkbright and P. Rienvatana, At. Absorpt. Newsl., 14 (1977) 105.
3 B. R. Culver and T. Surles, Anal. Chem., 47 (1975) 920.
4 M. W. Pritchard and R. D. Reeves, Anal. Chim. Acta, 82 (1976) 103.
5 S. Yasuda and H. Kakihama, Anal. Chim. Acta, 84 (1976) 291.
6 G. Tessari and G. Torsi, Anal. Chem., 47 (1975) 842.
7 R. E. Sturgeon, C. L. Chakrabarti and C. N. Langford, Anal. Chem., 48 (1976) 1792.
8 F. J. Fernandez and D. C. Manning, At. Absorpt. Newsl., 10 (1971) 3.
9 R. D. Ediger, G. Peterson and J. D. Kerber, At. Absorpt. Newsl., 13 (1974) 61.
10 R. D. Ediger, At. Absorpt. Newsl., 14 (1975) 127.
11 J. G. T. Regan and J. Warren, Analyst (London), 101 (1976) 220.
12 W. Frech and A. Cedergren, Anal. Chim. Acta, 88 (1977) 57.
13 D. C. Manning and W. Slavin, Anal. Chem., 50 (1978) 1234.
14 G. Lundgren, L. Lundmark and G. Johansson, Anal. Chem., 46 (1974) 1028.
15 R. Scobbie, Technical Topics, Varian Techtron Pty., Springvale, Vic., Australia, 1973.
16 T. H. Donnelly, J. Ferguson and A. J. Eccleston, Appl. Spectrosc., 29 (1975) 2.
17 T. Shigematsu, M. Matsui, O. Fujino and K. Kinoshita, Anal. Chim. Acta, 76 (1975) 329.
18 H. Branderberger and H. Bader, At. Absorpt. Newsl., 6 (1967) 101.
19 W. Lund and B. V. Larsen, Anal. Chim. Acta, 70 (1974) 299.
20 W. Lund and B. V. Larsen, Anal. Chim. Acta, 72 (1974) 57.
21 W. Lund, B. V. Larsen and N. Gundersen, Anal. Chim. Acta, 81 (1976) 319.
22 W. Lund, Y. Thomassen and P. Doyle, Anal. Chim. Acta, 93 (1977) 53.
23 L. Fairless and A. J. Bard, Anal. Lett. 5(7) (1972) 433.
24 L. Fairless and A. J. Bard, Anal. Chem., 45 (1973) 2289.
25 G. E. Batley and J. P. Matousek, Anal. Chem., 49 (1977) 2031.
26 F. O. Jensen, J. Dolezal and F. J. Langmyhr, Anal. Chim. Acta, 72 (1975) 245.
27 M. P. Newton, J. V. Chauvin and D. G. Davis, Anal. Lett., 6 (1973) 89.
28 M. P. Newton and D. G. Davis, Anal. Chem., 47 (1975) 2003.
29 J. B. Dawson, D. J. Ellis, T. F. Hartley, M. E. A. Evans and K. W. Metcalf, Analyst (London), 99 (1974) 602.
30 G. Torsi, Ann. Chim. (Rome), 67 (1977) 557.
31 E. Desimoni, F. Palmisano, L. Sabbatini and G. Torsi, Ann. Chim. (Rome), 69 (1979) 381.
32 G. Torsi, S. L. Paveri Fontana and G. Tessari, Ann. Chim. (Rome), 66 (1976) 69.
33 G. Torsi and G. Tessari, Anal. Chem., 45 (1973) 1812.
34 J. R. Moody and R. M. Lindstrom, Anal. Chem., 49 (1977) 2264.
35 T. M. Florence and G. E. Batley, Talanta, 23 (1976) 179.
36 Technical note 109-IM-10/72-PD, Princeton Applied Research Corp., Princeton, NJ, 1972.

37 W. R. Seitz, R. Jones, L. N. Klatt and W. D. Mason, Anal. Chem., 45 (1973) 840 (and references quoted therein).
38 L. R. P. Butler, P. F. S. Jackson and K. Kroger, Spectrosc. Lett., 4(6) (1971) 195.
39 D. G. Mitchell, W. N. Mills, J. S. Garden, Anal. Chem., 44 (1977) 1655.
40 I. L. Larsen, N. A. Hartmann and J. J. Wagner, Anal. Chem., 45 (1973) 1511.
41 W. Lund and M. Salberg, Anal. Chim. Acta, 76 (1975) 131.
42 E. D. Goldberg, Composition of Sea Water, Comparative and Descriptive Oceanography, Vol. 2, Interscience, New York, 1963.
43 E. Desimoni, F. Palmisano and L. Sabbatini, Anal. Chem., 52 (1980) 1889.

Analytica Chimica Acta, 124 (1981) 155—161

WAVELENGTH-MODULATED, CONTINUUM-SOURCE EXCITED ATOMIC FLUORESCENCE SPECTROMETRIC SYSTEM FOR WEAR METALS IN JET ENGINE LUBRICATING OILS USING ELECTROTHERMAL ATOMIZATION

T. F. WYNN[1], P. CLARDY[2], L. VAUGHN[3], J. D. BRADSHAW[4], J. N. BOWER[5], M. S. EPSTEIN[6] and J. D. WINEFORDNER*

Department of Chemistry, University of Florida, Gainesville, FL 32611 (U.S.A.)

(Received 23rd June 1980)

SUMMARY

A system for measuring atomic fluorescence of atoms produced via an electrically-heated graphite filament in a flame (acetylene/air or acetylene/nitrous oxide) and excited with a 300-W Eimac xenon arc lamp is described. The experimental system also included wavelength modulation for background emission/fluorescence/scatter correction and an optically-triggered electronic integrator for efficient monitoring of the analyte fluorescence signal. Copper, aluminum and molybdenum were determined in jet engine lubricating oil samples (1 μl) with no pretreatment. The determinations are evaluated with respect to the accuracy and repeatability criteria of the U.S. Joint Oil Analysis Program.

The determination of wear metals in aircraft engine lubricating oils is an essential part of preventive maintenance programs for the diagnosis of impending engine failure and the prevention of aircraft and personnel loss. The premises of this approach are that the presence of certain key metals and changes in their concentration in the lubricating oil signify deterioration of oil-wetted metallic parts in the engine as a result of friction, heat, or chemical reaction. The wear rate of the engine component containing the metal can be determined from changes in the metal concentration in the oil as a function of time. This approach has been used for more than three decades with excellent success.

The methods used for wear metal determinations must be fast enough for real-time input into the maintenance of the engine, simple enough for

---

Present addresses:
[1]577-68-7594, PSC 2, Maxwell AFB, AL 36112, U.S.A.
[2]American Hospital Supplies, Miami, FL, U.S.A.
[3]Frank J. Seiler Research Laboratory, FJSRL/NC USAF Academy, CO 80840, U.S.A.
[4]Georgia Institute of Technology, Atlanta, GA 30332, U.S.A.
[5]E. R. Squibb & Sons, Georges Road, New Brunswick, NJ 08903, U.S.A.
[6]Inorganic Analytical Research Division. National Bureau of Standards, Washington, DC 20234, U.S.A.

technicians to use, and capable of accurate multi-element determinations over a wide concentration range in an extremely complex matrix of oil [1, 2]. The two standard methods have been atomic absorption (a.a.s.) flame spectrometry and atomic emission spark (a.e.s.) spectrometry. The former technique has not historically been suitable for multi-element determinations although a sequential multi-element a.a.s. instrument (Perkin Elmer 5000) has been developed permitting measurement of 6 elements. The atomic emission technique is a simultaneous multi-element system but does not satisfy the repeatability and accuracy criteria for some of the important elements [1—3].

Other atomic emission systems based on the inductively-coupled plasma (i.c.p.) or the direct-current plasma (d.c.p.) are useful for the multi-element determinations, but because they employ solution nebulization procedures for sample introduction, they may be subject to severe errors when large wear metal particulates are present.

Electrothermal atomization techniques offer a distinct alternative to solution nebulization since there is no loss of wear metal particulates during sample introduction. In the present study, a carbon filament, electrothermal atomizer is used to effect the atomization of small volumes of oil. All sample "treatment" steps are performed during the ashing step prior to the atomization process. To prolong filament life and provide an inert atmosphere, the filament is placed in an argon sheath during the ashing and cooling cycles. During the atomization cycle, a flame surrounds the filament to improve the atomization characteristics of the filament by minimizing the cooling of atomized metals and formation of refractory compounds prior to excitation. Because of the wide linear dynamic range and low detection limits, atomic fluorescence spectrometry was chosen as the method for determination of the wear metals of interest. The use of a continuum source permits future expansion to a sequential multi-element system.

Wavelength modulation is used to optimize the signal-to-noise ratio (SNR) and provide background correction and an optically-triggered integrator is used to improve reproducibility. Several elements in jet engine oil correlation samples are determined by this approach.

EXPERIMENTAL

Apparatus and general layout

A schematic diagram depicting the experimental setup is shown in Fig. 1, and instrumental components and significant parameters are listed in Table 1. The system used now is an improved version of the one described by Molnar and Winefordner [4] and Vaughn [5].

The wavelength modulator used was similar to that described by Epstein and O'Haver [6], and consisted of a refractor plate driven by a torque motor and placed within the monochromator behind the entrance slit. An 80-Hz sinusoidal waveform was used to drive the torque motor and refractor plate.

TABLE 1

Instrumentation and parameters

Component	Description	Company
Monochromator	Jarrell-Ash 0.5-m, Ebert mount, Model 82-000, blaze angle at 400 nm, adjustable curved slits 100 μm, 7 mm slit height	Jarrell-Ash, Waltham, MA 02160
Detector	IP28 photomultiplier tube, 900 V	Hamamatsu
Detector power supply	Model 402 M Fluke Power Supply	John Fluke, Mfg. Seattle, WA
Amplifier	Ithaco Lock-in Synchronous Detector Model 391 A with l-f and 2-f modes, 400-ms time constant	Ithaco, Ithaca, NY, 14850
Preamplifier	Ithaco Model 164 with 10^4, 10^6, 10^8 V/A settings	
Furnace graphite	Poco Spectrographic Electrode Rods, Grades FXI and FX9I (FXI now AXF5QD61)	Poco Graphite, Inc., Decatur, TX 76234
	Bay Carbon BCI-100HD	Bay Carbon Inc., Bay City, MI 48707
Furnace power supply	SCR Power Supply, Model 10-250	Electric Measurements, Inc., Oceanport, NJ 07757
Excitation source	300-W Eimac xenon arc lamp at 20 A	Varian Associates, Eimac Division, San Carlos, CA 94070
Hollow-cathode lamp		Varian Associates, Eimac Division, San Carlos, CA 94070
Programming/ timing unit		Locally constructed [4]
Lenses	2 in. diameter spherical	Esco Products Oak Ridge Road, Oak Ridge NJ 07438
Mirror	6 in. spherical	
Atomizer		Locally constructed
Wavelength modulation function generator and torque motor driver[a]		Locally constructed
Quartz refractor plate[a]	Spectrosil, 1 in. × 1 in. × 1/8 in.	Esco Products
Torque motor[a]	Mechanics for Electronics	MFE Corp., Keewadin,
Modulation frequency[a]	Series R4-077 80 Hz	Dr., Salem, NH 03097
Integrator[a]	Optically Triggered	Locally constructed
Optical transistor[a]		Mounts locally constructed
Output[a]	Model 8000A Fluke digital voltmeter	
Recording oscilloscope[a]	Tektronix Model 549 storage scope wiht 1A1 dual trace plug-in and an oscilloscope camera	Tektronix, Inc., S.W. Millikan Way, Beaverton, OR 97005

[a]Addition or change to original system as studied by Vaughn [5].

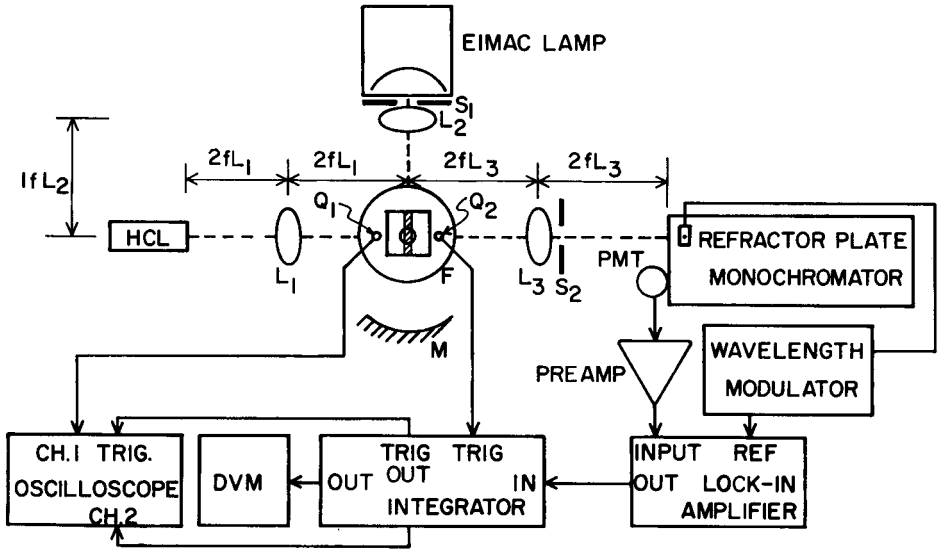

Fig. 1(a) Schematic diagram of experimental system. Lenses L_1, L_2, L_3 focus the source and the measurement beams. Focal lengths of the lenses are represented by *f*. Optical transistor, Q_1, is used for temperature measurements. Optical transistor, Q_2, is used to trigger the integrator. F is the furnace-burner combination. M is a 6-in. spherical mirror, S_1 and S_2 are 1-cm light stops. (b) Graphite filament (see Table 1 for materials). All dimensions in inches.

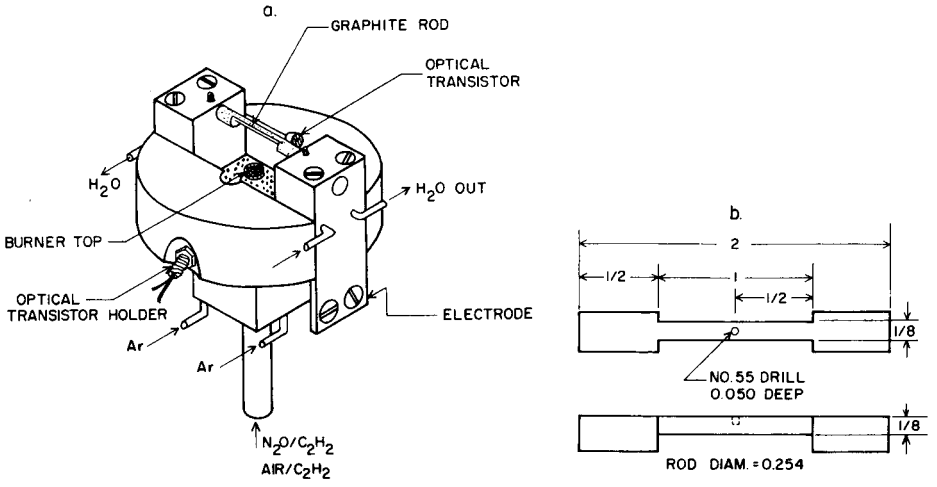

Fig. 2. Depiction of the combination graphite filament furnace and flame atomizer showing the location of the optical transistors.

A lock-in amplifier synchronized to the second harmonic of the plate oscillation frequency was used as the signal processor. The optimum wavelength scan interval ($\Delta\lambda$) was found to be 0.24 nm (for a monochromator slit width of 100 μm).

The atomizer (Fig. 2) consisted of a cylindrical bakelite block, 9.2 cm diameter and 2.6 cm high, with water-cooled copper blocks on either side to act as electrodes and supports for the filament. The graphite filaments were machined from 0.254-in. diameter spectrographic rods (see Table 1). The filament was held in place and electrical contact made through set screws in the copper blocks.

An aluminum block with fifty-six 1.3-mm diameter holes was inserted into the bakelite block to entrain an argon sheath around the filament. A capillary burner [7], consisting of 83 capillary tubes (1.0 mm i.d., 19 gauge, no. 324 stainless steel) and 3.8 cm long, supported either the acetylene air or acetylene/nitrous oxide flames.

Two optical transistors used in this instrumental system were mounted in the bakelite block with the lens permanently fixed on the filament center. One transistor used for temperature measurements had two caps, one with a 0.25-in. hole and provision for a neutral density filter and temperature measurements and one with a 1/64-in. hole for high (ca. >1500 K) temperature measurements. Temperature calibration was performed with a W-W/26% Rh thermocouple (up to ca. 2600 K) and with an optical pyrometer for higher temperatures. The second optical transistor was used to trigger the gated integrator (circuit diagram is available by writing J.D.W. or T.F.W.). The integrator had provisions for temperature adjustment to control the threshold of the trigger, a delay time, τ_{de}, adjustment to control the time between the trigger pulse and the initiation of the gate, and a gate time, τ_{ga}, adjustment. The optimization of τ_{de} and τ_{ga} was essential for good precision.

Reagents and standards

Oil standards were obtained from the Special Spectrometric Calibration Standards (Naval Air Rework Facility, Naval Air Station, Pensacola, FL). These standards contained Al, Cr, Cu, Fe, Pb, Mg, Ni, Si, Ag, Mo, Sn, and Ti at concentrations of 3, 10, 30, 50, and 100 ppm. The base oil was Conostan 85. Standards of 0.1, 1.0, and 5.0 ppm were prepared by diluting the oil standards with base oil (by weight). The oil correlation samples were synthetic and real samples in which elemental content had been independently determined by the U.S. Joint Oil Analysis Program (JOAP) laboratories and the results correlated.

Procedure

All samples were introduced with a calibrated 1-μl Micropettor-A syringe (Scientific Manufacturing Industries, Emeryville, CA). An ashing step, typically 800°C for 15 s, was used to destroy the organic matrix of the oil.

TABLE 2

Results of the oil correlation sample determinations

Sample	Cu				Mo				Al[e] ($\mu g\ g^{-1}$)			
	Trimmed[a] mean	This[b] work	%RSD	Meets criteria[c]	Trimmed[a] mean	This work	%RSD	Meets criteria[c]	Trimmed[a] mean	This work	%RSD	Meets criteria[c]
181	35.85	35	16	Y	—	—	—	—[d]	13.48	15.6	7	Y
182	35.85	32	5	Y	—	—	—	—[d]	11.51	13.0	27	Y
183	6.32	6.3	12	Y	—	—	—	—[d]	15.14	13.2	3	Y
184	5.46	5.0	11	Y	—	—	—	—[d]	13.14	10.1	15	Y
193	9.84	9.8	5	Y	40.87	42.	23	Y	—	—	—	—
194	8.40	9.3	4	Y	35.90	39.	10	Y	—	—	—	—
195	5.20	4.9	6	Y	—	—	—	—[d]	—	—	—	—
196	4.40	4.0	18	Y	—	—	—	—[d]	—	—	—	—
197	46.86	47	4	Y	—	—	—	—[d]	—	—	—	—
198	43.20	48	2	Y	—	—	—	—[d]	—	—	—	—

[a]This is the mean from 61 laboratories participating in the JOAP. [b]The regression equation for Cu data is $y = (1.017 \pm 0.04)\ x - 0.35 \pm 1.1$; $S_{yx} = 2.21$; $r = 0.993$. [c](Y) indicates that the results meet the criteria for repeatability and accuracy as set forth by JOAP. The JOAP accuracy and repeatability criteria for a given element are obtained by plotting the results (in $\mu g\ g^{-1}$) for each element in each pair of samples, e.g., each of the 61 laboratories will be a point on the graph of concentration of sample X vs. concentration of sample Y; where sample X and Y correspond to the pairs (181 and 182; 183 and 184; etc.). A rectangle is drawn with two sides parallel to the least-squares line and two lines perpendicular to the same line. The parallel lines of the rectangle are equally spaced from the least-squares line by a distance called the repeatability criteria and the two perpendicular lines of the rectangle are equally spaced from the JOAP trimmed mean value by a distance called the accuracy criteria. The accuracy and repeatability criteria are statistically based on the results from the 61 laboratories and differ for each element and sample pair. If a sample pair for a given laboratory falls within the rectangle, then that laboratory is said to meet the JOAP certification criteria [8]. [d]The trimmed mean values for Mo are atomic emission results. Also, since so few of the labs in JOAP determine Mo, these data had to be obtained by telephone from Pensacola NAS Interservice Oil Analysis Office. No data available for samples 181—184 or 195—198. [e]No results obtained for Al in samples 193—198).

In the absence of ashing, the "smoke" produced by the oil matrix during atomization resulted in a huge scatter signal which generated an excessive amount of photomultiplier shot noise, overloading the detection system.

Flow rates for the acetylene/nitrous oxide flame were 4.3 l min^{-1} and 7.2 l min^{-1}, respectively. All determinations with this flame (Al, Mo) were performed by bracketing each sample with two standards because of the short lifetime (ca. <10 runs) of the filaments in the hot flame. Possible methods of overcoming this problem are lowering the height of the filament in the flame and the use of other filament materials. In the cooler acetylene/air flame (Cu), several hundred determinations were possible before the filament had to be replaced.

The fluorescence lines used were 324.7 nm for Cu, 313.3 nm for Mo and 394.4 nm for Al. The filament atomization temperatures were 2300 K for Cu, 2950 K for Mo, and 2800 K for Al.

RESULTS AND DISCUSSION

Results for the oil samples are given in Table 2. The limit of detection based on three times the standard deviation of the blank for copper was 0.09 ppm (9×10^{-11} g). The limits of detection for molybdenum and aluminum were 0.4 ppm (4×10^{-10} g) and 1 ppm (1×10^{-9} g), respectively.

The numerical results and the regression equation for the copper data compare well with the JOAP correlation results for both real and synthetic samples. All of the sample pairs determined here met the JOAP criteria. While the detection limits observed are not significantly better than those for presently available analytical techniques, the accuracy observed, as illustrated by agreement with the JOAP results [8], shows that the present system has considerable potential. Modification of the furnace design and construction may improve detection limits (by increasing sample volume) and increase filament life when the acetylene/nitrous oxide flame is employed. The improved potential of a "total consumption" technique for the determination of elements in lubricating oils containing wear metal particulates as well as the simplicity of constructing a sequential multi-element atomic fluorescence spectrometer are significant incentives for further development of the system.

This research was supported by grant AF-AFOSR-F49620-80-C-005.

REFERENCES

1 R. Collacott, Chem. Britain, 13—2 (1977) 60.
2 C. A. Saba and K. J. Eisentraut, Anal. Chem., 51 (1979) 1927.
3 R. L. Miller, L. M. Fraser and J. D. Winefordner, Appl. Spectrosc., 25 (1971) 477.
4 C. J. Molnar and J. D. Winefordner, Anal. Chem., 216 (1974) 1417.
5 R. L. Vaughn, M.S. Dissertation, University of Florida, Gainesville, FL, 1978.
6 M. S. Epstein and T. C. O'Haver, Spectrochim. Acta, 30B (1975) 135.
7 H. Haraguchi and J. D. Winefordner, Appl. Spectrosc., 31 (1977) 195.
8 Joint Oil Analysis Program Technical Support Center, Naval Air Station, Pensacola, FL 32508, 1979.

Analytica Chimica Acta, 124 (1981) 163—168

REMOVAL OF CHLORIDE INTERFERENCE IN THE DETERMINATION OF CHROMIUM BY ATOMIC ABSORPTION SPECTROMETRY WITH ELECTROTHERMAL ATOMIZATION

KOJI MATSUSAKI*

Department of Industrial Chemistry, Technical College, Yamaguchi University, Tokiwadai, Ube 755 (Japan)

TAKASHI YOSHINO

Department of Industrial Chemistry, Faculty of Engineering, Yamaguchi University, Tokiwadai, Ube 755 (Japan)

YUROKU YAMAMOTO

Department of Chemistry, Faculty of Science, Hiroshima University, Higashisenda-machi, Naka-ku, Hiroshima 730 (Japan)

(Received 14th August 1980)

SUMMARY

Two mechanisms of chloride interference are described. The first arises from coordination of chloride to chromium(III), which can be prevented by addition of a masking agent such as tetraammonium—EDTA. The other is due to chloride salts remaining at the atomization step; this can be prevented by volatilizing the chlorides or converting them to oxides before atomization.

Atomic absorption spectrometry with a graphite furnace is widely used for determination of metals because of its high sensitivity and rapidity. However, interference from cations, anions, acids, organic substances, etc., is often encountered. In particular, severe interference is caused by chloride present originally in the specimen and/or added during preparation of the test solutions. On the basis of reactions taking place in the solid and/or gaseous state in the furnace, this chloride interference has been interpreted in terms of volatile compound formation [1—3], a vapour-phase process [4—6] and analyte occlusion in the matrix [7—10]. However, in previous work on aluminium [11], strontium [12] and chromate [13], it was found that the chloride interference is strongly related to the interaction between analyte and chloride ions in solution; this interaction is also affected by coexisting cations. This behaviour, therefore, has been interpreted on the basis of solution chemistry and it has been concluded that coordination of chloride not only to the analyte ion but also to the coexisting cations is a cause of interference in addition to the reactions in the solid and gaseous states as suggested previously [1—10]. The method of removal of the interference, therefore, is based on the prevention of chloro-complex formation

with analyte and coexisting cations, for example by adding masking agents such as EDTA. However, the interference mechanisms for aluminium and strontium ions seem to be different from that for chromate ions because chromate is an anion. Accordingly, chromium(III) is expected to be more similar to aluminium in its susceptibility to chloride interference than chromate, in solution, while it will be similar to chromate ion in the solid and gas phase reactions because the final state of both chromium(III) and chromate ions in the furnace will be the same. The chloride interference on chromium(III), therefore, has been investigated by a method similar to that used for aluminium and chromate ions.

EXPERIMENTAL

Apparatus and reagents

The apparatus used was that described previously [13]. All solutions were prepared from analytical-reagent grade chemicals and demineralized water, and stored in polyethylene bottles. The stock chromium(III) solution (1000 mg Cr l^{-1}) was prepared by dissolving chromium metal (99.99% pure) in nitric acid and diluting with 0.1 M acid.

Procedure

A 5-μl sample was deposited in the center of the graphite tube with the micropipette and dried, ashed and atomized with nitrogen flowing over the furnace at 5.5 l min^{-1}. The voltages and times for drying and atomization were always: dry for 30 s at 0.65 V (ca. 110°C) and atomize for 4 s at 7.0 V. The ashing step was varied as required. The absorption signals on atomization were recorded at 357.9 nm (0.2-nm bandwidth) and the peak height was taken as the analytical signal. A reagent blank was run under the same conditions and a suitable correction applied. The applied voltage between the atomizer terminals was measured with a suitable voltmeter, and the temperature in the centre of the furnace was measured with a Pt/PtRh thermocouple.

RESULTS AND DISCUSSION

Effect of chloride on chromium atomic absorption

Chloride was expected to show various effects in its interference on chromium(III), depending on the analytical conditions, as was found for aluminium, strontium and chromate ions. The factors which affected the chloride interference were the coexisting cations, the ashing temperature, the pH of the sample solution, and the standing time of the sample solution after the chloride had been added.

The effects of coexisting cations were measured for H^+, NH_4^+, Na^+, K^+, Mg^{2+}, Ca^{2+}, Sr^{2+}, Ba^{2+}, Cu^{2+}, Fe^{3+} and Al^{3+} in the range 10^{-5}—10^{-1} M; usually the pH was maintained at 3 (adjusted with hydrochloric acid) and the ashing

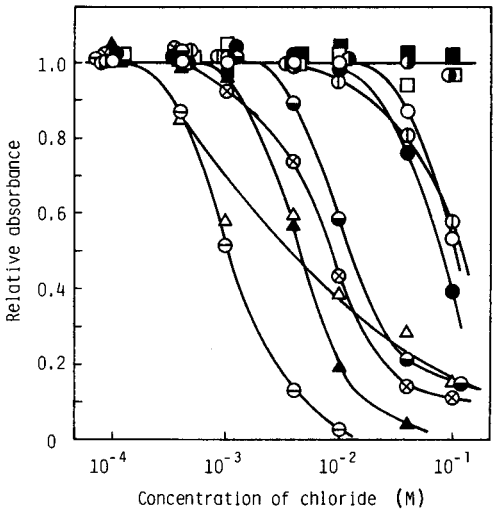

Fig. 1. Effect of some chlorides on the absorbance of chromium (0.1 mg l^{-1}) relative to that when the chlorides are absent. (□) HCl; (■) NH_4Cl; (○) NaCl; (●) KCl; (◑) $MgCl_2$; (◒) $CaCl_2$; (⊗) $SrCl_2$; (▲) $BaCl_2$; (⊖) $CuCl_2$; (⊙) $AlCl_3$; (△) $FeCl_3$. $AlCl_3$ and $FeCl_3$ at pH 1 and the others at pH 3. The solutions were not heated before measurement.

temperature at 550°C (30 s at 1.6 V). The results are shown in Fig. 1. The cations studied may be classified into three groups: those which showed negligible (H^+, NH_4^+ and Mg^{2+}), intermediate (Na^+, K^+ and Al^{3+}) and severe (Ca^{2+}, Sr^{2+}, Ba^{2+}, Cu^{2+} and Fe^{3+}) interference.

The effect of the ashing temperature on the interaction between analyte and chloride was measured in the presence of the various metal chlorides. The chloride interference in the presence of H^+, NH_4^+, Mg^{2+}, Na^+, K^+ and Al^{3+} disappeared completely at ashing temperatures higher than 110, 210, 470, 930, 930 and 850°C (30 s), respectively, as is shown for Na^+ in Fig. 2. However, the interference had not disappeared completely even at 1200°C when severely interfering metal chloride was present. This behaviour is similar to that of chromate [13]; such a chloride interference has been removed by volatilizing the chlorides or converting them to oxides before atomization, and a similar procedure is expected to be applicable to chromium(III). The strongly interfering chlorides have high vaporization temperatures; hence their interference is thought not to be removable during ashing, and the chlorides will be present during atomization, as was found for aluminium [11] and chromate [13].

The effect of pH was measured for 0.1 M solutions of various metal chlorides, the ashing temperature being kept at 350°C (30 s at 1.3 V); the pH was adjusted with hydrochloric acid and sodium hydroxide. As seen in Fig. 3 for sodium chloride, there is a severe suppression of the signal below pH 6. In alkaline media, only a slight effect is observed. This may be explained by formation of tetrahydroxochromate(III) ions [14] which are inert to chloride. Although the extent of the interference differed for different

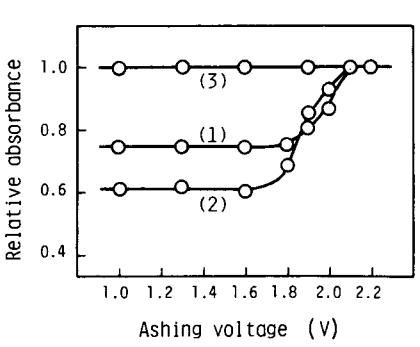

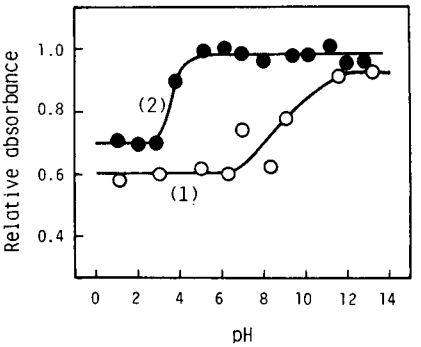

Fig. 2. Effect of ashing voltage on the relative atomic absorbance of chromium (0.1 mg l^{-1}) in the presence of 0.1 M NaCl at (1) pH 3.0, immediately after preparation; (2) pH 3.0, after heating for 3 h at 90°C; (3) pH 12.6 after heating as for (2).

Fig. 3. Effect of pH on the relative atomic absorbance of chromium (0.1 mg l^{-1}) in the presence of 0.1 M NaCl. (1) No further addition; (2) 0.01 M acetic acid added.

cations in acidic media, a very similar pH dependence was observed for all the other cations tested. In alkaline media, however, the reproducibility of the chromium signal was invariably poor, presumably because of loss of the analyte as a result of precipitation of coexisting cations as their hydroxides. When acetic acid was added instead of hydrochloric acid, the chloride interference diminished above pH 4, as shown for sodium in Fig. 3. Acetic acid (pK_a = 4.8) releases acetate ions at pH 4 which probably forms kinetically inert chromium(III) complexes [15] that are not attacked by chloride.

The effect of the standing time after chloride addition was measured after heating for 3 h at 90°C at pH 3.0 and 12.6. The absorbances of these solutions were recorded after ashing at different temperatures. The results are shown in Fig. 2. No chloride interference was observed for the solution of pH 12.6 at any ashing temperature. At pH 3.0, the extent of interference was greater after heating the solution. Figure 4 shows the spectra of acidic solutions containing 0.1 mg Cr(III) ml^{-1}. The two maxima shift toward longer wavelengths on heating. The $[Cr(OH_2)_6]^{3+}$ ion shows maxima at 407 and 575 nm, whereas $[Cr(OH_2)_5Cl]^{2+}$ has peaks at 430 and 605 nm, and $[Cr(OH_2)_4Cl_2]^{+}$ at 450 and 635 nm, etc. [16]. The bathochromic shift observed, therefore is in agreement with the formation of chloroaquochromium(III) ions on heating the solution.

In order to confirm that the chloride interference is caused by the coordination of chloride to chromium(III), the effect of chloride concentration on the atomic absorbance was examined. The chlorochromium(III) complex formation may be described as follows (ignoring coordinated water molecules):

$$Cr^{3+} + nCl^{-} \rightleftharpoons CrCl_n^{(3-n)+}$$

The equilibrium constant, $K = [CrCl_n^{(3-n)+}]/[Cr^{3+}]\,[Cl^{-}]^n$. The absorbance of

each of the solutions is given by $A = a_1[Cr^{3+}] + a_2[CrCl_n^{(3-n)+}]$, where a_1 and a_2 are constants. Also $[Cr^{3+}]_t = [Cr^{3+}] + [CrCl_n^{(3-n)+}]$, where $[Cr^{3+}]_t$ is the total concentration of chromium(III) present. For a solution containing no chloride, $A_1 = a_1[Cr^{3+}]_t$, and for a solution in which the formation of chlorochromium(III) complexes is complete, $A_2 = a_2[Cr^{3+}]_t$. Combination of these equations gives

$$(A_1 - A)/(A - A_2) = [CrCl_n^{(3-n)+}]/[Cr^{3+}] \quad (1)$$

The total concentration of chloride added, $[Cl^-]_t$, is approximately equal to $[Cl^-]$ under the present conditions, because the concentration of chloride is in very large excess. Figure 1 indicates that the absorbance is negligible when the formation of a chlorochromium(III) complex is complete. Thus $A_2 = 0$, hence $a_2 = 0$. Thus eqn. (1) becomes

$$\log [(A_1 - A)/A] = \log K + n \log [Cl^-]_t \quad (2)$$

Plots of $\log [(A_1 - A)/A]$ vs. $\log [Cl^-]_t$ for sodium chloride were linear with a slope of unity, indicating $n = 1$. This suggests that the chloride interference is attributable to the formation of monochlorochromium(III) ions.

Removal of the interference

Two methods for removal of the chloride interference may be suggested. The first is volatilization of the chloride, or conversion of the metal chloride to its oxide, before the atomization step. The other is the addition of a masking agent to the sample solution in order to prevent the coordination of the chloride to the analyte. The strongly interfering chlorides (Ca, Sr, Ba, Cu and Fe(III)) are difficult to remove completely simply by adjustment of

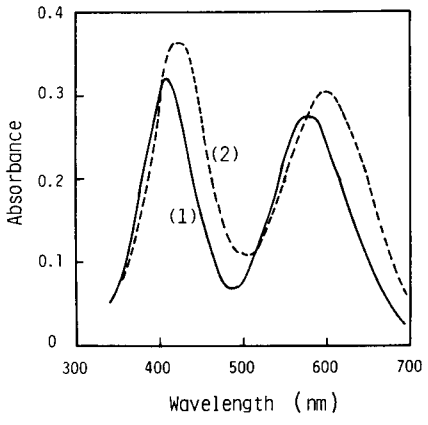

Fig. 4. Absorption spectra of chromium(III) (1 g l^{-1}) in 1.0 M NaCl at pH 3.0: (1) immediately after preparation; (2) after heating for 3 h at 90°C.

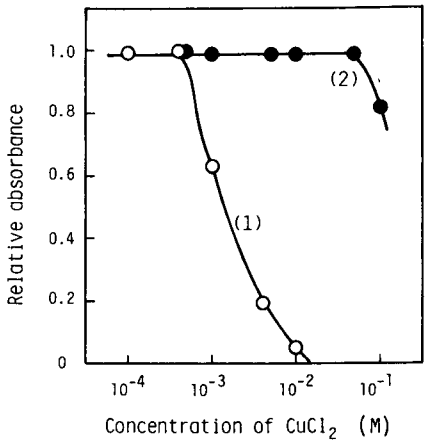

Fig. 5. Removal of $CuCl_2$ interference on chromium (0.1 mg l^{-1}) by addition of EDTA-$(NH_4)_4$: (1) no addition; (2) 0.05 M EDTA$(NH_4)_4$ added.

ashing temperature, and the standard addition method may result in fluctuating data. Addition of masking agents to the sample solutions containing these salts was therefore tried. As tetraammonium—EDTA had been successful for aluminium, strontium and chromate, it was also investigated for chromium(III). As shown in Fig. 5, EDTA removes the interference of copper(II) chloride; this was also observed for the other seriously interfering chloride salts. The success of the reagent arises not only from its masking ability, but because readily volatile ammonium chloride is also produced. The resulting EDTA complexes will be converted to oxides on heating. Tetraammonium-EDTA is also a good reagent for removing the chloride interference by Na^+, K^+ and Al^{3+}, even when lower ashing temperatures are used. In practice, the amount of additive needed and the pH of the sample solution, are best determined for each sample.

Chromium(III) reacts very slowly with ligands at room temperature [17] so that the concentration of chloro-complex formed may be affected by the standing time and temperature. Thus the extent of chloride interference on chromium(III) may differ for each sample. In particular, the method of sample preparation may affect the chloride interference. When the standard addition method is used, the added chromium(III) solutions must be heated at near boiling before instrumental measurement. Chromate ions react rapidly with chloride, so that the above procedure is not necessary, but a mixed sample of chromium(III) and chromate must be prepared carefully as mentioned above.

REFERENCES

1 D. A. Segar and J. G. Gonzalez, Anal. Chim. Acta, 58 (1972) 7.
2 J. Aggett and A. J. Sprott, Anal. Chim. Acta, 72 (1974) 49.
3 C. W. Fuller, Anal. Chim. Acta, 81 (1976) 199.
4 J.-Å. Persson, W. Frech and A. Cedergren, Anal. Chim. Acta, 92 (1977) 85, 95.
5 W. Frech and A. Cedergren, Anal. Chim. Acta, 82 (1976) 83.
6 E. J. Czobik and J. P. Matousek, Anal. Chem., 50 (1978) 2.
7 R. B. Cruz and J. C. van Loon, Anal. Chim. Acta, 72 (1974) 231.
8 J. Smeyers-Verbeke, Y. Michotte, P. van den Winkel and D. L. Massart, Anal. Chem., 48 (1976) 125.
9 D. J. Churella and T. R. Copeland, Anal. Chem., 50 (1978) 309.
10 J. A. Krasowski and T. R. Copeland, Anal. Chem., 51 (1979) 1843.
11 K. Matsusaki, T. Yoshino and Y. Yamamoto, Talanta, 26 (1979) 377.
12 K. Matsusaki, S. Murakami and T. Yoshino, Nippon Kagaku Kaishi, (1980) 1126.
13 K. Matsusaki, T. Yoshino and Y. Yamamoto, Anal. Chim. Acta, 113 (1980) 247.
14 C. F. Baes Jr. and R. E. Mesmer, The Hydrolysis of Cations, J. Wiley, New York, 1976, p. 211.
15 R. E. Hamm, R. L. Johnson, R. H. Perkins and R. E. Davis, J. Am. Chem. Soc., 80 (1958) 4469.
16 P. J. Elving and B. Zemel, J. Am. Chem. Soc., 79 (1957) 1281.
17 F. A. Cotton and G. Wilkinson, Advanced Inorganic Chemistry, Interscience, New York, 3rd edn. 1972, p. 386.

Analytica Chimica Acta, 124 (1981) 169—176

AN IMMOBILIZED IMMUNO-STIRRER FOR THE DETERMINATION OF CREATINE KINASE-MB ISOENZYME IN BLOOD SERUM

CHANG-LI YUAN[a], SHIA S. KUAN and GEORGE G. GUILBAULT*

Department of Chemistry, University of New Orleans, New Orleans, Louisiana 70122 (U.S.A.)

(Received 1st September 1980)

SUMMARY

An immobilized immuno-stirrer is described for the determination of creatine kinase-MB isoenzyme in blood serum. The IgG antibodies are immobilized on alkylamine glass beads using glutaraldehyde as cross-linking reagent, and the beads are packed into a rotating porous cell. After incubation with stirring, the CK-M isoenzymes in the blood serum sample are inhibited and are bound to the antibodies inside the stirrer. The residual CK-B isoenzyme activity is then determined spectrophotometrically or electrochemically. The binding capacity of the immuno-stirrer to CK-M isoenzyme was estimated to be 800 UI^{-1} with an average inhibitory efficiency of 97.8%. The within-day and day-to-day coefficients of variation were 5% and 4%, respectively, over a period of 52 days. An immuno-stirrer loaded with antibodies attached to cyanogen bromide-activated cellulose beads was also characterized, but the antibodies were not as stable as on glass beads.

The clinical significance of blood serum CK-MB, an isoenzyme of creatine kinase (E.C. 2.7.3.2), in the diagnosis of acute myocardial infarction has been recognized and accepted [1—3]. One of the clinically useful and reliable techniques for the determination of CK-MB is the immunoinhibition method [4, 5]. Being fast (life-saving), simple, safe and reliable, the immunoinhibition test has become more acceptable for practical use, particularly because no pretreatment is required. However, the instability of the soluble antibodies towards heat and microbial attack, their fragility, as well as their cost and batch-to-batch irreproducibility, have severely limited their use as routine analytical reagents. These limitations can be eliminated or minimized through immobilization [6—12]. The immobilization of antibodies has provided a more economical, stable, reproducible, selective means of immunoassay.

An immobilized antibody is one which is physically confined or localized in some way with retention of its immunological activity, and which can be used repeatedly and continuously. There are four principal methods for the immobilization of antibodies: physical adsorption, entrapment, protein cross-linking and covalent attachment. Of these, covalent coupling appears to be

[a]Present address: E. I. Dupont de Nemours, Wilmington, DE, U.S.A.

best because of the strong binding force which holds the antibodies in a stable conformation. The reusability of the covalently bound immunoadsorbents is another advantage. Their applications vary from detection or viruses and microorganisms [13—15], radioimmunoassay [16, 17], enzyme removal or isolation [18, 19] and studies on the antigenicity of antigen fragments [20].

Improved spectrophotometric [21] and electrochemical [22] methods have recently been described for the immunoassay of CK-MB. In this paper, an "immuno-stirrer" is described. It was designed to inhibit the creatine kinase M subunit as a pretreatment for the detection of cardio-specific CK-MB isoenzyme by both spectrophotometric and electrochemical techniques. Results obtained from this study are presented in detail.

EXPERIMENTAL

Apparatus

The kinetic measurements of creatine kinase (CK) and the residual CK (B subunit) were performed with a Cary 17 spectrophotometer, using the Oliver—Rosalki enzyme system (see below). A PAR 174H polarographic analyzer (Princeton Applied Research Corp., Princeton, NJ) was used for measurements with a three-electrode system.

An E.C. Motormatic motor control (Electro-Craft, Inc., Hopkins, MN) was used to maintain a steady stirring speed during assay. A Hall-effect digital sensor was employed to sense the magnetic field, and the trigger was amplified and displayed on a Heathkit frequency counter (Model CB-101 with modifications, circuit diagram available on request).

A Brinkman IC-2 circulator (Brinkman, Westbury, NY) was used to heat and pump water into a home-made cell to keep the temperature constant during assay; a laboratory immersion heater (Blue M Electric Co., Blue Island, IL) was occasionally used as an auxiliary heater.

Autopipettes (Finnpipette, Helsinki, Finland) of 5—50, 50—200, and 200—1000-μl capacities were used to deliver sera, substrates and reagents. A home-made rotating porous cell with removable lid was designed to facilitate easy loading and unloading of immobilized proteins [23—25]. The body was machined from polyethylene and at the bottom of the cell was drilled a hole into which a small cylindrical magnet was inserted and sealed by epoxy cement to keep the solution from reacting with the metal. The upper chamber, which accommodates the immobilized antibodies, had six holes drilled and a removable, tight-fitting cover. Nylon net (37-μm pore size, Tetko, Inc., NY) was glued onto the lid and around the wall inside the chamber using plastic rubber (Woodhill Chemical Sales Corp., Cleveland, OH) to prevent the immobilized antibodies from leaching out of the stirrer.

Reagents and solutions

Modified Oliver—Rosalki CK reagents (prepared according to the Dade formula; Dade Div. of American Hospital, Miami, FL) were: triethanolamine buffer (pH 7.0), 100 mM; creatine phosphate, 70 mM; glucose, 40 mM; magnesium acetate, 20 mM; adenosine diphosphate (ADP), 2 mM; $NADP^+$. 0.6 mM; adenosine monophosphate, 20 mM; glucose-6-phosphate dehydrogenase, 4.8 U/assay; hexokinase, 4.8 U/assay; reduced glutathione 18 mM (spectrophotometric assay) or 0.6 mM (electrochemical assay), obtained from Sigma Chemical Co., St. Louis, MO.

CK-M inhibiting antibodies were used (anti-human, from goats; E. Merck, Darmstadt, Germany). Each vial can be consituted to 2 ml, of which 0.1 ml can inhibit 800 U l^{-1} of CK-M by 99%.

The immobilization medium, sodium phosphate buffer, 0.1 M, pH 7.0, was prepared from $NaH_2PO_4 \cdot H_2O$ (Mallinckrodt). The characterization medium, triethanolamine buffer, 0.1 M, pH 7.0, was prepared from triethanolammonium chloride (Sigma).

A 2-ml portion of 50% dimethylsulfoxide and 2 ml of 0.05 M glycine—HCl buffer (pH 2.3) were used as the regeneration medium for the immobilized antibodies. Phosphate-buffered saline was used to wash away the organic solvent and acidic solution, and to restore the biological activity of the immobilized antibodies. It was prepared by adding 0.9% sodium chloride solution to 0.1 M, pH 7.0 sodium phosphate buffer. Borate-buffered saline was used to store the immobilized antibodies during refrigeration. It was prepared by adding 0.9% sodium chloride solution to 0.01 M, pH 8 sodium borate buffer.

Coupling reagents and carriers. Alkylamine porous glass beads (40—80 mesh) were supplied by Corning Glass Works (Corning, NY). Cellulose beads (65 mesh) were a gift from Dr. L. F. Chen, Department of Chemical Engineering, Purdue University, West Lafayette, IN. Glutaraldehyde (Eastman Kodak) and cyanogen bromide (Sigma) were used.

Immobilization procedures for Inh—CK-M antibodies

Immobilization on alkylamine glass beads [26—30]. Wash 0.25 g of alkylamine porous glass beads three times (5 ml each time) with double-distilled deionized (D^3) water in a 20-ml vial, then degas with 7 ml of D^3 water under vacuum in a desiccator for 10 min, until no more gas bubbles evolve from the glass beads, indicating that all the pores in the beads are filled with water. To these washed and drained beads, add 10 ml of 2.5% glutaraldehyde solution (25% glutaraldehyde diluted 1:10 with 0.1 M sodium phosphate buffer, pH 7), sufficient to cover the glass beads. Place the reaction mixture in a desiccator attached to the aspirator for 1 h to remove air and gas bubbles from the particles. Remove and filter the activated beads on a medium-porosity Gooch funnel and wash three times with distilled water (10 ml each time). Make sure that all the unbound glutaraldehyde is washed off.

Mix 1 ml (one half of the contents of the Merck vial) of antibody in sodium phosphate buffer (0.1 M, pH 7) with the alkylamine derivative prepared above. Allow to react in a cold room for 24 h, with gentle shaking. Wash the immobilized antibodies at least three times with the sodium phosphate buffer (pH 7) to remove unbound antibodies.

Immobilization on cellulose beads with cyanogen bromide [31—33]. Wash 0.3 g of 65-mesh cellulose beads three times (5 ml each time) with D^3 water in a 20-ml vial. Transfer the beads to a beaker containing 15 ml of acetonitrile and 10 ml of 0.1 M phosphate buffer in which 3 g of cyanogen bromide has been dissolved, and adjust the apparent pH of the solution to 11.0 ± 0.2. Activate the carrier at room temperature with shaking for 2 h, filter and wash successively with acetone (20 ml) and ethanol (20 ml).

Mix the activated beads with 1 ml of 0.1 M sodium phosphate buffer (pH 7) containing 1/2 of the contents of a vial of Inh-CK-M antibodies, as above. Carry out the coupling reaction with gentle shaking at 4°C. After 24 h, wash the product with the phosphate buffer (pH 7) to remove any unbound antibodies.

Assay procedures

Pretreatment before assay (stirring incubation). Mix 0.3 ml of CK-MB isoenzyme control or serum with 3 ml of 0.1 M triethanolamine buffer (pH 7) in a 10-ml beaker. Place the immuno-stirrer in the solution, which is held at 37°C with the use of the water-circulating cell. Stir at 200 rpm for 30 min.

Procedure. Place 1.1 ml of the CK solution obtained after pretreatment in a 1-cm^2 spectrophotometric quartz cell containing 1.0 ml of the modified reagent mixture. Initiate the reaction by the addition of 0.1 ml of $NADP^+$ solution (10 mg ml^{-1}), and record the rate continuously for 7 min at 500 nm. Measure the slope ($\Delta A \Delta t^{-1}$), to give a measure of the CK-MB activity. Alternatively, measure the residual activity amperometrically as described previously [22].

Regeneration. Put the immuno-stirrer, which has been used for 5 pretreatments, into the dimethyl sulfoxide regeneration medium. Stir at 200 rpm at 37°C for 20 min. The dimethyl sulfoxide lowers the surface tension of the liquid medium and breaks the Van der Waals' forces holding antibody to antigen in the complex (the pH 2.3 glycine—HCl buffer dissociates the complex by the change in pH.) Next, put the immuno-stirrer into the phosphate-buffered saline regeneration medium, and stir at 200 rpm and 37°C for 10 min to wash away the organic solvent and acidic solution. At the same time, this restores the biological capacity of the immobilized antibodies.

When not in use, keep the immuno-stirrer in a borate-buffered saline solution at 0—4°C to prevent microbial attack.

RESULTS AND DISCUSSION

Optimization of the assay procedure

The inhibitory efficiency (I.E.) is defined as

$$\text{I.E. } (\%) = 100(\text{T.A.}-\text{E.A.})/(\text{T.A.}-\text{R.A.})$$

where T.A. is total CK activity, E.A. is the experimental activity after immuno-stirring treatment, and R.A. is the residual activity (i.e., the B-subunit activity). Judging from the profile of I.E. vs. incubation time, maximum I.E. (100%) occurs after 25 min incubation at 37°C at 200 rpm (Fig. 1). To insure complete inhibition during the pretreatment, 30 min was used; this is believed enough to cover the clinically useful range.

A stirring rate of 200 rpm was found to give greatest inhibition. The I.E. tended to decrease at a higher stirring speed (300 rpm) because of three factors. The fast revolution caused a vortex on top of the stirrer which resulted in poor transport and bad contact between antigen and immobilized antibodies. It is hard to attain antigen—antibody equilibrium with fast rotation, and too vigorous rotation distorts the conformation of the macromolecules (i.e. antigen and/or antibody). A temperature of 37°C was chosen for incubation because the physiological feasibility of maximum formation of antigen—antibody complex is greatest at this temperature.

Studies on the regeneration of the immuno-stirrer

The regeneration procedure consists of two stages, the dissociation of the antigen—antibody complex, and the restoration of the inhibition capacity of

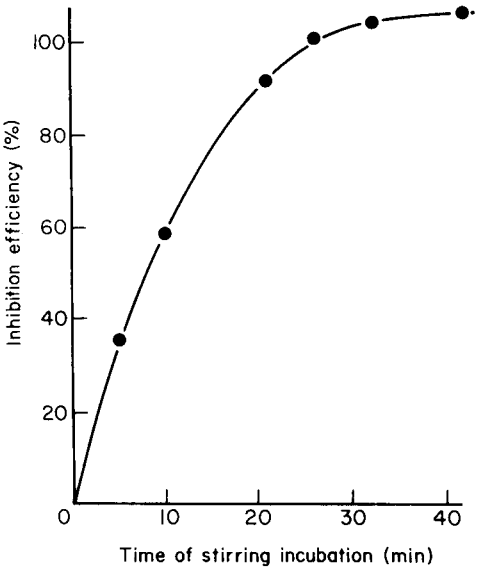

Fig. 1. The effect of time of stirring incubation on the inhibition efficiency.

the immobilized antibody. Regeneration was carried out at 37°C and 200 rpm. It is not necessary to regenerate the immuno-stirrer after each run. Since the inhibition capacity of the immuno-stirrer was sufficient to bind many more antigen molecules, the immuno-stirrer could be re-used five times without regeneration in routine clinical analysis.

The antibody molecules bind to the antigen through a variety of forces, which may include electrostatic, hydrophobic, Van der Waals' forces and hydrogen bonding. The dissociation of the complex can be achieved by a change in one or more parameters, such as ionic strength, pH, and addition of a competitive hapten, protein denaturants, chaotropic agents or surface tension-lowering agents. In the proposed method a 1:1 mixture of dimethyl sulfoxide [34] and 0.05 M pH 2.3 glycine—HCl buffer was used to dissociate the complex. A 20-min incubation at 37°C and 200 rpm was found to be sufficient for this purpose. Prolonged incubation would cause denaturation of the immobilized antibodies.

The second medium used to regenerate the immobilized immuno-stirrer was a phosphate-buffered saline solution (0.1 M, pH 7). Incubation for 10 min at 37°C with stirring at 200 rpm was found to be sufficient to clean away all traces of organic solvent and to restore the biological inhibitory capacity of the immobilized antibodies.

Performance characteristics of the immuno-stirrer

The inhibition efficiencies (I.E.) of the stirrer for a set of samples ranging from 100 to 900 U l^{-1} of CK-M were investigated. The efficiencies were 92—99% for up to 800 U l^{-1} of CK-M. At 900 U l^{-1} the I.E. dropped to 80%. Therefore the total inhibition capacity of an immuno-stirrer was estimated to be 800 U l^{-1}; the average inhibition efficiency was 97.8%.

A within-day precision study was done to evaluate the reliability of the immuno-stirrer for CK-MB determinations. Five determinations of normal (8.0 U l^{-1}) and of abnormal (187 U l^{-1}) samples were done; 5.5% and 4.6% were obtained as the coefficients of variation respectively. Ten serum samples were pooled as the matrix base for a recovery study. Cardiozyme controls (of known value) were added to the pooled sera to give CK-MB values of 33—168 U l^{-1}. The results (Table 1) show that the average recovery was 98.1%.

TABLE 1

Recovery study for pooled sera

Found (U l^{-1})	18.0	34.2	45.7	76.8	160.0
Expected (U l^{-1})	18.0	33.0	48.0	78.0	168.0
Recovery (%)	—[a]	103.6	95.2	98.5	95.2

[a]Calibration standard.

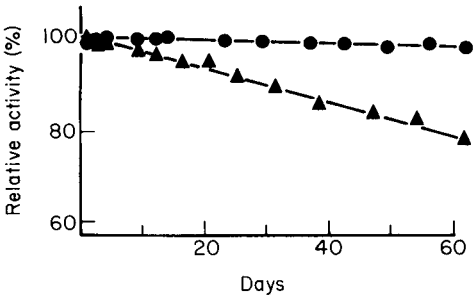

Fig. 2. The long-term operational stability of the immuno-stirrers. (•) Glutaraldehyde—alkylamine glass beads; (▲) cyanogen bromide cellulose beads.

Stability study. Two sets of immobilized immuno-stirrers, prepared from glutaraldehyde—alkylamine glass (g.a.g.) beads and cyanogen bromide-cellulose (c.b.c) beads were used for a long-term operational stability study. Each set of stirrers was run 52 times over a two-month span. The results are shown in Fig. 2. The g.a.g. beads showed a good response curve and constant activity with a day-to-day coefficient of variation of 4.0%; no loss of activity was evident by the end of the test. The c.b.c. beads gave a decrease in activity after 10 assays over three days, with a coefficient of variation of 8.4%. The poor stability could result from the more vigorous conditions of activation, which might result in a loss of the inhibition capacity of the immobilized antibodies. The good stability of the g.a.g. immuno-stirrer once again confirmed that glutaraldehyde is a very effective coupling agent [29] because the glutaraldehyde can be used under physiological conditions and causes only moderate changes in protein structure, with retention of the inherent immunological specificity.

Conclusions

The successful immobilization of CK-M antibodies through glutaraldehyde coupling to alkylamine glass beads, and the satisfactory loading of these immobilized antibodies onto a stirrer, have initiated a new dimension of application of an immuno-stirrer to analytical chemistry. By means of this immuno-stirrer, the cardio-specific isoenzyme CK-MB activity can be determined easily and reproducibly.

Each immobilized immuno-stirrer can be used for at least fifty-two assays efficiently (and possibly many more) thus greatly reducing the cost per assay. Furthermore the purity and activity of the CK-M antibodies vary widely from one manufacturer to another, and even from lot to lot; this has limited the use of soluble antibodies for routine assay in the clinical laboratories. Therefore, the use of the immobilized immuno-stirrer eliminates many problems of reproducibility and stability. Moreover, the whole assay takes only 30—40 min. This is extremely helpful to physicians for timely diagnosis of patients with myocardial infarction.

We thank Dr. Alfred Hew, Jr. (Hotel Dieu Hospital) for his generous supply of analyzed sera. Appreciation is expressed to the Dade Corporation (Miami, FL) for their kind provision of cardiozyme kits, the CK-M Merck antibody, and the Dade reagents kits.

REFERENCES

1 G. S. Wagner, C. R. Roe, L. L. Limbird, R. A. Rosati and A. G. Wallace, Circulation, 67 (1973) 263.
2 G. A. Moss, Creatine Kinase Isoenzymes: Methods and Clinical Significance, Worthington Biochemical Corporation, Freehold, NJ 07728, 1976.
3 M. A. Verat and D. W. Mercer, Circulation, 51 (1975) 855.
4 U. Wurzburg, N. Hennrich and H. Lang, Klin. Wschr., 54 (1976) 357.
5 D. Neumeier, W. Prellwitz, U. Wurzburg, M. Brundobler, M. Olbermann, H. J. Just, M. Knedel and H. Lang, Clin. Chim. Acta, 73 (1976). 445.
6 H. H. Weetall, in M. L. Hair (Ed.), The Chemistry of Biosurfaces, Vol. 2, M. Dekker, NY, 1972.
7 W. F. Line and M. J. Becker, in H. H. Weetall (Ed.), Immobilized Enzymes, Antigens, Antibodies and Peptides, Vol. 1, M. Dekker, NY, 1975.
8 I. Chibata, Immobilized Enzymes, Kodansha, Jpn., 1978.
9 O. R. Zaborsky, Immobilized Enzymes, CRC Press, Cleveland, OH, 1973.
10 D. H. Campbell and N. Weliky, in C. A. Williams and M. W. Chase (Eds.), Methods in Immunology and Immunochemistry, Vol. I, Academic Press, NY, 1967.
11 I. H. Silman and E. Katchalski, Ann. Rev. Biochem., 32 (1966) 873.
12 N. Weliky and H. H. Weetall, Immunochemistry, 2 (1965) 293.
13 J. Bozicevich, J. J. Bunim, J. Freund and S. B. Ward, Proc. Soc. Exp. Biol. Med., 97 (1958) 180.
14 J. Bozicevich, H. A. Scott and M. M. Vincent, Proc. Soc. Exp. Biol. Med., 114 (1963) 759.
15 H. H. Weetall and J. Bozicevich, 51st Annual Meeting, Fed. Am. Soc. Exp. Biol., Chicago, IL, 1967.
16 L. Wide and J. Porath, Biochim. Biophys. Acta, 130 (1966) 257.
17 T. Goodfriend, D. Ball, and S. J. Updike, Immunochemistry, 6 (1969) 481.
18 R. R. Williams and S. S. Stone, Arch. Biochem. Biophys., 71 (1957) 377.
19 R. R. Williams and S. S. Stone, Arch. Biochem. Biophys., 71 (1957) 386.
20 T. Webb and C. La Presle, Biochem. J., 91 (1964) 24.
21 C. Yuan, S. S. Kuan and G. G. Guilbault, Clin. Chem., in press.
22 C. Yuan, S. S. Kuan and G. G. Guilbault, Anal. Chem., January, 1981.
23 G. G. Guilbault and W. Stakbro, Anal. Chim. Acta, 76 (1975) 237.
24 J. W. Kuan, S. S. Kuan and G. G. Guilbault, Clin. Chem., 23 (1977) 1058.
25 H. S. Huang, S. S. Kuan and G. G. Guilbault, Clin. Chem., 23 (1977) 671.
26 D. Marchall, Biotech. Bioeng., 15 (1973) 447.
27 S. Avrameas and T. Ternynck, Immunochemistry, 6 (1969) 53.
28 D. J. Ford, R. Radin and A. J. Pesce, Immunochemistry, 15 (1978) 237.
29 S. Avrameas, Immunochemistry, 6 (1969) 43.
30 S. Avrameas, B. Taudou and S. Chuilon, Immunochemistry, 6 (1969) 67.
31 N. Weliky and H. H. Weetall, Immunochemistry, 9 (1972) 967.
32 L. D. Ryan and C. S. Vestling, Arch. Biochem. Biophys., 160 (1974) 279.
33 R. Axen, J. Porath and S. Ernback, Nature, 214 (1967) 1302.
34 C. J. van Oss, D. R. Absolom, A. L. Grossberg and A. W. Neumann, Immuno. Com., 8(1) (1979) 11.

Analytica Chimica Acta, 124 (1981) 177—183

CHLOROPHOSPHONAZO-*m*-NO_2, A NEW REAGENT FOR THE SPECTROPHOTOMETRIC DETERMINATION OF CERIUM SUB-GROUP RARE EARTH ELEMENTS IN THE PRESENCE OF YTTRIUM SUB-GROUP ELEMENTS

HSU CHUNG-GIN*, HU CHAO-SHENG, JIA XI-PING and PAN JIAO-MAI

Department of Chemistry, Shanghai Normal University, 3663 Chung Shan Road (N.), Shanghai (People's Republic of China)

(Received 28th July 1980)

SUMMARY

The synthesis of chlorophosphonazo-*m*-NO_2 is described. Cerium sub-group rare earth elements can be determined in the presence of 10—40 fold amounts of yttrium sub-group elements when the latter are masked by oxalic acid at pH 1.6. Under the experimental conditions employed, the apparent molar absorptivities of lanthanum and cerium at 666 nm are 9.5×10^4 and 9.3×10^4 l mol^{-1} cm^{-1}, respectively. Beer's law is obeyed for 0—12 μg of lanthanum or cerium in 25 ml of solution. The coefficients of variation for La and Ce are 0.37% and 0.92%, respectively.

2,7-Bisazo derivatives of chromotropic acid containing one or two functional groups (I) are sensitive reagents for the spectrophotometric determination of rare earths.

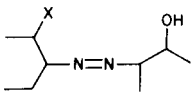

(I)

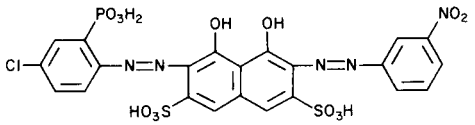

(II)

X = AsO_3H_2, PO_3H_2 or COOH

Among these reagents, arsenazo-III [1], arsenazo-M [2], dicarboxyarsenazo-III [3] and chlorophosphonazo-III [4, 5] have been used to determine total rare earths. Carboxynitrazo [6] and arsenazo-*p*-NO_2 [7, 8] have been reported to give sensitive colour reactions with cerium sub-group elements and to give no, or less sensitive reactions with yttrium sub-group elements, but have not been widely used. Chlorophosphonazo-*m*-NO_2 (CPA*m*N) II, one of the bisazo derivatives of chromotropic acid, containing one *o*-phosphono-*o'*-hydroxyazo group, can also be used as a reagent for rare earths. In this paper, the synthesis of CPA*m*N and its application in the determination of μg-amounts of cerium sub-group elements are described.

In acidic media, CPA*m*N is bright red and reacts with rare earth ions to form blue or green complexes. The complexes of yttrium sub-group elements are

decomposed by oxalic acid, whereas those of cerium sub-group elements are stronger, and exist in the presence of oxalic acid. This property can be utilized to create a selective method for the determination of cerium sub-group elements in the presence of yttrium sub-group elements.

EXPERIMENTAL

Apparatus

Absorbance was measured on a Hitachi Model 808 double-beam spectrophotometer with 1-cm cells. A Model pHS-29A pH meter (Shanghai 2nd Analytical Instruments Factory) was used with a combined glass electrode.

Synthesis of CPAmN

m-Nitroaniline (1 g) was mixed well with 16 ml of water and 4 ml of 12 M hydrochloric acid, dissolved by warming, and then diazotized by adding sodium nitrite (0.4 g in 2 ml of water) dropwise. Chlorophosphonazo-I (4 g, synthesized by a modification [9] of the method of Nemodruk et al. [10]) was dissolved in 16 ml of 10% lithium hydroxide solution and cooled to 0°C. The diazotized solution prepared was added with stirring, and the pH of the solution was adjusted to 9—10 with lithium hydroxide solution. After continuous stirring for 1—2 h, the solution was allowed to stand overnight, acidified to pH 1 with hydrochloric acid, and filtered after standing for several hours. The precipitate was dried at 80°C, ground, and soaked in 2 M hydrochloric acid for several hours, and then filtered and washed with 2 M hydrochloric acid. The product was again dried at 80°C, and 3 g (60%) of crude CPA*m*N was obtained.

Crude CPA*m*N (0.5 g) was dissolved in 150 ml of water and filtered. The solution was extracted with five 50-ml portions of (1 + 4) n-butanol—ethyl acetate. The aqueous phase was mixed with 10 ml of 12 M hydrochloric acid and extracted twice with 40 ml of n-butanol. After the organic phase had been washed with 25 ml of water, CPA*m*N in the n-butanol phase was back-extracted with 50 ml of 2% sodium hydroxide solution. The aqueous phase was washed with ethyl acetate, acidified with 20 ml of 12 M hydrochloric acid and left overnight. The precipitate was filtered, washed with 2 M hydrochloric acid and dried at 80°C. Two molecules of water contained in CPA*m*N were estimated by thermogravimetry (calculated 5.0%, found 5.2% H_2O).

The purity of CPA*m*N was checked by paper chromatography with a (5 + 2) mixture of 5% sodium citrate and 25% ammonia solution as eluent. A single blue band was obtained for the pure product. Element analysis confirmed the purity (calculated 9.68% N, 4.28%, P, 4.90% Cl; found 9.50% N, 4.16% P, 4.98% Cl). The absorption spectrum (Fig. 1) showed that the absorption maximum was at 545 nm with an apparent molar absorptivity of 3.85×10^4 l mol^{-1} cm^{-1}.

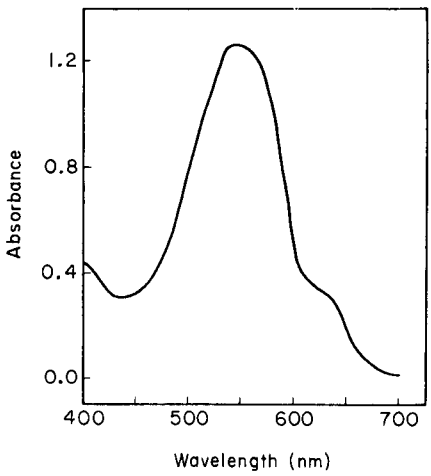

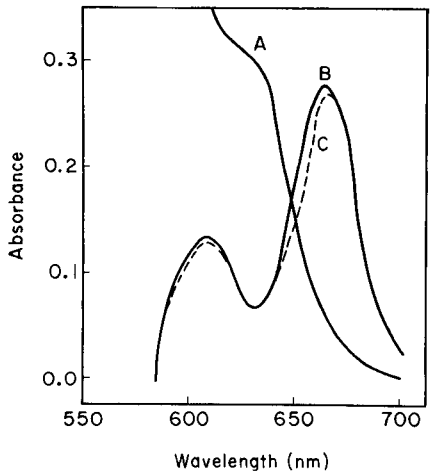

Fig. 1. Absorption spectrum of CPA*m*N (3.3×10^{-5} M) in 4×10^{-2} M HCl.

Fig. 2. Absorption spectra of CPA*m*N complexes of La and Ce in the presence and absence of oxalic acid: (A) CPA*m*N against water; (B) La—CPA*m*N against reagent blank, (C) Ce—CPA*m*N against reagent blank. La, 10.0 μg; Ce, 9.8 μg; CPA*m*N, 3.3×10^{-5} M; oxalic acid, 9.5×10^{-2} M; HCl, 4×10^{-2} M.

Reagents

The stock standard solutions of rare earths(III) were prepared by dissolving the oxides of lanthanum, praseodymium, samarium, europium, gadolinium, terbium, dysprosium, thulium, ytterbium (Specpure, Johnson—Matthey), neodymium, holmium, erbium, lutetium, yttrium (99.99%, Shanghai Chemicals Factory) in hydrochloric acid and the cerium oxide (99.99%, Shanghai Chemicals Factory) in a mixture of sulphuric acid and hydrogen peroxide, evaporating the excess of acid and diluting with (1 + 200) hydrochloric acid to a given volume. The solutions were standardized by EDTA titration with xylenol orange as indicator. The working standard solutions were prepared by diluting as required with (1 + 200) hydrochloric acid.

CPA*m*N solution (0.02%) was prepared by dissolving 0.02 g of CPA*m*N in 100 ml of water. The solution was stable for at least a month. Oxalic acid solution (3%) was prepared by dissolving 30 g of oxalic acid (A.R.) in 900 ml of water, adjusting the pH to 2.0 with ammonia and then diluting to 1 l with water. Cresol red solution (0.04%) was prepared by dissolving 0.04 g of cresol red (BDH) in 100 ml of 50% ethanol. The other reagents were of analytical grade; all the water used was deionized.

General procedure

The test solution containing not more than 12.0 μg of lanthanum or 11.7 μg of cerium was taken in a 25-ml volumetric flask; 1 ml of 1 M hydrochloric acid, 10 ml of 3% oxalic acid and 3 ml of 0.02% CPA*m*N solution were added successively and mixed well. The solution was then diluted to the

mark with water and the absorbance was measured at 666 nm in a 1-cm cell against a reagent blank. If the test solution was highly acidic, it was neutralized dropwise with 2 M sodium hydroxide to pH 2 (cresol red was used as a suitable indicator, unless a large amount of iron(III) was present) before the general procedure was applied.

RESULTS AND DISCUSSION

Absorption spectra

The absorption maximum of the reagent was at 545 nm (Fig. 1). The complexes of rare earths gave two peaks in the absence of oxalic acid. These were at 608 and 666 nm for lanthanum and cerium (Fig. 2) and at 610 and 657 nm for yttrium and ytterbium (Fig. 3).

In the presence of oxalic acid, the complexes of yttrium and ytterbium were completely masked (Fig. 3) while the complexes of lanthanum and cerium were almost unaffected. The more sensitive wavelength of 666 nm was chosen for the spectrophotometric measurements of lanthanum or cerium, measured against a reagent blank.

Behaviour of other rare earth elements

The absorbances of the complexes of the other rare earths were also measured at 666 nm against a reagent blank, in the presence of oxalic acid. Figure 4 shows that the absorbance relative to 10.0 μg of lanthanum, of the

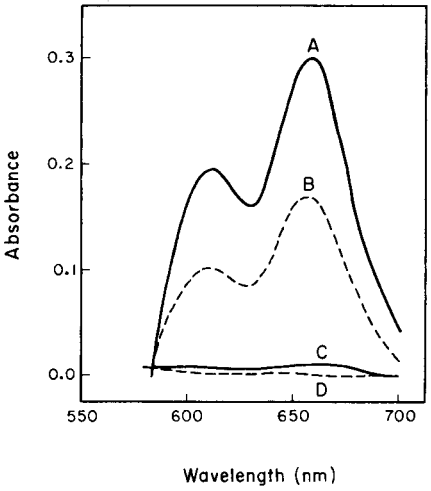

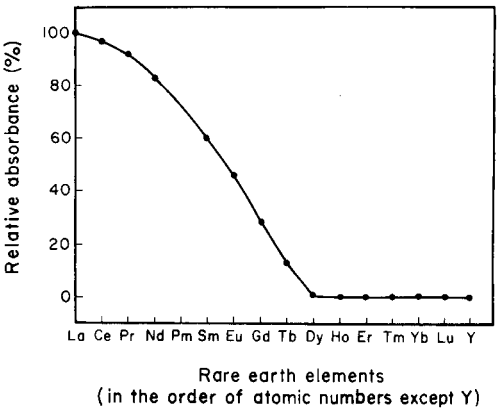

Fig. 3. Absorption spectra of CPA*m*N complexes of Y and Yb. (A) Y—CPA*m*N; (B) Yb—CPA*m*N in the absence of oxalic acid against reagent blank; (C) Y—CPA*m*N; (D) Yb—CPA*m*N in the presence of oxalic acid against reagent blank. Y, 10.4 μg; Yb, 10.2 μg; otherwise as for Fig. 2.

Fig. 4. Relative absorbances of CPA*m*N complexes of rare earths at 666 nm. CPA*m*N, 3.3×10^{-5} M; oxalic acid, 9.5×10^{-2} M; HCl, 4×10^{-2} M.

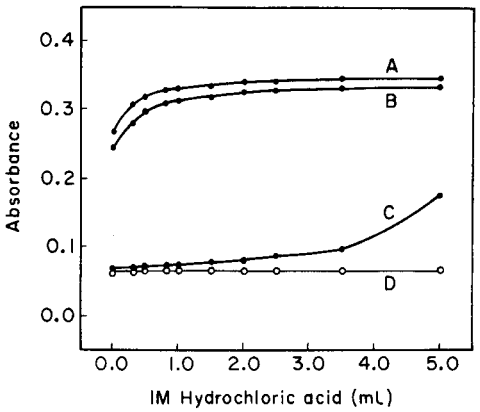

Fig. 5. Effect of amount of hydrochloric acid. (A) La, 10.0 μg; (B) Ce, 9.8 μg; (C), Y, 10.4 μg; (D) Yb, 10.2 μg and reagent blank against water; other conditions as for Fig. 4.

same weight of rare earth element, decreases with the increase in atomic number. From dysprosium to lutetium (including yttrium), the absorbances were negligible. This behaviour enables cerium sub-group elements to be determined in the presence of yttrium sub-group elements.

Effect of reaction conditions

The effect of the amount of hydrochloric acid in the presence of oxalic acid was examined in the range of 0.0—5.0 ml of 1 M hydrochloric acid. As shown in Fig. 5, the absorbances of the reagent blank and ytterbium complex were constant in this range, and that of yttrium complex slightly increased at high acidities, owing to the decomposition of its oxalate complex in the more acidic medium. The absorbances of the lanthanum and cerium complexes were almost unchanged in the range of 1.0—5.0 ml of 1 M hydrochloric acid; below 1.0 ml, the absorbances decreased gradually with the decrease of acidity, owing to the formation of the oxalate complexes.

For the determination of lanthanum or cerium in the presence of yttrium and ytterbium, the addition of 0.5—2.0 ml of hydrochloric acid was optimum, this corresponded to a pH range of 1.3—1.7 in the final solution. Usually, 1.0 ml of acid was introduced (pH ca. 1.6). If yttrium was absent, 5.0 ml of hydrochloric acid could be added (pH ca. 0.9) even when ytterbium was present.

Amounts of 8—12 ml of 3% oxalic acid solution were added for masking of yttrium sub-group elements; a greater amount of oxalic acid would slightly depress the absorbance of the lanthanum complex. Therefore, an addition of 10 ml of the oxalic acid is recommended. In 25 ml of solution, 2.0—5.0 ml of 0.02% CPA*m*N solution gave maximum absorbance for 10.0 μg of lanthanum, hence a 3.0-ml addition of CPA*m*N solution is recommended.

Characteristics of the complex

The coloured complexes were formed instantly and their absorbances were stable for at least 7 h. A study of the lanthanum—CPA*m*N complex, as determined by Job's method of continuous variations, showed that the metal-to-ligand ratio was 1:3 in the absence of oxalic acid.

Calibration graphs, precision and interferences

Calibration graphs were constructed according to the general procedure. Beer's law was obeyed for 0—12.0 μg of lanthanum or 0—11.7 μg of cerium in a 25-ml solution at 666 nm. In the absence of oxalic acid, Beer's law was obeyed for 0—18.0 μg of lanthanum or 0—17.6 μg of cerium. The apparent molar absorptivities of lanthanum and cerium at 666 nm, calculated from the slopes of the calibration graphs, were 9.5×10^4 and 9.3×10^4 l mol^{-1} cm^{-1}, respectively. The Sandell sensitivities were 1.5 ng La cm^{-2} and 1.5 ng Ce cm^{-2}. The coefficients of variation for the determination of 10.0 μg of lanthanum and 9.8 μg of cerium (10 determinations each) were 0.37% and 0.92%, respectively.

Solutions containing 10.0 μg of lanthanum and various amounts of 39 foreign ions besides the rare earths were prepared, and the general procedure was followed for the determination of lanthanum. As shown in Table 1, most of the ions did not interfere with the determination; 15 mg of iron(III) and 1.5 mg of uranium(VI) were tolerable, but thorium, zirconium and moderate amounts of calcium and barium would interfere.

Lanthanum was determined in the presence of various amounts of yttrium sub-group elements. The results are listed in Table 2. If an error of 10% in amounts is considered tolerable for the determination of 10.0 μg of lan-

TABLE 1

Effect of foreign ions on the determination of 10.0 μg of lanthanum

Foreign ion	Added (mg)	La found (μg)	Foreign ion	Added (mg)	La found (μg)	Foreign ion	Added (mg)	La found (μg)
Fe(III)	15	10.2	K(I)	5	9.8	U(VI)	1.5	10.5
Cu(II)	1	10.2	Bi(III)	0.1	10.0	Sc(III)	0.06	10.5
Co(II)	1	10.0	Mg(II)	1	10.4	Perchlorate	500	10.1
Cr(III)	1	10.4	Ba(II)	0.05	10.2	Nitrate	100	10.3
Al(III)	1	10.4	Ca(II)	0.04	10.2	Sulphate	100	10.0
Zn(II)	1	10.1	Th(IV)	0.003	10.1	Phosphate	150	9.7
Ni(II)	0.5	10.1	Zr(IV)	0.01	10.4	Dichromate	0.3	10.1
Pb(II)	0.5	10.1	Mo(VI)	1	9.8	Metaborate	3.6	10.3
Mn(II)	1	9.8	Hg(II)	1	9.7	Citrate	1000	9.7
Sn(IV)	0.3	10.0	V(V)	1	9.8	Tartrate	100	9.9
Sb(III)	0.3	9.9	W(VI)	1	9.7	Oxalate	290	9.6
Cd(III)	1	10.1	Ti(IV)	0.1	10.3	NTA	20	10.0
NH_4(I)	144	10.2	Nb(V)	1	10.4	EDTA	6.5	9.9

TABLE 2

Determination of 10.0 μg of lanthanum in the presence of yttrium sub-group elements

Rare earth	Added (μg)	La found (μg)	Rare earth	Added (μg)	La found (μg)	Rare earth	Added (μg)	La found (μg)
Dy	50	10.4	Tm	50	10.0	Lu	150	10.0
	100	10.9		100	10.3		200	10.2
	150	4.2		150	8.3		300	9.9
Ho	50	10.0	Yb	50	10.1		400	9.2
	100	10.5		100	10.6	Y	50	10.2
	150	5.3		150	9.4		100	10.6
Er	50	9.8		200	6.9		150	3.9
	100	10.4						
	150	8.8						

thanum, the tolerable limits for the yttrium sub-group elements (μg in parenthesis) are as follows: dysprosium (100), holmium (100), erbium (100), thulium (100), ytterbium (150), lutetium (400), yttrium (100).

Conclusions

The present method with CPA*m*N as a reagent for the spectrophotometric determination of cerium and lanthanum in the presence of yttrium sub-group elements is sensitive, selective and simple. Its sensitivity is superior to those of other 2,7-bisazo derivatives of chromotropic acid except for carboxynitrazo. Under the experimental conditions employed, 10—40-fold amounts of yttrium sub-group elements are tolerable, and 1.5 mg of uranium(VI) does not interfere, which is an advantage over the arsenazo-III or chlorophosphonazo-III methods.

The authors express their appreciation to Prof. Xia Yan and Prof. Yan Juan-Tan for their continuing support and valuable suggestions.

REFERENCES

1 S. B. Savvin, Zavod. Lab., 29 (1963) 131.
2 S. B. Savvin, R. F. Propistsova and R. V. Strel'nikova, Zh. Anal. Khim., 24 (1969) 31.
3 B. Buděšinký and K. Haas, Fresenius Z. Anal. Chem., 210 (1965) 263.
4 J. W. O'Laughlin and D. F. Jensen, Talanta, 17 (1970) 329.
5 T. Taketatsu, M. Kaneko and N. Kono, Talanta, 21 (1974) 87.
6 S. B. Savvin, T. V. Petrova and P. N. Romanov, Talanta, 19 (1972) 1437.
7 N. U. Perisic-Janjic, A. A. Muk and V. D. Canic, Anal. Chem., 45 (1973) 798.
8 E. B. Sandell and H. Onishi, Photometric Determination of Traces of Metals, Part I, 4th. edn., J. Wiley, New York, 1978, p. 467.
9 H. C. Liu, Y. X. Qu and B. C. Wu, Physical and Chemical Testing Communications, Chemistry Section, in Chinese, 2 (1979) 31.
10 A. A. Nemodruk, Yu. P. Novikov, A. M. Lukin and I. D. Kalinina, Zh. Anal. Khim., 16 (1961) 292.

Analytica Chimica Acta, 124 (1981) 185—192

SENSITIVE SPECTROPHOTOMETRIC DETERMINATION OF GERMANIUM AS METHYLENE BLUE 12-MOLYBDOGERMANATE

F. V. MIRZOYAN, V. M. TARAYAN* and E. KH. HAIRYAN

Institute of Inorganic and General Chemistry, Armenian Academy of Sciences and Yerevan State University (U.S.S.R.)

(Received 30th June 1980)

SUMMARY

The optimal conditions for the quantitative formation of 12-molybdogermanic acid and of its ion-associate with methylene blue, $(MB)_4[Ge(Mo_{12}O_{40})]$, are described. Dissolution of the centrifuged precipitate in acetone is used to provide a highly sensitive spectrophotometric method for the determination of 0.007—1.2 μg Ge ml^{-1} (ϵ = 4.5 × 10^5 l mol^{-1} cm^{-1}). Only silicon is a serious interference.

The spectrophotometric determination of germanium is usually preceded by its selective isolation as germanium tetrachloride by extraction or distillation. Thus the development of new spectrophotometric methods is usually carried out with the object of increasing sensitivity. In this respect, it is feasible to use basic dyes as reagents for the determination of molybdogermanic acid, as in theory the highest sensitivity can be achieved in this way, provided that all the hydrogen atoms in molybdogermanic acid are completely replaced by basic dye cations. However, investigations of such systems [1—5] have not resulted in the theoretically expected sensitivity, and the reproducibility has been far from satisfactory [6, 7].

Earlier, it was shown by the present authors [8—12] that the reproducibility of the results and the degree of substitution of hydrogen atoms in the heteropoly acid by dye cations (and therefore the sensitivity of the method) increased sharply when the reaction was carried out on the solid heteropoly acid after separation in a centrifuge. The investigation of molybdogermanic acid with the thiazine dyes, dimethylthionine and methylene green, to form a precipitate gave the conditions necessary for the complete substitution of molybdogermanic acid, but the molar absorptivities of the reaction products were relatively small [12]. The aim of the present work is to increase the sensitivity of the method for the determination of germanium by using molybdogermanic acid with methylene blue (MB), which has a large molar absorptivity.

EXPERIMENTAL

Reagents and apparatus

A 5×10^{-3} mol l^{-1} solution of germanium(IV) was prepared by dissolving weighed amounts of GeO_2 (guaranteed reagent, special) in distilled water by adding small amounts of sodium hydroxide. The final pH of the solution was 7.2.

Acetone, methylene blue and sodium oxalate were guaranteed reagent-grade, nitric acid (d = 1.41) was a guaranteed reagent, special, and $Na_2MoO_4 \cdot 2H_2O$ was pure. All the solutions were stored in polyethylene vessels.

Absorbances were measured with an SP-4A spectrophotometer, and the pH was measured with a pH-340 meter. The precipitates were separated by centrifuging the solutions for 1—2 min with a laboratory centrifuge CLK-1 at 3000 rpm.

Procedure

To the test solution containing 0.07—12.0 μg of germanium in a centrifuge tube, 0.5 ml of a 0.024 mol l^{-1} solution of sodium molybdate was added, and the pH was adjusted to 1.4—4.2 by adding nitric acid. The mixture was left for 10 min, and then 1.0—2.5 ml of 2 mol l^{-1} nitric acid and 0.5 ml of a 0.1% (w/v) solution of methylene blue were introduced. The solution was diluted to 10 ml by adding distilled water, and then mixed until a precipitate appeared. After centrifugation at 3000 rpm, the supernatant liquid was carefully decanted and the precipitate was dissolved in 10 ml of acetone containing 0.5 ml of 8 mol l^{-1} nitric acid. The absorbance of the acetone solution was measured at 660 nm in 0.1-cm cells against a distilled water blank taken through the whole procedure ($A_{blank} \leqslant 0.020$). Calibration graphs were prepared with aqueous germanium standards.

The abbreviations pH_i and pH_f are used below to denote the initial and final acidities necessary for the formation of molybdogermanic acid and the separation of MB—molybdogermanic acid compounds. The general method of investigation was described in detail earlier [12].

RESULTS AND DISCUSSION

Optimal conditions for the formation of molybdogermanic acid

The search for optimal acidity was not carried out on the basis of the absorbance of molybdogermanic acid which changes with acidity and molybdate concentration [13—15], but on the basis of the absorbance of the reaction product of methylene blue and molybdogermanic acid. In order to do this, it was necessary to establish by preliminary experiments, the final acidities of the medium at which molybdogermanic acid is not formed and at which molybdogermanic acid does not dissociate after its formation in a less acidic (pH_i) medium, but at which the product with methylene blue

is formed in maximum amount. The pH at which isopolymolybdate ions do not react with methylene blue had also to be studied. This acidity will depend on the nature of the heteropoly acid and on the dye. The pH which fulfilled all these criteria was 0.7 ± 0.1.

Figure 1 shows the dependence of the absorbance of acetone solutions of MB—molybdogermanic acid on pH_i, at various initial molybdate concentrations and at constant pH_f. The pH_i interval which allows the maximum formation of molybdogermanic acid is 1.4—4.2, provided that the initial molybdate concentration is 1.2×10^{-3}—2.4×10^{-3} mol l^{-1}. It might be thought that the equilibrium during the formation of molybdogermanic acid would be displaced as the result of the precipitation of the ion associate, but this does not occur. Almost the same interval of optimal pH_i was noted earlier in measuring the absorbance of molybdogermanic acid itself [16], and of analogous systems with other basic dyes [12].

This approach is interesting as a possible means of stabilizing and separating α- and β-molybdogermanic acid and other heteropoly acids [10, 13]. Such an approach is justified for investigating the formation conditions of a number of stable "non-coloured" heteropolymolybdic acids, such as those of aluminium, chromium and gallium, which usually absorb light at similar wavelengths to the isopolymolybdate ions.

In order to establish the minimum concentration of molybdate necessary for the quantitative formation of molybdogermanic acid, the dependence of the absorbance on the molybdate concentration was studied at pH_i 2.8 and pH_f 0.7. The maximum yield is given by molybdate concentrations exceeding $\geqslant 0.96 \times 10^{-3}$ mol l^{-1}. On increasing the concentration above 2.4×10^{-3} mol l^{-1}, the blank absorbance sharply increases (because isopolymolybdates are precipitated), and the absorbance of the required ion associate is decreased, apparently as the result of interaction of molybdogermanic acid with isopolymolybdate ions. If pH_f is decreased, the maximum tolerable molybdate concentration is increased.

Optimal conditions for the separation of the methylene blue—molybdogermanic acid product

It is necessary to establish the optimal acidity and molybdate concentration necessary for the maximum separation of the MB—molybdogermanic acid product and especially for minimizing the simultaneous separation of MB—isopolymolybdates, which have analogous spectral characteristics. Thus, the dependence of the absorbance upon pH_f was investigated at pH_i 2.2 (any value of pH_i can be chosen in the range 1.4—4.2). The molybdate concentration must be adequate for maximum formation of molybdogermanic acid (i.e. $\geqslant 0.96 \times 10^{-3}$ mol l^{-1}). The effect of pH_i at different molybdate concentrations is shown in Fig. 2. The largest interval of pH_f 0.45—1.0 over which the ion associate is separated in maximum yields is observed at 1.2×10^{-3} mol l^{-1} molybdate. On increasing the molybdate concentration, the MB—molybdogermanic acid product becomes stable in more acidic

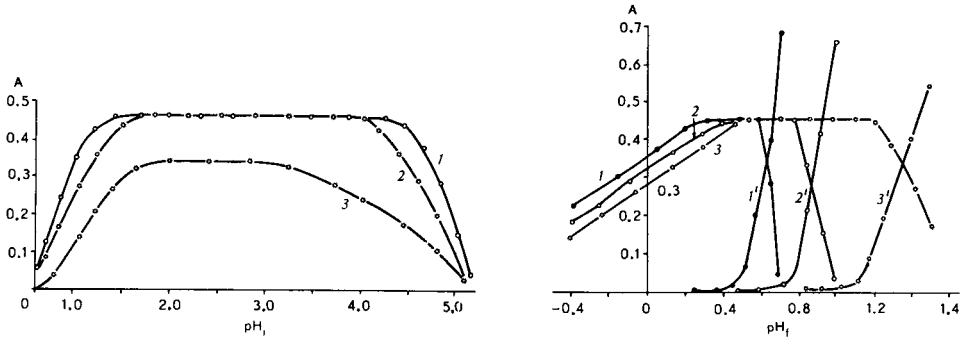

Fig. 1. The absorbance (A) as a measure of the extent of formation of molybdogermanic acid as a function of the initial pH. [Ge(IV)] = 1×10^{-5} M; [MB] = 1.5×10^{-4} M; pH_f = 0.7; A_{blank} = 0.00—0.02. [MoO_4^{2-}] = (1) 2.4×10^{-3} M; (2) 1.2×10^{-3} M; (3) 0.7×10^{-3} M.

Fig. 2. Effect of pH_f on the absorbance of germanium (1, 2, 3) and blank solutions (1′, 2′, 3′): [Ge(IV)] = 1×10^{-5} M; [MB] = 1.56×10^{-4} M; pH_i = 2.2; [MoO_4^{2-}] = (1, 1′) 4.8×10^{-3} M; (2, 2′) 2.4×10^{-3} M; (3, 3′) 1.2×10^{-3} M.

conditions, but the MB—isopolymolybdates are formed at considerably lower pH values than before (Fig. 2). For $\geqslant 1 \times 10^{-2}$ mol l^{-1} molybdate, the separation of a pure MB—molybdogermanic acid product becomes impossible.

The pH_f range, unlike that of pH_i, depends greatly on the nature of the basic dye [12]. Apparently this is due to the tendency of the basic dye to protolysis and to the water solubility of the products formed between methylene blue and molybdogermanic acid or isopolymolybdates. In order to eliminate the formation of basic dye isopolymolybdates, the masking effect of oxalate on isopolymolybdates may be used [3, 10, 12]. With this aim, the yield dependence of the MB—molybdogermanic acid product on the acidity was studied for various initial concentrations of oxalate and molybdate. The results are given in Fig. 3. In the presence of 1.2×10^{-3} mol l^{-1} molybdate, the introduction of 0.01 mol l^{-1} oxalate allows the pH range necessary for quantitative formation and separation of the MB—molybdogermanic acid product to be greatly extended into the less acidic range, to pH 4.2. In this pH range, MB—isopolymolybdates are not formed. At pH 0.5—1.2, quantitative separation of the MB—molybdogermanic acid product can be achieved even in the absence of oxalate (Fig. 2). Therefore, the masking effect of oxalate is exhibited at lesser acidities (pH 1.2—4.2). This makes it possible to separate the MB—molybdogermanic acid product under the conditions at which molybdogermanic acid is formed. A further 10-fold increase of the oxalate concentration allows the quantitative separation of the MB—molybdogermanic acid product at even higher pH values ($\leqslant$pH 6.0) in the complete absence of MB—isopolymolybdate (A_{blank} 0.01).

In the above experiments, the MB—molybdogermanic acid product was obtained and separated just after the addition of oxalate (which was added before the dye). Therefore from the practical point of view, it was necessary

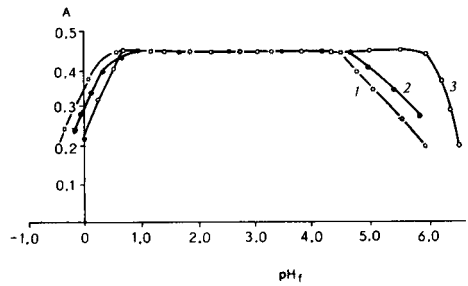

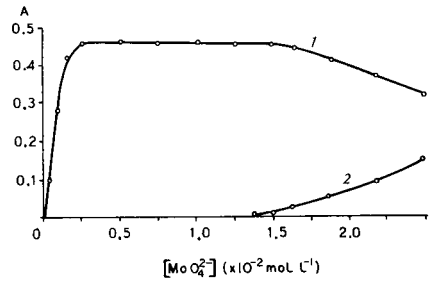

Fig. 3. Yield dependence (absorbance) of the ion associate on final acidity at various initial concentrations of oxalate and molybdate ions. [Ge(IV)] = 1 × 10^{-5} M; [MB] = 1.56 × 10^{-4} M; pH_i = 2.2; (MoO_4^{2-}) = (1, 2) 1.2 × 10^{-3} M; (3) 6.0 × 10^{-3} [$C_2O_4^{2-}$] = (1) 0.01 M; (2, 3) 0.10 M.

Fig. 4. Absorbance dependences of germanium (1) and blank solutions (2) on molybdate concentration. [Ge(IV)] = 1 × 10^{-5} M; pH_i = 2.2; pH_f = 4.0; [$C_2O_4^{2-}$] = 0.1 M; [MB] = 1.56 × 10^{-4} M.

to determine the stability of molybdogermanic acid in the presence of oxalate. It was found that on introduction of 0.1 mol l^{-1} oxalate, molybdogermanic acid is stable for less than 15—20 min (and in 0.01 mol l^{-1} oxalate, up to 30 min). For this reason, the solid MB—molybdogermanic acid product must be obtained and separated during this adequately long period.

Experiments were carried out to establish the upper limit of the molybdate concentration which allows the quantitative separation of the pure MB—molybdogermanic acid product. The results given in Fig. 4, show that the maximum yield is assured at 1 × 10^{-3}—1.5 × 10^{-2} mol l^{-1} molybdate. A further increase of the molybdate concentration favours the separation of MB—isopolymolybdates and thereby raises the absorbance of the blank solution, and leads to a decreased yield of the MB—molybdogermanic acid product, as described above.

Finally, the methylene blue concentration must influence the yield of the MB—molybdogermanic acid product and MB—isopolymolybdates. In all the above experiments, the concentration of the dye was kept constant at 1.56 × 10^{-4} mol l^{-1}. Tests were carried out at different concentrations of MB, both in the absence of oxalate (pH_f = 0.7, [MoO_4^{2-}] = 1.2 × 10^{-3} mol l^{-1}) and in its presence (pH_f = 4.0, [MoO_4^{2-}] = 1.2 × 10^{-3} mol l^{-1}, [$C_2O_4^{2-}$] = 0.01 mol l^{-1}). Quantitative yields of the (ϵ = 4.5 × 10^5 l mol^{-1} cm^{-1}), when MB—isopolymolybdates are completely absent, are obtained from 1.25—6.20 × 10^{-4} mol l^{-1} dye solutions, under both conditions. Further increase in the MB concentration leads to the separation of isopolymolybdates.

Thus, contrary to the literature data on the rigidity of the conditions required for obtaining basic dye—molybdogermanic acid compounds, it has been shown that the MB—molybdogermanic acid product can be quantitatively separated over fairly large ranges of concentrations of the components, which makes the method readily applicable for the determination of germanium-(IV).

The composition and analytical properties of methylene blue—molybdogermanic acid

The ratio of the main components, MB and molybdogermanic acid (MGA) in the compound studied was determined by the method of isomolar series. The tests were carried out both in the presence and absence of oxalate and by studying two different total concentrations of the components. The results are shown in Fig. 5. They show a ratio MB:MGA = 4:1, irrespective of the total concentration of the isomolar series components and the different conditions. The validity of the composition is confirmed by the fact that the molar absorptivity of the acetone solutions of MB—molybdogermanic acid product which is 4.5×10^5 l mol^{-1} cm^{-1}, is four times that of an acetone solution of MB itself (1.1×10^5 l mol^{-1} cm^{-1}). This also provides evidence of the quantitative formation and separation of the MB—molybdogermanic acid product. This was also estimated by determination of the germanium content in the corresponding precipitates with use of phenylfluorone [17, 18] after decomposition with nitric acid.

The MB—molybdogermanic acid product obtained both from the β-isomer of molybdogermanic acid (pH_i 1.8) and the α-isomer (pH_i 4.0), was analysed for its molybdenum content. The precipitate $(MB)_4MGA$, containing 1×10^{-7} mol of germanium, after being separated in a centrifuge, was dissolved in the same tube in 2.5 ml of concentrated sulphuric acid (d = 1.83). The solution was transferred to a 25-ml measuring flask. The test-tube was washed several times with small portions of distilled water and the washings were also transferred to the same measuring flask. Molybdenum(VI) in the solution was determined by a thiocyanate spectrophotometric method [19]. In order to avoid the superposition of the spectral bands of the dye and the molybdenumthiocyanate complex, the complex was extracted into 10 ml of butyl acetate. In preliminary experiments, it was established that the introduction of germanium(IV) and MB did not affect the light absorption characteristics of the butyl acetate extracts of the molybdenum thiocyanate complex and that the complex was quantitatively recovered by a single extraction. A blank test was carried out simultaneously. The results of six parallel tests showed that, irrespective of pH_i (and therefore irrespective of which isomer of molybdogermanic acid is formed, the ratio Mo:Ge in the compound studied remains constant at 11.89 ± 0.12), i.e. the MB—molybdogermanic acid product is based on 12-molybdogermanic acid.

The compound $(MB)_4MGA$, with its very high molar absorptivity is of value for the determination of trace amounts of germanium(IV). The limit of detection of the proposed method, based on the results of 16 parallel blank tests and the 3 s criterion, is 5.4 ng ml^{-1} (in a final volume of 10 ml). The upper limit of determination is 1.2 μg Ge ml^{-1} (s_r = 0.01). To establish the lower limit, various amounts of germanium in pure solutions were determined and the s_r values were calculated. For each concentration 16 parallel determinations were made. Figure 6 shows the dependence of the relative standard deviations on germanium concentration. The lower limit

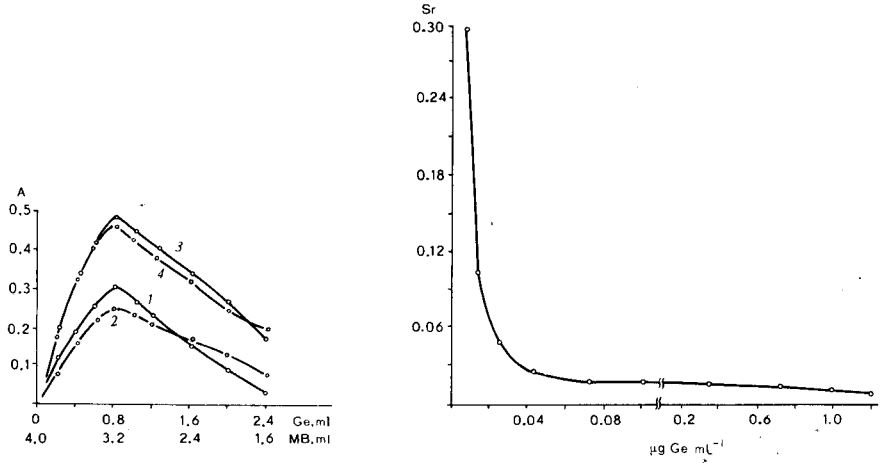

Fig. 5. Isomolar series for the MB—molybdogermanic acid system.* A_{blank} = 0.000; (1, 3) pH_f = 4.0; (2, 4) pH_f = 0.7. Total concentration of [MB] + [Ge]: (1, 2) 4.0 × 10^{-5} M; (3, 4) 8.0 × 10^{-5} M.

Fig. 6. Dependence of relative standard deviation (s_r) upon concentration of germanium.

of determination, considered as the concentration which has s_r = 0.3, is 7 ng Ge ml^{-1}. Thus the method, apart from being highly sensitive, is also notable for the large concentration range over which it is applicable. It takes 30—35 min to carry out 20 parallel determinations.

The determination of 10^{-5} mol l^{-1} germanium is possible in the presence of many other elements. At pH_i 1.5, where interferences are expected to be less than at higher acidities, the following could be tolerated (mol ratio in parentheses): B (500), Ga (100), Al (25), Fe(III) (20), In (10), Hg (II) (10), PO_4^{3-} (20) and AsO_4^{3-} (10). Fairly large amounts of alkaline and alkaline earth elements and Cu, Co and Ni do not interfere. Silicon always gives high results.

The accuracy was checked on germanium-containing standard minerals (No. 791-76, 3.83% Ge and 792-76, 4.97% Ge), and also by standard addition to various germanium-containing iron ores (10 ppm—0.1% Ge, following a preliminary separation of germanium(IV) as germanium tetrachloride. The results were all satisfactory.

REFERENCES

1 L. I. Ganago and I. A. Prostak, Dokl. Akad. Nauk B. SSR, 13 (1969) 345.
2 Gr. Popa and I. Paralescu, Talanta, 16 (1969) 315; Rev. Chim. (Bucharest), 21 (1970) 43.
3 L. I. Ganago and I. A. Prostak, Zh. Anal. Khim., 26 (1971) 104.
4 L. I. Ganago and I. A. Prostak, Izv. Vyssh. Uchebn. Zaved. Khim. Khim. Tekhnol., 14 (1971) 1165.
5 V. P. Zhivopistsev and T. B. Cherepanova, Zh. Anal. Khim., 32 (1977) 974.
6 D. N. Lisitsina, D. P. Shtcherbov and I. A. Talatinova, Zb. Issledovanie v oblesti Khimicheskikh i phizicheskikh metodov analiza mineralnovo sirya, Vip. 3, Alma-Ata, izd. Kazims, 1973, p. 38.

7 V. A. Nazarenko and G. V. Phlyantikova, Zh. Anal. Khim., 32 (1977) 1225.
8 V. M. Tarayan, F. V. Mirzoyan and Z. A. Karapetian, Dokl. Akad. Nauk Arm. SSR, 63 (1976) 168.
9 F. V. Mirzoyan, V. M. Tarayan and Z. A. Karapetian, Arm. Khim. Zh., 30 (1977) 25; 31 (1978) 152; Zavod. Lab., 44 (1978) 1184; Zh. Neorg. Khim., 23 (1978) 3026.
10 F. V. Mirzoyan, V. M. Tarayan and Z. A. Karapetian, Zh. Anal. Khim., 34 (1979) 1515.
11 F. V. Mirzoyan, V. M. Tarayan and A. A. Petrossian, Arm. Khim. Zh., 31 (1978) 597.
12 F. V. Mirzoyan, V. M. Tarayan and E. Kh. Hayrian, Arm. Khim. Zh., 32 (1979) 106.
13 R. A. Chalmers and A. G. Sinclair, Anal. Chim. Acta, 33 (1965) 384.
14 F. Chauveau, P. Souchay and R. Schall, Bull. Soc. Chim. Fr., (1959) 1190.
15 A. Halasz and E. Pungor, Talanta, 18 (1971) 557, 565.
16 W. Kemula and S. Rosolowski, Roczn. Chem., 34 (1960) 835.
17 V. A. Nazarenko, N. V. Lebedeva and R. V. Ravitskaya, Zavod. Lab., 24 (1958) 9.
18 V. A. Nazarenko and N. V. Lebedeva, Zb. Nauchnikh trudov, Giredmet, 2 (1959) 63.
19 L. B. Zaitchikova, Zavod.Lab., 15 (1949) 1025.

Analytica Chimica Acta, 124 (1981) 193—200

SOME PYRIDYLAZO COMPOUNDS AS SENSITIVE REAGENTS FOR THE SPECTROPHOTOMETRIC DETERMINATION OF NICKEL

K. OHSHITA

Laboratory of Chemistry, Daido Institute of Technology, Minami-ku, Nagoya (Japan)

H. WADA* and G. NAKAGAWA

Laboratory of Analytical Chemistry, Nagoya Institute of Technology, Showa-ku, Nagoya (Japan)

(Received 15th August 1980)

SUMMARY

Six 2-(2-pyridylazo)-5-alkoxyphenol derivatives were synthesized, and their application to the spectrophotometric determination of nickel was studied; 2-(2-pyridylazo)-5-methoxyphenol and the corresponding ethoxyphenol are very sensitive and selective. The molar absorptivity of the nickel chelate of the former is 11.3×10^4 l mol^{-1} cm^{-1}. A solvent extraction procedure for the selective determination of 1—8 μg of nickel is described.

1-(2-Pyridylazo)-2-naphthol (PAN) has been widely used as a very sensitive reagent for the spectrophotometric determination of nickel [1]. In an attempt to prepare an even more sensitive reagent, six 2-(2-pyridylazo)-5-substituted phenols have been synthesized and their properties as nickel reagents studied. Among these reagents, 2-(2-pyridylazo)-5-methoxyphenol (PAP-5-OMe) and 2-(2-pyridylazo)-5-ethoxyphenol (PAP-5-OEt) were found to be much more sensitive reagents than PAN.

EXPERIMENTAL

Preparation of azo compounds (see Table 1)

The various 2-aminopyridines used were diazotized with freshly prepared butyl nitrite in the presence of sodium amide in diethyl ether by heating under reflux for several hours. After the solution had been cooled, the precipitate was filtered, washed with diethyl ether and stored in a desiccator over silica gel. An ethanolic solution of the appropriate substituted phenol was added to the 2-diazopyridine in ethanol, carbon dioxide bubbled through for 1 h, and the mixture allowed to stand overnight. The precipitate was then filtered and recrystallized from ethanol or ethanol—water mixture. The results of elemental analyses and the melting points of the compounds synthesized are shown in Table 1.

TABLE 1

Elemental analyses[a] and melting points of the 2-(2-pyridylazo)-5-alkoxyphenol derivatives tested

Compound[b]	C(%)	H(%)	N(%)	Br(%)	m.p. (°C)
PAP-5-OMe	63.2(62.9)	4.9(4.85)	18.1(18.3)		175
PAP-5-OEt	64.0(64.2)	5.3(5.4)	17.1(17.3)		150
5-Me-PAP-5-OMe	64.7(64.2)	5.4(5.4)	17.0(17.3)		267
5-Br-PAP-5-OMe	45.9(46.8)	3.2(3.3)	13.6(13.6)	25.6(25.9)	210
3,5-Br-PAP-5-OMe	37.5(37.2)	2.3(2.35)	10.6(10.9)	41.6(41.3)	231
PAP-5-OMe-6-Me	63.2(64.2)	5.3(5.4)	17.3(17.3)		190

[a]The numbers in parentheses indicate the calculated values. [b]PAP-5-OMe, 2-(2-pyridylazo)-5-methoxyphenol; PAP-5-OEt, 2-(2-pyridylazo)-5-ethoxyphenol; 5-Me-PAP-5-OMe, 2-(5-methyl-2-pyridylazo)-5-methoxyphenol; 5-Br-PAP-5-OMe, 2-(5-bromo-2-pyridylazo)-5-methoxyphenol; 3,5-Br-PAP-5-OMe, 2-(3,5-dibromo-2-pyridylazo)-5-methoxyphenol; PAP-5-OMe-6-Me, 2-(2-pyridylazo)-5-methoxy-6-methylphenol.

Reagents and apparatus

Each azo compound was dissolved in ethanol or dioxan.

Metal ion solutions. A standard solution of nickel was prepared from analytical-grade nickel sulfate and standardized with 0.01 M EDTA. A copper(II) solution was prepared by dissolving copper (99.99%) in dilute nitric acid. A cobalt(II) solution was prepared from analytical-grade cobalt(II) chloride and standardized by EDTA titration with the use of xylenol orange—1,10-phenanthroline as indicator. Other metal solutions were prepared from their analytical-grade nitrates, sulfates or chlorides.

Buffer solutions. Acetic acid—sodium acetate (2 M, pH 3—6), 2 M potassium dihydrogenphosphate—sodium hydroxide (pH 6—8), and 2 M ammonia—ammonium chloride (pH 8—10) were used.

Reagent-grade chloroform was used without further purification. All water used had been redistilled from a hard-glass vessel.

A Shimazu Model UV-200 spectrophotometer and a Hitachi-Horiba pH meter Model F-7 were used.

General procedure for investigation of reagents

To a 50-ml separatory funnel, transfer a metal ion solution and a reagent solution. If necessary, warm the mixture on a water bath. Add 2 ml of buffer solution and dilute with water to 20 ml. If necessary, warm again. After cooling, extract with exactly 10 ml of chloroform. Measure the absorbance of the chloroform extract in a 1-cm cell against chloroform.

Procedure for determination of nickel (1—8 μg)

To a 50-ml separatory funnel, transfer 5—10 ml of sample solution, add 1 ml of 1 M sodium thiosulfate solution and 0.3 ml of a 0.2% (w/v) solution of PAP-5-OMe in methanol. Heat the mixture for 5 min on a boiling water

bath. Add 2 ml of the 2 M phosphate buffer solution to adjust the pH to 7, and dilute to about 20 ml with water. Heat again for a few min. After cooling, extract with 3 ml of chloroform. Transfer the chloroform phase to another separatory funnel. Add 0.1 ml of the 0.2% (w/v) PAP-5-OMe solution to the aqueous phase, heat, and extract again with 3 ml of chloroform: repeat this procedure. Combine the three chloroform phases and shake for 5 min with 20 ml of 0.2 M ammonia—ammonium chloride buffer solution (pH 9) containing 0.5 ml of 0.4% (w/v) potassium periodate solution. Transfer the chloroform phase to a 10-ml volumetric flask, and dilute to the mark with pure chloroform. Measure the absorbance at 520 nm in a 1-cm cell against a reagent blank.

RESULTS AND DISCUSSION

Acidity constants of the azo compounds

All the reagents are soluble in aqueous dioxan solution. The dissociation equilibria can be written as

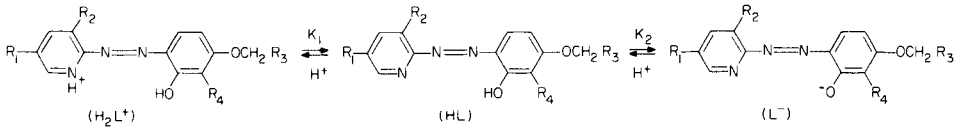

The acidity constants, $K_{a1} = [H^+][HL]/[H_2L^+]$ and $K_{a2} = [H^+][L^-]/[HL]$, were determined by Hildebrand and Reilley's method [2], with the results shown in Table 2.

Absorption spectra of the metal chelates

The azo compounds studied react with many metal ions as do other pyridylazo compounds. The absorption spectra of metal chelates extracted in chloroform were measured; some are shown in Fig. 1. The spectra of PAP-5-OEt and 5-Br-PAP-5-OMe chelates were very similar to those of the PAP-5-OMe chelates. PAP-5-OMe-6-Me chelates were not extracted quantitatively. In the case of PAP-5-OMe and PAP-5-OEt, the absorbance of the

TABLE 2

Acidity constants of the reagents at μ = 0.1 (KNO_3) and 25°C in aqueous dioxan

Reagent	pK_{a1}	pK_{a2}	H_2O:dioxan	Reagent	pK_{a1}	pK_{a2}	H_2O:dioxan
PAP-5-OMe	3.15	7.80	9:1	5-Br-PAP-5-OMe	<1	7.75	4:1
	3.30	7.40	—[a]	3,5-Br-PAP-5-OMe	<1	9.55	3:2
PAP-5-OEt	3.20	7.75	9:1	PAP-5-OMe-6-Me	3.00	8.15	4:1
5-Me-PAP-5-OMe	2.95	9.55	4:1	PAP-4-OMe[b]	2.50	8.73	9:1

[a]Pure water. [b]2-(2-Pyridylazo)-4-methoxyphenol [3].

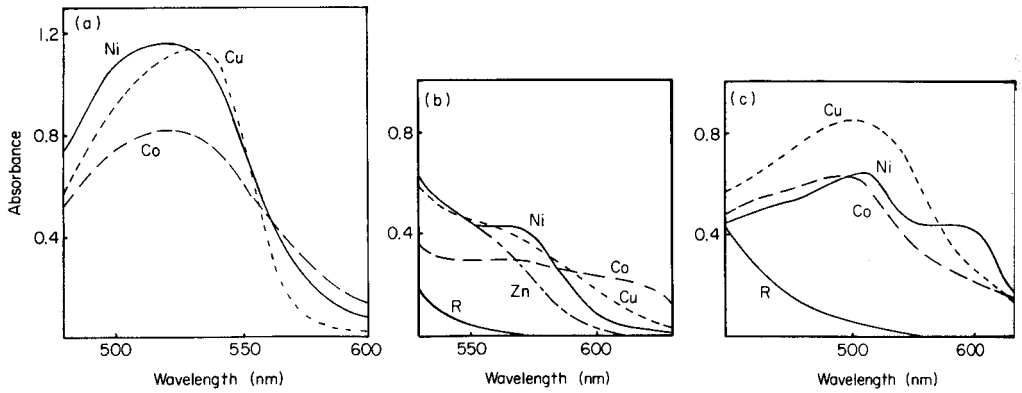

Fig. 1. Absorption spectra of metal chelates in chloroform: (a) PAP-5-OMe; (b) 5-Me-PAP-5-OMe; (c) 3,5-Br-PAP-5-OMe. Ni—6.19, Cu—6.42, Co—5.89, Zn—6.50 μg; 0.5 ml of 0.2% reagent.

reagent was negligible at the wavelength of maximum absorption of the nickel chelate. The molar absorptivities of the nickel, copper(II) and cobalt(II) chelates are shown in Table 3. The molar absorptivities of the nickel chelates with PAP-5-OMe and PAP-5-OEt are extremely high. It has been reported [4] that the sensitivity of 2-(5-bromo-2-pyridylazo)-5-dimethylaminophenol for nickel is higher than that of 2-(2-pyridylazo)-5-dimethylaminophenol (DMPAP), but this effect of bromine substitution is not evident for the present reagents (Table 3).

Composition and stability constants of nickel chelates

The mole ratio of nickel to PAP-5-OMe in the extracted chelates was established as 1:2 from the results of the continuous variations method. The stability constant of the nickel chelate of PAP-5-OMe was determined in water and in 10% dioxan solution by spectrophotometry; that of PAP-5-OEt was only determined in 10% dioxan. The straight-line portions of the

TABLE 3

Molar absorptivities of metal chelates

Reagent	Nickel		Copper		Cobalt(II)	
	ϵ ($\times 10^4$ l mol^{-1} cm^{-1})	λ_{max} (nm)	ϵ ($\times 10^4$ l mol^{-1} cm^{-1})	λ_{max} (nm)	ϵ ($\times 10^4$ l mol^{-1} cm^{-1})	λ_{max} (nm)
PAP-5-OMe	11.3	520	11.3	530	8.1	523
PAP-5-OEt	10.8	522	11.2	530	8.6	526
5-Me-PAP-5-OMe	4.2	565	4.5	540	2.4	565
5-Br-PAP-5-OMe	9.9	528	10.3	550	6.5	534
3,5-Br-PAP-5-OMe	5.7	552	7.9	550	6.0	544
DMPAP[a]	9.5	545	6.1	540	8.9	530
PAN[b]	5.0	570	2.2	564	2.7	550

[a] 2-(2-Pyridylazo)-5-dimethylaminophenol [3]. [b] 1-(2-Pyridylazo)-2-naphthol [1].

absorbance—pH plots were used for the calculations. At pH 5—6 the predominant reagent species is HL, therefore the equilibrium constants for the formation of the nickel chelates were $K_1 = [H^+][NiL^+]/[HL][Ni^{2+}]$ and $K_2 = [H^+]^2[NiL_2]/[HL]^2[Ni^{2+}]$. In the presence of a large excess of nickel (2.0×10^{-3} M) compared with reagent (2.0×10^{-5} M), the expression for K_1 can be written as

$$\log [NiL^+]/[HL] = \log K_1 + \log [Ni^{2+}] + pH$$

A plot of $\log [NiL^+]/[HL]$ vs. pH yielded a straight line with a slope of 1 in each case. The equilibrium constant K_1 was determined from the intercept of the straight line on the pH axis and the corresponding stability constant was calculated from $\beta_1 = [NiL^+]/[Ni^{2+}][L^-] = K_1/K_{a2}$.

In the presence of excess of reagent (8.0×10^{-5} M) over nickel (4.0×10^{-6} M), NiL_2 should be formed, and the expression for K_2 can be written as

$$\log [NiL_2]/[Ni^{2+}] = \log K_2 + 2 (\log [HL]) + 2 (pH)$$

A plot of $\log [NiL_2]/[Ni^{2+}]$ vs. pH yielded a straight line with a slope of 2. The equilibrium constant was determined from the intercept as before, the corresponding stability constant being calculated from $\beta_2 = [NiL_2]/[Ni^{2+}][L^-]^2 = K_2/K_{a2}^2$. The results are shown in Table 4. These formation constants are smaller than those of the analogous PAN chelates [1, 5].

Effect of pH on the extraction of the chelates

The absorbances of the various chelates extracted into chloroform at different pH values were measured at the maximum absorption wavelength of the chelates. Some results are shown in Fig. 2. The behaviour of PAP-5-OEt was similar to that of PAP-5-OMe. In the cases of 5-Me-PAP-5-OMe and 3,5-Br-PAP-5-OMe, the nickel chelates can be completely extracted above pH 4, but for PAP-5-OMe and PAP-5-OEt pH >6 is necessary for complete extraction.

Determination of nickel with PAP-5-OMe

The nickel chelate of PAP-5-OMe could be extracted with chloroform, 1,2-dichloroethane or isoamyl alcohol, but not with carbon tetrachloride or benzene. The extraction—pH curves are shown in Fig. 3. Chloroform gave constant absorbance over the widest pH range. As seen in Fig. 2a, the nickel

TABLE 4

Stability constants of nickel chelates, μ = 0.1 (KNO_3), 25°C

	PAP-5-OMe		PAP-5-OEt	PAN[a]
	(H_2O)	(10% dioxan)	(10% dioxan)	(1:1 dioxan) [1]
$\log \beta_1$	5.45	5.70	5.45	14.0
$\log \beta_2$	11.5	12.2	12.0	27.6

[a] At 14°C.

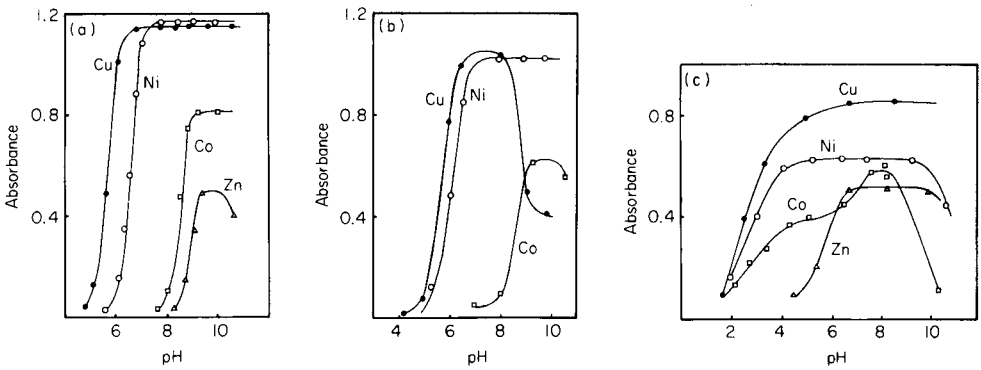

Fig. 2. Effect of pH on extraction: (a) PAP-5-OMe; (b) 5-Br-PAP-5-OMe; (c) 3,5-Br-PAP-5-OMe. Amount of metals and reagent as Fig. 1.

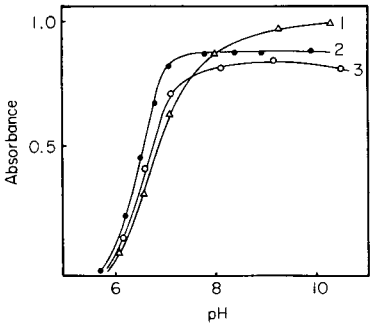

Fig. 3. Effect of solvent on the extraction of Ni—PAP-5-OMe (Ni, 4.90 μg; 0.5 ml of 0.2% PAP-5-OMe solution): (1) isoamyl alcohol; (2) chloroform; (3) 1,2-dichloroethane.

chelate of PAP-5-OMe can be extracted quantitatively in the pH range 7.5—10. The cobalt(II) chelate, however, is extracted at pH $\geqslant$7.5. Therefore, if the sample contains cobalt, nickel should be extracted at pH 7.0. Since the recovery of nickel is about 92% at this pH, three extractions with 3-ml portions of chloroform should be carried out.

The maximum absorbance for 5 μg of nickel was obtained with 100 μg of PAP-5-OMe (0.2% solution, 0.05 ml). However, 0.3 ml of 0.2% solution was used for the first extraction, and 0.1 ml each for the second and third extractions, to accommodate samples which contain other metals that form chelates with PAP-5-OMe. Under the recommended procedure based on these results, Beer's law is obeyed for 1—8 μg Ni/10 ml of chloroform. The Sandell sensitivity is 0.52 ng Ni cm^{-2}.

Effect of other ions. At pH 7, the copper(II)—PAP-5-OMe chelate is extracted, while the zinc chelate is not extracted. Cadmium, manganese(II), iron(III) and chromium(III) do not react with PAP-5-OMe at pH 7. If >20 μg

of cobalt is present, it is partly extracted at pH 7. Copper(II) (<60 μg) could be masked by prior addition of 1 ml of 1 M sodium thiosulphate.

Since suitable masking agents for cobalt could not be found, the back-extraction of copper(II), nickel and cobalt from the chloroform extract was studied. After the copper(II), nickel or cobalt(II) chelate had been extracted into chloroform from aqueous solution at pH 7, 9 or 10, respectively, the organic phase was shaken with various solutions for 5 min. The results are shown in Table 5. When the chloroform phase was shaken with ammonia—ammonium chloride buffer solution (pH 9) containing potassium periodate, cobalt was back-extracted, while nickel was not. The effect of ammonia and potassium periodate concentrations on the back-extraction of cobalt and the absorbances of the nickel and cobalt chelates in chloroform at 520 nm were examined (Table 6). The best results were obtained when 20 ml of 0.2 M ammonia—ammonium chloride solution containing 0.2—1.0 ml of 0.4% potassium periodate was used: up to 200 μg of cobalt can be tolerated under these conditions.

Results of the determination of nickel in the presence of various metals by the recommended procedure are given in Table 7.

TABLE 5

Back-extraction (%) of Cu, Ni and Co with various solutions

Solution	Cu (3 μg)	Ni (5 μg)	Co (5 μg)	Solution	Cu (3 μg)	Ni (5 μg)	Co (5 μg)
0.01 M EDTA	100	100	100	0.01 M $Na_2S_2O_3$	80	20	1
0.01 M HCl	100	100	100	0.01 M $Na_4P_2O_7$	84	0	94
0.01 M diethyldithiocarbamate	100	100	100	0.2 M NH_3—NH_4Cl (pH 9) (0.02% in KIO_4)	46	0	98
0.01 M KCN	100	100	100	0.1 M HOAc—NaOAc (pH 4)	100	97	100

TABLE 6

Back-extraction with NH_3—NH_4Cl—KIO_4 (pH 9) after extraction of Ni and Co at pH 7

NH_3—NH_4Cl conc.[a] (M)	Absorbance of $CHCl_3$ phase		Vol. 0.4% KIO_4 (ml)[b]	Absorbance of $CHCl_3$ phase	
	Co (50 μg)	Ni (5 μg)		Co (50 μg)	Ni (5 μg)
0	0.252	0.950	0.2	0.045	0.950
0.2	0.045	0.950	0.5	0.045	0.950
0.3	0.043	0.950	1.0	0.045	0.950
0.5	0.040	0.900	2.0	0.043	0.940
1.0		0.820	5.0		0.893

[a]19.5 ml of pH 9.0 buffer plus 0.5 ml of 0.4% KIO_4. [b]Added to 0.2 M buffer to give a total volume of 20.0 ml.

TABLE 7

Effect of other ions on the determination of nickel (4.90 μg)

Other ion	Added (μg)	Ni found (μg)	Other ion	Added (μg)	Ni found (μg)
Fe(III)	500	4.87	Cd(II)	500	4.90
Zn(II)	500	4.90		1000	4.82
	1000	4.95	Co(II), (III)	100	4.90
Mn(II)	1000	4.90		200	4.95
Cr(III)	1000	4.90	Cu(II)	50	4.87

In the presence of cobalt, without nickel the absorbance is only 0.030 greater than when cobalt is absent; this change, however, is almost constant in the presence of less than 200 μg of cobalt. Thus, for accurate work, the calibration graph should be prepared from nickel standard solutions containing a similar amount of cobalt to that in the sample.

This investigation was partially supported by a Grant-in-Aid for Scientific Research No. 454180 from the Ministry of Education, Science and Culture (Japan).

REFERENCES

1 T. Dono, G. Nakagawa and H. Wada, Nippon Kagaku Zasshi, 82 (1961) 590. G. Nakagawa and H. Wada, Bunseki Kagaku, 10 (1961) 1008. G. Nakagawa and H. Wada, Nippon Kagaku Zasshi, 84 (1963) 636. S. Shibata, in H. A. Flaschka and A. J. Barnard, Jr. (Eds.), Chelates in Analytical Chemistry, M. Dekker, New York, 1972.
2 G. H. Hildebrand and C. N. Reilley, Anal. Chem., 29 (1958) 258.
3 H. Wada, Bunseki Kagaku, 21 (1972) 543.
4 S. Shibata, M. Furukawa and K. Tôei, Anal. Chim. Acta, 66 (1973) 397.
5 R. G. Anderson and G. Nickless, Analyst, 92 (1967) 207.

Analytica Chimica Acta, 124 (1981) 201—209

A NEW GRAPHICAL METHOD FOR DETERMINING STABILITY CONSTANTS OF WEAK AND POLYNUCLEAR COMPLEXES

J. J. BERZAS NEVADO*, A. ARREBOLA RAMÍREZ and M. ROMÁN CEBA

Department of Analytical Chemistry, Faculty of Sciences, University of Extremadura, Badajoz (Spain)

(Received 31st March 1980)

SUMMARY

A graphical method is proposed for differentiating mono- and poly-nuclear complexes as well as for determining the stability constants of weak complexes. The method is based on the effect of dilution on the degree of dissociation of the complex. The precision for log K is ±0.02 for a degree of dissociation between 30 and 70%. The greatest values for log K that can be determined are 4.3, 12.4, 7.5 and 10.7 for 1:1, 2:2, 2:1 and 3:1 ligand: metal complexes, respectively. If log $K_1 \geqslant 5.7$, the method permits log K_2 to be determined if simultaneous complexes are formed.

The present paper describes a new spectrophotometric method for determining stability constants of weak complexes, as well as for differentiating mononuclear and polynuclear complexes (e.g. AB and A_2B_2). The method is based on the effect of dilution on the degree of dissociation of the complexes. There are other methods based on the same effect which have been applied to the determination of stability constants [1—3]. In all these methods, solutions containing ligand and cation in a stoichiometric ratio, but at different concentrations, are used. They permit large stability constants to be determined, but they have a very important limitation in that they do not usually give an accurate value when there are two complexes of a metal ion in equilibrium with the free or solvated metal ion.

When work is done with stoichiometric ratios, the problem mentioned above will arise, unless the equilibrium constant of one of these reactions is so high that the concentration of free metal ions is negligible. However, when an excess of ligand is used, it is easier to avoid the presence of free metal ions, and thus it should be possible to determine the stability constants for the other equilibria. Also, the new method proposed in this paper, when an excess of ligand is used, permits the stability constants of very weak complexes to be determined.

THEORY

For the equilibrium $mA + nB \rightleftharpoons A_mB_n$ (where $m, n \geqslant 1$), the stability constant is $K = [A_mB_n]/[A]^m[B]^n$. Let a and b be the initial concentrations

of A and B, respectively, and assume that there is a constant mole ratio $r = a/b \gg m/n$. Under these conditions, the degree of complexation α_c is

$$\alpha_c = [A_mB_n]/[A_mB_n]_{max} = [A_mB_n]n/b = E/E_{o(b)}$$

where E is the absorbance difference between complex and ligand and $E_{o(b)}$ is the absorbance for complete complexation at reactant concentration b, i.e., when $\alpha_c = 1$.

At equilibrium, the concentrations of the complex and reactants will be $[A_mB_n] = b\alpha_c/n$, $[B] = b(1 - \alpha_c)$ and $[A] = b(r - m\alpha_c/n)$. Substituting these expressions into the stability constant equation and simplifying gives

$$K = \alpha_c/[nb^{m+n-1}(r - m\alpha_c/n)^m (1 - \alpha_c)^n] \quad (1)$$

Replacing α_c by $E/E_{o(b)}$, rearranging and extracting the nth root gives

$$E^{1/n}/\left[b^{(m+n-1)/n}\left(r - \frac{m}{n}\frac{E}{E_{o(b)}}\right)^{m/n}\right] = (nKE_{o(b)})^{1/n}\left(1 - \frac{E}{E_{o(b)}}\right) \quad (2)$$

Provided that the Lambert–Beer law is obeyed, when an initial concentration b° is diluted by a factor β, the corresponding value of $E_{o(b^\circ)}$ is decreased by the same factor, i.e., $b = b^\circ/\beta$, and $E_{o(b)} = E_{o(b^\circ)}/\beta$. Substitution of b and $E_{o(b)}$ into eqn. (2) gives

$$Y = (\beta E)^{1/n}\Big/\left[(b^\circ/\beta)^{(m+n-1)/n}\left(r - \frac{m}{n}\frac{\beta E}{E_{o(b^\circ)}}\right)^{m/n}\right] = (nKE_{o(b^\circ)})^{1/n} \times \left(1 - \frac{\beta E}{E_{o(b^\circ)}}\right) \quad (3)$$

A plot of Y against βE gives a straight line.

When $b^\circ/\beta \to \infty$, $Y \to 0$ and $\beta E \to E_{o(b^\circ)}$. Thus, the intersection of the straight line with the abscissa provides the value of $E_{o(b^\circ)}$. The slope of the straight line is $(nK/E_{o(b^\circ)}^{n-1})^{1/n}$, which allows the calculation of the stability constant. In order to plot Y, the left-hand side of eqn. (3), against βE, it is necessary to make an approximation, since the unknown term $E_{o(b^\circ)}$ appears in the ordinate. This can be effected if $E_{o(b^\circ)}$ is considered as the greatest experimental value obtained for βE. This is acceptable when the work is done with a mole ratio $r > 10$.

The method proposed provides for the differentiation of mono- and polynuclear complexes. Suppose that the stoichiometry of a complex corresponds to $m/n = 1$. If a plot of $\beta E/(b^\circ/\beta)(r - \beta E/E_{o(b^\circ)})$ against βE gives a curve, then $(\beta E)^{1/2}/(b^\circ/\beta)^{3/2}(r - \beta E/E_{o(b^\circ)})$ can be plotted. If a straight line is obtained, it confirms that the complex is 2:2 and not 1:1. The fact that the straight line and the curve have the same limit, $E_{o(b^\circ)}$, aids in differentiating between the two complexes.

Accuracy and precision of the method

For plotting Y against βE, it is necessary to make an approximation, which affects the accuracy of the method. Generally, the bigger the mole ratio r, the greater the accuracy. However, for a particular value of the concentration b, the expression $dK/Kd\alpha_c$ gives the relative error in K with respect to the degree of complexation α_c. Equation (1) can be differentiated to give

$$dK/Kd\alpha_c = \{1 + \alpha_c[m^2/n(r - m\alpha_c/n) + n/(1 - \alpha_c)]\}/\alpha_c$$

By approximation to finite increments, the following expression is obtained

$$\Delta K/K = \{1 + \alpha_c[m^2/n(r - m\alpha_c/n) + n/(1 - \alpha_c)]\}\,\Delta\alpha_c/\alpha_c$$

The precision of the method depends on the values α_c and $\Delta\alpha_c$, the latter being the precision of the measurement of α_c. If a reasonable value for $\Delta\alpha_c$ such as ±0.01 is accepted, the relative errors can be calculated as a function of α_c. Data for a 1:1 complex and $r = 10$ are shown in Table 1. As can be seen, the precision of log K is within ±0.02 when the degree of complexation is 30—70%.

APPLICATIONS

When the degree of complexation is 95%, the precision in log K cannot be better than ±0.1, so this α_c value must be considered the highest for which the method is applicable.

From this value, eqn. (1) permits, for a given mole ratio and different stoichiometries, the calculation of the values of the expression

$$\log Kb^{m+n-1} = \log K(E_{o(b^\circ)}/\beta\epsilon)^{m+n-1}$$

where ϵ is the molar absorptivity of the complex.

$E_{o(b^\circ)}$ can be considered to have a value close to 1, and as $\beta = 1$ when the considered value for b is a maximum, the highest values of log K which can be determined by this method can be calculated. For $r = 10$, $\log(K/\epsilon^{m+n-1}) = 0.3$ for a 1:1 complex, 0.4 for a 2:2 complex, −0.5 for a 2:1 complex, and −1.3 for a 3:1 ligand:metal complex. Values of ϵ of 10^4 l mol^{-1} cm^{-1} are

TABLE 1

Precision of the method

α_c	$dK/Kd\alpha_c$	$\Delta K/K$	$\Delta \log K$	α_c	$dK/Kd\alpha_c$	$\Delta K/K$	$\Delta \log K$
0.05	21.2	0.212	±0.10	0.60	4.2	0.042	±0.02
0.10	11.2	0.112	±0.05	0.70	4.8	0.048	±0.02
0.20	6.3	0.063	±0.03	0.80	6.3	0.063	±0.03
0.30	4.8	0.048	±0.02	0.90	11.2	0.112	±0.05
0.40	4.2	0.042	±0.02	0.95	21.1	0.211	±0.10
0.50	4.1	0.041	±0.02				

usual for complexes with organic ligands, so values of log K up to 4.3, 12.4, 7.5 and 10.7, respectively, can be determined by the method.

Simultaneous formation of two complexes

Consider the simultaneous formation of two complexes

$$A + B \rightleftharpoons AB \text{ and } AB + A \rightleftharpoons A_2B$$

K_1 and K_2 are the successive stability constants of the complexes. If $K_1 \gg K_2$, and when $r = a/b$ is large, the formation of AB dominates the equilibria. Under such conditions it is possible to determine K_2 by using the method proposed in this paper, by considering this equilibrium as a reaction of 1:1 stoichiometry between AB and A. The necessary and sufficient conditions to carry this out are that AB and A_2B have different molar absorptivities at the wavelength used, and that K_1 must be sufficiently large so that the concentration of free metal ions is negligible. This condition can be considered as met when the degree of complexation is at least 98%.

Equation (1) permits the value of the degree of complexation to be calculated as a function of log Kb^{m+n-1}. Figure 1 shows the corresponding plot for a 1:1 complex at two values of r. When $\alpha_c \geqslant 0.98$ and $r = 10$, log $K_{1b} \geqslant 0.7$. Diluting to $b = 10^{-5}$ M gives log $K_1 \geqslant 5.7$. A final condition is that the molar absorptivity of AB must be known. Thus, if K_1 is sufficiently large

$$\alpha_c^{A_2B} = (E - E_{o(b)}^{AB})/(E_{o(b)}^{A_2B} - E_{o(b)}^{AB}) = E'/E'_{o(b)}$$

where E is the absorbance difference between a complex and the ligand.

The value of $E_{o(b)}^{AB} = E_{o(a)}^{AB}$ (when $a = b$), can be experimentally determined by operating with excess of metal ions, so that A_2B is not formed in appreciable quantity, and by having $\alpha_c^{AB} \geqslant 98\%$. In effect, taking into account that $a =$

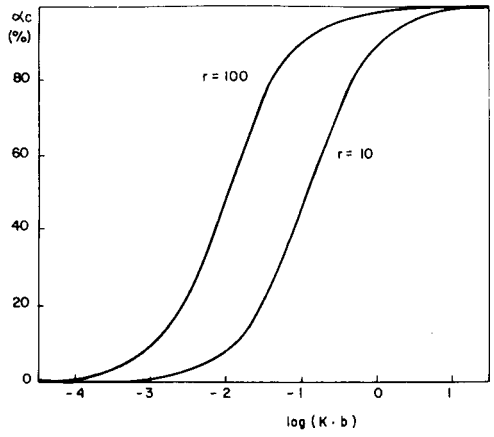

Fig. 1. Degree of complexation for a 1:1 complex as a function of log (Kb) for $r = 10$ and $r = 100$.

[A] + [AB] + 2[A_2B], equations for the degree of complexation of AB and A_2B can be obtained

$$\alpha_c^{AB} = [AB]/a = K_1[B]/(1 + K_1[B] + 2K_2[AB]) \quad (4)$$

$$\alpha_c^{A_2B} = 2[A_2B]/a = 2K_2[AB]/(1 + K_1[B] + 2K_2[AB]) \quad (5)$$

$[A_2B]$ is insignificant when $\alpha_c^{AB}/\alpha_c^{A_2B} \geqslant 100$, so for $r' = b/a = 11$, $K_1/K_2 \geqslant 20$. With this value, eqn. (4) permits $K_1[B]$ to be calculated when $\alpha_c^{AB} \geqslant 0.98$. Thus it can be calculated that $K_1[B] \geqslant 100$. For $a = 10^{-4}$ M, [B] = 10^{-3} M and $\log K_1 \geqslant 5.0$.

If the three conditions mentioned above are achieved, and $m = n = 1$, the general eqn. (3) can be written as

$$\beta E'/(b^\circ/\beta)\,(r - 1 - \beta E'/E'_{o(b^\circ)}) = K_2 E'_{o(b^\circ)}\,(1 - \beta E'/E'_{o(b^\circ)}) \quad (6)$$

However, when a mixture of monomeric and dimeric complexes is formed, this period is not applicable.

EXPERIMENTAL

Reagents and apparatus

All reagents were of analytical-reagent grade.

Monopotassium orotate solution (2.5×10^{-3} M) was prepared by dissolving 0.4855 g of the salt (Schuchardt) and diluting to 1 l with demineralized water. A 5.0×10^{-4} M copper(II) solution was prepared by diluting a 3.13×10^{-2} M solution standardized with 8-quinolinol. Samples were buffered with acetic acid/sodium acetate and ammonia/ammonium chloride solutions. Pseudopurpurin (1,2,4-trihydroxyanthraquinone-3-carboxylic acid) solution (2.5×10^{-4} M) was prepared by dissolving 0.0750 g of compound (Pfaltz and Bauer) and diluting to 1 l with ethanol. An aqueous 5.0×10^{-4} M palladium(II) solution was prepared by diluting a 1.11×10^{-2} M solution standardized with dimethylglyoxime.

A Beckman 25 spectrophotometer and Crison pH meter 74 were used.

Procedure

Mixtures of A and B at constant mole ratio $r = a/b > 5$ but of different concentrations, $b = b^\circ/\beta$, were prepared. Their absorbances, E, were measured against reference solutions prepared with the same ligand concentration, but no cation.

For a chosen b°, β is calculated for each concentration. The product βE is plotted as abscissa versus the corresponding ordinate calculated from the values βE, b°/β and r. As the dilution factor β is increased, the cell path-length l should be increased by a factor similar or proportional to β, in such a way that β/l is constant. In this way the absorbance measured gives the value of βE directly, so that α_c is measured more precisely and the precision of the method is improved.

RESULTS

Copper—orotic acid system

The study of the $E = f(\text{pH})$ curve and the application of Job's method showed that for pH values below 6.0 only one complex, of 1:1 stoichiometry, is formed, whereas at pH > 6.0, 1:1 and 2:1 ligand:cation complexes are produced. The 2:1 complex has its greatest stability at pH ⩾ 9.5.

Determination of log K_1 in acidic medium. The stability constant was determined at different pH values, a b° value of 10^{-4} M, and $r = a/b = 10$. The results obtained at pH 4.02 are shown in Table 2. The values of the ordinate for a 1:1 complex with respect to βE (at several pH values) are plotted in Fig. 2, producing straight lines which intersect the abscissa to give a value of 0.710 for $E_{o(b^\circ)}$ which leads to a molar absorptivity of 7.1×10^3 l mol^{-1} cm^{-1}. In the same figure, the corresponding values for a 2:2 complex have been plotted, giving a curve. This clearly indicates that the complex is 1:1 and not 2:2. By substitution of the values found for $E_{o(b^\circ)}$ and the slopes of the straight lines into the expression for the slope, the following values for log K_1 can be calculated: 3.06 (pH 3.27), 3.37 (pH 3.62), 3.80 (pH 4.02), 4.31 (pH 4.60).

Determination of log K_2 at pH 9.45. This constant was determined for $b^\circ = 10^{-4}$ M and $r = a/b = 10$. In Table 3 the results obtained for a 1:1 and a 2:1 complex are shown. In both cases, the corresponding plots are curves (Fig. 3). This fact indicates that there are two complexes in equilibrium in accordance with the data deduced by the application of Job's method.

The data obtained by application of eqn. (6) for a 1:1 reaction are shown in Table 4. The value of $E^{AB}_{o(b^\circ)}$ was not determined experimentally, as mentioned in the discussion of the simultaneous formation of two complexes; the value 0.710 determined in the study of this complex in acidic medium was used.

TABLE 2

Data for copper(II)—orotic acid at pH 4.02 for 1:1 and 2:2 complexes ($r = 10$, $b^\circ = 10 \times 10^{-5}$ M)

b°/β [Cu(II)] ($\times 10^{-5}$ M)	E (310 nm)	βE	Y_{AB}[a]	$Y_{A_2B_2}$[b]
2	0.077	0.385	2057	741×10^3
4	0.197	0.492	1340	302×10^3
6	0.330	0.550	1009	176×10^3
8	0.464	0.580	803	118×10^3
10	0.600	0.600	667	86×10^3

[a]For $m = n = 1$, $\beta E/[(b^\circ/\beta)(r - \beta E/E_{o(b^\circ)})]$. [b]For $m = n = 2$, $(\beta E)^{1/2}/[(b^\circ/\beta)^{3/2}(r - \beta E/E_{o(b^\circ)})]$.

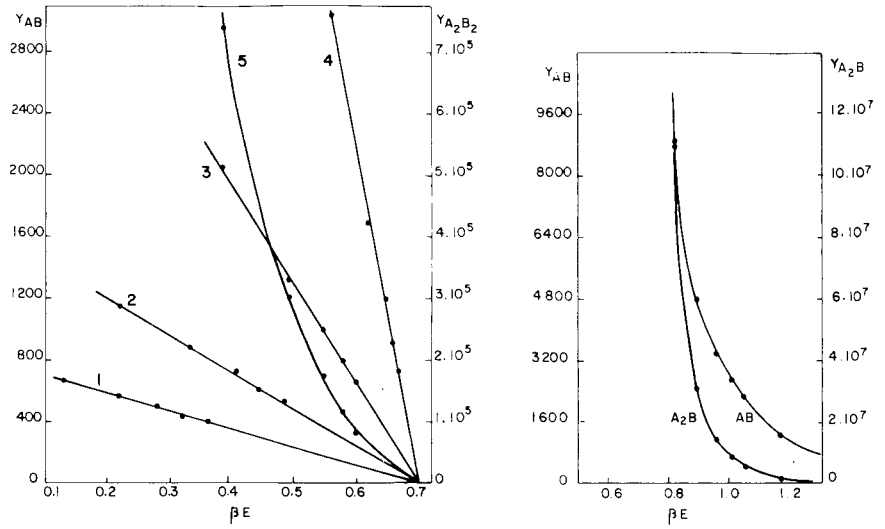

Fig. 2. Determination of log K_1 at several pH values for the copper(II)—orotic acid system. pH = (1) 3.27, (2) 3.62, (3) 4.02, (4) 4.60, (5) 4.02 (A_2 B_2).

Fig. 3. Plots at pH 9.45 for the copper(II)—orotic acid system obtained by application of eqn. (3) for 1:1 and 2:1 complexes.

TABLE 3

Data for copper(II)—orotic acid at pH 9.45 for 1:1 and 2:1 complexes by application of eqn. (3) (r = 10, b° = 10 × 10^{-5} M)

b°/β [Cu(II)] (× 10^{-5} M)	E (310 nm)	βE	Y_{AB}[a]	Y_{A_2B}[b]
1	0.082	0.820	8824	1112 × 10^5
2	0.180	0.900	4843	312 × 10^5
3	0.286	0.954	3465	152 × 10^5
4	0.402	1.004	2748	92 × 10^5
5	0.522	1.044	2294	62 × 10^5
10	1.160	1.160	1289	18 × 10^5

[a]See footnote (a), Table 2. [b]For m = 2, n = 1, $\beta E/[(b^\circ/\beta)^2 (r - 2\beta E/E_{o(b^\circ)})^2]$.

Figure 4 is a plot of the ordinate values against $\beta E'$, producing a straight line which intersects the abscissa to give a value of 0.720 for $E'_{o(b^\circ)}$. This value permits the molar absorptivity of the 2:1 complex to be calculated

$$\epsilon^{A_2B} = E^{A_2B}_{o(b^\circ)}/b^\circ = (E^{AB}_{o(b^\circ)} + E'_{o(b^\circ)})/b^\circ = (0.710 + 0.720)/10^{-4} =$$

14300 l mol^{-1} cm^{-1}

TABLE 4

Data obtained by application of eqn. (6) for copper(II)—orotic acid (pH = 9.45, r = 10, $b^\circ = 10 \times 10^{-5}$ M)

b°/β [Cu(II)] ($\times 10^{-5}$ M)	E (310 nm)	βE	$\beta E' = \beta E - E^{AB}_{o(b^\circ)}$	$\beta E'/\frac{b^\circ}{\beta}\left[(r-1) - \frac{\beta E'}{E'_{o(b^\circ)}}\right]$
1	0.082	0.820	0.110	1256
2	0.180	0.900	0.190	1070
3	0.286	0.954	0.244	962
4	0.402	1.004	0.294	880
5	0.522	1.044	0.334	808
10	1.160	1.160	0.450	562

By substitution of the value found for $E'_{o(b^\circ)}$ and the slope of the straight line into the expression for the slope, log K_2 can be calculated to be 3.30.

Palladium(II)—pseudopurpurin system

Román et al. [4] determined the stoichiometry of this complex in an ethanol—water medium by various procedures, finding the existence of only a 2:2 complex.

The stability constant was determined for $b^\circ = 2 \times 10^{-5}$ M and r = a/b = 5 (metal/ligand) in a 72% ethanol—water medium, 0.4 M in ethanolamine. The

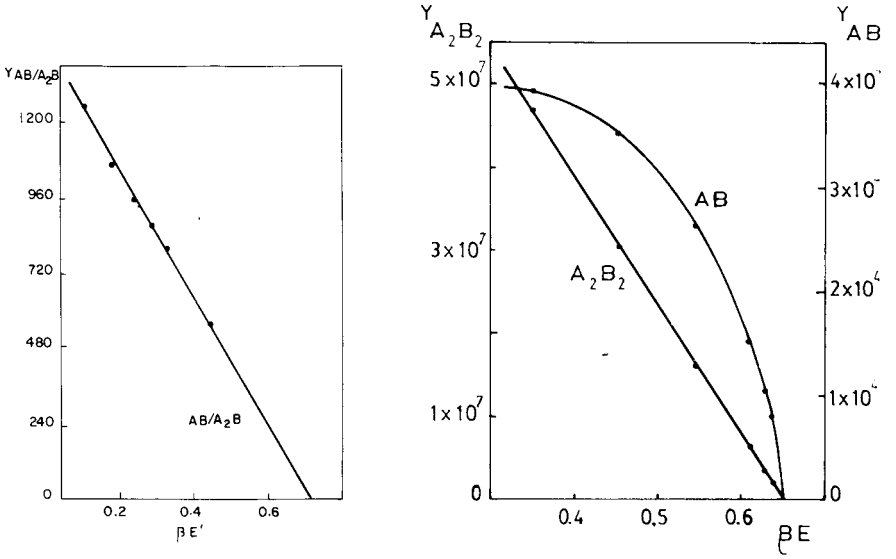

Fig. 4. Determination of log K_2 at pH 9.45 for the copper(II)—orotic acid system by application of eqn. (6).

Fig. 5. Determination of log K for the 2:2 palladium(II)—pseudopurpurin complex.

TABLE 5

Data for the palladium(II)—pseudopurpurin system for 1:1 and 2:2 complexes (r = 5, b° = 2 × 10^{-5} M)

b°/β [Pseudopurpurin] (M)	E (670 nm)	βE	Y^a	Y^b
2 × 10^{-6}	0.035	0.350	39.3 × 10^3	47.0 × 10^6
3 × 10^{-6}	0.068	0.455	35.3 × 10^3	30.3 × 10^6
5 × 10^{-6}	0.136	0.545	26.2 × 10^3	15.9 × 10^6
1 × 10^{-5}	0.306	0.612	15.1 × 10^3	6.1 × 10^6
1.5 × 10^{-5}	0.475	0.630	10.5 × 10^3	3.4 × 10^6
2 × 10^{-5}	0.640	0.640	8.0 × 10^3	2.2 × 10^6

[a]See footnote (a), Table 2. [b]See footnote (b), Table 2.

results obtained assuming 1:1 and 2:2 complexes are presented in Table 5. Figure 5 presents graphically the values of the ordinate in the βE function for 1:1 and 2:2 complexes, giving a curve and a straight line, respectively. This clearly indicates that the complex is 2:2 and not 1:1. The value found for $E_{o(b^\circ)}$ (0.650) and the slope of the straight line (15.54 × 10^7) gives $\log K$ = 15.89.

REFERENCES

1 K. S. Klausen, Anal. Chim. Acta, 44 (1969) 377.
2 B. W. Budesínský, J. Inorg. Nucl. Chem., 31 (1969) 1345.
3 D. V. González García, A. Arrebola Ramírez and M. Román Ceba, Talanta, 26 (1979) 215.
4 M. Román Ceba, A. Fernández Gutiérrez and A. Muñoz de la Peña, Third Annual Meeting of the Portuguese Chemical Society, Coimbra (1980), communication 11P18.

Analytica Chimica Acta, 124 (1981) 211—213

Short Communication

THE DETERMINATION OF TUNGSTEN BY ELECTRON PARAMAGNETIC RESONANCE SPECTROMETRY

M. V. KRISHNAMURTHY

Radiochemistry Division, Bhabha Atomic Research Centre, Trombay, Bombay 400085 (India)

(Received 28th July 1980)

Summary. Electron paramagnetic resonance is used to determine tungsten in the range 5—400 $\mu g\ ml^{-1}$. Tungstate is reduced to tungsten(V) in the presence of thiocyanate in acidic medium and detected as the tungsten(V)—thiocyanate complex in amyl acetate after extraction. Molybdenum does not interfere; vanadium (>5 mg) interferes. The relative standard deviation for mid-range concentrations is about 3%.

The determination of tungsten is of great interest in the analytical chemistry of refractory materials. Tungsten forms a paramagnetic tungsten(V) complex with thiocyanate ions in acidic medium under reducing conditions [1—3] and this complex can be detected by the electron paramagnetic resonance technique. Interferences are few with this technique.

Experimental

Reagents. Sodium tungstate dihydrate (analytical reagent, BDH) was used as the standard substance; 0.4049 g, 0.3423 g and 0.1591 g of sodium tungstate were dissolved in 0.5% NaOH solution in 100-ml standard flasks to prepare three independent standard solutions. Working solutions were prepared daily by suitable dilution. Amyl acetate (A.R. grade) was equilibrated with the tin(II) chloride solution (see below) for use as the organic extractant. Freshly prepared solutions and analytical-reagent grade chemicals were used throughout.

Procedure. The initial steps are similar to the procedure for the spectrophotometric determination of tungsten [2, 3]. The aliquot of tungsten solution (0.5—2 ml) is mixed with 2 ml of 50% (w/v) potassium thiocyanate solution and 5 ml of 7% (w/v) tin(II) chloride solution in concentrated hydrochloric acid and shaken thoroughly. The solution is then diluted to 12 ml with tin(II) chloride solution. The reduction to tungsten(V) is complete after 50 min. The solution is extracted twice with 5-ml portions of amyl acetate for 2 min each time in a separating funnel. The coloured extracts are combined in a 10-ml standard flask and the solution is diluted to the mark.

The Varian V-4502 x-band e.p.r. spectrometer used was fitted with a V-4533 multipurpose cavity employing 100 kHz modulation and detection. The tungsten extract was transferred to a Varian quartz sample tube (3 mm i.d.) and cooled to liquid nitrogen temperature. Spectral recordings were obtained by using a Varian quartz insert liquid nitrogen Dewar; 100 kHz modulation was set at "1000" on the field modulation unit for all the samples studied and the 100 kHz amplifier gain was adjusted as required. Calibration of the amplifier gain was done as recommended by the manufacturer. The microwave power was kept constant at about 50 mW. There was no power saturation effects. A set of seven spectral recordings were taken for each sample in duplicate to calculate the average value of the spectral derivative amplitude. The concentration range of tungsten studied was 0.5—400 μg ml^{-1}.

Results and discussion

Tungsten(V) has the $5d^1$ outer electron configuration. The tungsten complex formed with thiocyanate is not definitely known but is assumed to be $WO(SCN)_5^{2-}$, similar to the halide complexes WOX_5^{2-} found in acidic media [4]. Tungsten is hexacoordinated with axial distortion. The e.p.r. spectrum obtained for the tungsten complex in amyl acetate medium at the liquid nitrogen temperature is shown in Fig. 1. The observed spectrum is a singlet arising from the $\frac{1}{2} \rightleftharpoons -\frac{1}{2}$ transition, and consists of two overlapping components caused by g-anisotropy. The hyperfine structure of ^{183}W ($I = \frac{1}{2}$) with an isotopic abundance of 14.48% is also observed. The line width of the low field component is ca. 22 gauss. The e.p.r. parameters were found to be $g_{\|} = 1.795 \pm 0.005$, $g_{\perp} = 1.820 \pm 0.005$ and $A_{\|} = 150 \pm 5$ gauss which agree with the values reported for several known tungsten(V) complexes [5].

The e.p.r. spectral intensity is proportional to the observed derivative amplitude. The average signal derivative amplitude obtained for the low field component was plotted against concentration of tungsten for the ranges 5—50 μg ml^{-1} and 10—400 μg ml^{-1} (Fig. 2), and linear graphs were obtained. The relative standard deviation of measurements about midrange in the lower concentration range was about 3%, but less in the higher concentration range because of the increase in signal to noise ratio. The lower limit of detection was 0.1 μg ml^{-1}.

The interfering effects from other metal ion impurities were studied to ascertain their influence on the conversion to tungsten(V) and on the e.p.r. spectral observation. Diamagnetic impurities have no influence on the e.p.r. spectra. There was no interference from monovalent ions like Na^+, K^+, Rb^+, Ag^+, NH_4^+; divalent ions like Mg^{2+}, Ca^{2+}, Sr^{2+}, Ba^{2+}, Zn^{2+}, Cd^{2+}, Pb^{2+}, Sn^{2+}; trivalent ions like Al^{3+}, La^{3+}; tetravalent ions like Zr^{4+}, Sn^{4+}, Ce^{4+}, Th^{4+}; or uranyl ions up to levels of 100 mg. Paramagnetic metal ions like Ti^{3+}, Cr^{3+}, Fe^{3+}, Cu^{2+}, Fe^{2+}, Mn^{2+}, Ni^{2+}, Co^{2+}, Ce^{3+}, Sm^{3+}, Eu^{3+}, Gd^{3+} did not interfere at the 10 mg level. Molybdenum did not interfere as the molybdenum(V) complex formed [5] has a g-value of 1.94 which is very different from that of the tungsten(V) complex. Vanadium(IV) is coextracted from

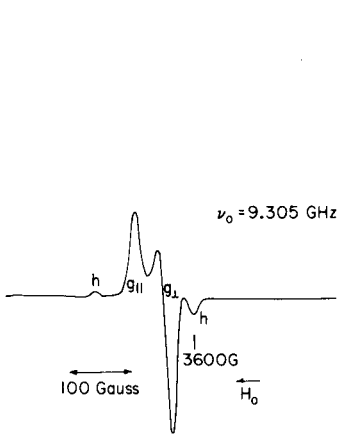

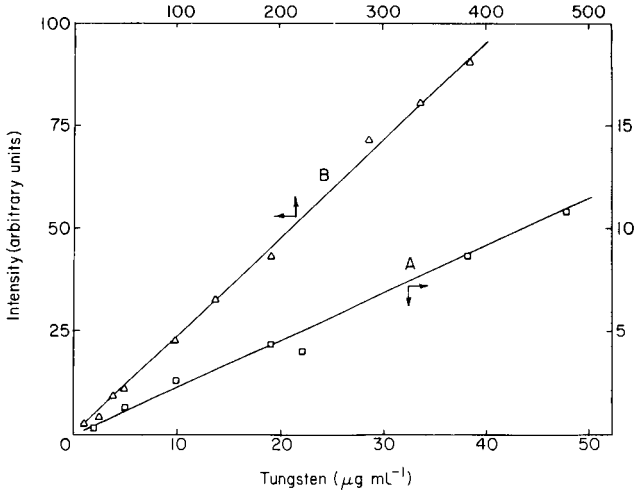

Fig. 1. E.p.r. spectrum of the tungsten(V)—thiocyanate complex in amyl acetate at the liquid nitrogen temperature. $g_{\parallel}$ and $g_{\perp}$ refer to the parallel and perpendicular components in the spectrum. The low intensity lines marked 'h' are the hyperfine lines (parallel components) from the ^{183}W isotope.

Fig. 2. Calibration plots of e.p.r. signal intensity (derivative amplitude) vs. concentration of tungsten for the concentration ranges 5—50 μg ml^{-1} (A) and 10—400 μg ml^{-1} (B).

thiocyanate medium and gives rise to an e.p.r. spectrum with a g-value of 1.964 and extensive hyperfine structure [5] (I = 7/2 for ^{51}V). The extreme hyperfine lines interfere with the tungsten(V) spectrum when vanadium is present at a level greater than 5 mg. It has been observed [1, 2] that the acidity of the medium should be $\geqslant$8 M to prevent the formation of other reduced species like W(III) or W(IV), and in the present studies the acidity was maintained at about 8 M. Several chemical procedures have been developed to bring tungsten impurities occurring in a variety of materials into solution [6]; these procedures can be advantageously used in the determination of tungsten by the proposed method.

The author is greatly indebted to Dr. M. V. Ramaniah, Director, Radiological Group, and Dr. P. R. Natarajan, Head, Radiochemistry Division, for their encouragement, and to Dr. B. D. Joshi for his kind cooperation.

REFERENCES

1 H. Freund, M. L. Wright and R. K. Brookshier, Anal. Chem., 23 (1951) 781.
2 C. E. Crouthmel and C. E. Johnson, Anal. Chem., 26 (1954) 1284.
3 E. B. Sandell, Colorimetric Determination of Traces of Metals, Interscience, New York, 1959, pp. 886—889.
4 H. E. Kon and N. E. Sharpless, J. Phys. Chem., 70 (1966) 105.
5 B. A. Goodman and J. P. Raynor, in H. J. Emeleus and A. G. Sharpe (Eds.), Advances in Inorganic Chemistry and Radiochemistry, Vol. 13, Academic Press, New York, 1970, pp. 236, 237, 252—254.
6 W. T. Elwell and D. F. Wood, Analytical Chemistry of Molybdenum and Tungsten, Pergamon, Oxford, 1971, pp. 103—115.

Analytica Chimica Acta, 124 (1981) 215—219

Short Communication

SPECTROPHOTOMETRIC DETERMINATION OF CITRIC ACID BY AN ENZYMATIC METHOD WITH 2-(4-IODOPHENYL)-3-(4-NITROPHENYL)-5-PHENYL-2H-TETRAZOLINIUM CHLORIDE

STEFANO GIROTTI, ROLANDO BUDINI*, ENRICO GATTAVECCHIA and DOMENICA TONELLI

Chemical Institute "G. Ciamician", University of Bologna, Bologna (Italy)

(Received 15th August 1980)

Summary. The procedure is based on the method of Möllering and Gruber in which the decrease in NADH absorbance caused by dehydrogenase reactions is monitored. Final reaction with the tetrazolium reagent improves the sensitivity to give a useful range of 2—100 μM citrate. Most naturally occurring carboxylic acids and phenolic substances do not interfere. The method is applicable to vegetable tissue after a simple extraction with poly(vinylpyrrolidone).

Many methods are available for determining DL-citric acid. Since chemical methods [1—4] have poor selectivity, a preliminary separation is necessary when mixtures of acids are to be analysed. That is generally done by chromatographic techniques which either require considerable time or lack the desired accuracy and precision [5—7]. As far as good selectivity and rapidity are concerned, enzymatic methods appear to give the best results [8, 9]. However, if biological samples such as vegetable tissue are analyzed, problems may arise because of interferences from other compounds (e.g., polyphenols) occurring in relatively high concentrations. In this communication, a simple and rigorous method for determining citric acid is described and its applicability to vegetable samples is verified. It is a modification of the enzymatic spectrophotometric method of Möllering and Gruber [10], whose original method is based on the measurement of a decrease in NADH absorbance caused by dehydrogenase reactions. In the modified procedure, a redox reaction in which 2-(4-iodophenyl)-3-(4-nitrophenyl)-5-phenyl-2H-tetrazolium chloride (INT) is reduced by NADH to a red formazan [11] is coupled to the reaction sequence. The overall reaction scheme is

$$\text{DL-Citrate} \xrightleftharpoons{\text{citrate lyase}} \text{oxaloacetate} + \text{acetate}$$

$$\left\{\begin{array}{l}\text{Oxaloacetate} + \text{NADH} + \text{H}^+ \xrightleftharpoons{\text{L-malate dehydrogenase}} \text{L-malate} + \text{NAD}^+ \\ \text{Pyruvate} + \text{NADH} + \text{H}^+ \xrightleftharpoons{\text{L-lactate dehydrogenase}} \text{L-lactate} + \text{NAD}^+\end{array}\right.$$

$$\text{NADH} + \text{H}^+ + \text{INT} \xrightleftharpoons{\text{diaphorase}} \text{NAD}^+ + \text{formazan}$$

Pyruvate can be formed from oxaloacetate if oxaloacetate decarboxylase is present in the sample.

The absorbance at 492 nm, the wavelength of maximum absorption of the formazan, is proportional to the original DL-citrate concentration. The proposed method has the advantage of having good sensitivity and a short analysis time (10—25 min).

Experimental

Apparatus. Measurements were made on a Perkin-Elmer 124 double beam spectrophotometer equipped with a Lauda K 4 R thermostat. Samples were taken with Oxford pipettes.

Reagents. All the chemicals were of analytical grade and used as received. The enzymes citrate oxaloacetate—lyase (CL; EC 4.1.3.6; specific activity 8 IU mg^{-1}), L-malate—NAD oxidoreductase (MDH; EC 1.1.1.37; specific activity 1200 IU mg^{-1}), L-lactate—NAD oxidoreductase (LDH; EC 1.1.1.27; specific activity 550 IU mg^{-1}), NADH—lipoamide oxidoreductase (diaphorase; EC 1.6.4.3; specific activity 80 IU mg^{-1}), and the Test Combination-Foodstuff-UV kit (were all from Boehringer, Mannheim). All solutions were prepared with twice-distilled water. Glycylglycine buffer solutions (0.5 M) containing zinc chloride (5 mM), NADH (0.23 mM), and Triton X-100 (2%, v/v) at different pH values were obtained by adding 5 M sodium hydroxide to the stock buffer solution. Citrate working standard solutions were prepared by diluting the stock solution (2.5 mM) with water immediately before use. The following reagents were prepared for the assay of citric acid with INT: CL (6.5 mg ml^{-1}); a mixture containing MDH (0.5 mg ml^{-1}), LDH (2.5 mg ml^{-1}) and ammonium sulphate (3.2 M); a mixture containing diaphorase (1 mg ml^{-1}), INT (0.6 mM) and sucrose (5 mM).

Procedure. Pipette into cuvettes 1.5 ml of buffer solution (pH 7.8), 0.2 ml of sample (citrate standard solution or vegetable extract), 0.02 ml of MDH and LDH solution and 0.05 ml of CL solution. Mix thoroughly, and measure the absorbance at 492 nm in a 1-cm cell (zero absorbance) against a blank consisting of buffer solution, at 25 ± 0.05°C. Add 1.0 ml of diaphorase—INT solution and, after stirring, record the change in absorbance with time. Measure the true absorbance change by the end-point method [12]. Determine the absorbance of a blank of identical composition in which water replaces an equal volume of CL solution. Subtract the former absorbance from the latter, the differences in absorbance being proportional to the DL-citric acid concentration.

The light-sensitivity of INT must be taken into account both in storage of solution and in the determination. Direct sunlight must be avoided at all times and a calibration curve must be obtained for each new set of reagents.

Results

Effect of reaction variables. Glycylglycine buffer proved to give the best results in the determination of citric acid with diaphorase and INT. Phosphate buffer was rejected owing to its ability to precipitate zinc ions which are well-known activators of citrate lyase [10]. Triethanolamine was discarded

TABLE 1

Absorbance (at 492 nm) and reaction time as a function of the temperature for 4.3×10^{-5} M citrate solutions

Temp. (°C)	Absorbance	S.d. (n)[a]	Time (min)	Temp. (°C)	Absorbance	S.d. (n)[a]	Time (min)
10	0.612	0.025 (10)	25	30	0.592	0.021 (10)	10
20	0.600	0.020 (10)	18	40	0.584	0.027 (10)	5

[a]Standard deviation from mean (evaluated from n observations).

in view of the application to vegetable samples, as triethanolamine might react with phenols which are widely distributed in plant tissues. The effect of pH was studied over the range 7—10. Optimal activity of the whole enzymatic system was obtained at pH 7.8; this pH was used in all further determinations.

Under the above conditions the effect of temperature on the chromogen formation was studied. The results are reported in Table 1. Because there is little variation in absorbance at reaction temperatures between 10 and 40°C, a deviation of 1—5°C would not cause a significant change in absorbance thus the reaction can be also carried out at room temperature without thermostatting the cell compartment.

Analytical results. Standard solutions of citric acid (2—100 μM) were assayed under the recommended conditions. The calibration graph was calculated by the method of least squares. The correlation coefficient for 10 different samples was 0.9999 and the linear equation was: Absorbance = 0.0138 [citric acid (μM)] + 0.0007.

Discussion

The proposed method is about four times as sensitive as that of Möllering and Gruber [10]. When standard solutions were analysed by the U.V. Test (Boehringer) based on the Möllering and Gruber method, the resulting linear equation is: Absorbance = 0.0031 [citric acid (μM)] + 0.0001, and the correlation coefficient is 0.9980. The sensitivity is improved because the formazan formed has a higher molar absorptivity than NADH [11]. The two methods have about the same accuracy and precision. With 3.7×10^{-5} M solutions of citric acid, the standard deviation (and coefficient of variation) resulting from the application of the present method and U.V. method based on 10 measurements each were 0.29 (4.1%) and 0.31 (4.4%), respectively.

DL-Citric acid was also determined with the present method in the presence of other biologically important acids. As can be seen from the data of Table 2, the present method retains good selectivity and precision in these conditions. Oxaloacetic, pyruvic and glycolic acids show only a little interference. Perhaps the former two acids interfere because they are involved in the first two steps of the assay, the latter because it is an inhibitor of LDH [13].

TABLE 2

Determination of citric acid in the presence of other compounds

Composition of solution[a]	Citric acid recovered (mg l^{-1})	Recovery (%)	S.d. (n)[b]	Composition of solution[a]	Citric acid recovered (mg l^{-1})	Recovery (%)	S.d. (n)[b]
1) Citric acid	96.7	99.7	2.2 (10)	1) + glycolic acid[c]	92.0	94.8	3.7 (1
1) + L-malic acid	96.1	99.1	3.0 (10)	1) + L-glutamic acid	97.2	100.2	2.8 (1
1) + pyruvic acid[c]	92.5	95.4	4.2 (11)	1) Maleic acid	96.3	99.3	1.3 (1
				1) + oxaloacetic acid	92.7	95.6	4.9 (1
1) + L(+)lactic acid	99.6	102.7	2.5 (10)	1) + catechol	94.9	97.8	1.8 (1
1) + fumaric acid	98.7	101.8	1.8 (10)	1) + resorcinol	98.6	101.7	2.4 (1
1) + oxalic acid	95.2	98.2	1.5 (10)	1) + hydroquinone	97.8	100.8	3.0 (1
1) + D-tartaric acid	95.6	98.6	2.1 (10)	1) + (+)pyrocatechol	97.6	100.6	2.7 (1
1) + acetic acid	97.8	100.8	3.4 (10)	1) + pyrogallol	88.8	91.6	3.8 (1
1) + DL-succinic acid	94.7	97.6	1.3 (10)	1) + caffeic acid	92.8	95.7	1.5 (1

[a]Each solution contained 97.0 mg l^{-1} citric acid; the second component was added at the 100 mg l^{-1} level unless otherwise specified. [b]Standard deviation from mean (evaluated from n observations). [c]50 mg l^{-1} added.

When citric acid is determined by the UV Test, which is based on the first three steps of the reaction sequence, the same interferences occur, supporting the view that these acids interact with MDH and LDH. Their interference is appreciable only if they are present in large amounts. Therefore their effect is negligible if the assay is performed on vegetable tissues in which these acids are present at low concentrations [14].

The assay of citric acid was also carried out in the presence of some phenolic compounds, which might be expected to interfere in the analysis of vegetable samples. From Table 2 it appears that the recovery of citric acid was quite satisfactory in the presence of every phenol tested, except for caffeic acid and pyrogallol. Perhaps, that is due to interaction with MDH [15]. To avoid this interference, poly(vinylpyrrolidone) can be used during the extraction of citrate from organic tissues, because of its high blocking capacity for polyphenolic substances [16]. The applicability of the assay to biological substrates was investigated on ripe strawberries (cv. Gorella). The extraction was done as described previously [17] using insoluble poly-(vinylpyrrolidone). When citrate was determined by the UV Test, the mean value was 7.1 mg g^{-1} (fresh weight) of strawberries. This result is in good agreement with the data in Table 3 obtained by the present method. The present assay for citrate is highly selective, sensitive, accurate and precise, and may be applied to the determination of citrate in samples such as vegetable tissue, without the need for accurate chromatographic separations.

TABLE 3

Determination of citric acid in strawberries (cv. Gorella)

Citrate added (mg g^{-1})	Citrate recovered (mg g^{-1})	Recovery (%)	S.d. (n)[a]
0	7.35	100.0	0.2 (8)
5.10	12.25	98.4	0.3 (8)
10.04	17.10	98.8	0.2 (8)

[a]Standard deviation from mean (evaluated from n observations).

REFERENCES

1 J. W. Munson and R. Bilous, J. Pharm. Sci., 66 (1977) 1403.
2 J. Morot-Gaudry, M. Z. Nicol and E. Jolivet, J. Chromatogr., 87 (1973) 425.
3 M. Y. Kamel and Z. A. El-Awamry, Microchem. J., 23 (1978) 445.
4 D. R. Nelson and R. W. Rinne, Plant Cell Physiol., 18 (1977) 393.
5 M. Bourzeix, J. Guitraud and F. Champagnol, J. Chromatogr., 50 (1970) 83.
6 A. Sasson and S. P. Monselise, J. Am. Soc. Hort. Sci., 102 (1977) 331.
7 V. T. Turkelson and M. Richards, Anal. Chem., 50 (1978) 1420.
8 J. V. Passonneau and J. G. Brown, in H. U. Bergmeyer (Ed.), Methods of Enzymatic Analysis, Vol. 3, Academic Press, London, 1974, p. 1565.
9 G. G. Guilbault, S. H. Sadar and R. McQueen, Anal. Chim. Acta, 45 (1969) 1.
10 H. Möllering and W. Gruber, Anal. Biochem., 17 (1966) 369.
11 H. Möllering, A. W. Wahlefeld and G. Michal, in H. U. Bergmeyer (Ed.), Methods of Enzymatic Analysis, Vol. 1, Academic Press, London, 1974, p. 136.
12 H. U. Bergmeyer, in H. U. Bergmeyer (Ed.), Methods of Enzymatic Analysis, Vol. 1, Academic Press, London, 1974, p. 102 and 308.
13 G. W. Schwert and A. D. Winer, in P. D. Boyer, H. A. Lardy and K. Myrback (Eds.), The Enzymes, Vol. 7, Academic Press, London, 1963, p. 127.
14 A. C. Hulme, in A. C. Hulme (Ed.), The Biochemistry of Fruits and Their Products, Vol. 1, Academic Press, London, 1970, p. 171.
15 R. T. Wedding, C. Hansch and T. R. Fukuto, Arch. Biochem. Biophys., 121 (1967) 9.
16 J. C. Gray, Phytochem., 17 (1978) 495.
17 S. Girotti, R. Budini, D. Tonelli and P. Paganelli, Ann. Chim., 3 (1980) 247.

Analytica Chimica Acta, 124 (1981) 221—224

Short Communication

THE FLUORESCENCE PROPERTIES OF *o*-PHTHALALDEHYDE DERIVATIVES OF IODINATED AMINO ACIDS

J. N. MILLER* and H. THAKRAR

Department of Chemistry, Loughborough University of Technology, Loughborough, Leicestershire LE11 3TU (Gt. Britain)

(Received 14th October 1980)

Summary. The preparation and fluorescence properties of *o*-phthalaldehyde (OPT) derivatives of several iodoamino acids have been studied and compared with those of glycine and tyrosine. Incorporation of successive iodine atoms in the tyrosine and thyronine structures produces increasing quenching of the fluorescence of the OPT derivatives, presumably by the internal heavy atom effect, without significant changes in the spectral distribution. Addition of anti-thyroxine (T4) antiserum to OPT-labelled T4 has no effect on its fluorescence properties.

The determination of iodinated amino acids (tyrosine and thyronine derivatives) is of great importance because of the use of these compounds as indicators of thyroid function in clinical chemistry. Determinations of thyroxine (3,3′,5,5′-tetraiodothyronine, T4) and 3,3′,5-triiodothyronine (T3) are particularly frequently required in blood serum at ng ml^{-1} and lower levels. The need for analytical methods combining sensitivity and specificity has restricted the number of useful techniques: in practice either high-performance liquid chromatography (h.p.l.c.) or competitive binding immunoassays have been used almost exclusively. Fluorescent derivatives of the analyte molecules are of value in conjunction with both these techniques. Thus fluorescence immunoassays for T4 [1, 2] and T3 [3] have been described, using fluorescein [1] and fluorescamine [2, 3] as the fluorescent labels. Iodoamino acids have also been determined by h.p.l.c. [4, 5] though apparently not with the aid of fluorimetric detection.

Smith [1] found that a fluorescein derivative of thyroxine was markedly less fluorescent than other fluorescein—amino acid conjugates; the fluorescence of fluorescein—T4 was, however, enhanced on binding to anti-T4 antibodies. It was suggested that the iodine atoms of T4 quenched the fluorescence of the fluorescein conjugate via the heavy-atom effect, the effect being in some way reduced or abolished in the presence of specific antibody. Handley et al. [2] found that the much more readily prepared fluorescamine [6] derivatives of T4 and T3 also showed enhanced fluorescence on binding to appropriate antibodies. Initially it was assumed [2] that a similar mechanism was responsible, but later work [3, 7], showed that the quantum yields

of fluorescamine derivatives of iodoamino acids were similar to those of derivatives containing no iodine atoms, and it is now believed that a different mechanism, involving the disruption of exciplexes, is operating [8].

In the light of these results it was apparent that the fluorescence properties of the *o*-phthalaldehyde (OPT) derivatives of iodinated amino acids would be of great interest. This reagent forms highly fluorescent derivatives with primary amines and amino acids in the presence of thiols [9]: the structures of the products have recently been elucidated [10]. OPT has been used in the determination of non-iodinated amino acids by h.p.l.c.—fluorimetry [11, 12] and the properties of OPT derivatives of such amino acids have been studied [13]. It is claimed that the chemical yields in OPT— amino acid reactions are higher than those of fluorescamine—amino acid reactions, and that the OPT products offer up to ten times more fluorimetric sensitivity. Many authors reported that OPT derivatives are relatively unstable, although careful choice of thiol compound and solvent can minimise this problem [13—15].

Experimental

Corrected excitation and fluorescence spectra were obtained at room temperature using a Perkin-Elmer MPF-44B spectrofluorimeter fitted with a DCSU-2 correction accessory. For quantitative studies, the wavelengths were 339 and 454 nm and the spectral bandwidths were 8 nm and 12 nm in the excitation and emission monochromators, respectively. Quantum yields were determined by the comparative method, with the OPT derivative of glycine as standard ($\phi_f = 0.39$ [13]).

o-Phthaldialdehyde (Pierce Chemical Co., Rockford, IL), ethanethiol and 2-mercaptoethanol (BDH Ltd., Poole, Dorset), and proteins and L-isomers of amino acids (Sigma Chemical Co. and Calbiochem-Behring) were used as received. Antisera were from RIA (UK) Ltd. (Sunderland). Other chemicals were of analytical reagent grade; water was triply distilled from silica and passed through a 0.2-μm filter (Amicon, High Wycombe).

Stock solutions (1 mM) of amino acids were prepared in nitrogen-purged 0.1 M borate buffer, pH 10, and stored at 4°C. OPT/ethanethiol and OPT/2-mercaptoethanol solutions were made up afresh whenever possible, but could be stored for short periods in the dark at 0°C: they contained 1 mM OPT and 2 mM thiol in borate buffer. Amino acids were labelled by a modification of the procedure of Butcher and Lowry [16]. Equal volumes (100 μl) of amino acid stock solution and OPT/thiol reagent were mixed, allowed to react for 2 min at room temperature in the dark, and then diluted to 5 ml with 0.5 M NaOH.

Results and discussion

The reaction of the amino acids with OPT was rapid, the fluorescence rising to a maximum intensity after ca. 120 s and decreasing slowly thereafter. As previously reported [15], ethanethiol yielded more stable derivatives

TABLE 1

Fluorescence quantum yields of OPT derivatives with ethanethiol as the thiol reagent

Compound	ϕ_f	Compound	ϕ_f
Glycine	0.39[a]	3,5-Diiodothyronine	0.030 ± 0.002 (3)
Tyrosine	0.340 ± 0.015 (3)	3,5,3'-Triiodothyronine (T3)	0.023 ± 0.002 (3)
Thyronine	0.23 (1)	3,3',5'-Triiodothyronine	0.020 ± 0.001 (3)
3-Iodotyrosine	0.060 ± 0.005 (3)	(reverse T3)	
3,5-Diiodotyrosine	0.050 ± 0.002 (3)	Thyroxine (T4)	0.014 ± 0.001 (3)

[a]Reference value. Figures in parentheses indicate the number of determinations.

than 2-mercaptoethanol, and stability and fluorescence background problems were minimised by treating the reaction mixtures with alkali. While the excitation and fluorescence spectra of all the OPT derivatives were very similar, their fluorescence intensities varied substantially. The quantum yield values in Table 1 show clearly that iodine atoms strongly quench the fluorescence. A single iodine atom exerts a major quenching effect, with further iodine atoms producing additional, though smaller, reductions in quantum yield. This behaviour is in complete contrast to that of fluorescamine derivatives of the iodoamino acids, in which the quenching effect of the iodine atoms is small [7]. OPT derivatives will thus be less suitable than fluorescence derivatives in combined h.p.l.c.—fluorimetric analyses. It is also noticeable that the hydroxylated aromatic ring in thyroxine exerts a separate quenching effect: OPT—thyronine has a lower quantum yield than OPT—tyrosine, and 3,5-diiodothyronine shows a similar reduction in ϕ_f compared with 3,5-diiodotyrosine. The effects of the hydroxylated ring and its substituents on the quantum yields of the OPT derivatives are indeed at least as great as those of the tyrosine ring: thus OPT—"reverse T3" and OPT—T3 have similar quantum yields which are lower than that of OPT—diiodothyronine. Model-building studies (Orbit molecular models) show that OPT—thyronines may adopt conformations in which the hydroxylated aromatic ring is close to the isoindole moiety of the fluorescent group: such conformations would permit π-electron interactions that might be responsible for the observed effects of the ring. Indirect evidence for the short-range nature of the iodine (heavy atom) quenching effect was revealed by a comparison of the OPT derivatives of the proteins human serum albumin and porcine thyroglobulin. These derivatives showed similar fluorescence intensities, even though thyroglobulin contains > 1% by weight of iodine: the iodine atoms are presumably not close to the amino groups at which OPT derivatives are formed.

OPT—T3 did not show any significant enhancement of fluorescence on mixing with anti-T3 antiserum at pH 9. Fluorescence enhancement immunoassays of the types developed with fluorescein and fluorescamine as labels would thus not be feasible for OPT derivatives of iodinated amino acids.

We thank the Medical Research Council for a grant to purchase the spectrofluorimeter; H. T. is in receipt of a Science Research Council Studentship.

REFERENCES

1 D. S. Smith, FEBS Lett., 77 (1977) 25.
2 G. Handley, J. N. Miller and J. W. Bridges, Proc. Chem. Soc. Anal. Div., 16 (1979) 26.
3 G. Handley, Ph.D. Dissertation, Loughborough University, 1979.
4 M. T. W. Hearn, W. S. Hancock and C. A. Bishop, J. Chromatogr., 157 (1978) 337.
5 N. M. Alexander and M. Nishimoto, Clin. Chem., 26 (1979) 1063, Abstract no. 002.
6 M. Weigele, S. L. De Bernardo, J. P. Tengi and W. Leimgruber, J. Am. Chem. Soc., 94 (1972) 5927.
7 F. Reiterer, F. Nachtmann, G. Knapp and H. Spitzy, Mikrochim. Acta (I) (1978) 115.
8 J. N. Miller, G. Handley, C. S. Lim and J. W. Bridges, submitted.
9 M. Roth, Anal. Chem., 43 (1971) 880.
10 S. S. Simons, Jr. and D. F. Johnson, J. Org. Chem., 43 (1978) 2886.
11 D. W. Hill, F. H. Walters, T. D. Wilson and J. D. Stuart, Anal. Chem., 51 (1979) 1338.
12 P. Lindroth and K. Mopper, Anal. Chem., 51 (1979) 1667.
13 R. F. Chen, C. Scott and E. Trepman, Biochim. Biophys. Acta, 576 (1979) 440.
14 S. S. Simons, Jr. and D. F. Johnson, Anal. Biochem., 90 (1978) 705.
15 S. S. Simons, Jr. and D. F. Johnson, Anal. Biochem., 82 (1977) 250.
16 E. C. Butcher and O. H. Lowry, Anal. Biochem., 76 (1976) 502.

Analytica Chimica Acta, 124 (1981) 225—227

Short Communication

APPLICATION OF A SIMPLE PRECONCENTRATION SCHEME TO THE DETERMINATION OF ISOPROPYLMETHYLPHOSPHONOFLUORIDATE AT TRACE LEVELS IN WATER

WILLIAM K. FOWLER*, JOSIAH E. SMITH and HERBERT C. MILLER

Southern Research Institute, 2000 Ninth Avenue South, Birmingham, AL 35255 (U.S.A.)

(Received 23rd July 1980)

Summary. The procedure for the preconcentration and determination of isopropylmethylphosphonofluoridate (Sarin) involves extraction of the sample with chloroform, preconcentration of the vaporized extract on a Porapak Q plug, and direct thermal desorption of the adsorbed material into a gas chromatograph. Precise determinations at concentrations down to approximately 67 pg ml^{-1} are possible.

Frequently a need exists for preconcentration of liquid samples or sample extracts that are to be separated by gas chromatography, and several preconcentration techniques are available for this purpose [1—7]. However, many of these techniques may be too complex or time-consuming for effective application to certain problems. Moreover, many preconcentration schemes are intolerably imprecise or are useful only for the determination of very volatile or very nonvolatile compounds.

This communication describes a simple method that has been used successfully for the preconcentration and gas chromatographic separation of the toxic isopropylmethylphosphonofluoridate (Sarin or GB) from water. Because existing methods lack either needed sensitivity [8] or selectivity [9], this new method with both the required sensitivity and selectivity was developed. The method entails the volatilization of a liquid sample extract in a tube filled with glass wool, the collection of the vapor of interest by adsorption on a solid sorbent, and the thermal desorption of the collected species into a gas chromatograph. A related procedure has been applied to another compound [10]. With the developed method, Sarin could be determined in water at concentrations down to approximately 67 pg ml^{-1}.

Experimental

Fabrication of preconcentrator tubes. A 111-mm length of 3-mm o.d., 1.8-mm i.d. standard borosilicate glass tubing was fire-polished at one end. Into the other end were inserted (in order), a spacer made of glass capillary melting point tubing, a small plug of silanized glass wool, approximately 12.5 mg of 50/80-mesh Porapak Q (Supelco, Inc., Bellefonte, PA), another silanized glass wool plug, and another capillary spacer. Finally, the unpolished

end of the tube was fire-polished to complete the fabrication of the preconcentrator tube. The capillary spacers were retained within the tube by the natural constriction at each end attributed to the fire polishing process. The tubes were conditioned prior to use by heating them overnight at 200°C with nitrogen flowing through them at 30 ml min^{-1}.

The preconcentrator tube was connected by means of teflon tubing to a 7-mm o.d., 5-mm i.d., 76-mm long tapered glass pipet dropper tube filled with silanized glass wool. The other end of the preconcentrator tube was attached to an air sampling pump.

Preparation of calibration standards. Standard solutions of Sarin were prepared in 2×10^{-4} M H_2SO_4 because Sarin is subject to rather rapid hydrolysis at certain other pH levels [11]. Appropriate quantities of neat liquid Sarin were first dissolved in reagent-grade chloroform, and the chloroform solutions were then added in microliter quantities to 1.5-ml portions of 2×10^{-4} M H_2SO_4 in conical glass centrifuge tubes with teflon-lined caps. Next, the containers were capped, and the chloroform—water mixtures were mixed thoroughly by agitation for 45 s with a vortex mixer. Seven standards were prepared, with the final concentrations of Sarin covering the range 0.067—0.80 ng ml^{-1}.

Extraction. Each sample (1.5 ml) was extracted with 100 μl of reagent-grade chloroform. The two-layer mixtures were mixed with a vortex mixer for 45 s and then centrifuged for 5 min to separate the phases. The chloroform phase was then withdrawn from beneath the supernatant aqueous layer with a 100-μl syringe and transferred to a preconcentrator tube as described below.

Preconcentration. The entire chloroform extract from a single sample or standard was injected by syringe directly into the glass wool inside the tapered dropper tube while air was being drawn into the tube at a rate of 100 ml min^{-1} by a pump. The glass wool caused a large increase in the air—solution surface contact area, and therefore evaporation of the solution was rapid. Pumping was maintained for 4 min to ensure that all vapors of Sarin and chloroform were swept into the sorbent bed.

Desorption, separation, and measurement. A Model 275-HA gas chromatograph (Tracor Instrument Co., Austin, TX), equipped with a phosphorus-specific flame photometric detector (FPD), was employed. The injection port was modified according to Method A of a previous publication [12] in order to permit thermal desorption from the sorbent tubes directly into the gas chromatographic column. Chromatographic peak areas were estimated manually as the height × width at half-height. The mixed phase analytical column consisted of 5% QF-1 and 3% DC-200 coated onto 60/80-mesh Gas-Chrom Q and packed into a 183-cm length of 3-mm o.d., 1.6-mm i.d. teflon (TFE) tubing. The temperatures of the column oven, injection port, and detector block were 105, 200, and 150°C, respectively, while the flow rates of nitrogen carrier gas, detector hydrogen, and detector air were 20, 100, and 100 ml min^{-1}, respectively.

Results and discussion

A linear least-squares fit of detector signal (s) versus concentration (c) for the seven standards yielded an equation $s = (227 \pm 12\ mm^2\ ml\ ng^{-1})c + (4 \pm 6\ mm^2)$ with a standard error of estimate (S_{yx}) of 8.3 mm^2 for signals between 20 and 189 mm^2, for concentrations between 0.067 and 0.80 ng ml^{-1}, and a correlation coefficient of 0.993. The calibration standard of lowest concentration, 0.067 ng ml^{-1}, generated a chromatographic peak amplitude of about 10 times the peak-to-peak noise amplitude at the baseline.

Six additional standards in the range 0.16—0.75 ng ml^{-1}, processed as "unknowns" by another analyst using the calibration data, yielded a least-squares fit of found (y) versus known (x) concentrations of $y = (0.88 \pm 0.02)x + (0.05 \pm 0.01$ ng $ml^{-1})$ with S_{yx} = 0.012 ng ml^{-1} and r = 0.999. The minimum and maximum differences between known and found values were 0.00 and 0.05 ng ml^{-1}.

Of the 100 μl of chloroform employed for each extraction, recoveries of chloroform were between 70 and 80 μl with an average of 76 μl, and no mathematical compensation for variations in extractant volume was used. Presumably, the losses of chloroform were due primarily to evaporation. The equilibrium distribution coefficient of Sarin between chloroform and water is 31.2 [13], and thus about 60% of the total Sarin in each aqueous standard was extracted.

It is concluded that the method is effective for the preconcentration and determination of Sarin at trace levels in water. The method requires about 10 min per sample after calibration, and in principle, it can be applied to the determination of most substances of sufficient volatility in other types of samples and sample extracts.

The work presented herein was performed under a U.S. Army Contract. The assistance of Mark A. Carter is gratefully acknowledged.

REFERENCES

1 E. S. K. Chian, P. P. K. Kuo, W. J. Copper, W. F. Cowen and R. C. Fuentes, Environ. Sci. Technol., 11 (1977) 282.
2 P. P. K. Kuo, E. S. K. Chian, F. B. De Walle and J. H. Kim, Anal. Chem., 49 (1977) 1023.
3 Z. Voznakova, M. Popl and M. Berka, J. Chromatogr. Sci., 16 (1978) 123.
4 D. J. Schultz, J. F. Pankow, D. Y. Tai, D. W. Stephens and R. E. Rathbun, J. Res. U.S. Geol. Surv., 4 (1976) 247.
5 H. Bargnoux, D. Pepin, J. L. Chabard, V. Vedrine, J. Petit and J. A. Berger, Analusis, 5 (1977) 170.
6 V. Leoni, G. Puccetti, R. J. Colombo and A. M. D'Ovidio, J. Chromatogr., 125 (1976) 399.
7 J. Zerbe, Chem. Anal. (Warsaw), 22 (1977) 575.
8 B. Gehauf and J. Goldenson, Anal. Chem., 29 (1957) 276.
9 H. O. Michel, E. C. Gorden and J. Epstein, Environ. Sci. Technol., 7 (1973) 1045.
10 J. F. Mazur, G. E. Podolak and B. T. Heitke, Am. Ind. Hyg. Assoc. J., 41 (1980) 66.
11 J. Epstein, Science, 170 (1970) 1396.
12 W. K. Fowler, C. H. Duffey and H. C. Miller, Anal. Chem., 51 (1979) 2333.
13 R. W. Rosenthal, R. Proper and J. Epstein, J. Phys. Chem., 60 (1956) 1596.

Analytica Chimica Acta, 124 (1981) 229—231

Short Communication

THERMOMETRIC AND POTENTIOMETRIC TITRATIONS OF MODIFIED GLASS SURFACES

RICHARD J. KVITEK, PETER W. CARR and JOHN F. EVANS*

Department of Chemistry, University of Minnesota, 207 Pleasant Street S.E., Minneapolis, MN 55455 (U.S.A.)

(Received 19th September 1980)

Summary. Glass surfaces modified with N-2-aminoethyl-3-aminopropyltrimethoxysilane have been titrated with copper(II) by constant rate thermometric titration and by manual potentiometric titration with Gran plot end-point location. The results indicate that the titrant reacts with the bound ligand in a two-step process, with the thermometric titration responding to the first step and the potentiometric titration responding to the combined steps.

Immobilized organic functional groups have been used extensively during the past five years in several areas of analytical chemistry, e.g. for preconcentration of metals [1], in immobilized enzyme reactors [2], and for electrode modification [3—4]. In the case of bound ligands, the amount of ligand is most often measured via elemental determination or determination of the metal-binding capacity. Direct titration of modified glass surfaces in water by acid—base titration is compromised by the slow dissolution of the silica matrix at pH greater than 7 [5]. It should be noted that indirect redox titrations for the determination of bound diol groups, have been successfully carried out [6].

The purpose of this communication is to report the first direct thermometric and potentiometric titrations of chemically modified porous glass surfaces. Controlled pore glasses (CPG) modified by reaction with N-2-aminoethyl-3-amino-propyltrimethoxysilane (en-silane) were titrated with copper(II) sulfate with thermometric end-point detection. These titrations were done with 0.4 M copper sulfate in unbuffered 0.1 M $NaNO_3$, the initial pH being 9.5. A well defined end-point is evident in Fig. 1. Replicate titrations indicate that the end-point corresponded to 1.64 ± 0.14 μmol m^{-2} of copper-binding sites. Titrations at different rates of titrant addition such that the end-point time varied from 1 to 5 min indicated the absence of kinetic end-point errors [7]. Conventional calibration techniques indicated an apparent enthalpy of -17 ± 1 kcal mol^{-1} of copper(II).

Direct potentiometric titration of the same material using a copper(II)-selective electrode produced an extremely drawn-out titration curve, typical of the titration of a polyelectrolyte or the presence of a multiplicity of

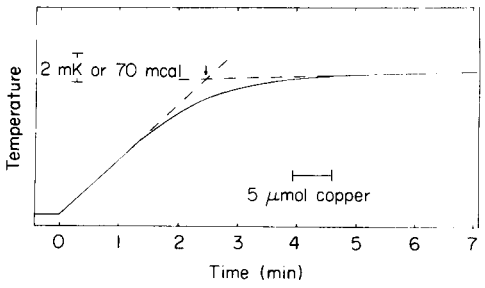

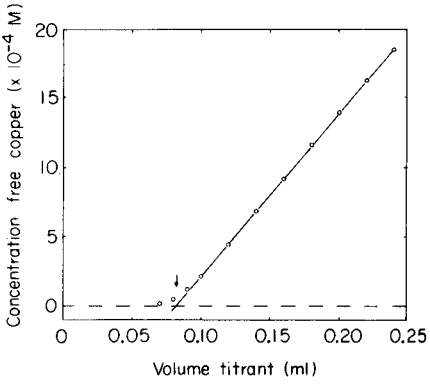

Fig. 1. Thermometric titration of en-silane modified CPG (en-CPG) with copper(II). Conditions: 0.12 g of en-CPG in 35 ml of 0.1 M $NaNO_3$ titrated with 0.4 M $CuSO_4$, rate of titrant addition 7.4 μmol min^{-1}. Initial pH of analyte solution was ca. 9.5, final pH was ca. 5.5. Arrow indicates end-point of titration.

Fig. 2. Gran plot of the potentiometric titration of en-CPG with copper(II). Conditions: 0.10 g of en-CPG in 30 ml of 0.1 M $NaNO_3$ titrated with 0.4 M $CuSO_4$ with copper-selective electrode and saturated calomel reference. Arrow indicates end-point of titration.

types of binding sites. A Gran plot [8] of these data yielded a well defined end-point as illustrated in Fig. 2. Replicate determinations indicated the presence of 3.12 ± 0.08 μmol m^{-2} of copper-binding capacity. Based on the assumption of a 2:1 ligand/copper(II) ratio [9], this is in good agreement with both elemental (nitrogen) assays of bound ligand (3.26 ± 0.16 μmol m^{-2} copper-binding capacity) and the total copper-binding capacity (3.66 ± 0.22 μmol m^{-2}) found by the method of Leyden et al. [9]. Direct injection potentiometric experiments showed that copper(II) uptake is very rapid, i.e. 99% reaction takes place in less than 5 s.

The difference in the thermometric and potentiometric end-points is real and is attributed to the fact that there are two steps of reaction, the second step having an experimentally unobservable reaction enthalpy and resulting in a $Cu(II)en_2$ complex. The ability of thermometric titrimetry to discriminate between successive steps in a reaction or to distinguish amongst classes of sites is well known [10]. A more detailed report on these observations will be forthcoming.

R. J. K. acknowledges the financial support of the 3M Company in the form of a fellowship. Acknowledgment is made to the donors of The Petroleum Research Fund, administered by the ACS for partial support of this research (grant 10733-G3) and to the National Institutes of Health (grant R01-GM27581-01).

REFERENCES

1 D. E. Leyden and G. H. Luttrell, Anal. Chem., 47 (1975) 1612.
2 R. S. Schifreen, D. A. Hanna, L. D. Bowers and P. W. Carr, Anal. Chem., 49 (1977) 1929.
3 K. D. Snell and A. G. Keenan, J. Chem. Soc., Chem. Soc. Rev., 8 (1979) 259.
4 R. W. Murray, Acc. Chem. Res., 13 (1980) 135.
5 R. K. Iler, The Chemistry of Silica, Wiley—Interscience, New York, 1979, p. 47.
6 F. E. Regnier and R. J. Noel, J. Chromatogr. Sci., 14 (1976) 316.
7 P. W. Carr and J. Jordan, Anal. Chem., 45 (1973) 634.
8 G. Gran, Analyst, 77 (1952) 661.
9 D. E. Leyden, M. L. Steele, B. B. Jablonski and R. B. Somoano, Anal. Chim. Acta, 100 (1978) 545.
10 J. Barthel, Thermometric Titrations, Wiley—Interscience, New York, 1975, p. 53.

Analytica Chimica Acta, 124 (1981) 233—236

Short Communication

DIFFERENTIAL PULSE POLAROGRAPHIC DETERMINATION OF TRACES OF MOLYBDENUM IN SOLAR-GRADE SILICON†

PIER LUIGI BULDINI*

C.N.R.-Istituto LAMEL, Via de' Castagnoli 1, 40126 Bologna (Italy)

DONATELLA FERRI

Istituto Chimico, Facoltà di Ingegneria, Università di Bologna, 40136 Bologna (Italy)

(Received 4th February 1980)

Summary. After dissolution of silicon with hydrofluoric and nitric acids and matrix volatilization as hexafluorosilicic acid, 0.2 M nitric acid and 1.8 M ammonium nitrate are added to the residue. Molybdate is then determined by means of its catalytic wave in nitrate media. The limit of determination is ca. 0.1 $\mu g\ g^{-1}$ and calibration graphs are linear up to 0.2 μg Mo(VI) ml^{-1}.

For extensive development of solar cell devices, silicon considerably cheaper than that now available is needed for crystal growth and cell fabrication. Contamination levels for solar-grade silicon are less important than those for semiconductor-grade stock, yet cell performance remains a function of metal impurity content. The acceptable impurity levels depend on the tolerable cell efficiency and on the method of cell manufacture. At present, molybdenum concentrations in feedstock to achieve specific solar cell performance levels are accepted as 40 $\mu g\ g^{-1}$ for a relative efficiency $\eta = 0.9\ \eta_0$, about 25 $\mu g\ g^{-1}$ for $\eta = 0.95\ \eta_0$, and about 2.5 $\mu g\ g^{-1}$ for $\eta \approx \eta_0$, where η_0 is the efficiency of a typical baseline device.

Molybdenum contents are usually determined by spark-source mass spectrometry (detection limit 0.03 $\mu g\ g^{-1}$ [1]) or by neutron activation analysis (detection limit about 0.03 ng g^{-1} [2]). For the analysis of silicates, atomic absorption spectrometry is useful down to the low $\mu g\ ml^{-1}$ level [3—5], but solvent extraction may be needed to avoid interferences and to lower the detection limit.

Voltammetric techniques have been applied to the determination of molybdenum in silicates [6—9] but the catalytic molybdenum wave in nitrate media has not previously been utilized. In acidic nitrate solutions molybdate ion gives an exceptionally high polarographic current and the well-shaped wave is suitable for trace analysis; the method has been applied to the determination of molybdenum in steels [10].

†Presented at the Heyrovsky Memorial Congress on Polarography, Prague, August 1980.

Although chemical methods cannot reach the high sensitivity of the more sophisticated physical methods, it is shown below that relatively inexpensive apparatus allows the detection limits required by advanced technologies to be achieved. The proposed method is based on silicon dissolution with hydrofluoric and nitric acids, matrix volatilization as hexafluorosilicic acid, and differential pulse polarography.

Experimental

Reagents. Electronic-grade chemicals were used and normal precautions for trace analysis were taken throughout the work. Reagents and solutions were stored in polyethylene bottles, and polyethylene volumetric ware was used. All plastic ware and PTFE vessels were filled with 8 M ammonia solution, left overnight and rinsed thoroughly before use in order to remove every trace of molybdate ions.

Working standards were prepared daily by diluting stock Mo(VI) solutions (1000 μg ml^{-1}) obtained from ammonium molybdate tetrahydrate in twice-distilled water.

Apparatus. The silicon samples were dissolved in PTFE test tubes fitted with 29/32 sockets, which were placed in a temperature-programmed aluminium block (Berghof, Tubingen, Germany); this heating device is equipped with 29/32 cones so that filtered air can be passed into the test tubes.

The AMEL (Milan) Model 472 Multipolarograph used was equipped with a Model 460 stand, a 5-ml microcell, a mercury dropping electrode ($m^{2/3}$ = 1.79), an Ingold Model 303/NS saturated calomel reference electrode and an Ingold Model Pt-805/NS platinum ring counter electrode. Instrumental conditions were: pulse height 100 mV, drop time 2 s and scan 2 mV s^{-1}. Solutions were deaerated with pure nitrogen for 2—3 min before analysis, and thermostatted at 25.0 ± 0.1°C.

Procedure. The preliminary sample treatment followed earlier recommendations [11, 12]. Clean the samples (usually large pieces) by washing and degreasing with trichloroethylene—acetone—methanol and ultrasonic treatment. After etching with hydrofluoric—nitric acids (1 + 1), wash in running twice-distilled water, dry in a nitrogen stream, and powder finely in a mill fitted with an agate cell.

Place 10—100 mg of sample in a PTFE test tube; add 2 ml of 65% HNO_3 and 5 ml of 12 M HF. After the initial reaction has ceased, place the tube in the heating device with the PTFE cone in position, and heat at 50°C for 1 h. Then heat at 110°C for 2 h, while passing filtered air through the tube. Only a small residue remains. Then add 2 ml of 2 M HNO_3, shake well to dissolve any residue, and add 3 ml of 2 M NH_4NO_3—1 M NH_3 solution. Transfer the solution to a polarographic cell, deaerate and record the polarogram from 0 to −0.4 V (vs. SCE). Measure the peak height at −0.21 V and compare it with a calibration curve. Figure 1 shows a typical polarogram with the method of peak measurement. The calibration graph obtained under the recommended conditions is linear up to 0.2 μg Mo(VI) ml^{-1}.

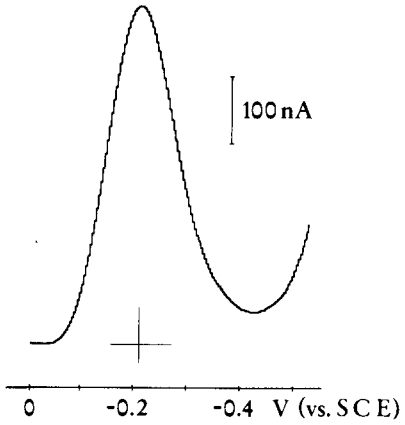

Fig. 1. Typical polarogram for molybdenum (0.30 μg g^{-1}) in solar-grade silicon, showing the method of peak measurement.

Results and discussion

To check the proposed method, several blocks of semiconductor silicon were tested: no molybdenum was found. When these samples were spiked to contain 0.25, 0.5 and 1 μg Mo(VI) g^{-1} and re-analysed, the recoveries varied from 99—101%. The results obtained on five contaminated blocks are shown in Table 1; again a 0.25 μg g^{-1} spike gave a 99—101% recovery. When the prescribed conditions are used, the proposed method permits determinations of molybdenum levels as low as 100 ng g^{-1}, with a relative standard deviation of 1—2%.

The optimal polarographic working conditions have been previously reported [10]. No cations were found that cause interferences on the catalytic wave of molybdate; of the impurities found in metallurgical-grade silicon, only chromium(VI), copper(II) and iron(III) have reduction potentials near −0.21 V, but these potential interferences are never present at concentration levels high enough to interfere, because the catalytic effect greatly enhances the molybdate wave.

Of the dopants used in silicon technology, only phosphorus might cause problems through molybdophosphate formation. It was shown, however, that phosphorus, even at high dopant levels (20 μg g^{-1}), caused no difficulty. The procedure is simple, rapid and suitable for routine trace analysis.

TABLE 1

Tests on contaminated silicon blocks with recoveries of 0.25 μg Mo(VI) g^{-1} spikes

Sample	233616	73151	96777	127692	79899
Mo found (μg g^{-1})	0.25	0.40	0.30	0.55	0.20
Recovery (%)	101	101	100	99	100

The authors thank Profs. D. Nobili and P. Lanza for their helpful suggestions.

REFERENCES

1 Performance characteristics, Mass Spectrometer Type MS-7, Associated Electrical Industries Ltd.
2 General Activation Analysis Data Sheet, Multi-Element Survey Analysis of Silicon, General Activation Analysis, San Diego, CA, U.S.A.
3 C. H. Kim, C. M. Owens and L. E. Smythe, Talanta, 21 (1974) 445.
4 D. Hutchinson, Analyst (London), 97 (1972) 118.
5 V. B. Schweizer, At. Absorpt. Newsl., 14 (1975) 137.
6 H. Holzapfel, O. Guertler and B. Tempel, Fresenius Z. Anal. Chem., 235 (1968) 413.
7 I. L. Beleuta and C. Bratu, Radiochem. Radioanal. Lett., 2 (1968) 233.
8 Z. A. Gallai, N. M. Sheina, N. V. Polikardova and T. V. Pleshakova, Zh. Anal. Khim., 30 (1975) 1148.
9 T. Ya. Belova, L. P. Volkova and K. S. Pakhomova, Zavod. Lab., 44 (1978) 1176.
10 P. Lanza, D. Ferri and P. L. Buldini, Analyst (London), 105 (1980) 379.
11 P. L. Buldini, D. Ferri and P. Lanza, Anal. Chim. Acta, 113 (1980) 171.
12 P. Lanza and P. L. Buldini, Anal. Chim. Acta, 85 (1976) 69.

Analytica Chimica Acta, 124 (1981) 237—241

Short Communication

DETERMINATION OF SACCHARIN IN ELECTROPLATING BATHS BY DIFFERENTIAL PULSE AND A.C. POLAROGRAPHY†

MANFRED GEISSLER*, BARBARA SCHIFFEL and CLAUS KUHNHARDT

Forschungsinstitut für NE-Metalle, VEB Mansfield Kombinat "Wilhelm Pieck", 9200 Freiberg—Sachs (German Democratic Republic)

(Received 25th June 1980)

Summary. Saccharin can be determined in palladium, gold and nickel electroplating baths by differential pulse polarography or second-harmonic a.c. polarography after extraction with an ethyl acetate/carbon tetrachloride mixture and after masking the noble metal with cyanide. Detection limits lie between 0.025 and 0.005 g l^{-1}. Bath components such as chloride, nitrate, sulfate, phosphate, glucose, citrate, Fe^{3+}, Sn^{4+}, Cr^{3+}, Ni^{2+} and Pb^{2+} do not interfere.

Saccharin is a commonly used brightener in nickel, palladium and gold electroplating baths, and is also applied in the electrolytic production of nickel. It is decomposed electrochemically and must thus be added periodically to the baths. Its determination in electroplating solutions has always been difficult. Dubsky [1] has reviewed the methods for the determination of saccharin in nickel electroplating baths, recommending a derivative d.c. polarographic method [2], which does not involve separation of the compound from the solution. Rooney and Jones [3] determined saccharin by linear sweep polarography in hydrochloric acid medium after extraction with diethyl ether and back-extraction with sodium hydroxide solution. The polarographic methods were reported to be highly selective.

In the work described here, the determination of saccharin in palladium and gold baths was studied by d.c., derivative d.c., square-wave, differential-pulse and a.c. polarography.

Very recently, Sontag and Kral [4] have described the differential pulse polarographic determination of saccharin in alcohol-free drinks, and the identification of the reaction products at the DME.

Polarographic behaviour of saccharin

D.c. polarography. Nejmann [5] and Dubsky [1] showed that, in acidic and alkaline solutions, saccharin gives a wave close to the potential of hydrogen reduction: the saccharin wave can be separated from the hydrogen wave by recording the derivative curve [1]. However, the present studies showed

†This paper was presented at the Analytiktreffen, Neubrandenburg, November, 1979.

that the saccharin waves could not be evaluated quantitatively even using the derivative curves. Acidic, ammoniacal and alkaline supporting electrolytes were tested, including tetramethylammonium hydroxide and EDTA. The d.c. polarographic wave (and its first derivative) was best defined in 0.1 M HCl. However, with this supporting electrolyte, saccharin could not be determined in palladium baths containing palladium tetrammine dinitrate. Palladium decreased the hydrogen overvoltage and caused a high current at about +0.1 V so that high counter-current compensation had to be used and irreproducible waves with large drop variations were recorded. At higher acidities, $Pd(NH_3)_2Cl_2$ ("yellow salt") was precipitated. Although the high current flow at the beginning of the polarogram was eliminated, the reproducibility of the saccharin wave was not improved as the palladium was not precipitated quantitatively. Well-defined saccharin waves were recorded in 0.005—0.05 M HCl—0.05 M KCl solutions at pH 1.2—3.5, but again the method was unsuitable for application to palladium baths.

The reduction of saccharin was also studied by square-wave polarography, with the same supporting electrolytes as above, but broad and irreproducible peaks showing many interferences were obtained.

Differential pulse polarography. When differential pulse polarography (d.p.p.) was used with acidic and alkaline supporting electrolytes, saccharin gave well-defined and reproducible peaks (Fig. 1). In > 0.2 M HCl, the peak height was constant. The best defined peak was obtained in 0.5 M HCl with a peak potential E_p = −1.1 V (vs. SCE). Ammoniacal supporting electrolytes containing EDTA gave smaller peaks (E_p = −1.74 V), whose heights decreased with rising pH. As shown by Sontag and Kral [4], the undissociated form of saccharin was reduced in strong acid and the dissociated form reduced in weakly acidic and alkaline media: the reduction of the dissociated saccharin required a larger expenditure of energy. The half-widths of the peaks showed only small differences (W = 63 mV in acidic and 69 mV in alkaline media), indicating that the reaction reported by Sontag and Kral [4] was irreversible. In practice, 0.5 M HCl was used as the supporting electrolyte

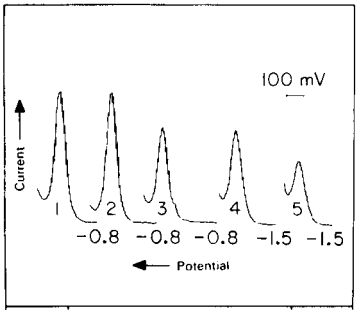

Fig. 1. Differential pulse polarograms of 4 × 10^{-4} M saccharin in various media: (1) 1.0 M HCl; (2) 0.5 M HCl; (3) 0.05 M HCl; (4) 0.1 M NH_3 + 0.1 M NH_4Cl + 0.05 M EDTA; (5) 2 M NH_3 + 0.5 M NH_4Cl + 0.5 M EDTA. ΔV = 20 mV.

in the analytical determination of saccharin in palladium baths. Well-defined peaks suitable for quantitative evaluation were obtained (Fig. 1, curve 2).

With saccharin concentrations greater than 2 g l^{-1} and a high enough dilution of the original bath in 0.5 M HCl, it was possible to record a saccharin peak free of interference from palladium. When lower concentrations had to be determined, a larger sample volume had to be added to the supporting electrolyte; "yellow salt" was then precipitated and the unprecipitated palladium interfered. It was necessary therefore to eliminate this interference by separating palladium from saccharin (see below).

Second-harmonic a.c. polarography. In 0.5 M HCl, saccharin gave a well-defined peak of half-width W = 74 mV at E_p = −1.08 V (vs SCE), when second-harmonic a.c. polarography (120 Hz, amplitude 10 mV) was applied. The double-peak usually found for reversible electrode processes in this technique did not occur, showing that the saccharin was reduced irreversibly. Compared with the d.p.p. peak the a.c. polarographic one had its more negative peak front at or near the base line; when standard solutions were studied, the calibration curve thus passed through the origin.

Separation of palladium from saccharin

Initially, attempts were made to separate the palladium from the bath and to determine the saccharin in the remaining solution by d.p.p. Precipitation of "yellow salt" (see above) and reduction of palladium(II) to the metal by hydrazine monochloride in ammoniacal solution were both unsuitable. The separation of saccharin by extraction with ethyl acetate [1] thus seemed to be more promising. The sodium saccharinate had first to be converted by acidification to the imide, the only compound that could be extracted. Extraction was possible only from a hydrochloric acid medium; nitric acid was co-extracted and interfered with the saccharin polarographic peak, whereas the phase separation was bad from sulphuric acid solutions. The precipitation of "yellow salt" caused by acidification with hydrochloric acid also inhibited phase separation. After precipitation of palladium with hydrazine, saccharin could easily be extracted from the acidified solution but subsequent evaporation of the solvent resulted in saccharin losses.

Further experiments were therefore carried out, in order to improve the phase separation after extraction with ethyl acetate, and to mask the palladium. A mixture of ethyl acetate and carbon tetrachloride (1 + 1) decisively improved the phase separation without any change in the percentage extraction of saccharin. A practical advantage was that the extraction mixture was the denser phase. Potassium cyanide was found suitable for masking palladium: the tetracyanopalladate(II) anion is very stable, its stability constant being pK_4 = 51.6 [6], whereas that of $[Pd(NH_3)_4]$ $(NO_3)_2$ is pK_4 = 29.6 and that of the Pd—EDTA complex is pK_{PdY} = 26.4 [7]. Experiments showed that $[Pd(CN)_4]^{2-}$ is not decomposed by hydrochloric acid and is not extracted by the carbon tetrachloride—ethyl acetate mixture.

Experimental

Equipment. The polarographs used were the OH-105 model for d.c. and a.c polarography and the OH-104 model for square wave polarography (Radelkis, Budapest, Hungary). A voltammetric analyzer (VA1) for Tast, triangular wave and differential pulse polarography was constructed in this laboratory. The dropping mercury electrode was used with a saturated calomel reference electrode or a platinum wire auxiliary electrode.

Reagents. The reagents were hydrochloric acid (12.5 M, d = 1.18), potassium cyanide (10% solution), carbon tetrachloride (p.a.), ethyl acetate (p.a.) and ammonia/ammonium chloride (0.5 M solution). For the saccharin standard solution, saccharin was precipitated from a solution of sodium saccharinate with hydrochloric acid, filtered and dried, and 50 mg of saccharin was dissolved in 50 ml of 0.1 M NaOH.

Analytical procedure. Depending on the saccharin content and the preliminary dilution of the palladium bath, pipette 1—20 ml of the sample into a 50-ml separating funnel and dilute with distilled water to about 20 ml. Depending on the palladium content, add 10% potassium cyanide solution (8 ml of 10% KCN solution for ca. 35 g Pd l^{-1}). Using a fume hood and powerful suction, add 4 ml of 12.5 M HCl (d = 1.18) and extract for 2 min with a mixture of 20 ml of ethyl acetate and 20 ml of carbon tetrachloride. Transfer the organic phase to a second separating funnel and discard the aqueous phase after treatment with iron(II) sulphate. Re-extract the saccharin from the organic phase with 20 ml of 0.5 M ammonia/ammonium chloride solution by shaking for 1 min. Discard the organic phase and transfer the aqueous phase to a 50-ml measuring flask. Boil away the solvent residues, add 3 ml of 12.5 M HCl (d = 1.18) and dilute with distilled water to the mark. Deaerate a part of the solution in the polarographic cell by passing a stream of nitrogen through it for 3 min. Record the differential pulse polarogram from —0.85 V (vs. SCE) to the hydrogen evolution. Measure the peak with reference to the blank current (see Fig. 2, curve 1). Calculate the saccharin content either from a calibration curve or by the standard addition

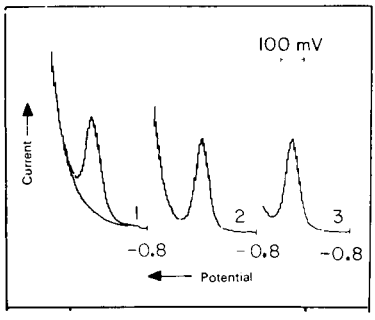

Fig. 2. Differential pulse polarograms of saccharin in palladium, gold and nickel baths after separation by extraction: (1) Pd bath, saccharin 0.73 g l^{-1}; (2) Au bath, saccharin 3.6 g l^{-1}; (3) Ni bath, saccharin 0.4 g l^{-1} ΔV = 20 mV. Blank current and measured peak height are given for curve (1).

method: in the latter case, add saccharin standard solution to a separate fraction of the bath and analyze by the same procedure.

Alternatively, the a.c. polarographic curve of saccharin may be recorded with reference to the blank current. The concentration is again determined using a standard solution or a calibration curve. In such procedures, the amplitude was 10 mV and the frequency 120 Hz.

Results

This method was applied to the determination of saccharin in palladium, gold and nickel electroplating baths (Fig. 2). For cyanide gold baths the addition of potassium cyanide was omitted. For determinations of saccharin in nickel baths, the method was tested with a Watts type bath containing $NiSO_4$ (250 g l^{-1}), $NiCl_2$ (50 g l^{-1}) and boric acid (25 g l^{-1}).

When the d.p.p. method was used for palladium baths, the working range was 0.2—5 mg of saccharin per 50 ml of sample solution, and the limit of determination was 0.01 g l^{-1} of bath. In two typical analyses with a pulse amplitude of 20 mV and a pulse duration of 100 ms, the statistical data were: (1) saccharin content found 0.73 g l^{-1}, s = 0.007 g l^{-1} (P = 95%, n = 16), and the confidence interval of the mean $\Delta\bar{x}$ = ± 0.015 g l^{-1}; (2) saccharin content found 0.031 g l^{-1}, s = 0.00045 g l^{-1} (P = 95%, n = 20), $\Delta\bar{x}$ = ± 0.001 g l^{-1}.

For gold baths, the limit of determination for saccharin by d.p.p. was 0.005 g l^{-1}. The coefficient of variation was 1.8% at a saccharin level of 3.6 g l^{-1} (n = 16).

When second-harmonic a.c. polarography was applied to palladium baths, the working range was 0.1—2 mg of saccharin per 50 ml of sample solution, and the limit of determination 0.025 g l^{-1} of bath. For a typical sample, the saccharin content found was 0.340 g l^{-1}, s = 0.0165 g l^{-1} (P = 95%, n = 24), $\Delta\bar{x}$ = ±0.007 g l^{-1}.

Other bath components such as Cl^-, NO_3^-, SO_4^{2-}, PO_4^{3-}, glucose, citrate, Fe^{3+}, Sn^{4+}, Cr^{3+}, Ni^{2+}, and Pb^{2+} do not interfere with these determinations.

REFERENCES

1 I. Dubsky, Metalloberfläche, 24 (1970) 85.
2 A. V. Krusenstjern and M. Yuguchi, Metalloberfläche, 20 (1966) 320.
3 R. C. Rooney and D. L. Jones, Electroplat. and Metal Finish, 17 (1964) 49.
4 G. Sontag and K. Kral, Fresenius Z. Anal. Chem., 294 (1979) 278.
5 M. B. Nejmann, Zh. Anal. Khim., Moskva, 10 (1955) 175.
6 H. C. Hedrich and Ch. J. Raub, Metalloberfläche, 31 (1971) 512.
7 J. Kragten, Talanta, 25 (1978) 239.

Analytica Chimica Act, 124 (1981) 243

Errata

R. D. Braun, The Electrochemical Reactions of Copper(II) and Copper(I) Chloride in N,N-Dimethylformamide.
Anal. Chim. Acta, 120 (1980) 111—120.

p. 116. Line 24 of the text should read:
p − q is found to be 1 ... instead of p − q is found to be 2, as in the text.
The equation on line 26 of the text should read:
$CuCl_4^{2-} + e = CuCl_3^{2-} + Cl^-$ ... instead of $CuCl_4^{2-} + e = CuCl_2^{2-} + 2Cl^-$, as in the text.

p. 119. The equation near the bottom right-hand side of the electrochemical equations should read:

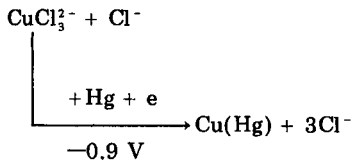

instead of

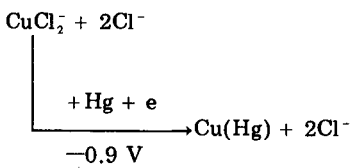

as in the text.

p. 120. On lines 2, 4 and 33, $CuCl_2^-$ should read $CuCl_3^{2-}$.

ACA announcements

ANNOUNCEMENTS OF MEETINGS

1981 BENEDETTI-PICHLER AWARD: CALL FOR NOMINATIONS

The American Microchemical Society is Soliciting nominations for its 17th annual Benedetti-Pichler Award. This award is given in recognition of service to microchemistry in its broadest sense, including research, application, administration, teaching, or other means of promoting the advancement of microchemistry. The nominee need not be a member of the society. Nominations should be made in writing, stating the reason for nomination and citing the work of the nominee. All nominations must be received by April 1, 1981. Nominations and requests for further information should be addressed to: Lisa Hallquist, J.T. Baker Chemical Co., 222 Red School Lane, Phillipsburg, NJ 08865, U.S.A.

CALENDAR OF FORTHCOMING MEETINGS

March 9–13, 1981 Atlantic City, U.S.A.	**1981 Pittsburgh Conference** Contact: John A. Queiser, Programme Chairman, 1981 Pittsburgh Conference, 2523 Greenboro Lane, Pittsburgh, PA 15220, U.S.A. Tel: 412 795–7110.
March 23–June 5, 1981 Uppsala, Sweden	**Course: Biochemical Separation Methods** Contact: Secretary, Eva Linder, Institute of Biochemistry, University of Uppsala, Box 576, S–751 23 Uppsala, Sweden.
Apr. 8–10, 1981 Amsterdam, The Netherlands	**Mass Spectrometric Isotopes and Elemental Analysis** Contact: Dr. E. Hebeda, Laboratory for Isotopes/Geology, De Boelelaan 1085, NL-1081 HV Amsterdam, The Netherlands.
Apr. 13–16, 1981 Cardiff, Wales United Kingdom	**International Symposium on Electroanalysis in Clinical Environmental and Pharmaceutical Chemistry** Contact: Short Courses Section (Electroanalysis Symposium), UWIST, Cardiff CF1 3NU, Wales, United Kingdom. (Further details published in Vol. 116, No. 1)
April 22–24, 1981 Noordwijkerhout, The Netherlands	**Joint NL – UK Symposium on Quantitative Organic Analysis** Contact: Dr. B. Griepink, Secretary of Analytical Chemistry Section of the Royal Netherlands Chemical Society, c/o Analytical Chemistry Laboratory, Croesestraat 77A, 3522 AD Utrecht, The Netherlands. (Further details published in Vol. 118, No. 2)
Apr. 26–May 1, 1981 Singapore, Republic of Singapore	**1st Asian & Pacific Chemistry Congress** Contact: The Congress Secretary, 1st ASPAC Congress, c/o Singapore Professional Centre, 129 B, Block 23, Outram Park, Singapore 0316, Republic of Singapore.
May 3–7, 1981 Hindenlang, (Bavarian Alps), F.R.G.	**4th International Symposium on Capillary Chromatography** Contact: Dr. J. Rijks, Laboratory of Instrumental Analysis, University of Technology, P.O. Box 513, NL–5600 MB Eindhoven, The Netherlands.
May 5–8, 1981 Gatlinburg, TN, U.S.A.	**Separation Science and Technology for Energy Applications** Contact: A.P. Malinauskas, Oak Ridge National Laboratory, P.O. Box X, Oak Ridge, TN 37830, U.S.A.

May 11–15, 1981 Avignon, France	**Vth International Symposium on Column Liquid Chromatography** Contact: Prof. G. Guiochon, Ecole Polytechnique, Laboratoire de Chimie Analytique Physique, Route de Saclay, 91128 Palaiseau Cedex, France. (Further details published in Vol. 118, No. 1)
May 18–20, 1981 Jekyll Island, Georgia, U.S.A.	**11th Annual Symposium on the Analytical Chemistry of Pollutants** Contact: Prof. Dr. Roland W. Frei, The Free University, De Boelelaan 1083, 1081 HV Amsterdam, The Netherlands.
May 20–22, 1981 Eger, Hungary	**Symposium on the Analysis of Steroids** Contact: Prof. S. Görög, c/o Hungarian Chemical Society, 1061 Budapest VI., Anker köz 1, Hungary.
June 1–5, 1981 Stresa, Lago Maggiore, Italy	**2nd European Symposium on Organic Chemistry** Contact: Prof. Giorgio Modena, Istituto di Chimica Organica, Via Marzolo, 1, 35100 Padova, Italy.
June 16–17, 1981 Venice, Italy	**1st International Symposium on Chromatography in Biochemistry, Medicine and Environmental Research** Contact: Dr. A. Frigerio, Italian Group for Mass Spectrometry in Biochemistry and Medicine, c/o Istituto di Ricerche Farmacologiche "Mario Negri", Via Eritrea 62, 20157 Milan, Italy. Tel: 35.54.546.
June 18–19, 1981 Venice, Italy	**8th International Symposium on Mass Spectrometry in Biochemistry, Medicine and Environmental Research** Contact: Dr. A. Frigerio, Italian Group for Mass Spectrometry in Biochemistry and Medicine, c/o Istituto di Ricerche Farmacologiche "Mario Negri" Via Eritrea 62 20157 Milan, Italy. Tel: 35.54.546.
June 22–26, 1981 Veldhoven, The Netherlands	**4th International Symposium on Affinity Chromatography and Related Techniques** Contact: Dr. T.C.J. Gribnau, Organon Scientific Development Group, P.O. Box 20, 5340 BH Oss, The Netherlands. (Further details published in Vol. 118, No. 1)
June 23–27, 1981 Karl–Marx–Stadt, D.D.R.	**Tagung Festkorperanalytik** Contact: Dr. K. Danzer, Technische Hochschule, Karl–Marx–Stadt, Sektion Chemie und Werkstofftechnik, PSF 964, 9010 Karl–Marx–Stadt, D.D.R. (Further details published in Vol. 118, No. 2)
July 5–10, 1981 Swansea, Wales	**The Third Swansea Summer School of Automatic Chemical Analysis** Contact: Prof. D. Betteridge, Department of Chemistry, University College of Swansea, Singleton Park, Swansea SA2 8PP, Great Britain.
July 6–9, 1981 Strasbourg, France	**27th IUPAC Symposium on Macromolecules** Contact: Secretariat, Macro 1981, Société de Chimie Industrielle, 28, rue Saint-Dominique, 75007 Paris, France.
July 12–17, 1981 Exeter, Great Britain	**5th International Conference on NMR Spectroscopy** Contact: Dr. J.F. Gribnau, Royal Chemical Society, Burlington House, London W1V 0BN, Great Britain.
Aug. 3–7, 1981 Denver, Col., U.S.A.	**30th Denver Conference on Applications of X-Ray Analysis** Contact: Mrs. Mildred Cain, Denver Research Institute, University of Denver, Denver, CO 80208, U.S.A. Tel: (303) 753–2141.

Aug. 16–22, 1981 Vancouver, Canada	**28th Congress International Union of Pure and Applied Chemistry** Contact: Congress Secretariat, 28th IUPAC Congress, c/o The Chemical Institute of Canada, 151, Slater Street, Suite 906, Ottawa, Ontario, Canada K1P 5H3.
Aug. 20–21, 1981 Helsinki, Finland	**Symposium on Harmonisation of Collaborative Analytical Studies** Contact: Dr. H. Egan, Laboratory of the Government Chemist, Cornwall House, Stamford Street, London SE1 9NQ, Great Britain.
Aug. 23–28, 1981 University of Auckland, New Zealand	**Golden Jubilee Conference "Chemistry in the Service of Man"** Contact: Dr. D.J. McLennan, Chemistry Dept., Univ. of Auckland, Auckland, New Zealand.
Aug. 23–28, 1981 Espoo, Finland	**Euroanalysis IV – Triennal Conference of the Federation of European Chemical Societies** Contact: Professor L. Niinistoe, Department of Chemistry, Helsinki University of Technology, SF–02150 Espoo 15, Finland. (Further details published in Vol. 109, No. 1)
Aug. 23–28, 1981 Canberra, Australia	**Sixth Australian Symposium on Analytical Chemistry** Contact: Hon. Secretary, Miss B.J. Stevenson, P.O. Box 1397, Canberra City, A.C.T. 2601, Australia.
Aug. 30–Sep. 5, 1981 Vienna, Austria	**XI International Congress of Clinical Chemistry – IV European Congress of Clinical Chemistry** Contact: Congress Secretariat, Interconvention, P.O. Box 35, A-1095 Vienna, Austria. Tel. (0222) 42 13 52.
Sep. 1–4, 1981 Siofok, Hungary	**3rd Danube Symposium on Chromatography** Contact: Hungarian Chemical Society, H–1368 Budapest, P.O.B. 240, Hungary. Tel: Budapest 427–343. (Further details published in Vol. 115)
Sep. 1–4, 1981 Aberdeen, Scotland	**ESTA 2 – The Second European Symposium on Thermal Analysis** Contact: Dr. F.P. Glasser, Chairman of the Organising Committee, ESTA 2, Department of Chemistry, University of Aberdeen, Meston Walk, Old Aberdeen, AB9 2UE, Scotland.
Sep. 4–8, 1981 Tokyo, Japan	**9th International Conference on Atomic Spectroscopy and XXII Colloquium Spectroscopicum Internationale** Contact: The Japan Society for Analytical Chemistry, 9th ICAS/XXII CSI, Gotanda Sanhaitsu, 26-2 Nishigotanda 1-chome, Shinagawa-ku, Tokyo 141, Japan. (Further details published in Vol. 118, No. 1)
Sep. 21–24, 1981 Loughborough, England	**Particle Size Analysis Conference** Contact: P.J. Lloyd, PSA 81 Conference, Particle Technology Group, Chemical Engineering Department, University of Technology, Loughborough, Leics. LE11 3TU, Great Britain. (Further details published in Vol. 120)
Sep. 22–25, 1981 Leipzig, D.D.R.	**Analytiktreffen 1981 – Strukturanalytische Methoden in der Stereochemie** Contact: Sektion Chemie der KMU Leipzig, Liebigstrasse 18, DDR–7010 Leipzig, D.D.R.
Sep. 28–Oct. 1, 1981 Barcelona, Spain	**16th International Symposium on Advances in Chromatography** Contact: Professor A. Zlatkis, Chemistry Department, University of Houston, Houston, Texas 77004, U.S.A.

Sep. 29–Oct. 2, 1981 Basle, Switzerland	**ILMAC'81 – 8th International Exhibition of Laboratory Chemical Engineering, Measurement and Automation Techniques in Chemistry** Contact: D. Gammeter, Secretariat, ILMAC '81, Postfach, CH–4021 Basle, Switzerland. Tel: 061–2620 20.
Nov. 23–25, 1981 Barcelona, Spain	**2nd International Congress on Analytical Techniques in Environmental Chemistry** Contact: Dr. J. Albaigés, General Secretary, Plaza de Espana, Barcelona–4, Spain. Tel: 223–31 01.
April 14–16, 1982 Amsterdam, The Netherlands	**12th Annual Symposium on the Analytical Chemistry of Pollutants** Contact: Prof. Dr. Roland W. Frei, The Free University, De Boelelaan 1083, 1081 HV Amsterdam, The Netherlands.
Aug. 30–Sep. 3, 1982 Vienna, Austria	**9th International Mass Spectrometry Conference** Contact: Interconvention, P.O. Box 105, A–1014 Vienna, Austria. (Further details published in Vol. 120)
Aug. 28–Sep. 2, 1983 Amsterdam, The Netherlands	**9th International Symposium on Microchemical Techniques** Contact: Symposium Secretariat, c/o Municipal Congress Bureau, Oudezijds Achterburgwal 199, 1012 DK Amsterdam, The Netherlands. Tel: (020) 552 3459

(continued from back cover)

Printed in The Netherlands.

CONTENTS

(continued on inside page of cover)